Sequential detection methods for spread-spectrum code acquisition

Ravi, K. V.

Award date:
1991

Awarding institution:
University of Bath

SEQUENTIAL DETECTION METHODS FOR SPREAD-SPECTRUM CODE ACQUISITION

Submitted by K. V. RAVI

for the degree of Ph.D.,

of the University of Bath

1991

COPYRIGHT

K. V. Ravi.

ProQuest LLC
789 East Eisenhower Parkway
P.O. Box 1346
Ann Arbor, MI 48106-1346

ACKNOWLEDGMENTS

I would like to express my sincere thanks to Dr. R .F .Ormondroyd for his constant encouragement and guidance throughout the course of this research.

I also wish to thank the Commonwealth Scholarship Commission and the British Council for their provision of a Commonwealth Scholarship to carry out this research.

I would also like to acknowledge the support provided by the Indian Space Research Organization for allowing a study leave to pursue research.

SYNOPSIS

In this research, the performance of a novel initial code acquisition technique, called sequential detection, for direct-sequence spread-spectrum systems suitable in low SNRs is analyzed using a Monte-Carlo computer simulation approach. This technique employs a variable-dwell time discrete step serial-search which is optimum in the sense of minimum mean acquisition time for a given probability of detection and false alarm. A new variant of the sequential detector using quantization of the log-likelihood function is considered and its performance analyzed. This sequential detector employs a uniform quantizer with the minimum number of quantization levels $Q = 32$, which are determined to give the performance closer to the ideal sequential detector. Three variants of the sequential detector namely, the quantized log-likelihood sequential detector, an ideal log-likelihood sequential detector and a biased square-law sequential detector are considered and their comparative performance is analyzed for various channel impairments in the predetection SNR range -4dB to 10dB.

All three variants are optimized with respect to critical system parameters namely, the upper and lower thresholds, input SNR and design SNR, and the optimum or a range of near-optimum values of these parameters are determined. The acquisition performance of all three variants are also analyzed and compared for the cases with data modulation and no data modulation. In addition, the effect of code rate Doppler offset and residual carrier Doppler offset on the acquisition performance of the sequential detector is also analyzed and compared for both the cases with data modulation and no data modulation for all the variants of the detector when operating at their optimum design SNR. The degradation in the acquisition performance due to the presence of a CW jammer and a pulse jammer waveform is also analyzed and compared for all variants. Finally, the performance of the sequential detector is compared with other common types of serial search methods using a fixed-dwell serial search and a digital matched filter, and its performance is shown to be superior particularly at lower SNRs, which is a promising performance for the new detector.

CONTENTS

CHAPTER 1

INTRODUCTION

Most modern communication systems conventionally aim at the optimum utilization of the basic communication resources namely, the power and the bandwidth. In many situations, however, various channel impairments, which may be intentional or unintentional, impose severe degradation in the performance of these systems to render them practically unusable. Communications in a tactical military environment and channels with severe multipath fading and interference are examples of such situations. Spread-spectrum systems, which are classical wideband systems, exhibit better immunity in such circumstances and provide survivable communications while conventional communication techniques degrade significantly or fail to operate completely.

Spread-spectrum systems typically employ an rf bandwidth, which is much in excess of the information bandwidth, achieved by means of modulating the data with a spreading function (which is usually a high-rate pseudorandom code sequence). The common methods of achieving this are by using a direct-sequence (DS) spreading or by frequency-hopping (FH), however, other forms of spreading are also employed depending upon the application. The information from these spread signals is usually recovered by a despreading process using a correlation receiver using either active correlation or matched filtering. This despreading is achieved by using a code sequence which is a replica to the one used in the transmitter and synchronized with the received signal. In general, spread-spectrum modulation can be considered as a two stage modulation in which the information signals are modulated by a spreading function as well as an rf carrier employing common modulation techniques (either PSK or FSK or analog modulation) and this can be compared with a conventional wideband system such as FM or PCM in which data modulation directly spreads the spectrum of the signal. The generic spread-spectrum system is shown in figure 1.1.

Spread-spectrum signals exhibit certain unique characteristics compared with conventional communication signals generated by the common modulation techniques. Usually, the cost

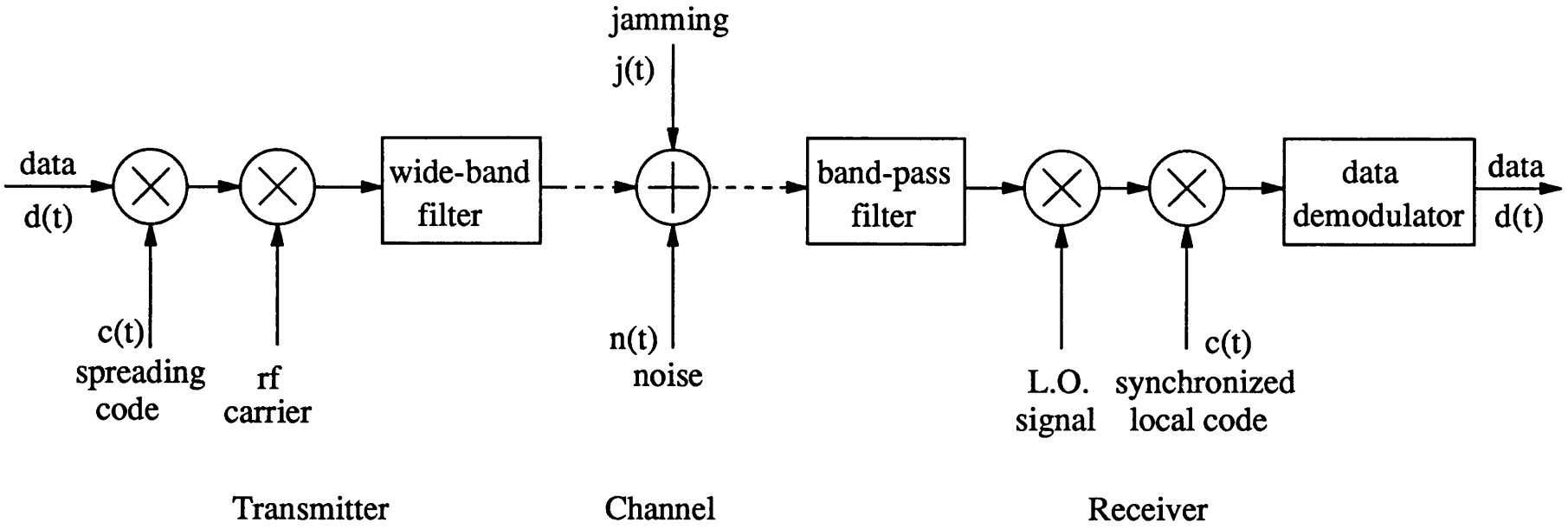

Figure 1.1 Schematic diagram of a generic DS spread-spectrum system.

of using spectrum spreading can be traded against the benefits associated with energy spreading. However, in certain circumstances, when communications are intermittent in an interference-limited environment, spread-spectrum systems can even be spectrally efficient as the multiple accessing interference contributed by the low duty users can be reduced by inherent user inactivity (as for the case of micro cellular mobile radio schemes and certain data communication networks) [1,2]. Thus, spread-spectrum signals find various applications namely:

a. low power density signalling (satellite communication down-links)

b. low probability of interception, LPI (covert communications)

c. anti-jam applications

d. interference rejection

e. multipath protection (fading and mobile channels)

f. multiple accessing (code division multiple access, CDMA and frequency-hop multiple access, FHMA)

g. secure communications (military and civilian)

h. improved spectral efficiency (for special cases) and

i. ranging (satellite navigation and chirp radar)

This wide range of applications is made possible by a number of characteristics of spread-spectrum signals which are achieved from the unique nature of the spreading and despreading processes. For example, as the information signal is spread out over a much wider rf bandwidth, the power spectral density of the spread-spectrum signal is reduced and it is then quite difficult to identify spread-spectrum signals in normal levels of background white noise, and this provides protection against interception. When the received spread-spectrum signals undergo despreading at the receiver, the channel noise in the information bandwidth is spread over the spread bandwidth while the desired signal is despread into the data bandwidth. Thus, the actual channel noise which gets in to the demodulator is reduced significantly relative to the desired signal power after the despreader. This provides the spread-spectrum process with a *processing gain* which can be manipulated to achieve either the anti-jamming and interference rejection capabilities or the multiple access capability which can be achieved by using a set of orthogonal spread-spectrum codes. These capabilities directly depend on the spreading ratio or the processing gain. However, spread-

spectrum processing does not combat the effects of white noise (as in case of FM or PCM) in the channel as the bandwidth expansion is achieved by a function which is independent of the information signal, rather than being uniquely related to the information signal. Therefore, the requirement on the information signal-to-noise ratio (SNR) for demodulation of a spread-spectrum signal is unaltered. As a multiple accessing system, spread-spectrum techniques can also provide *graceful* degradation as the number of users of the system increases by trading bit error rate for number of users. This may be compared with TDMA or FDMA systems in which the maximum number of users is generally fixed by the available total number of time slots or frequency slots (assuming no demand-assignment). When used as a ranging signal, the spread-spectrum signal is capable of resolving the time delay ambiguity more accurately, thus improving the precision in ranging.

Thus, the major characteristics of spread-spectrum signals achieved by spectral spreading and despreading can be summarized as: reduced power flux density, low detectability, anti-jam capability, anti-interference capability, anti-eavesdrop and anti-spoof capability, multiple-accessing capability and precision ranging.

Even though spread-spectrum techniques have been used in the military scenario for communication and radar applications for a long time, with the well known earliest developments taking place in the 1950's, these have begun to find wide-spread use in civilian applications over the last decade. In satellite communications, with increasing demand for a reduced power flux density, spectral spreading is found to be attractive, particularly on the down links [3]. With the emerging global navigation systems such as GPS, RDSS etc., spread-spectrum techniques provide precise ranging and position location to an accuracy of the order of 10 metres for a number of civilian land mobile and avionic applications [4,5]. Satellite based data communication networks employing CDMA for improved spectral efficiency have already been in commercial use [10]. Spread-spectrum multiple accessing has been proposed and studied for cellular land mobile radio and various forms of transmission techniques namely, FH-DPSK, FH-MFSK etc., are in the experimental or in the trial stage [6-8]. Spread-spectrum mobile radio has also been used for countering fading dispersive channels like hf radio etc., [9]. Recently, spread-spectrum techniques have been widely considered for various satellite based data networks [10], local area networks [11], indoor wireless communications (portable radio telephones) [12,13], mobile satellite communications [14] and wide-band packet radios for multipath environments [15]. In

addition, some spread-spectrum multiple access systems have also been reported to have been implemented using integrated-circuit (IC) realizations for various commercial applications [16].

1.1 Types of spectrum spreading

Depending upon the type of data spreading used, spread-spectrum signals can be classified into four major types.

a) Direct-sequence (DS)

b) Frequency-hopping (FH)

c) Time-hopping (TH)

d) Chirp

Figure 1.2 shows the schematic diagram of a DS spread-spectrum system. In digital direct-sequence (DS) spread-spectrum systems, a high-rate pseudorandom code is modulo-2 added either synchronously or asynchronously with the information-bearing digital signals. In the case of analog information rather than digitized information this is directly multiplied with the pseudorandom code to generate the spread signal rather than modulo-2 added. This operation performs spectrum spreading but to avoid excess utilization of the bandwidth, the transmit signals are normally filtered over the null-to-null rf bandwidth of the spread-spectrum signal, as approximately 90% of the total energy is contained within this bandwidth (assuming rectangular pulses with no pulse shaping). The power spectral density of a typical DS spread-spectrum signal is shown in figure 1.3. At the receiver, the incoming signal is despread by correlating with a local replica code which is synchronized to the one at the transmitter and the information signal is recovered from the despread signal using the appropriate data demodulator. The processing gain of the DS spread-spectrum system is normally expressed as the ratio of the pseudorandom code rate to the data rate (or sometimes the ratio of spread bandwidth to the information bandwidth).

In frequency-hopped (FH) spread-spectrum systems, the carrier frequency is *hopped* between the frequencies which are selected pseudorandomly from a set of contiguous or non-contiguous frequencies. In the frequency-hopping system, as shown schematically in figure 1.4, the carrier is generated by an agile frequency synthesizer whose frequency is digitally controlled by a data word representing one of the hop frequencies. These numbers are generated pseudorandomly and are the *n-tuple* data words from a conventional PN code

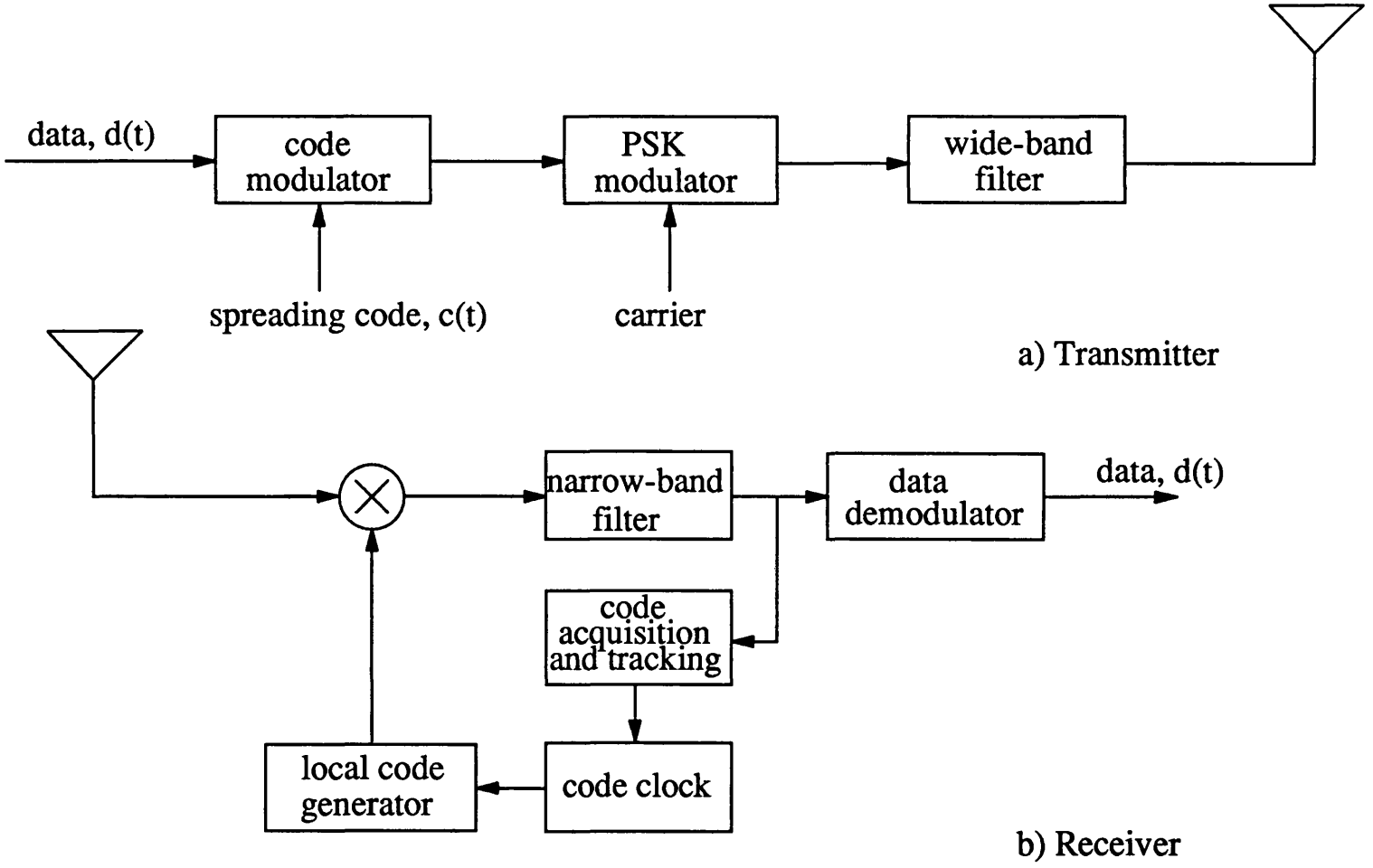

Figure 1.2 Simplified schematic diagram of a direct-sequence spread-spectrum system.

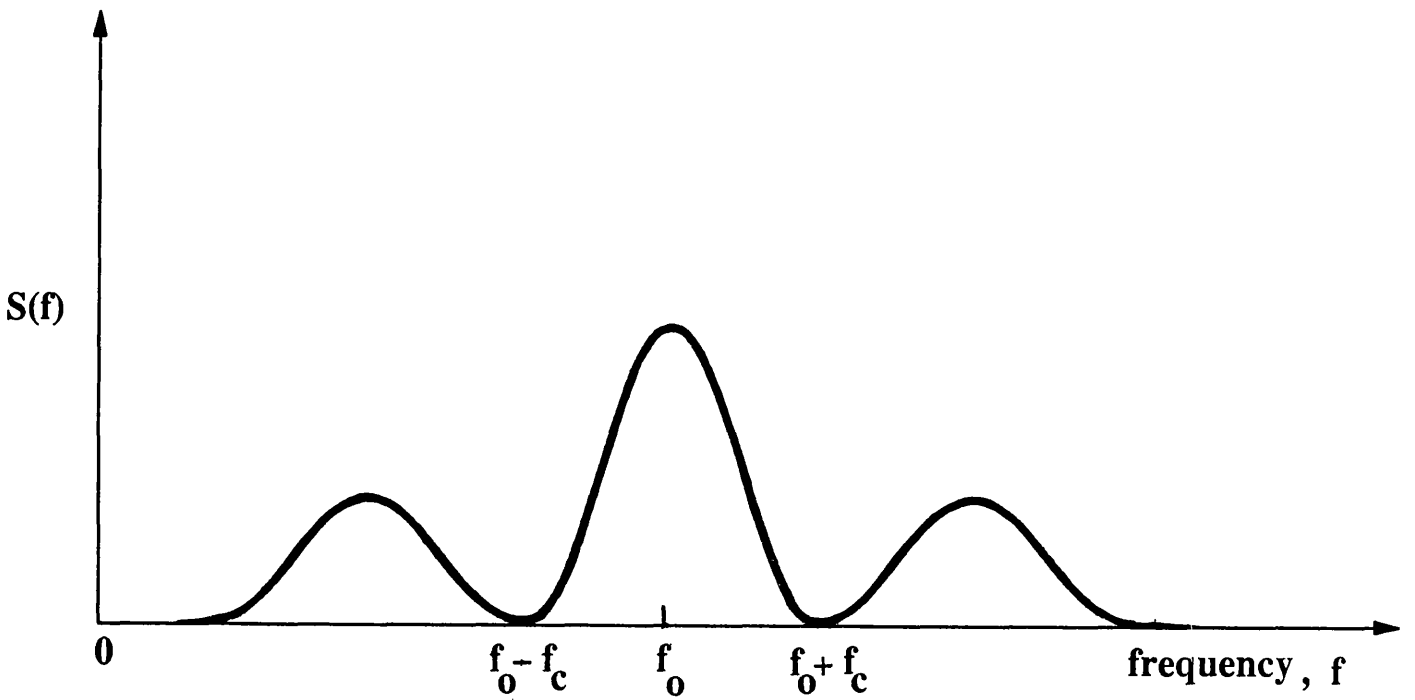

Figure 1.3 Power spectral density of a spread-spectrum signal.

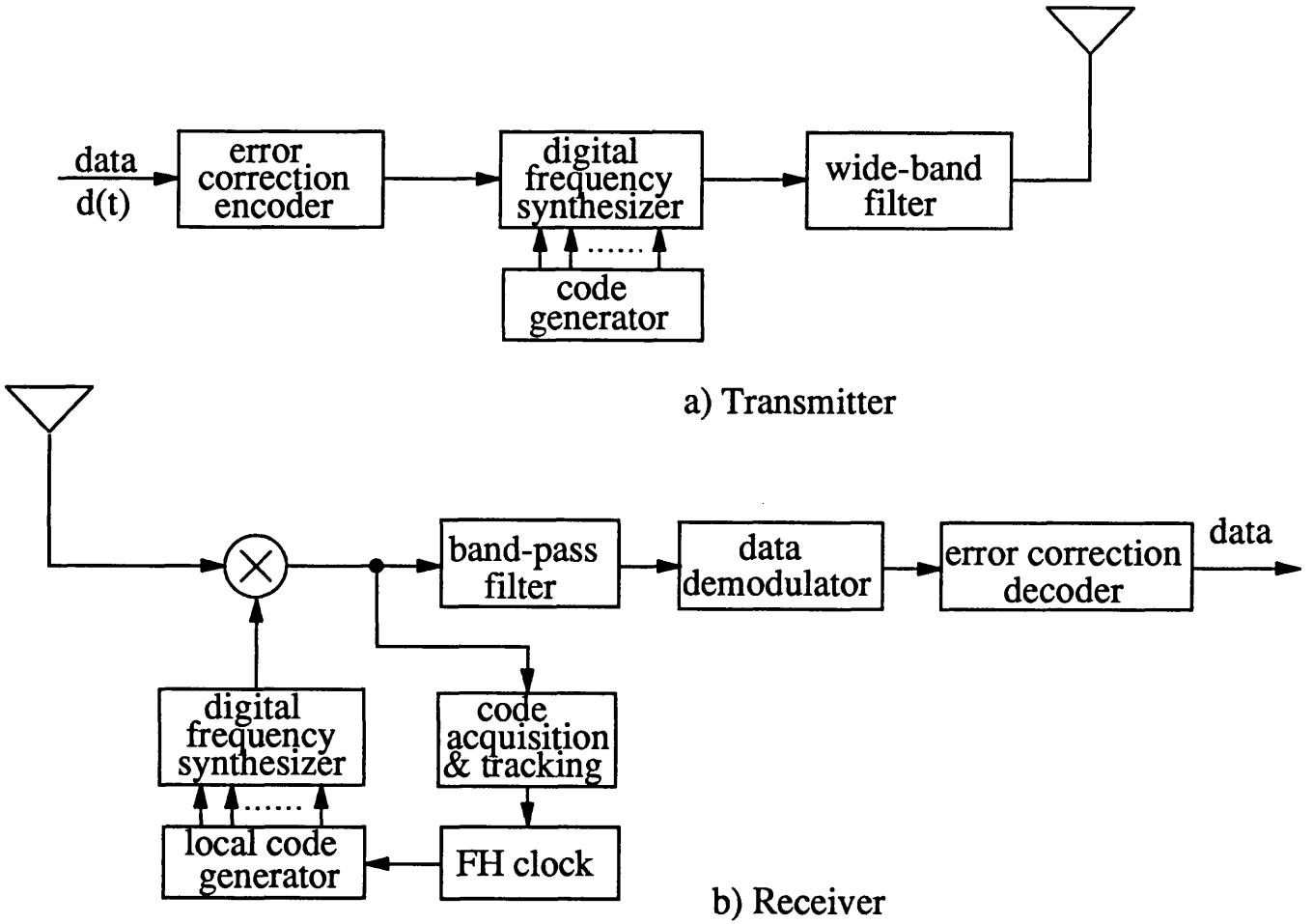

Figure 1.4 Schematic diagram of frequency-hopping spread-spectrum system.

feedback shift register generator and the data bit to be transmitted. The data bit is normally impressed on the carrier using FSK modulation by adding it as one of the bits in the *n-tuple*, generally as the least significant bit to produce smallest frequency change (with the *n-1* bits coming from the code generator). In the receiver, a local frequency synthesizer synchronized to the transmitter synthesizer ensures that the incoming signal is translated to a single IF frequency.

The processing gain of an FH system is determined by the number of frequencies over which the carrier hops while the hop rate depends upon the agility of the synthesizer, the number of hop frequencies and the final data bit error rate. Depending upon the hop rate, the frequency-hopping can be considered as *slow hopping*, *medium hopping* or *fast hopping*. The slow frequency-hopping system uses a single hop per several data bits while fast frequency-hopping system employs several hops (multiple hops) per data bit. The medium hopping system, however, uses the intermediate situation where hop rate is almost same as date rate. Fast frequency-hopping takes advantage of the frequency diversity gain and this provides a better error rate and improves immunity to partial band jamming.

The output spectral width of the frequency-hop modulator is dependent on the frequency spacing and the number of tones. Usually, tones are spaced far enough apart so that the transmitted signals are orthogonal. The specific frequency spacing and the bandwidth of the dehopped signal are decided by the hop rate (chip rate) or the data rate, depending upon the application (slow, medium or fast hopping) while the highest hop rate is usually limited by the switching speed of the synthesizer. In slow hopping the minimum frequency spacing is decided by the data bandwidth while in fast hopping it is decided by the chip rate. However, in FH systems, it is often possible to use overlapping channels with significant overlap of the transmit spacing (for example, the centre of one channel might fall at a null of the adjacent channel) when the rf bandwidth is restricted while keeping the chip rate high. In frequency-hopping, any interference on one hop may destroy all of the data bits in that hop causing very high bit error rate (BER), thus, the use of error correction coding is essential to recover the lost data bits to avoid excessive increase in the BER. This interference may be easily caused by the self generated inter-symbol interference within the receiver itself due to the settling time of the synthesizer or due to multipath interference or by any deliberate jamming and interference signals.

A third method of spectrum spreading is time-hopping (TH) in which a burst of information

carrier is transmitted for a short time duration, with the time slot selected pseudorandomly under the control of a high rate PN code, from a slotted time frame. It is similar to a simple pulse modulation system with the transmitter being turned on and off using the code sequence. The fourth type of spectrum spreading which is not common in communication systems but is often used in radar applications is the chirp waveform which spreads the bandwidth by sweeping the carrier frequency. Chirp signals are characterized by pulsed rf signals with the frequency during the pulse period, varied according to some known way. Normally, this form of modulation uses either linear frequency modulation or nonlinear frequency modulation to generate either up-chirp or down-chirp waveforms. Despreading is done by compressing the chirp signals using matched filters, employing dispersive delay lines (frequency dispersive filters). The processing gain of chirp signals is determined by their time-bandwidth product. Thus, these signals realize spread-spectrum modulation without necessarily employing coding and are advantageous in radar applications as significant power saving is possible. In addition to these direct form of spread-spectrum techniques various hybrid forms viz., DS/FH, DS/TH, FH/TH, DS/FH/TH etc., can also be used depending upon the application.

1.2 Merits and demerits of spread-spectrum signal types

There are certain specific merits and demerits in using different types of spread-spectrum modulation. Direct-sequence spread-spectrum signals offer best noise and anti-jam performance (for a wideband jammer), best discrimination against multipath and are the most difficult to detect. However, in a multiple-access environment, where several users communicate with a common base station simultaneously, they suffer from a near-far problem. This is due to the nearer, and hence stronger signals swamping out the weaker signals by using up the available processing gain. Direct-sequence systems require a wideband channel with relatively less phase distortion. They also require fast code generators and limits on the available bandwidth limit the processing gain to only 20dB - 30dB. In addition, synchronization of transmitter and receiver code generators is a vital process for signal reception and this can be a lengthy process in direct-sequence systems.

Frequency-hopping systems provide the greatest amount of theoretical spreading or processing gain as it is dependent mainly on the number of frequencies available from the synthesizer. It does not always need a contiguous spectrum. It is less affected by the near-far problem as the FH system is an avoidance type system rather than an averaging type of

system as in case of the DS. It is also relatively fast to achieve initial code acquisition due to its considerably lower chip rate since coarse acquisition is normally achieved by methods like *camp and wait* techniques which can dismiss the incorrect cells quickly unlike methods that use a long dwell-time for the dismissal of each incorrect cell (like serial-search with active correlator which will be discussed in chapter 2). However, it needs a complex frequency synthesizer and requires error correction to improve the bit error rate. As the FH receiver normally uses non-coherent message demodulation, it is 3dB poorer against thermal noise compared to a coherent DS receiver. It is also not useful for ranging applications.

Time-hopping has high bandwidth efficiency, simpler implementation than FH and no near-far problem if coordinated (as it is also an avoidance type system). However, it is preferable when the transmitter is average power limited rather than peak power limited since the transmission is in bursts which causes the peak power to be usually high. It also needs error correction due to its potential mutual burst interference. The initial acquisition time is similar to that of DS type for a given bandwidth, which is usually long. The hybrid forms of spread-spectrum signals can combine the averaging and the avoidance nature of each spread-spectrum technique to take the best advantage of the particular methods while avoiding the disadvantages associated with each technique.

1.3 Codes for spread-spectrum signals

The spread-spectrum signals are normally generated using pseudorandom codes which are usually at high-rate for DS signals, however, the code rate for FH signals is usually much lower as it depends on the hop rate. For all types of spread-spectrum signal, successful despreading at the receiver requires these codes to have an impulse like periodic correlation function (two level) to give a maximum auto-correlation when the code delay is zero (inphase) and a minimum auto-correlation when the code delay is more than one chip (out of phase). The code set to which these codes belong should also possess minimum cross-correlation to provide minimum mutual interference. Normally, these codes are selected from a set of maximal length PN sequences (*m-sequences*) or Gold codes. Maximal length PN codes provide a triangular correlation function, with a minimum and uniform cross-correlation. Gold codes also provide a triangular correlation function, but they also exhibit minor side lobes with a varying degree of correlation for different code delays. However, these codes provide a larger code set than maximal length PN sequences for a given code length, and hence find wide-spread use in multiple accessing applications. Other families of

codes having good correlation properties such as Quadrature Residue (QR) sequences, Hall sequences, Kasami sequences and Kronecker sequences (rapid synchronization capability) also find application in spread-spectrum systems, the precise application being dependent upon the exact properties of the code set being used.

1.4 Reception of spread-spectrum signals

The fundamental requirement of the spread-spectrum receiver is the correct recovery of the information bearing signals from the noise corrupted low power density spread-spectrum signal. The main task of a spread-spectrum receiver is to despread the information from the high-rate, low power density received spread-spectrum signal to a high power density, low bit rate information signal. For direct-sequence spread-spectrum systems this is normally achieved by using a correlation receiver which may use either active or passive correlation. The active correlator employs the multiplication of the received signal with a local code replica followed by integrate and dump filtering whereas the passive correlator uses either matched filtering or convolution (using CCD or SAW convolvers). For successful data recovery, the despreader output needs to be maximized to provide the best demodulator performance. The energy in the despread signal is maximized when the received PN code is phase synchronized with a local replica PN code (in case of active correlation) since this results in the maximum correlation between the two codes. Thus, one of the primary functions of the receiver is to achieve accurate synchronization of the transmitter and local codes as rapidly as possible to minimize the down time of the communication link. Once the correct synchronization of the PN code is achieved, then the despreader performs the correlation of the incoming signal with the synchronized local code and recovers the information signal. Code phase acquisition is normally carried out before the carrier phase synchronization (using non-coherent detection) and hence, it is done at very high noise levels typically at input SNRs less than -30dB, depending on the processing gain.

The process of acquiring code phase synchronization imposes severe constraints particularly at very low SNRs due to excessive false alarms and poor detectability. Spread-spectrum code synchronization is normally carried out in two stages. In many spread-spectrum systems, the receivers use either active or passive correlators to carry out the synchronization process and employ search logic to acquire the coarse initial alignment of the locally generated replica of the PN code with the incoming PN signal. This coarse code alignment is called *initial acquisition*, in which synchronization is normally acquired to within an accuracy of about

half a code chip. The remaining code phase error is then corrected in a closed loop tracking system to achieve minimum possible phase error. This process of fine synchronization is normally called *code tracking*. Tracking loops such as the delay-lock loop and tau-dither loop etc., are popularly used for this purpose.

The other problem of spread-spectrum reception is in its efficient data recovery after the despreading process for which various modulation techniques (BPSK, QPSK, MSK etc.,) in conjunction with a variety of error correction coding techniques (block or convolutional) can be employed. The analyses of such techniques and their performance have been presented by many researchers. The anti-jamming and interference rejection capabilities in the presence of various types of jammers or interferers for such spread-spectrum receivers have also been of research interest recently.

1.5 Initial PN code acquisition

Code synchronization is the most critical aspect of the receiver functions and within this, initial code acquisition is the most sensitive component as it takes the longest time to achieve. Consequently, it has attracted intensified research interest in modelling, analysis and optimization. Initial code acquisition can be achieved using one of a number of methods all of which make use of the triangular auto-correlation function of the PN sequences to indicate whether coarse lock has been achieved or not. The randomness of the acquisition process arises mainly because of the initial uncertainty about the code phase offset. However, the correlator output, on which the lock decision is made, is also affected by various other factors such as the front-end receiver additive white Gaussian noise (AWGN), unknown carrier phase (non-coherent receivers), possibly the carrier frequency offset (Doppler), the possible presence of random data during acquisition, channel distortion (eg., fading channels) and additive interference and jamming. A less evident cause of randomness in direct-sequence spread-spectrum systems stems from the partial correlation between the incoming code and the local code which causes spurious correlation signals.

The key components of the acquisition system are the search strategy and the detector structure. The detectors employ either coherent or non-coherent detection and may use either an active correlator with a fixed or variable dwell-time (integration time) or a passive matched filter. They also use a specific statistical testing philosophy namely, Bayes or Neyman-Pearson or others. The search strategies commonly employed are the serial search or maximum-likelihood (parallel) or sequential estimation. In all these cases the overall

acquisition performance depends on the optimum search strategy and the optimum detector performance. Often, it is the trade off between the acquisition performance and hardware complexity that governs the choice of a search strategy. The choice of the detector is dependent on the type of the receiver's decision criterion and also on the choice of the search strategy itself.

A significant amount of research work concerning the optimization of search strategies can be found in the literature. As the main interest has always been to improve the speed and/or lock probability (or overall acquisition probability) of the search in low SNR environments, the serial search strategy has been adopted in many cases rather than either sequential estimation which fails at low SNRs or the maximum *a posteriori* probability (MAP) technique (described in chapter 3) which is considered to be prohibitively complex to implement. Among the serial search strategies, the single and multiple dwell and the expanding window variable dwell types have received considerable attention and many generalized analyses and unified approaches to the analysis of these strategies, have been presented. However, detector optimization has not received equal attention and needs to be explored further. The use of non-coherent detectors with various dwell time integrators, such as single, multiple and variable dwell times, employing either active or passive correlators have been analyzed by a number of researchers. However, the serial search disregards any information gathered during the search which could also be used to alter the direction of the search to further reduce the acquisition time. For this reason, the serial search is theoretically suboptimum compared to maximum *a posteriori* technique and hence further gains in performance are still possible by employing optimum detectors and optimum searches with the serial search. Although the variable dwell time expanding window search can reduce this gap to some extent, the sequential detector, which also uses a variable dwell time, offers good improvement and a better promise both in terms of performance and simplicity.

The sequential detector on the other hand is *conceptually known to be optimum* in the sense of minimum mean dismissal time for a given probability of detection and false alarm compared with any other detectors, including sequential or non-sequential types (without considering the detectors that use any form of adaptation). This type of detector has been used generally in radar detection for sequential range processing but its use in communication systems is very limited indeed. The theoretical analysis for the performance of the sequential detector has been found to be quite difficult because of the multiple integral

equations, the solutions for which are very difficult, if not impossible. Further, the solutions have a complex relationship with the threshold levels, bias and input SNR and for many cases they are unwieldy. The various approximate theoretical analyses for the sequential detector available in the literature fail to satisfy the moderate to high SNR situations and hence, in this thesis the Monte-Carlo computer simulation has been used to investigate the optimum performance of the sequential detectors for spread-spectrum acquisition under these conditions and also in low SNR conditions. The various practical difficulties affecting the acquisition performance namely, presence of data modulation, Doppler shift and jamming or interference have also been simulated in this work and the performance of a number of variants of sequential detector is analyzed.

1.6 Goals of the present research

The main objectives of the research reported in this thesis are:

i) to investigate the optimum acquisition characteristics of the sequential detector for direct-sequence spread-spectrum code acquisition using a Monte-Carlo computer simulation

ii) the simulation and analysis of a quantized log-likelihood sequential detector (QLD) to obtain the minimum number of quantization levels and to assess its performance under these conditions

iii) the simulation and analysis of a biased square law sequential detector (BSD)

iv) the comparative analysis of the QLD and BSD with the ideal log-likelihood sequential detector (LLD) in the absence and the presence of data modulation.

v) the analysis of the QLD, BSD and LLD in the presence of code rate Doppler offset and residual carrier Doppler offset, and data modulation.

vi) the analysis of the degradation of acquisition performance for the QLD, BSD and LLD due to CW interference and pulse jamming.

vii) a comparative evaluation of the LLD with the single-dwell detector and the digital matched filter.

1.7 Organization of the thesis

The thesis is organized into eight chapters. The first chapter has introduced the different types of spread-spectrum signals with their advantages and disadvantages. The problems

associated with the reception of spread-spectrum signals have been addressed and the critical aspects of code synchronization and its significance in the reception has been discussed. The critical problem of this research interest, namely *the faster initial code acquisition in low SNRs for direct-sequence spread-spectrum signals using optimum sequential detectors* has also been introduced and the aims of this research have been outlined. An introduction to the organization of the rest of the thesis is also presented in this chapter.

In the second chapter, the classification of the PN code acquisition schemes based on two different criteria will be introduced. Based on these classifications, various types of code acquisition techniques commonly in use are reviewed and their analytical performances compared. The generalized analysis methods employed in the analysis of these techniques namely, the unified theory using flow graph techniques, the equivalent circular state diagram approach and the direct method using algebraic combinatorial approaches are discussed and the important results on the application of these methods to each of the acquisition techniques is presented. The analytical difficulties involved in using these methods with the sequential detector will also be highlighted.

In the third chapter, the statistical decision theory applied to hypothesis testing of the general signal detection problem, with particular emphasis on the sequential detection problem, is introduced. The decision criteria and the optimum decision rules for an optimum detector are described and the merits and demerits of these decision rules (eg., Bayes, Neyman-Pearson, minimax, MAP etc.,) highlighted. Sub-optimum detection (nonparametric detection) is also introduced briefly with the performance measures and the significance of the receiver operating characteristics (ROC) outlined. The fundamental differences between a fixed sample size and a variable length test are described together with the sequential probability ratio test (SPRT). The major performance criteria of a sequential test viz., the operating characteristic function (OCF) and the average sample number (ASN) function are introduced. The applications of sequential detection theory to the code acquisition of spread-spectrum signals is described and the existing research work in this area is reviewed. In addition, the complexities in the analysis of sequential detection are highlighted and the biased square law detector with its low SNR approximations is described.

In chapters 4-7, the computer simulation models employed are presented together with the various observations and analyses of the performance of these code synchronization systems. In particular, the fourth chapter presents all the computer models and the signal models used

to simulate the three variants of the sequential detector for the acquisition of direct-sequence spread-spectrum signals in the presence and the absence of data modulation, and the code rate and residual carrier Doppler frequency offsets together with their mathematical representation are presented . The software techniques used to realize the various functional blocks in the system model for both transmit and receive sides are described along with the channel models employed for simulating the various channel impairments namely, Gaussian noise, jamming and interference. In addition, the computer models for a more conventional single-dwell detector and a digital matched filter detector are presented. Finally, the Monte-Carlo computer simulation procedure developed to assess the statistical performance of all the detectors is explained.

In the fifth chapter, first, the performance of three variants of the sequential detector in the absence of data modulation is presented. The effect of the number of quantization levels of the uniform quantizer, Q, on the acquisition performance of the quantized log-likelihood sequential detector, is shown and compared with the performance of an ideal log-likelihood sequential detector, leading to the choice of minimum acceptable number of quantization levels. Using an approximate model to the ideal log-likelihood function, the biased square law sequential detector, is also analyzed and the performance of three variants of the sequential detector are compared. In the second part of this chapter, the optimization of the three detectors with respect to various critical system parameters is presented from which the optimum system parameters or the range of near-optimum values are derived. Two stages of optimization with respect to: i) the upper and the lower thresholds, and ii) the input SNR and the design SNR is shown together with the three dimensional optimization characteristics for each pair of the system parameters.

In the sixth chapter, first, the effect of data modulation on the acquisition performance of the QLD and BSD are compared with that of the LLD. The data modulation degradation for each variant of the sequential detector with identical system parameters is assessed and new results on the acquisition performance of the sequential detector in the presence of random data modulation is presented. In the second part, the analysis is extended to include the presence of residual carrier and code rate Doppler frequency offsets and the acquisition performance for all three variants of sequential detector is then compared. This analysis examines, for the first time, the effect of both carrier and code Doppler on the mean acquisition time of a sequential detector. The degradation in the acquisition performance due

to the presence of data modulation and Doppler shift is also analyzed with each detector operating at its optimum design SNR in predetection SNR range -4dB to 10dB.

The seventh chapter is also organized into two parts. The first part presents the acquisition performance of the sequential detector in the presence of CW interference and pulsed jamming. Results on the degradation of acquisition performance due to CW interference and pulse jamming with various duty factors are presented for a range of jammer-to-signal power ratio (J/S) and input SNR due to Gaussian noise. In the second part, the Monte-Carlo simulation is extended to two other common forms of serial-search PN code acquisition namely, the single-dwell detector and the digital matched filter and the acquisition performance is compared with that of the sequential detector. The critical dependence of the mean acquisition time on the threshold and dwell-time for both the digital matched filter and the single-dwell detector is also analyzed and the optimization of these parameters, carried out to obtain minimum mean acquisition time, is presented. The theoretical performance of a single-dwell serial-search acquisition, evaluated numerically using a two-dimensional optimization of the mean acquisition time, with the threshold, dwell-time and input SNR is also presented and compared with its simulated acquisition performance, and shown to be in a close agreement.

The eighth chapter presents the synopsis of the simulation results and a discussion from which final conclusions are reached. The significant achievements of this research are highlighted and the scope for further work outlined.

1.8 References

1) J.P. Costas, "Poisson, Shannon and the Radio Amateur", Proc IRE, vol. 47, pp 2058-2068, Dec 1959.

2) B.R. Vojcic, R.L. Pickholtz and I.S. Stojanovic, "A comparison of TDMA and CDMA in microcellular radio channels", ICC'91, vol. 2. pp 866-870, June 1991.

3) W.K.Alem, "Spread-spectrum acquisition and tracking performance for shuttle communication links", IEEE Trans. on comm., vol-com-26, no. 11, pp 832-840, November 1978.

4) E.D. Holm and E.E. Westerfield, "A GPS fast acquisition receiver", NTC'83, pp 214- 218, November 14-16, 1983.

5) R.D. Briskman, "Radio determination satellite service", Proceedings of the IEEE, vol. 78, no. 7, pp 1096-1106, July 1990.

6) P.M.C. Lal, V.S. Palsule, K.V. Ravi, "Applications of frequency-hopped spread-spectrum techniques: An overview", IETE Technical Review, vol. 3, no. 5, pp 210-220, 1986.

7) G.R. Cooper and R.W. Nettleton, "A spread-spectrum technique for high capacity mobile communications", IEEE Trans. on comm., vol-VT-27, pp 264-275, November 1978.

8) D.J. Goodman *et al* , "Frequency-hopped multilevel FSK for mobile radio", BSTJ, vol. 59, pp 1257-1275, September 1980.

9) P.J Munday *et al* , "Jaguar-V frequency-hopping radio system", IEE Proc, Pt F, p 213, June 1982.

10) N.Abramson, "VSAT data networks", Proceedings of the IEEE, vol. 78, no. 7, pp 1267-1274, July 1990.

11) C.T. Spracklen *et al*, "Spreadnet- A spread-spectrum local area network", Jou. of IERE, vol. 57, no. 1, pp 12-16, January/February 1987.

12) K. Yamada, K. Daikoku and H. Usui, "Performance of portable radio telephone using spread-spectrum", IEEE Trans. on comm., vol.com-32, no. 7, pp 762-768, July 1984.

13) K. Pahlavan and M. M Chase, "Spread-spectrum multiple access performance of orthogonal codes for indoor radio communications", IEEE Trans. on comm., vol.com-38, no. 5, pp 574-577, May 1990.

14) K.S. Gilhousen, "Increased capacity using CDMA for mobile satellite communication", IEEE Sel. Areas in comm., vol. 8, no. 4, pp 503-514, May 1990.

15) J.H. Fischer *et al*, "Wide band packet radio for multipath environments", IEEE Trans. on comm., vol.com-36, no. 5, pp r564-576, May 1988.

16) D.C. Kemdirim, J.S. Wight, "DS SSMA with some IC realizations", IEEE Sel. Areas in comm., vol. 8, no. 4, pp 663-674, May 1990.

CHAPTER 2

CODE ACQUISITION IN DIRECT SEQUENCE SPREAD SPECTRUM RECEIVERS

2.1 INTRODUCTION

Despreading of the pseudo-noise modulated spread-spectrum signal is usually accomplished by means of a local replica of the PN code in the receiver which is synchronized to the one superimposed on the incoming waveform. Correlation of the incoming signal with the synchronized local PN code replica then produces the desired despreading process. The process of synchronizing the local and received PN signals is normally achieved in two stages. Initially, a coarse alignment of the two PN signals is produced to within a small (typically less than a chip) residual relative timing offset. This process is referred to as *PN acquisition*. Once the incoming PN code has been acquired, a fine synchronization system takes over and continuously maintains the best possible waveform alignment by means of a closed loop operation. This process is referred to as *PN tracking*.

The problem of code acquisition has attracted considerable research attention recently and many results have been reported. However, with the increasing need for spread-spectrum receivers to operate in lower SNR environments, and with longer code lengths, the need for more efficient acquisition under severe noise conditions is also growing. Two important parameters that constrain the choice of an acquisition scheme are the mean acquisition time and the hardware complexity. In this chapter, various acquisition schemes suitable for rapid acquisition of direct-sequence PN signals in low SNR environments are reviewed. The acquisition performance of some of the latest proposals pertaining to the rapid acquisition schemes are also considered and analyses of their performance are compared. The optimum acquisition method using a variable integration time for faster acquisition namely, *sequential detection* will also be discussed.

2.2 ACQUISITION TECHNIQUES - A CLASSIFICATION

The common denominator among almost all the PN acquisition techniques is that the received signal is first correlated with the local replica PN signal to produce a measure of correlation between the two signals. These methods make use of the large correlation output when the codes are in synchronization and the low correlation value when the codes are out of synchronization by one chip or more. This correlation measure is then processed by a suitable detector/decision rule and search strategy to decide *whether the two codes are in synchronism* and *what to do if they are not.* Thus, the differences between the various schemes depend on:

i) the type of detector (and decision strategy) which is dependent on the form of the received signal and the particular application,

ii) the nature of the search algorithm which acts on the detector outputs to reach the final verdict.

2.2.1 Based on the type of detector

All known types of detectors for PN acquisition can be classified into either coherent or non-coherent. The *non-coherent detectors* assume no knowledge of the carrier phase and consequently, they generally comprise a bandpass filter centered at the frequency of the received PN signal followed by a square-law envelope detector, an integrate and dump circuit which operates over a finite time interval and a simple threshold device. The *coherent detector* assumes that the receiver is capable of determining good estimates of the carrier phase and frequency, thus the carrier must be demodulated prior to PN despreading. This is usually very difficult because the power in the carrier has been spread to result in a very low power density. The coherent detector typically employs a low pass filter followed by an optimum Bayes detector or, instead, just a simple threshold device.

Depending upon the integration time the detectors can also be classified as either fixed or variable integration time types. The *fixed integration type* can be further subdivided into single-dwell and multiple-dwell types based on whether the detector's decision is made on the basis of a single fixed time observation of the received signal plus noise or many such observations. Depending on the duration of the observation, *single-dwell* detectors can be further differentiated according to whether they use *partial or full period* code correlation. The *multiple-dwell* detectors make decisions based on the threshold comparison test

following a threshold exceedance of the first dwell output, which is then verified using the additional dwells in combination with further threshold tests in accordance with a specified verification algorithm to produce a final decision. The verification algorithm can be of the type in which the code phase position is *immediately rejected* (Di Carlo and Weber) [1] or dismissed as soon as any dwell output fails to satisfy its threshold exceedance test. Other types of verification modes, often referred to as *search/lock strategies* (Hopkin's) [2] (*or non-immediate rejection*) either employ algorithms which require repeated threshold testing of a given dwell output or use a majority logic type of decision based on the outcome of each of the total set of multiple-dwell threshold tests.

For the case of *variable integration time* detectors, the dwell time, being the time for a continuously integrated stochastic process to exceed a threshold, is a random variable. This kind of acquisition scheme, with a variable integration time detector, typically employs the classical method of sequential detection which finds its roots in the detection of radar signals [3] and will be discussed in section 2.3.4.

Based on the rate at which the decisions are made on each code phase under test, detectors can be classified as high decision rate detectors or low decision rate detectors. The matched filter (passive correlator) PN acquisition systems typically fall under the *high decision rate* detectors as these structures make decisions on the out-of-sync code phase offsets between incoming and local codes at the PN chip rate or an integer multiple of it. *Low decision rate* detectors employ active correlation and make these decisions at a rate much slower than chip rate often at the code repetition rate or a multiple of it.

A final classification of detector types is based on the criterion for deciding between in-sync and out-of-sync hypotheses. For example *Bayes* decision criterion minimizes the average risk whereas the *Neyman-Pearson* criterion minimizes the probability of missed detection (error of the second kind) for a given probability of false alarm (error of the first kind). Figure 2.1 presents the summary of the various classifications based on the detector types.

2.2.2 Based on the type of search algorithm

PN acquisition schemes can be classified into three categories based on the search strategy employed:

i) Maximum-likelihood (parallel))

ii) Sequential estimation

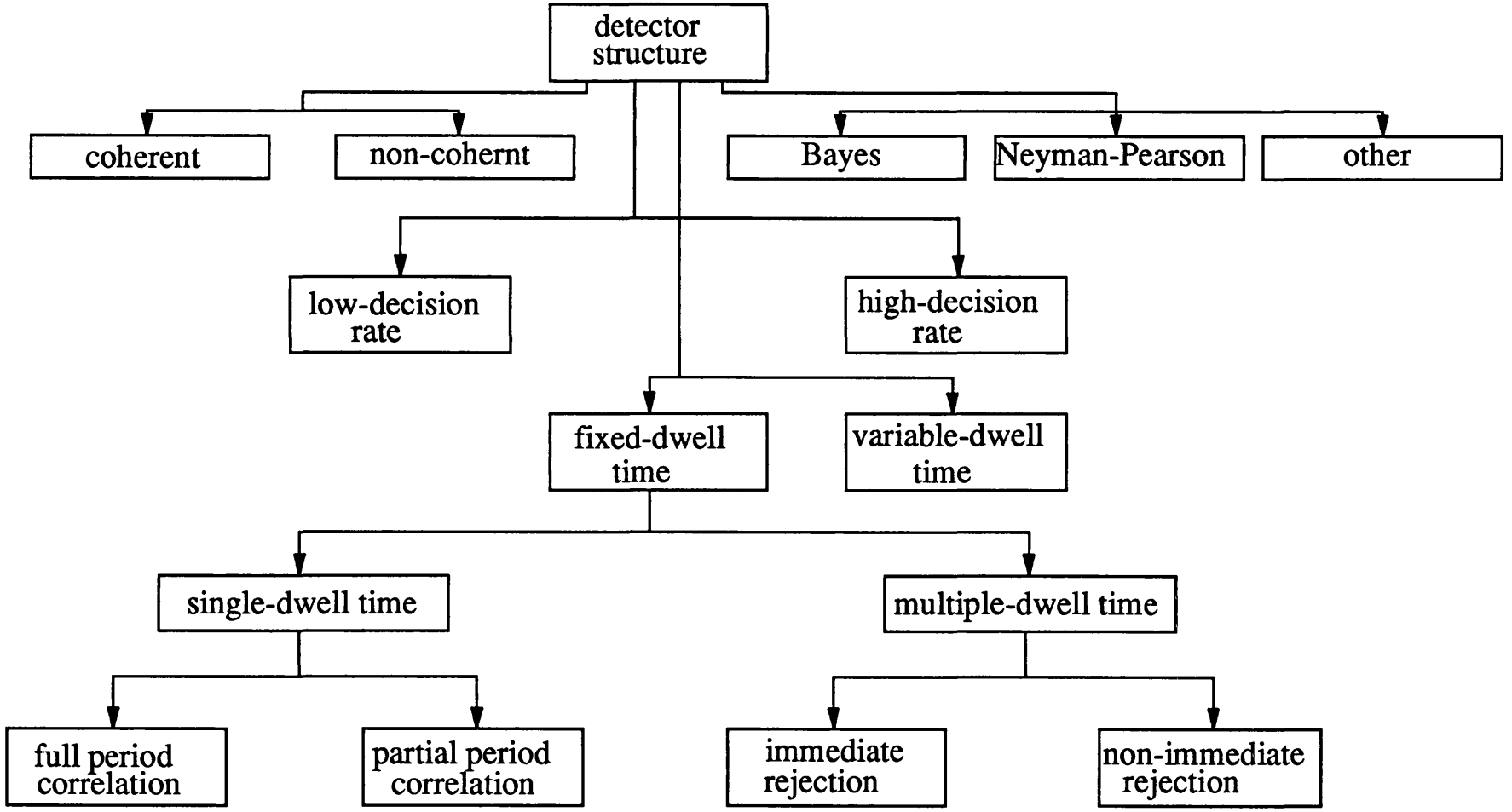

Figure 2.1 Classification of acquisition schemes based on detector type.

iii) Serial search.

This classification of search strategies is summarized in figure 2.2.

2.2.2.1 Maximum-likelihood

These algorithms correlate the received PN signal with all possible code positions (or perhaps fractional code positions) of the local code replica. All the correlations are performed in *parallel* with the corresponding detector outputs pertaining to the observations made on the same received signal. The local code phase position that produces the maximum detector output is chosen as the correct PN code.

The maximum-likelihood algorithm can also be implemented in a *serial* fashion, by correlating the received signal serially with all possible code positions of the local code replica and storing the corresponding detector outputs. At the end of the test the correct code position is chosen as the one with maximum detector output. Thus, in both cases a clear advantage is that a definite decision is made after only a single examination of all code phase positions, or a single search through the entire code period. However, for longer codes, the complexity of parallel implementation or the time required to search the entire code and reach the synchronization decision in the serial version is often prohibitive.

2.2.2.2 Rapid acquisition by sequential estimation (RASE)

This scheme, first introduced by Ward [4] makes the best estimate of the incoming PN signal and loads the first 'n' received PN code chips (n being the number of stages in the code generator) into the receiver code generator and this forms the initial state of the local code generator. The receiver code thus generated is correlated with the incoming signal and the threshold is examined at the end of a predetermined examination interval. The correlation is continued if the test passes, otherwise, a new estimate is made and the test is repeated. An obvious advantage with this scheme is that the acquisition is rapid as long as the 'n' consecutive estimates are correctly made. However, at lower SNRs the probability of correctness with which the initial estimate is made (P_c) is reduced and the probability of estimating the n consecutive bits falls drastically, and hence the technique looses its advantage. In general, rapid acquisition is only possible with moderate SNRs, ie., down to -15dB.

A modified RASE called *Recursion Aided Rapid Acquisition Sequential Estimation,*

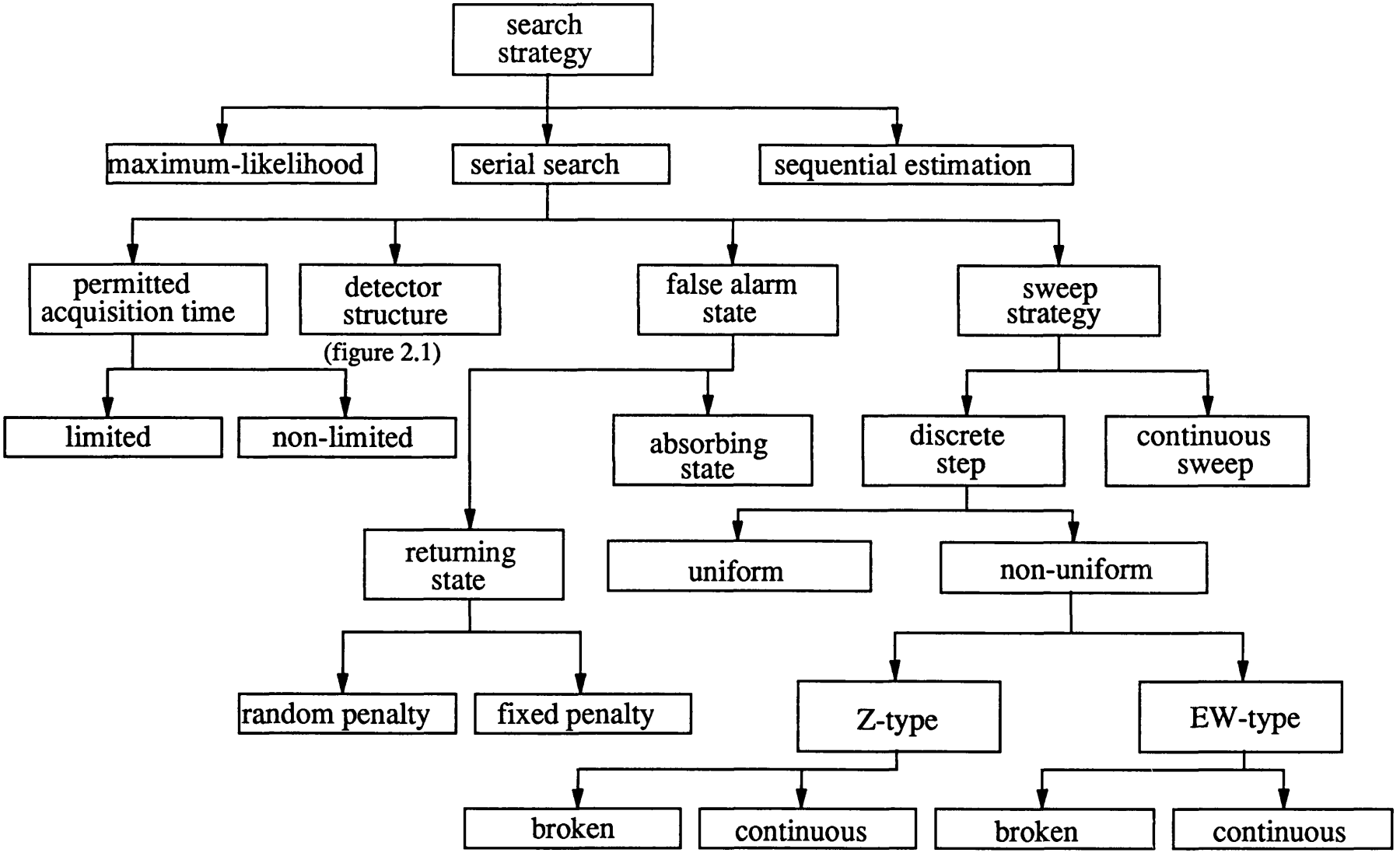

Figure 2.2 Classification of acquisition schemes based on search strategy.

RARASE [5], employs a sync-worthiness-indicator (SWI) formed by the addition of the estimated code chips to determine when the shift register should switch from the reload to the track condition. Compared with RASE, which only has a simple detector, RARASE can achieve an acquisition time reduction by a factor of 7.5 (for n = 15 shift register). Other modifications of RASE using the recursive relation of the PN codes to improve the initial n-chip estimate have also been investigated which use majority logic voting on independent n-chip estimates [6], threshold decoding type of estimator [7] and by replacing the simple threshold decisions with a Bayes detector [8]. Nevertheless RASE, RARASE and their variants can only offer good performance down to moderate SNRs.

2.2.2.3 Serial search

First proposed by Sage [9], a serial search is performed by linearly varying the time difference between the PN modulation on the incoming carrier and the PN waveform generated at the receiver. A continuous decision process is used to determine when synchronization is reached. Such a continuous search system is referred to as *sliding correlator* PN acquisition. Since the test for synchronization is based on a continuous decision process, this method can yield a shorter acquisition time when compared with the serial realization of the maximum-likelihood technique as the search can terminate anywhere within the uncertainty region rather than having to wait until the end of the code period. Often, however, several passes of search through the uncertainty region are required to achieve lock, particularly when the SNR is poor. When compared with the RASE system, the serial acquisition technique can provide shorter acquisition time for input SNRs worse than -15dB. Thus, this type of technique is attractive for low SNR environments.

In recent years, the trend has been to accomplish the variation of time difference between incoming and local PN waveforms by a discrete stepping process wherein the phase of the local PN code is stepped at uniform increments in time, advanced or retarded by a fixed amount (typically a fraction of a chip). This *discrete-step* serial search of the uncertainty region can be accomplished by a uniform search from one end to the other or by a non-uniform search (making use of *a priori* information), typically starting at the minimum code phase uncertainty, and expanding as a function of time to higher uncertainty. Such an *expanding window search* or the simpler *Z-type search* strategies are well suited for applications with very long codes in which it is not feasible to search the entire code, but it does require some *a priori* information regarding the code phase, through some means. One

method of obtaining this is to have very accurate crystal clocks both in the transmitter and the receiver which are initially synchronized and maintain accurate time even when not phase locked. Other situations are when a short preamble code is used or while resynchronizing from the successful acquisition previously held.

A further subclassification of search strategies depends on time elapsed before reaching the acquisition. Systems in which the search is allowed to proceed as long as necessary to achieve acquisition with a given fidelity are classified as having *nonlimited acquisition time.* These are the systems typically employed in applications where information modulation is always present. Search strategies with *limited acquisition time* are usually used in systems where the information modulation only commences when the PN code acquisition has been achieved, viz. push-to-talk systems. In such cases, acquisition must be achieved within a fixed time (usually less than a second or so) to a high overall probability of acquisition.

The detector classification can also be based on the way false alarm states are handled, and thus the serial search strategies can be classified as being of the returning state or absorbing state types. In normal circumstances the occurance of noise causes a false alarm state to be generated and after a given amount of time (false alarm penalty time) which is a random variable, (but is often mathematically modelled as being fixed) the system will return to the acquisition mode and continues searching where it last left off. Such a recoverable false alarm state is referred to as a *returning state.* Occasionally entry into a false alarm state is catastrophic as the system cannot recover from this event. In this instance code acquisition is completely lost and thus this type of false alarm state is referred to as an *absorbing state.*

2.3 PERFORMANCE OF ACQUISITION TECHNIQUES

The primary requirement of the acquisition scheme is to reduce the mean acquisition time for a given level of background noise and interference. Various factors contribute to the poor acquisition performance of the receiver, namely, the presence of data modulation on the PN carrier, Doppler shift, jamming and interference etc. The performance of a particular acquisition scheme is governed by the various parameters relating to the search/lock strategies employed, the detector type and integration time used. In this section, the parameters influencing each of the acquisition schemes described are identified and analytical results for the acquisition performance are discussed. The various methods employed for the analysis of the search techniques are also described.

Performance measures

A common measure of performance is the mean-time to acquisition, defined as the average time elapsed from the initiation of acquisition to the completion of it. However, for the case of burst-mode communication systems, a more appropriate criterion is to consider the probability of successfully acquiring an anticipated spread-spectrum burst within a given time. Thus, the probability of detection and probability of false alarms will be more suitable criteria. The related parameters, such as false alarm penalty time, mean-time to lose-lock etc., also need to be considered wherever appropriate. However, to obtain the complete statistical description of the acquisition process, the probability density function *(pdf)* of the acquisition time is required from which various moments can be obtained. This *pdf* can be analytically obtained from the generating function formed by the transition probabilities of the acquisition process modelled as discrete Markovian process. However, obtaining the generating function and the closed loop solutions for the *pdf* are not easy in all the cases and often approximations are required. In some cases, the solutions are normally limited to the first two moments of the acquisition time.

2.3.1 Serial search acquisition techniques

In a simple serial search acquisition system using a sliding correlator with continuous decision, the mean acquisition time in ideal conditions when the signal is not corrupted is simply:

$$T_{acq} = \frac{L}{2\Delta f_c} \tag{2.1}$$

where L is the length of the PN code in chips and Δf_c is the difference in clock frequency between the local code generator and the incoming PN code. However, the presence of noise causes the decision reliability to deteriorate because it reduces the probability of detection and furthermore causes false alarms to occur due to the noise on the correlation signal samples exceeding the threshold. The mean acquisition time in such circumstances depends on the probability of detection P_d, probability of false alarms P_{fa} (or equivalently the false alarm rate n_{fa}), the false alarm penalty time T_P and the specific search/lock strategy used to counter the false alarms.

Numerous researchers have investigated these problems and derived expressions for the mean acquisition time and its moments with different search/lock strategies and have also

analyzed the statistics of the acquisition time function. All these analyses are reviewed here with respect to each search technique.

2.3.2 Continuous search sliding correlator

In the continuous sweep serial search, the local PN generator runs at a frequency $f_c + \Delta f_c$ which differs from the clock frequency $f_c = 1/T_c$ of the incoming PN code by a small amount $\Delta f_c \ll f_c$. Thus, the epoch difference between both the codes vanishes at instants of time which are $L/\Delta f_c$ apart (L being the PN code length in chips) generating a train of impulses at the correlator output which are triangular pulses of width $2/\Delta f_c$. These pulses are detected by the non-coherent detection circuit and tested against a preset threshold. The first detected impulse declares the hit and sets the local clock to f_c and activates the tracking loop. For the sliding correlator with Δf_c as the slip rate between the two codes, the probability of false alarms and miss detection have been derived as a function of the carrier-to-noise ratio and search rate by Sage [9]. The effects of false alarm and miss detection were accounted for and the expressions for the mean acquisition time were derived by Pandit [10] as:

$$T_{acq} = \frac{L}{\Delta f_c}(1 + n_{fa}\, T_P)\left[\frac{1}{P_d} - 0.5\right] \tag{2.2}$$

where P_d is the probability of detection, n_{fa} is the false alarm rate and T_P is the false alarm penalty time.

The quantities P_d and n_{fa} depend on the SNR at the receiver input and the threshold level set by the acquisition circuit and can be determined using the methods of signal detection theory or measured experimentally. The effects of self-noise and decorrelation on the sliding correlator was found to place an upper limit on *the search rate* and this problem was studied by Ormondroyd and Comley and analytic expressions were fitted to extend the observations for cases with longer code lengths [11].

2.3.3 Discrete search sliding correlator

The sliding correlator with discrete search (or the stepping correlator) has received major attention recently and various schemes with uniform stepping and non-uniform stepping have been considered. For the case of uniform stepping, both single-dwell systems and multiple-dwell systems with immediate rejection verification mode have been analyzed. The non-uniform stepping strategies have also been analyzed using a unified approach based on the use of equivalent circular state diagrams [18] and generalized algebraic characterization

[20].

2.3.3.1 Single-dwell serial search

In this type of system the received signal plus noise is actively correlated with the local replica of the PN code and then passed through a predetection bandpass filter. The filtered output is passed through a standard type non-coherent square-law envelope detector to remove the effects of data modulation. The detector output is next integrated for a fixed time duration τ_d called the *dwell time* in an integrate and dump circuit (post-detection integration) and then compared with a preset threshold. Equivalently, a low pass version of a single-dwell search scheme employs in-phase and quadrature-phase carrier reference signals and the despread and demodulated signals in both the channels are passed through low pass filters, square-law detecting the low pass signals and summing to produce the required signal for post detection integration. Both these detectors are shown in figures 2.3 and 2.4.

Through a Markov chain model of the acquisition process, Holmes and Chen have derived the mean-time to acquisition with and without code rate Doppler [12]. A more complete description of the single-dwell acquisition has been presented by Di Carlo and Weber [13] by deriving an alternate system performance viz., the probability of successful synchronization as a function of all critical design parameters of the acquisition system.

The total time uncertainty to be resolved is $T_{un} = N_u T_c$, where N_u is the number of code chips in the uncertainty region and is normally set equal to the code length, L. Typically, the received and the local PN codes are aligned to within half a chip period ($T_c/2$) and hence the total number of code phase alignments (which are usually referred to as *cells*) would be $q = 2N_u$. The mean acquisition time, T_{acq}, of the single-dwell acquisition scheme, in the absence of code Doppler, due to the method presented by Holmes and Chen assuming that the number of cells to be searched $q \gg 1$ is:

$$T_{acq} = \frac{(2-P_d)(1+KP_{fa})}{2P_d} q\tau_d \tag{2.3}$$

where P_d and P_{fa} are the detector decision probabilities, K is the false alarm penalty factor (false alarm verification time, $T_P = K\tau_d$ sec) and τ_d the dwell time.

The variance of the acquisition time σ^2_{acq} has also been derived as:

$$\sigma^2_{acq} = \tau_d^2 (1 + K P_{fa})^2 q^2 \left[\frac{1}{12} - \frac{1}{P_d} + \frac{1}{P_d^2} \right] \tag{2.4}$$

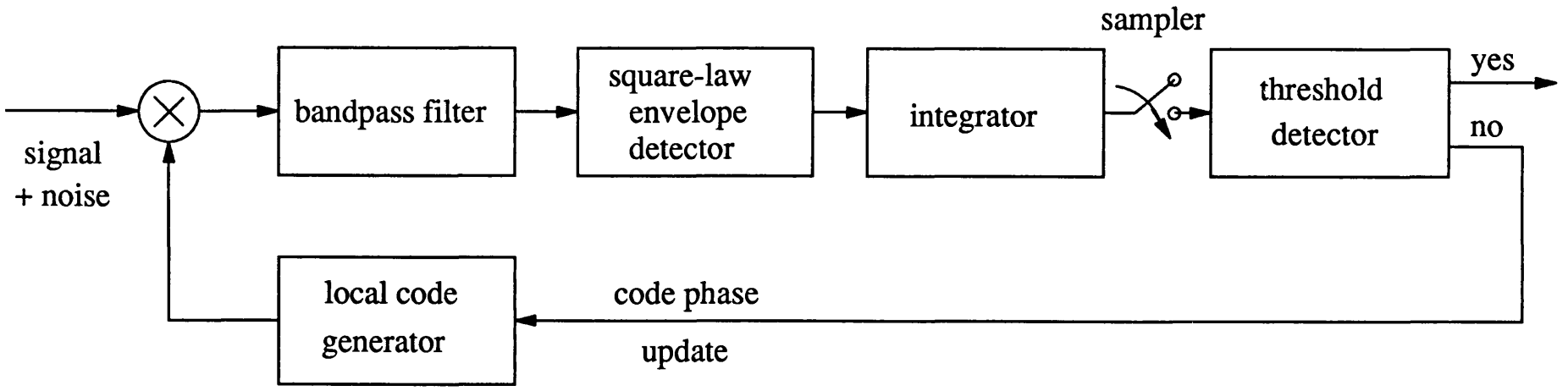

Figure 2.3 Schematic diagram of a non-coherent single-dwell detector : bandpass version

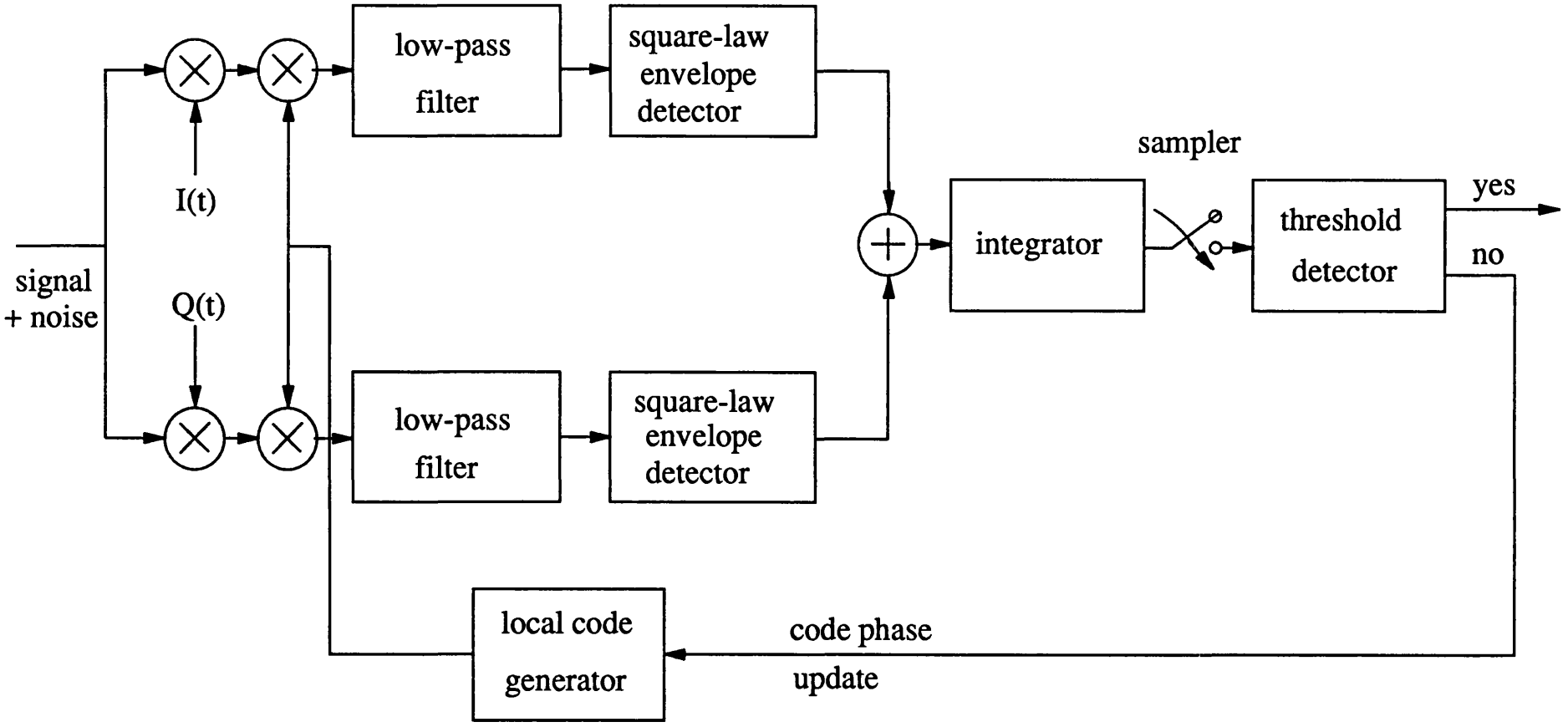

Figure 2.4 Schematic diagram of a single-dwell detector : low-pass version

The effect of Doppler on the acquisition performance is twofold. First, it smears the relative code phase during the acquisition dwell time which has the effect of increasing or reducing the probability of detection depending on the code phase and algebraic sign of the Doppler rate. Secondly, Doppler also affects the effective code sweep rate which in the extreme case can reduce it to zero causing the search time to increase greatly. Though it is very difficult to exactly account for the Doppler, *as far as the effective sweep rates are concerned* the Doppler has been accounted for and the modified expressions for T_{acq} and σ^2_{acq} to a first approximation are given as:

$$T_{acq} = \frac{(2-P_d)(1+KP_{fa})\,N_u\tau_d}{2P_d \mid \frac{\Delta T_c}{T_c} + \tau_d\,\Delta f_c + K\,\tau_d\,\Delta f_c\,P_{fa} \mid} \tag{2.5}$$

$$\sigma^2_{acq} = \frac{(1+K\,P_{fa})^2\,N^2\left[\frac{1}{12} - \frac{1}{P_d} + \frac{1}{P_d^2}\right]}{\left[\frac{\Delta T_c}{T_c} + \tau_d\,\Delta f_c + K\,\tau_d\,\Delta f_c\,P_{fa}\right]^2} \tag{2.6}$$

where

$\Delta T_c/T_c$= step size of search in fractions of a chip (typically ½)

Δf_c = code Doppler in chips which can be either positive or negative

$\Delta f_c \tau_d$ = PN code phase timing shift due to code doppler during dwell time

$\Delta f_c K \tau_d$ = code phase shift during list verification

The mean acquisition time with Doppler $T_{acq\mid Doppler}$ and its variance $\sigma^2_{acq\mid Doppler}$ can be expressed in terms of $T_{acq\mid no-Doppler}$ and $\sigma^2_{acq\mid no-Doppler}$ respectively as shown below:

$$T_{acq\mid Doppler} = \frac{T_{acq\mid no-Doppler}}{\mid 1 + \frac{q'}{N_u}\,\Delta f_c\,\tau_d\,(1+K\,P_{fa}) \mid} \tag{2.7}$$

$$\sigma^2_{acq\mid Doppler} = \frac{\sigma^2_{acq\mid no-Doppler}}{\left[1 + \frac{q'}{N_u}\,\Delta f_c\,\tau_d\,(1+K\,P_{fa})\right]^2} \tag{2.8}$$

where $\frac{N_u}{q'} = \frac{\Delta T_c}{T_c}$ represents *the mean search update* (denoted μ) in the absence of Doppler (or equivalently the step size of the search in fractions of a chip) with q' as the number of cells in the absence of Doppler ($q' = q$ for $\Delta f_c = 0$).

Similarly, by the substitution of the equivalent *mean search update*, into the original equations the Doppler rate can also be taken into account [14].

The probability of detection P_d and probability of false alarm P_{fa} depend on SNR, the acquisition system parameters, namely τ_d and the type of detector, and can be derived based on signal detection theory [15], as given below:

If the envelope detector output is sampled at a rate $1/T \leq B$ where B is the predetection filter bandwidth, which ensures sufficient sample decorrelation, then the samples can be treated as independent identically distributed (iid) random variables. Then the detector probabilities can be approximated with a Gaussian assumption of the integrator output (for a large BT) and given by:

$$P_{fa} = Q[\beta] \tag{2.9}$$

$$P_d = Q[(\beta - \sqrt{B\tau_d}\gamma)/\sqrt{1+2\gamma}] \tag{2.10}$$

where $Q[x]$ is the Gaussian probability integral with β and γ given by

$$\beta = (\eta - B\tau_d)/\sqrt{B\tau_d} \tag{2.11}$$

$$\gamma = A^2/2\sigma^2 \tag{2.12}$$

where A is the *rms* amplitude of the correlator signal and $\sigma^2 = N_o B/2$ is the variance of the noise process where N_o is the single-sided noise spectral density. For a required P_d, P_{fa}, given γ, B and η the necessary dwell time τ_d can be determined easily. However, the basic design problem is to choose the optimum threshold and the dwell time that can provide a minimum mean acquisition time for a given input SNR. Since both P_d and P_{fa} are functions of the threshold, dwell time and γ, and they are transcendentally related; the optimization problem requires the equations to be solved numerically. The optimization of the single-dwell detector is considered in chapter 7.

2.3.3.2 Search/lock strategy (SLS)

An accurate analysis of code acquisition must explicitly account for the strategy by which the search and lock functions are monitored. The transition from search mode (coarse acquisition) to lock mode (tracking) is important as it has twofold effect on the overall code synchronization process. First, it yields a verification which establishes the validity of a *hit* produced by the search algorithm before the control is taken over by the tracking. This is important as the false alarms, if unchecked, can have significant impact on the acquisition time due to the longer integration time used during lock mode to assure high probability of detection and thereby ensuring that the detector does not declare loss of synchronization prematurely. Secondly, it continuously monitors the lock mode and determines when to reinitialize the search mode based on loss of synchronization. Hopkins [2] has analyzed such a *search/lock strategy* (SLS) for a single-dwell acquisition system, as shown in figure 2.5,

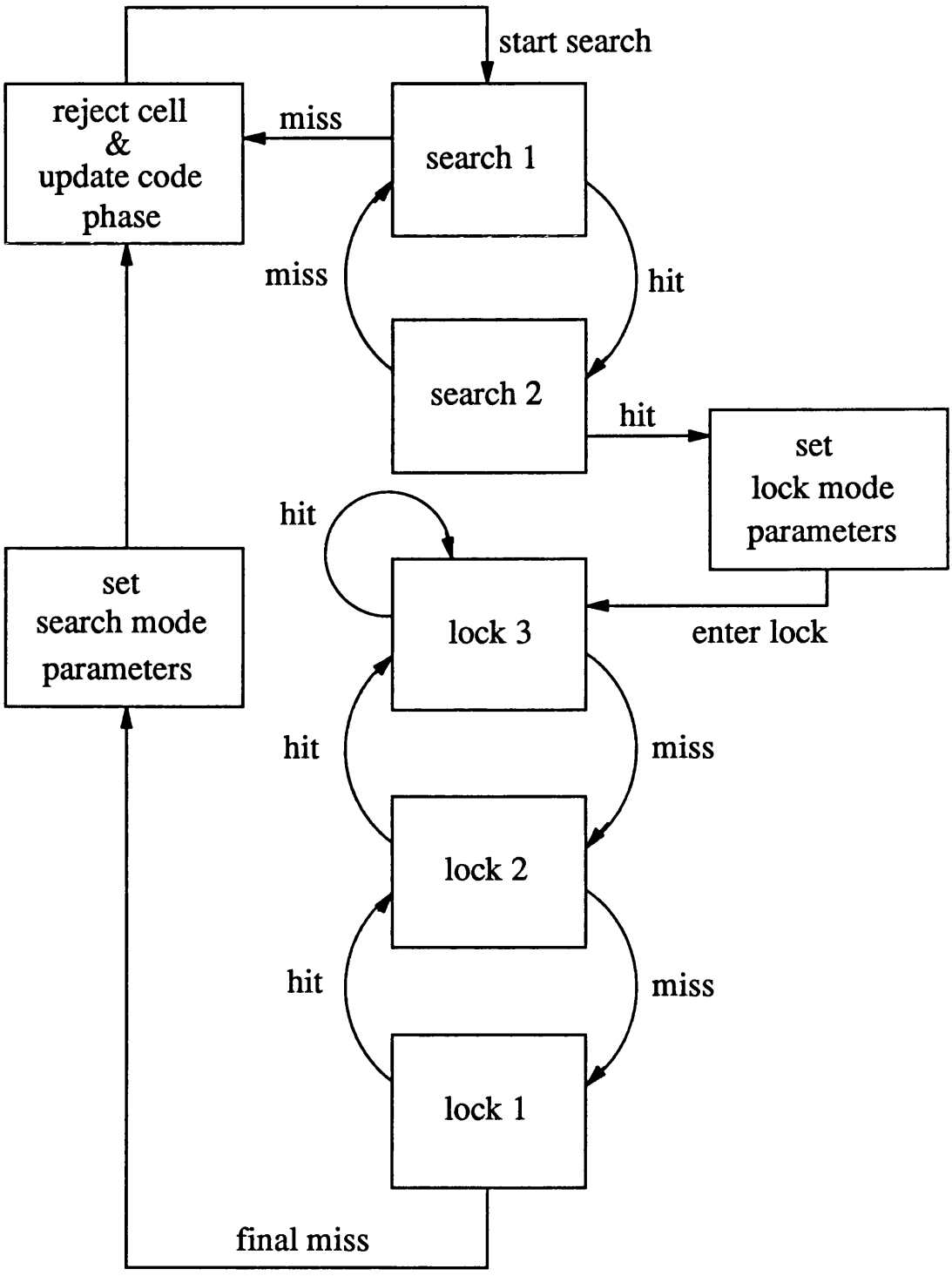

Figure 2.5 A search/lock strategy

(Hopkin's up-down counter strategy)

using identical dwell-times (τ_{d1}) for both search and lock modes. In this, the first test of a cell (state 1) causes a hit to the next state (stage 2) and a hit in state 2 to enter the *lock mode.* In the *search mode* a miss in state 1 results in immediate rejection of the cell and a phase step to the next cell, a miss in state 2 causes a return to state 1. Once the lock mode is entered a single miss will not cause a return to search. This SLS is analogous to a counter with four possible counts 0, 1, 2 and 3 and an initial count of 1 with 3 for the lock mode. This type of SLS is called an *up-down counter strategy.* A significant feature of this SLS is that *the detector parameters are changed upon entering the lock mode* to ensure a very high probability of detection (P_d). A Markov chain model with absorbing boundaries (states with no transition, ie., starting and ending states), was employed to analyze the SLS and the expression for mean time to acquisition was derived as:

$$T_{acq} = \frac{N_u \bar{\tau}_d}{2}\left[\frac{2-P_L}{P_L}\right] \tag{2.13}$$

where P_L is the probability of entering lock and $\bar{\tau}_d$ is the mean dwell time for an incorrect cell.

The variance of the acquisition time was found to be:

$$\sigma^2_{acq} = \bar{\tau}_d^2 N_u \left[\frac{1}{12} + \frac{1}{P_L^2} - \frac{1}{P_L}\right] \tag{2.14}$$

The probability of acquiring lock P_L is determined from the knowledge of state transition probabilities (in fact, P_L is the probability of going from state 1 to state 3 and can be related to probability of detection for the search mode). $\bar{\tau}_d$ is the mean time to reach state 0 to 6 and can be related to the dwell time and the probabilities of false alarm in the search and lock modes [2]. To include the effects of code Doppler or its derivatives, the modifications to the mean search update, μ can be made as suggested earlier.

2.3.3.3 Equivalence of single-dwell search with continuous sweep

Often, the performance results obtained for the discrete stepping search system can be extended to the continuous sweep procedure, using an equivalence of the system parameters. Thus $q\tau_d$ is equivalenced with $L/\Delta f_c$ to equivalently search one code period. Further, $KP_{fa} = (K\tau_d)(P_{fa}/\tau_d)$, hence for the continuous system $K\tau_d$ is equivalenced to the false alarm penalty time T_P and P_{fa}/τ_d is equivalenced with the false alarm rate $n_{FA} = P_{fa}(q\Delta f_c/L)$.

2.3.3.4 Double dwell serial search acquisition

The mean acquisition time of the single-dwell serial search system depends on the mean

dwell time for each cell with incorrect code phase and the false alarm penalty time factor K. When both τ_d and P_{fa} are large, this can lengthen T_{acq} significantly. In order to reduce the acquisition time of the serial search it is required to discard the cells containing no signal (ie., the out-of-sync and the potential false alarm states) as soon as possible, still keeping the advantage of longer integration time for the cell containing the wanted signal in-lock signal to improve the decision reliability. This technique reduces the required mean dwell time, simultaneously improving the probability of detection. Thus a double-dwell system, in which the search is performed during the first dwell time τ_{d1} and the verification is performed in the second dwell time τ_{d2}, significantly improves the acquisition performance over the single-dwell scheme as those cells without the wanted correlation signal can be rejected in the search mode itself.

Double-dwell search schemes with a search/lock strategy, similar to *Hopkin's up-down counter strategy*, however, employing two different integration times in the search mode and three verification stages which can employ longer integration time, has been analyzed by Holmes and Chen [12] and Di Carlo and Weber [1], and expressions for mean acquisition times were obtained as a function of various search parameters and system parameters. The analysis by Di Carlo and Weber derives expressions for more general multiple-dwell schemes and obtains results for the two-dwell system as a special case, while Holmes and Chen extended the analysis using a Markov chain model of the acquisition process of a single-dwell scheme to that of the double-dwell scheme.

The expressions for mean acquisition time and variance without code Doppler for a double-dwell search scheme are given by [1,12]:

$$T_{acq} = \frac{(2-P_d)}{2P_d}\left[\tau_{d1} + \tau_{d2} P_{fa1} (1 + K P_{fa2})\right] q \tag{2.15}$$

$$\sigma^2_{acq} = \tau^2_{d1} + \tau^2_{d2} P^2_{fa1} (1 + K P_{fa2})^2 q^2 \left[\frac{1}{12} - \frac{1}{P_d} + \frac{1}{P_d^2}\right] \tag{2.16}$$

with $q \gg P_{fa2} K (K+1)$ and $q \gg 1$

where

τ_{d1} = first dwell time

τ_{d2} = second dwell time

$P_d = P_{d1} P_{d2}$ product of detection probabilities of dwell times one and two, respectively

P_{fa1} = false alarm probability of the first dwell

P_{fa2} = false alarm probability of the second dwell

K = penalty for a false alarm at the second detector (number of τ_{d2} units of time)

The equations can also be modified to account for code Doppler by replacing q by N_u/μ where μ is the *mean search (code phase) update* in chips given by:

$$\mu = \frac{\Delta T_c}{T_c} + \tau_{d1}\Delta f_c + P_{fa1}\,\tau_{d2}\,\Delta f_c + P_{fa1}\,P_{fa2}\Delta f_c \qquad (2.17)$$

2.3.3.5 Multiple-dwell serial search

The multiple-dwell serial search strategy is a more general type of serial search in which *the examination interval* is not constrained to be a fixed period of time. Instead, the examination interval consists of a series of shorter dwell periods with the decision being made after each dwell time. Thus, an incorrect waveform alignment can be discarded in a shorter period of time than is possible with the single-dwell time technique. This capability to *quickly discard* the incorrect alignments significantly reduces the overall acquisition time, especially when a large number of possible alignments are to be examined.

The general form of the *N-dwell serial search acquisition system* (as referred by Di Carlo and Weber) is shown in figure 2.6. The received PN signal, plus noise, is multiplied by the local PN signal and the output is fed to each of the N non-coherent detectors. The i_{th} detector is characterized by a detection probability, P_{di}, a false alarm probability, P_{fai}, and the dwell time τ_{di}. The detector dwell times are assumed to be ordered such that:

$$\tau_{d1} \leq \tau_{d2} \leq \tau_{d2} \leq \ldots\ldots\ldots \leq \tau_{dN} \qquad (2.18)$$

The decisions are made by sequentially examining the N detector outputs (starting with the first) and applying the following *algorithm.*

Step 1: If *all* the N detectors (tested in succession) indicate that the present cell is correct (produces a threshold crossing) then the decision is made to stop the search.

Step 2: If *any* one of the detectors fails to indicate that the present cell is correct (fails to produce a threshold crossing), then the decision is made to continue the search and the local code generator is updated (retarded), whereupon the next cell is examined.

The *N integrate and dump (I & D)* circuits initiate their integration at the same time but dump at later and later time instants.

Though this represents the conceptual realization, in practice the N, I & D circuits would be realized by a single continuous-time integrator whose output is sequentially sampled (but

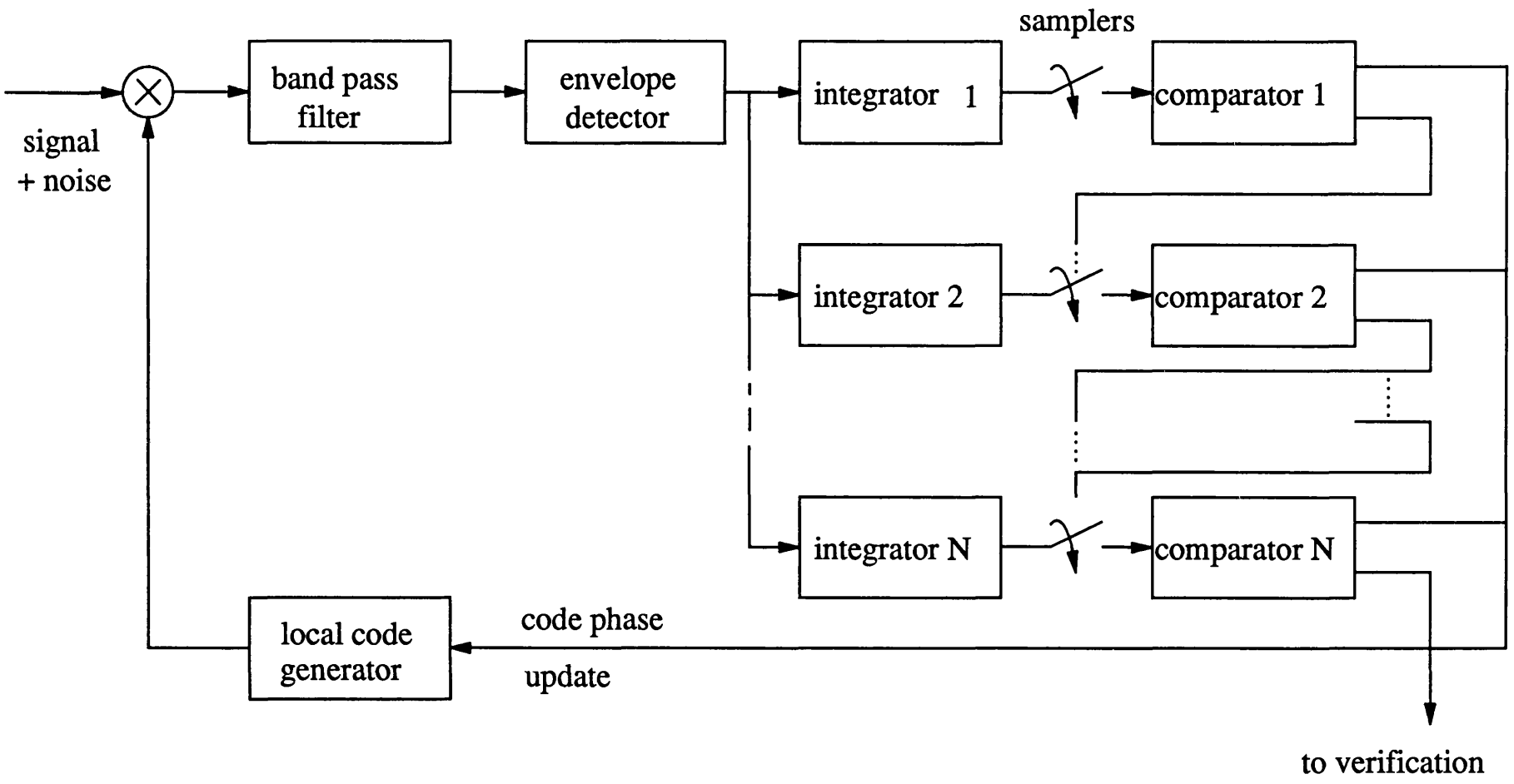

Figure 2.6 Schematic diagram of an N-dwell serial search system.

not dumped) at time constants $\tau_{d1}, \tau_{d1}+\tau_{d2}, \ldots\ldots, \tau_{d1}+\tau_{d2}+\ldots\ldots+\tau_{di}$ *depending on the outcomes of the first i - 1 threshold comparisons.*

The false alarm penalty time, T_P, when all N detector outputs exceed their respective thresholds for a cell which does not correspond to the correct code alignment, can be modelled as an integer multiple of the additional time required by the N^{th} dwell

$$T_P = K_N(\tau_{dN} - \tau_{dN-1}) \tag{2.19}$$

The statistical properties of the acquisition strategy are obtained using a Markov chain model and a flow graph representation of the N-dwell system by Di Carlo and Weber [1] and the expressions for mean and variance of the acquisition time were found to be:

$$T_{acq} = q\,\frac{(2-P_d)}{2P_d}\sum_{j=1}^{N}\left[\, t_j \prod_{i=1}^{j-1} P_{fai} + P_{FA}\,T_P\,\delta_{jN}\right] ; \qquad q>>1 \tag{2.20}$$

$$\sigma^2_{acq} = q^2\left[\frac{1}{12}-\frac{1}{P_d}+\frac{1}{P_d^2}\right]\left\{\sum_{j=1}^{N} t_j\left[\prod_{i=1}^{j-1} P_{fai} + P_{FA}\,T_P\,\delta_{jN}\right]\right\}^2 \tag{2.21}$$

where t_j is the additional time necessary to make the j^{th} decision given that the present cell has not been rejected at the $(j-1)^{th}$ decision.

$$t_j = \tau_{dj}, \quad j=1,\ldots N \tag{2.22}$$

if the detectors are reinitialized after each decision (integrate and dump) and

$$t_j = \tau_{dj} - \tau_{dj-1}, \quad j=1,\ldots N \tag{2.23}$$

if the detectors are not reinitialized.

P_D and P_{FA} are the overall system detection probability and false alarm probability which are expressed, in terms of the conditional probabilities per cell basis, as:

$$P_D = \sum_{i=1}^{N} P_{di} \tag{2.24}$$

$$P_{FA} = \sum_{i=1}^{N} P_{fai} \tag{2.25}$$

P_{di} = conditional probability of detecting the correct cell given that it has been successfully detected by previous $(i-1)$ detectors.

P_{fai} = conditional false alarm probability which is the conditional probability that the i^{th} detector chooses an incorrect cell given that the previous $(i-1)$ detectors have also chosen it.

δ_{jN} = the Kronecker delta function defined as

$$\delta_{ij} = \begin{cases} 1 & i=j \\ 0 & i\neq j \end{cases} \tag{2.26}$$

For the *special case of* $N = 1$, $K_1 = K$ the above expressions readily reduce to those of the *single-dwell search* system. When compared with the single-dwell search, it is apparent

from the expressions that for the same false alarm penalty time, i.e. $K\tau_d = K_N(\tau_{dN} - \tau_{dN-1})$, the N-dwell system can yield a smaller acquisition time than the single-dwell system if

$$\sum_{j=1}^{N}\left[\prod_{i-1}^{j-1} P_{fai}\right](\tau_{dj} - \tau_{dj-1}) < \tau_d \tag{2.27}$$

Thus, the ability to design the *N-dwell* system to satisfy the above equation depends on the functional relationship between the conditional false alarm probabilities and dwell times. The system detection probability P_D, and false alarm probability P_{FA} can be approximated from the signal detection theory as in the case of the single-dwell detector.

From the computation results of cases with, $N = 1, 2, 3$ by Di Carlo and Weber a significant conclusion was reached that *the reduction in average acquisition time obtained by increasing the number of dwells is significant from one to two. Additional but only nominal improvement is gained when more than two dwells are used.*

2.3.4 Variable dwell time schemes or sequential detection

These schemes employ *sequential detection methods* stemming from the original work by Wald [3] which has been applied to radar detection theory. The design philosophy is based on the minimization of the acquisition time by quickly dismissing the false sync positions, allowing it to integrate over a much longer time interval during the single cell which contains the correct code alignment.

Though multiple-dwell schemes achieve this by increasing the integration time in discrete steps, sequential detectors allow the integration time to be continuous and replace the multiple threshold tests by a continuous test of a single dismissed threshold.

The corresponding search strategy is designed so that the mean time to dismiss the false sync is much smaller than the single-dwell system. Thus, since the search spends virtually all its time dismissing false sync positions, the mean acquisition time of sequential detection PN acquisition system will be much less than that of the single-dwell system.

The generalized sequential detection acquisition system is shown in figure 2.7. This employs a square-law envelope detector to remove the data modulation and operates identically to a single-dwell system except that the integrator or accumulator samples are a transformed version of the envelope detector samples. The output of the integrator would, typically follow along the integrated mean of the square-law detector output (N_oBt or $N_oB(1+\gamma)t$), depending upon whether the cell under test corresponds to *noise only* or *signal plus noise.*

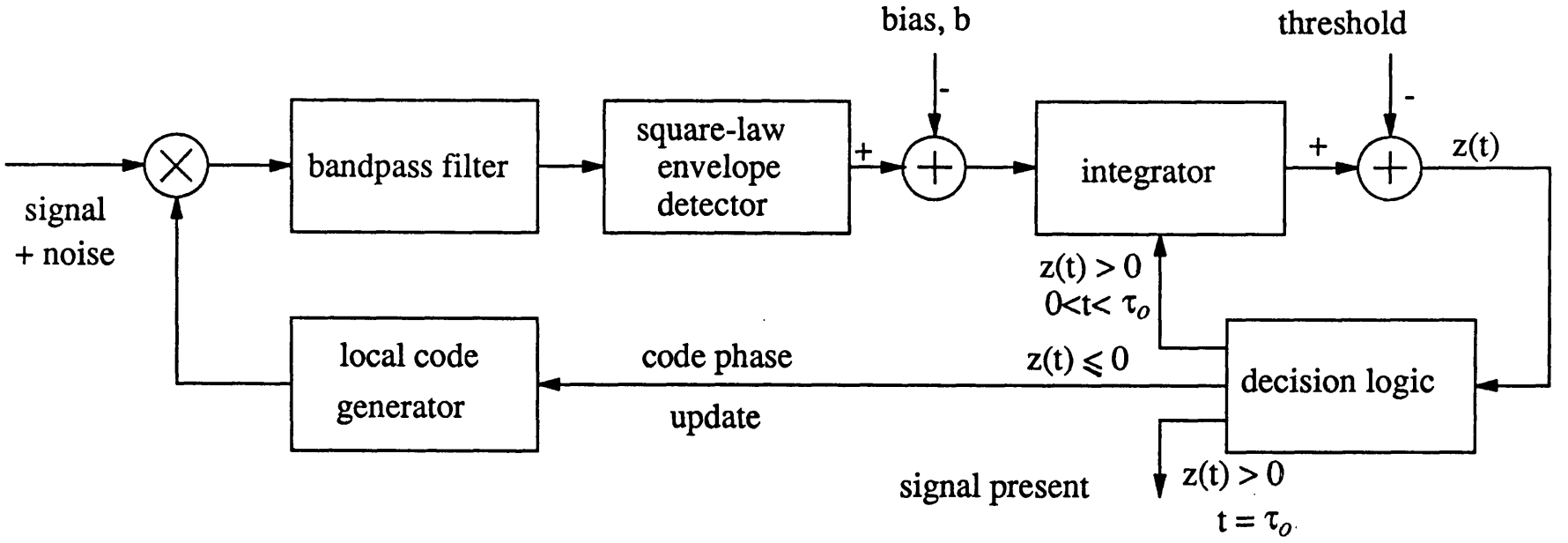

Figure 2.7 Schematic diagram of a generalized serial-search sequential detection system (with time-out feature)

For both these hypotheses the integrator output would tend to increase with time, but at different slopes. By subtracting a bias voltage b, such that $N_oB < b < N_oB(1+\gamma)$, the integrator output will tend to decrease linearly with a slope $(N_o B - b)$, when the noise only is present, and increase linearly with slope $(N_oB(1+\gamma) - b)$ when the signal plus noise is present, as illustrated in figure 2.8. By setting a negative threshold a code epoch is dismissed when the integrator output falls below it. The smaller the magnitude of this threshold, the faster the integrator output will dip below it if it contains no wanted signal. This provides the basis of a *quick dismissal*. However, since the smaller magnitude of threshold can more likely dismiss the signal plus noise also (ie., a false dismissal), a compromise threshold value must be chosen for a relatively quick dismissal of the false sync, but which tends to allow the true sync position to remain above threshold.

There are two ways of determining a true sync event (and a false alarm). One way is by designation of truncation time, say τ_o. On reaching this interval without declaring the wrong epoch causes the declaration of the signal. This is called *a truncated sequential test* and the test truncation time τ_o is referred to as the *time-out* of the sequential detector. The time-out feature in some cases is replaced by a test against a second positive threshold in which case the signal is declared to be present as soon as the integrator output rises above the positive threshold, rather than remaining above the lower negative threshold for all $0 < t < \tau_o$. This is the *two-threshold sequential detection system* and indeed, is the more classical type, representing a direct application of the sequential hypothesis testing originally discussed by Wald. A complete description of two-threshold sequential detection scheme with optimum decision criteria will be discussed in chapter 3.

2.4 GENERAL ANALYSIS OF SERIAL SEARCH SCHEMES

Various researchers have used combinatorial arguments or simplified flow graph techniques with transform domain methods for analyzing straight serial search strategies from a characteristic function or a generating function. In some cases, the analysis is extended to optimized expanding window searches and the derivations are obtained through laborious steps. These analyses use many assumptions [16]-[22] and their results are valid only for the specific cases assumed.

Generalization of the serial search analysis to include many other specific cases has been carried out using unified theory and circular state diagrams in *transform domain* by

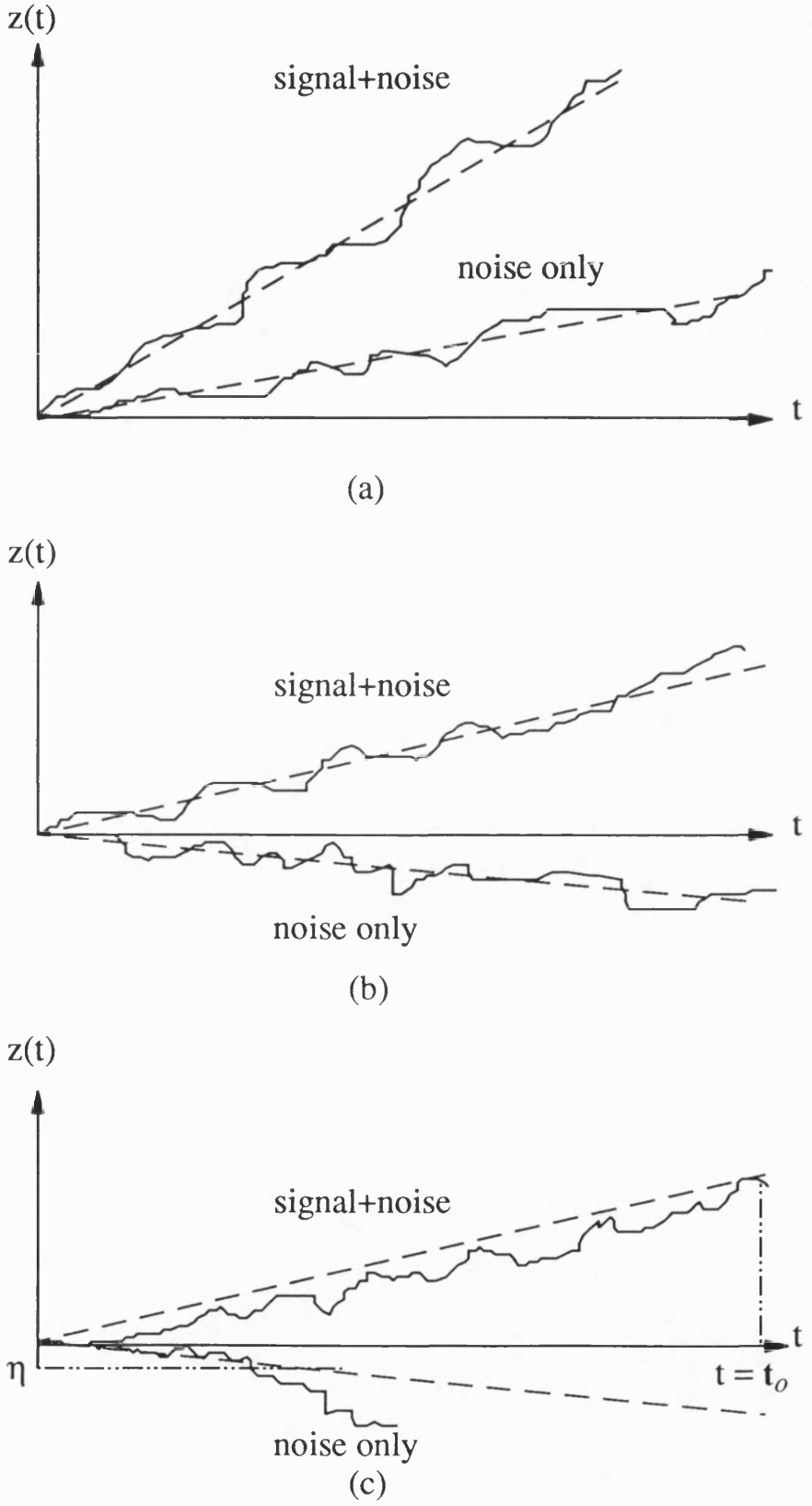

Figure 2.8 Typical growth rate of the integrator output for a sequential detector: (a) no bias (b) with bias (c)with threshold dismissal and test truncation

Polydoros and Weber [17], and, Polydoros and Simon [18]. A *time domain* method using a rapidly converging infinite series to obtain the *pdf* and the first two moments of the mean acquisition time has also been presented by Meyr and Polzer [23]. A direct approach for the analysis of strategies for serial search using both time domain and the transform domain techniques has been presented by Jovanovic [21]. Pan, Dodd and Kumar [22] have recently presented an analysis for straight serial search strategies with fixed dwell times using a modified flow graph which permits the use of a generalized lock strategy and allows the false alarm time to be treated as a random variable. In this work, the distribution of the acquisition time has been obtained directly by use of an extended generalization of Bernoulli trials. This analysis is more general and requires fewer assumptions and approximations compared with the other analyses which use a fixed penalty false alarm time. It is also suitable for single and multiple-dwell schemes and can be extended for Z-search and expanding window searches.

The following sections describe these general analysis methods used for analyzing the serial search strategies and the results obtained using these methods are also discussed.

2.4.1 Unified approach to serial search

This is a general theory of analysis applicable to serial search acquisition schemes proposed by Polydoros and Weber [16]. It provides a general extension to the previous state diagram or flow graph technique originally suggested by Holmes and Chen [12]. The theory is based strictly on *transform domain techniques* and is formulated to be general enough to encompass the past theoretical methods as well as the more recent ones and allows for significant freedom when modelling the receiver structure. It accounts for arbitrary choices for: 1) cell logic (verification mode), 2) search logic (serial search strategy), 3) prior information and 4) the form of spectral spreading such as DS or FH.

Using this approach the generating function is obtained by substituting various path gains of the flow graph, representing all possible state transitions as appropriate to the acquisition scheme, in the generalized characteristic (or generating) function, from which the mean acquisition time and its variance can be obtained. The applicability of the proposed theoretical framework was illustrated, by considering the cases of simple examples, viz. single and multiple dwell. The various branch gains were defined and the expressions for mean acquisition time were obtained which readily agree with the previous results. Following a similar approach, a matched filter non-coherent acquisition system was also analyzed and the mean acquisition time for both uniform and worstcase assumptions were

derived.

In a parallel effort, Holmes and Woo [24], Weinberg [19] and Braun [20] have used *combinatorial arguments* to derive expressions for a more sophisticated serial search strategy which is a class of *expanding window technique* (which will be discussed in the next section). The unified theoretical framework has also been later generalized to provide results for any arbitrary serial search strategy, such as the *Z-search and the expanding window search* by Polydoros and Simon [18].

2.4.2 Equivalent circular state diagram approach

The circular state diagram method was first used as a tool for modelling and analyzing the complete acquisition behaviour of *straight (uniform) serial search* schemes using the unified theoretic approach by Polydoros and Weber. The method was generalized using equivalent circular state diagrams and extended to *include arbitrary serial search* strategies by Polydoros and Simon [18] in which two classes of *non-uniform serial search* strategies, *viz., Z-search and expanding window search*, were considered. In this work, also the generating or characteristic function of the stochastic process is derived through a transform domain description.

The advantage of this technique is that it circumvents the complicated combinatorial arguments used in the analyses employing a transform domain description of the stochastic acquisition process by Braun [20] and Weinberg [19]. It allows a simple and more systematic evaluation of the generating function of the process using the well-known flow graph reduction techniques.

2.4.3 A direct approach to analysis of serial search strategies

A direct approach to obtain the statistics of the mean acquisition time of serial search strategies was presented and various Z-search and expanding window search strategies were compared by Jovanovic [21]. This technique *combines the idea of algebraic characterization of the search with the transform domain methods* and is a general unified technique yielding many other known results as special cases.

One of the major advantages of this technique is that the effect of the search strategy on the moments of the acquisition time can be isolated from the effect of the detection/verification time.

Using this approach several conclusions regarding the comparative performance of the continuous/broken, centre/edge Z-searches and expanding window search have been confirmed. Two alternative search strategies namely, i) uniformly expanding alternate (UEA) and ii) non-uniformly expanding alternate (NUEA) were also proposed and their performances were compared. Both these strategies perform tests by jumping sequentially on cells following the order of decreasing *a priori* probability. An optimum search strategy based on *the maximum a posteriori* (MAP) method was also analyzed to establish *an absolute and uniform basis* of comparison with the suboptimal strategies.

Based on these comparisons it was shown that the non-uniformly expanding alternate (NUEA) strategy achieves a performance which is indeed very close to the theoretical limit showing essentially the same performance as the MAP search.

2.5 NON-UNIFORM SEARCH STRATEGIES

The straight serial search strategies (uniform) considered hitherto have assumed that the *a priori* pdf of the signal location across the uncertainty region is *uniform*, ie., the correct cell is equally likely to occur in any of the q cells searched in one complete pass. When the *a priori* pdf signal location is in some sense *peaked rather than uniform ie., non-uniform* then the optimum search strategy should begin with searching in the region where the likelihood of finding the signal is the highest. The *expanding window search and the Z-search schemes* achieve this objective. Both these search strategies can employ either continuous or broken (with a fast rewinding) searches and also can start at either the centre or the edge of the uncertainty region. These search strategies are shown in figure 2.9.

The analyses of the non-uniform search strategies have been carried out by a number of researchers using the above general approaches and by using combinatorial methods. The analysis of two subclasses of Z-search (continuous/centre and broken/centre) and expanding window search schemes using *the equivalent circular state diagram approach* was presented by Polydoros and Simon [18] and the results are discussed here. In their analysis, the unified approach was applied to the non-uniform search case *simply by translating the motion of the specific search strategy under consideration into a circular motion along an equivalent circular state diagram*, analogous to the one used for the uniform search.

A. Continuous/Centre Z-search

This search, as shown in figure 2.9, is initiated at the centre of the code phase uncertainty

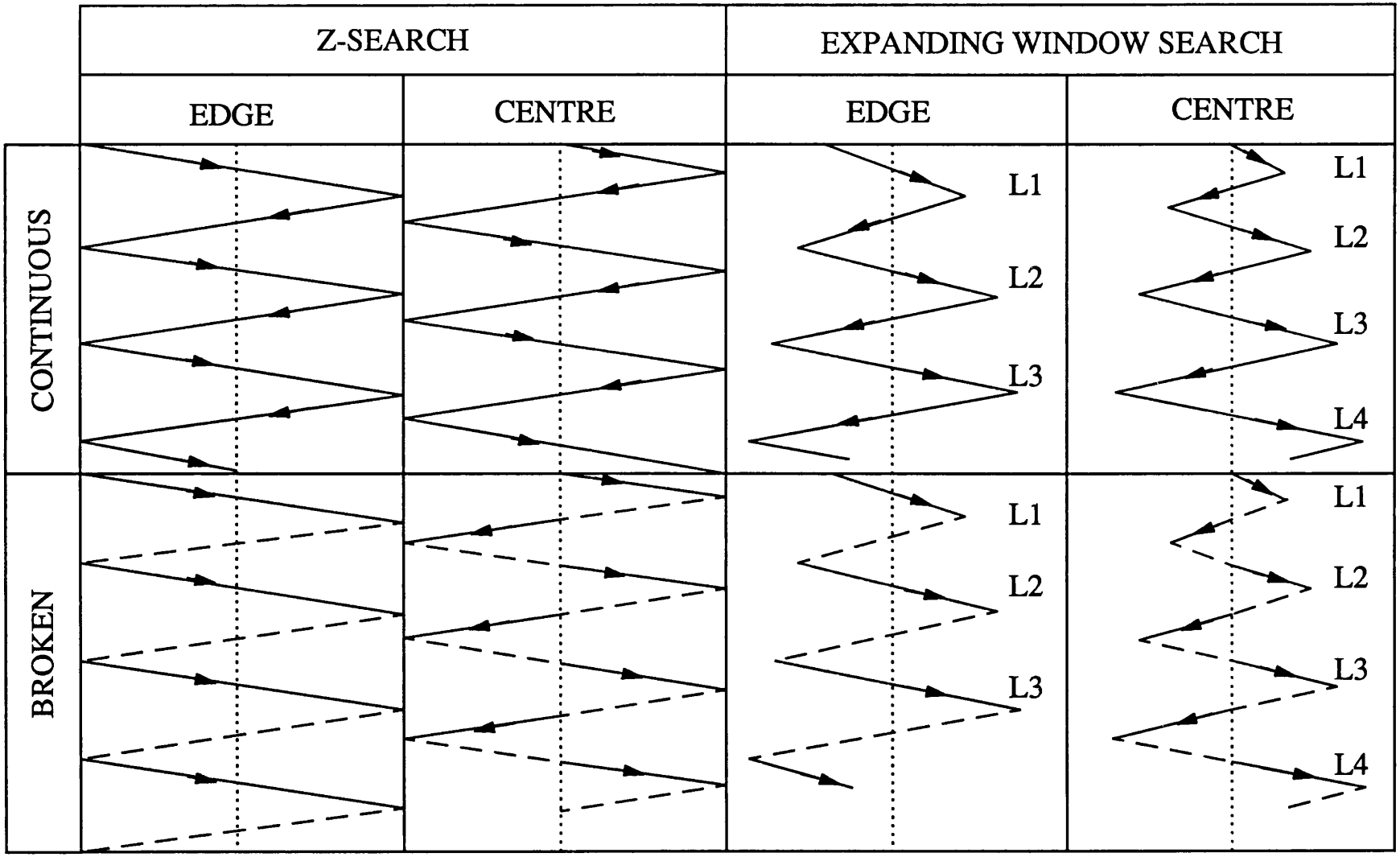

Figure 2.9 Z-search and Expanding window search schemes

region and proceeds until the end in the direction of decreasing *a priori* probability and reverses its direction every time the boundaries are reached. Assuming the location of the true sync state is at the centre (for a triangular *a priori* distribution), the search process will meet it once during each sweep.

Following the steps of flow graph reduction techniques, the generating function can be derived from which acquisition statistics can be obtained. Thus, the mean acquisition time for continuous/centre Z-search can be found to be [18]

$$T_{acq\,|\,cont} = \tau_d \left[\frac{1}{P_d} + \frac{2(1 + KP_{fa})q\,(3-3P_d+P_d^2)}{3P_d(2-P_d)} \right] \quad \text{for } \textit{large } q \tag{2.28}$$

B. Broken/Centre Z-search

This is similar to the continuous/centre Z-search with the exception that the same cells are not searched twice in a row (figure 2.9). Instead, when one of the boundaries is reached, the local code is quickly rewound to the centre and the search continues in the opposite direction. Following the identical steps using circular state diagrams the mean acquisition time has been obtained as

$$T_{acq\,|\,broken} = \tau_d \left\{ \frac{1}{P_d} \left[1 + \left[\frac{4-3P_d}{2} \right] \frac{T_r}{\tau_d} \right] + \frac{(1+KP_{fa})q}{P_d} \left[1 - \frac{7}{12} P_d \right] \right\} \quad \text{for } \textit{large } q \tag{2.29}$$

The *improvement in the mean acquisition time* using a broken rather than a continuous/centre Z-search can be approximated to (for large q)

$$\frac{T_{acq\,|\,cont}}{T_{acq\,|\,broken}} = \frac{2(3-3P_d+P_d^2)}{3(2-P_d)\left(\frac{7}{12}P_d\right)} \tag{2.30}$$

The maximum improvement factor occurs for $P_d = 1$ and has the value 1.6, ie., a 37.5% saving in acquisition time.

For more general cases where the *a priori probability distribution, π_j is arbitrary but symmetric* ($P_d = 1$, q large), the *improvement factor* is

$$\frac{T_{acq\,|\,cont}}{T_{acq\,|\,broken}} = \frac{2\sum_{j=1}^{q/2} j\pi_j + \frac{q}{2}}{2\sum_{j=1}^{q/2} j\pi_j + \frac{q}{4}} \tag{2.31}$$

which is *lower and upper bounded* by

$$\frac{6}{5} \le \frac{T_{acq\,|\,cont}}{T_{acq\,|\,broken}} = 2 \tag{2.32}$$

corresponding to *a priori distributions*

$$\pi_1 = \pi_q = \tfrac{1}{2} \qquad (2.33)$$
$$\pi_j = 0 \; ; \; j \neq 1, q$$

and

$$\pi_{q/2} = \pi_{\frac{q}{2}+1} = \tfrac{1}{2} \qquad (2.34)$$
$$\pi_j = 0 \; ; \; j \neq \frac{q}{2}, \frac{q}{2}+1$$

Thus regardless of the a priori probability distribution, the broken/centre Z-search potentially offers *an improvement of at least 20% and at most 100%* over the continuous centre Z-search. Of course, for $P_d < 1$ these improvements will decrease accordingly.

C. Expanding window search

This method was, first, analyzed using combinatorial methods and laborious derivations by Holmes and Woo [24], Braun [20] and Weinberg [19] as an optimum serial search strategy and the improvement in the acquisition time in comparison with the uniform window search was shown. However, a more general approach using *equivalent circular state diagrams* was presented by Polydoros and Simon [18]. Results of this method are discussed briefly here.

Polydoros and Simon considered a class of expanding window search strategies with two representative cases which differ in the way the search is continued once the entire uncertainty region has been searched without success. In one case, search repeats by starting from the smallest window while in the other case it starts repeating from the largest window.

Using this method, the expanding window single-dwell serial search strategy was *optimized in terms of the required number of partial windows, parameterized by the prior distribution of the phase uncertainty.* From the results, it was observed that *there exists an optimum number of sweeps* N_{opt} *for* $P_d < 1$; *while for* $P_d = 1$, $N_{opt} = 1$ *implying that the continuous/centre Z-search is the optimum.* The effect of *peakness* of the prior distribution on the performance was also studied for a *truncated Gaussian distribution* and it was seen that the more peaked the distribution the more one gains by using expanding window search rather than the Z-search. The value of N_{opt} was also observed to increase with decreasing P_d and it was concluded that *as the reliability of individual cell tests decreases one has to rely more on the prior information and, thus, spend more time around the peak (more windows).* The higher peak distribution was also observed to result in a large N_{opt} than the more dispersed one. Thus, optimizing the system at lower P_d was found to be essential in view of the gain in acquisition time reduction.

2.6 RAPID ACQUISITION BY SEQUENTIAL ESTIMATION (RASE)

The sequential estimation acquisition scheme, first proposed by Ward [4], can provide significant improvement in the mean acquisition time as long as the SNR is not very low. Rapid acquisition is achieved by directly loading the estimated initial status into the local code generator of the PN despreader as shown in figure 2.10. This technique presumes that the incoming signal is baseband, thus correlation is done at baseband and the Gaussian noise is the only interference. The implication for direct-sequence PN receiver is that *the coherent carrier phase tracking has to be established before code acquisition.*

The scheme in its original form is extremely vulnerable to interfering signals because the decisions are made at the chip rate rather than at the data rate. This means that the detector operates in the very poor SNR at the input of the spread-spectrum receiver. Errors in detecting the n consecutive bits lead to the wrong initial code state being inserted into the local code generator with which the system try's to acquire lock. After the examination period a new set of n bits are loaded (if the test fails) and the process is repeated. Thus, the system is not particularly useful for multiple access or in tactical radio environments characterized by bursty communications in severe jamming. However, it can be useful for precision ranging or for continuously operating strategic links in relatively good SNR conditions.

Ward has derived the expressions for acquisition time as a function of false alarm, false dismissal probabilities (P_{fa},P_{fd}), and examination time, T_e, as

$$T_{acq,RASE} = \frac{T_e}{P_c^n(1-P_{fa})(1-P_{fd})} \tag{2.35}$$

where P_c is the correctness probability of the estimated bit which is a function of input SNR. P_{fa} and P_{fd} are functions of the threshold, examination period and P_c.

The experimental performance has been compared with that of the stepping correlator and the *improvement factor* is found to be (for large SNR) a function of SNR.

$$\frac{T_{acq}}{T_{acq,RASE}} = 2^{(n-1)}P_c^n \tag{2.36}$$

where n is the shift register length.

For large SNR, the improvement factor approaches half the number of bits in the sequence, while for very small SNR the average acquisition time of sequential estimator is *twice* that of stepping correlator.

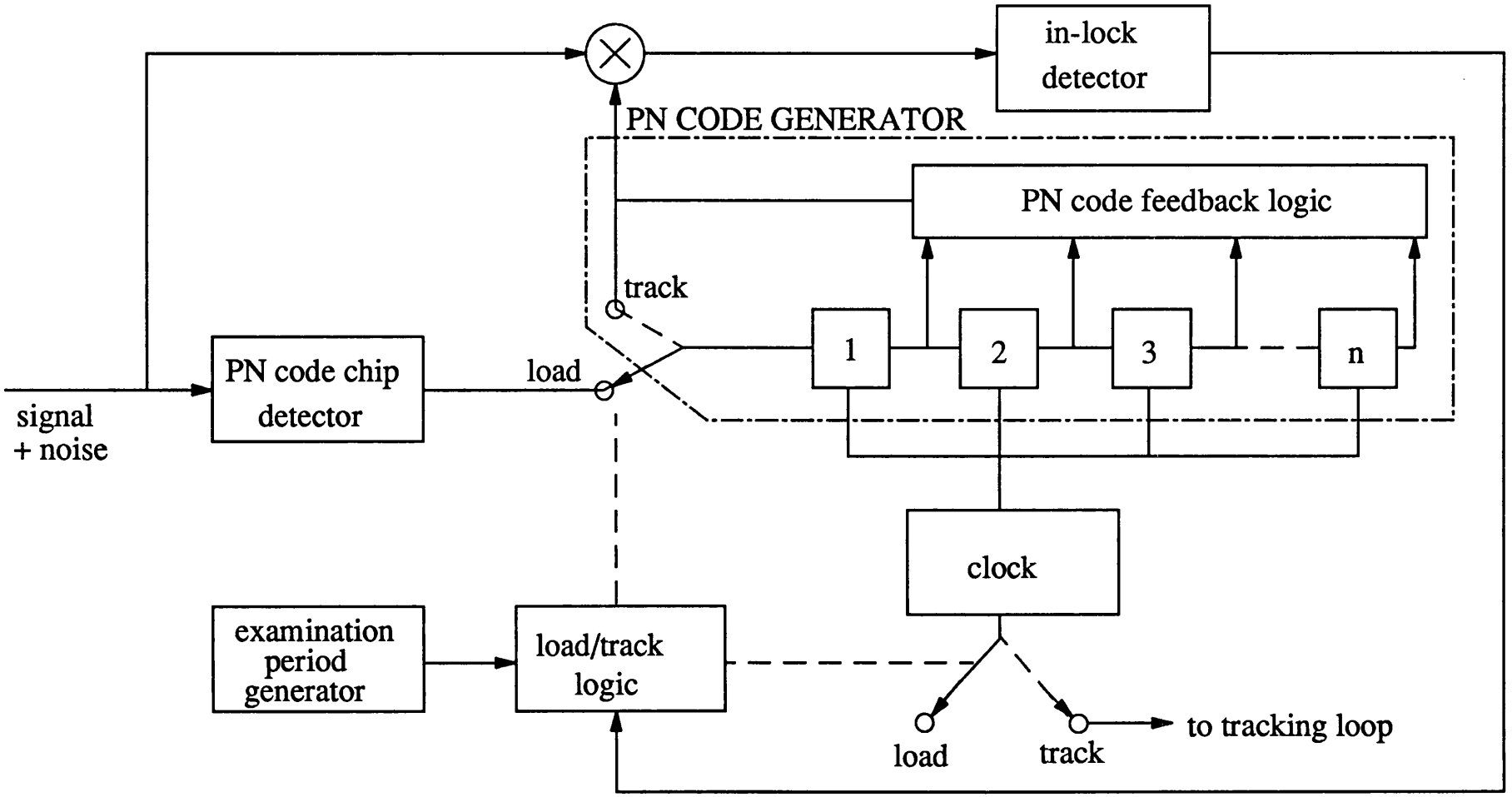

Figure 2.10 Rapid acquisition by sequential estimation (RASE)

The effects of Doppler and self noise have been also accounted for and the expressions for acquisition time and the threshold then takes the form:

$$T_{acq,RASE} = \frac{T_e}{P_c^n(1-P_{fa}^2)(1-nf_d/f_c)} \tag{2.37}$$

f_c, the nominal frequency and f_d, the frequency difference due to Doppler.

2.6.1 Recursive Aided RASE (RARASE)

Ward and Yiu [5] have suggested an *improved method of sequential estimation* by using the recursive relation of the PN sequences to determine if a short estimate of the state of the received PN signal is probably correct, thus discarding the high proportion of incorrect initial state estimates with relatively simple logic. The modified scheme is shown in figure 2.11. The average acquisition time for RARASE has been derived as

$$T_{acq,RARASE} = \frac{T_e}{P_c^n}(P_c^2 + 3(1-P_c)^2) \tag{2.38}$$

for one 3 input mod-2 adder in the *sync-worthiness-indicator* (SWI) as shown in figure 2.11. The improvement factor over RASE system is

$$\frac{T_{acq,RARASE}}{T_{acq,RASE}} = P_c^2 + 3(1-P_c)^2 \tag{2.39}$$

The number of checks can be increased to more than one bit for better decision reliability by adding more number of adders and thus for m, 3 input mod-2 adders in SWI [5]

$$\frac{T_{acq,RARASE}}{T_{acq,RASE}} = (P_c^2 + 3(1-P_c)^2)^m \tag{2.40}$$

The analytical expression for the probability of attempting to track for a *general overlapping SWI implementation* is difficult. However, for a particular case of fully overlapped SWI implementation with a single 3 input mod-2 adder and a counter which requires n successive *attempt tracking* outputs from the mod-2 adder before placing it in track mode, the improvement factor is given by

$$\frac{T_{acq,RARASE}}{T_{acq,RASE}} = \frac{1}{P_c^n}\left[P_c^{2n} + \sum_{j=1}^{n}\sum_{x=0}^{j-1}\frac{n}{j}\binom{j}{x}\binom{n-j-1}{j-x-1}P_c^{2n-3j+2x}(1-P_c)^{3j-2x}\right] \tag{2.41}$$

The improvement for n=15 is an impressive factor of 40 at higher SNRs and the improvement is shifted towards smaller values of SNR compared to the non-overlapping RARASE implementation. However, for typical SNRs it varies from 2 to about 20 with largest for SNRs of -3dB to -6dB and may be significant as low as -20dB.

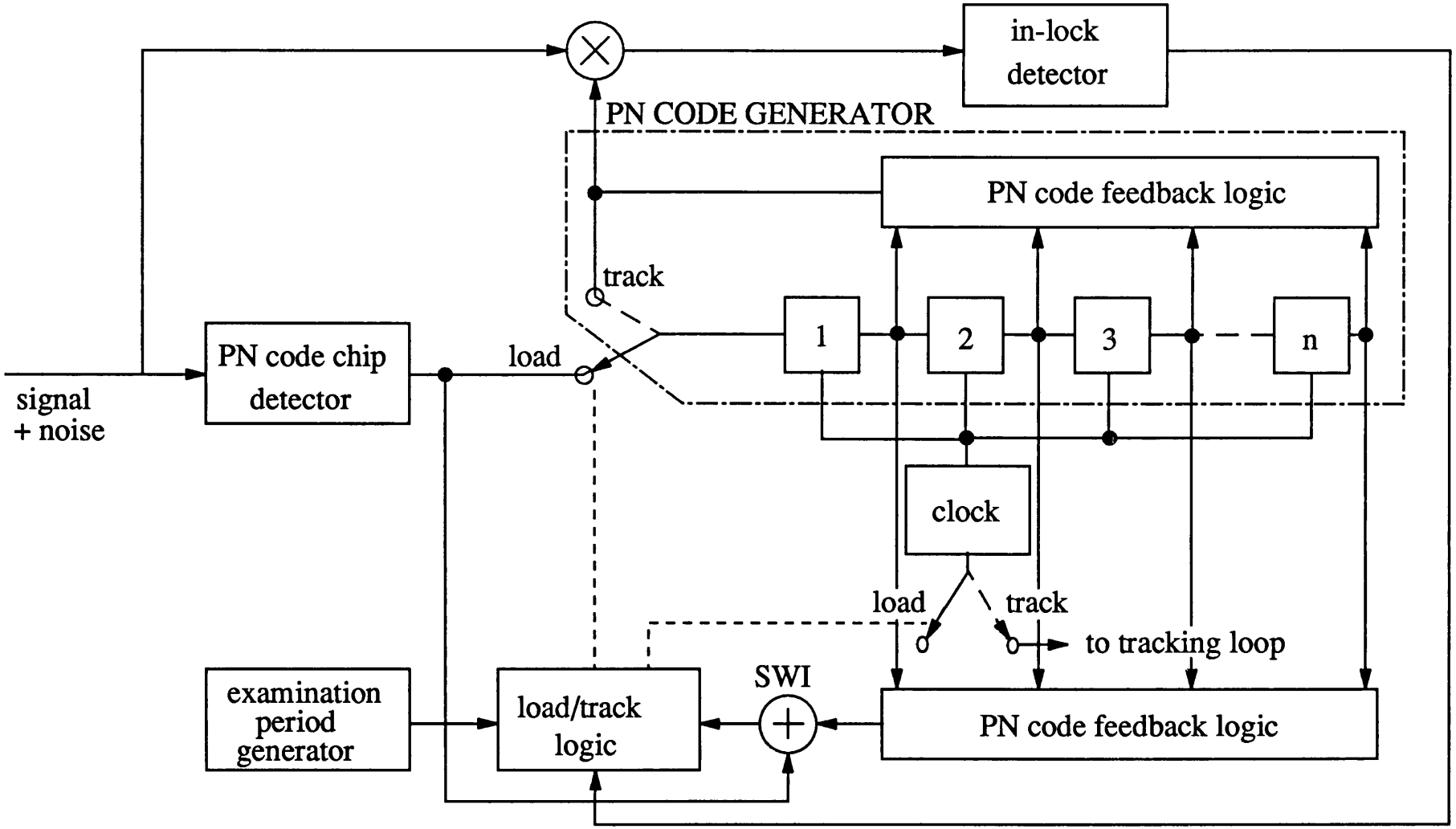

Figure 2.11 Recursive aided rapid acquisition by sequential estimation (RARASE)

2.6.2 Modifications to RASE/RARASE

RARASE schemes employing *sequential detection* as a phase checking system have also been analyzed by Ward and Yiu [5] in which each sync-worthy phase estimate is checked with a variable examination time made up of a series of examination intervals. At the end of the examination interval a hard *not-in-lock* decision or a soft *probable-in-lock* decision is made. The not-in-lock decision results in a continued search for the sync-worthy phase estimate, while the *probable-in-lock* decision results in continued examination of the same phase and the resetting of the threshold parameter. After a certain number of successive *probable-in-lock* decisions have occurred a *hard-in-lock* decision is made, resulting in no further examination. The average *number of examination intervals* (NEI) used per sync-worthy phase estimate has been derived as:

$$NEI = 1 + P_c \sum_{i-1}^{j} \prod_{k=1}^{i} (1 - P_{fdk}) + Q \sum_{i=1}^{j} \prod_{k=1}^{i} P_{fak} \tag{2.42}$$

where Q=1–P_c with P_c is the probability that a phase presented to the detector is correct and P_{fdk}, P_{fak} are the probability of false dismissal and false alarm at the end of k^{th} examination interval. The steps for computation of these probabilities were presented and the NEI was computed [5].

The analysis of sequential detection RASE becomes more complicated due to the interrelation between phase estimation and phase checking times. Thus, *the explicit formulation of improvement factor has not been derived.* However, computer iteration procedures have been employed to solve the problem.

Alem and Weber have applied the *optimal Bayes detector* for the acquisition of a baseband PN code using sequential estimation [8]. The performance of the system in terms of P_{fa} and P_{fd} in the range of SNR = -20db to -30db has been numerically calculated. Kilgus [6] suggested obtaining a number (n) of independent estimates of each of the n chips and making *a majority logic vote among all n estimates* to determine the initial n chip estimate. Pearce and Ristenblatt [7] suggest *a threshold decoding type* of estimator similar to that used for block codes. Recently, Chiu and Lee [25] have suggested an *improved sequential estimation* (ISE) based on *an extended characteristic polynomial* which can extend the use of RASE for both the m sequence and the converted m sequence. The mean acquisition of ISE has also been derived through the generating function flow graph technique as:

$$T_{acq,ISE} = \frac{1 + (1-P_c^{m+1})\, K\, P_{fa}}{P_c^{m+1} P_d} T_e \tag{2.43}$$

where

$$T_s = (m+1+L)T_c \tag{2.44}$$

T_c, chip duration, m - shift register length

P_c, chip correctness probability

with rest of the symbols as defined earlier.

2.7 PN CODE ACQUISITION USING MATCHED FILTERS

Active correlators integrate over a period of time which may be of the order of a few code lengths which is called dwell-time, τ_d for each threshold test. This imposes a basic limitation on the search speed since the reference code can be updated only after intervals of τ_d. The search rate of a DS acquisition scheme can be significantly increased with a passive correlator device such as *matched filter* (MF) which provides the real time search capability (for each incoming code chip, code phase is searched within a code chip period or even less). In the matched filter correlator each T_c segment (chip time) of the received waveform participates in $MT_c/\Delta T_c$ decisions where ΔT_c is typically of the form $2^{-n}T_c$ (for $n = 0, 1, 2, ...$), M is an integer constituting a fundamental design parameter as $MT_c/\Delta T^c$ is essentially equal to the number of memory locations in the correlator's shift register. *This multiple use of the received waveform is the key to the rapid acquisition idea.*

The non-coherent matched filter detector makes a decision every T_c sec; at the same time the decision is based on a correlation time of MT_c sec. In the continuous case, the incoming PN code plus noise is involved in the correlation with a finite segment of PN waveform (M chips) and the continuous time output is tested against a threshold to determine when acquisition has occurred. The input continuously slides past the stationary (not running in time) stored PN waveform replica until the two are synchronized, at which point the threshold would be exceeded and the local PN generator enabled. As the PN spreading waveform is typically biphase modulated on a carrier whose phase is as yet unknown, the matched filter acquisition system must be implemented either in a bandpass version or an equivalent low pass version. In the *bandpass case*, a bandpass matched filter is used whose maximum output is detected by a square-law envelope detector, while in the *low pass version*, in-phase and quadrature-phase carriers with arbitrary phase but known or estimated frequency are used to demodulate the received signal, followed by baseband matched filtering of each demodulated signal. The matched filter outputs are then non-coherently

combined to produce the desired correlation measure for threshold testing. Both these versions are shown in figures 2.12 and 2.13.

Conceptually, PN matched filters can be implemented as a tapped delay line followed by a passive filter matched to a single PN chip waveform. Attempts to develop advanced concepts which allow the matched filters to be programmable have led to intensive investigations of *Surface Acoustic Wave* (SAW) convolvers, *Charge Coupled Device* (CCD) correlators and digital techniques. The basic limiting factors are the *length and hardware complexity* of the matched filter which grows proportionally with the length of the sequence to be detected.

Many schemes have been proposed for PN acquisition with matched filters and some implementation results have also been reported in the literature. Grieco has proposed the use of CCDs [26] and has also analyzed the inherent limitations of CCD matched filters [27]. The design of CCD pseudo-noise matched filters has been presented by Magil *et al* [28], whilst Milstein *et al* have proposed the use of an SAW devices for spread-spectrum receivers [29]. Dostert and Pandit have presented the performance of a PN synchronization circuit employing SAW tapped delay line matched filter [30] and a wideband spread-spectrum modem, using a pair of SAW convolvers as programmable matched filters, has been reported by Hjelmstad and Skaug [31]. A similar implementation scheme using SAW convolvers as programmable matched filters for a hybrid DS/FH spread-spectrum scheme has been implemented by Kowatsch [32]. Milstein, Gevargiz and Das have also proposed a rapid acquisition scheme, using parallel SAW convolvers [33]. Use of *subsequence matched filtering* (SMF) has been proposed to improve acquisition performance by Mark and Blake [34].

In the development of the structure of matched filters, Baier has proposed a non-coherent low cost digital matched filter (DMF) with binary quantization which shows good performance for signals with a large time-bandwidth product [35]. A comparison of the SNR degradation with non-coherent DMF with one bit quantization suggested previously by Turin [36] has been carried out and the results show that *the extended DMF outperforms Turin's DMF by as much as 3dB*. Couturier, Wight and Pearce [37] have implemented a non-coherent four phase DMF and experimentally verified the *Baier's theory* of complex valued envelope matched filtering while Levita [38] has analyzed the performance of the digital matched filter for multilevel signals.

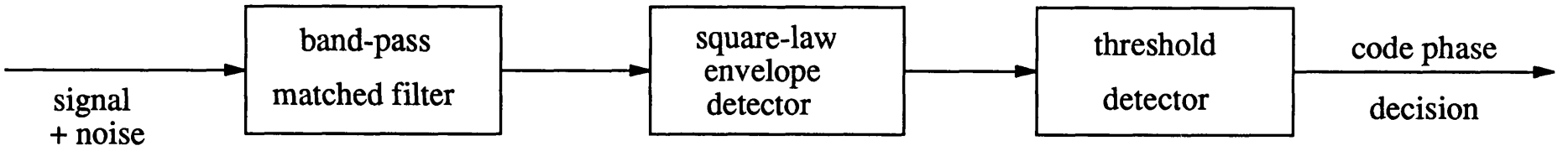

Figure 2.12 Schematic diagram of a matched filter: band-pass version

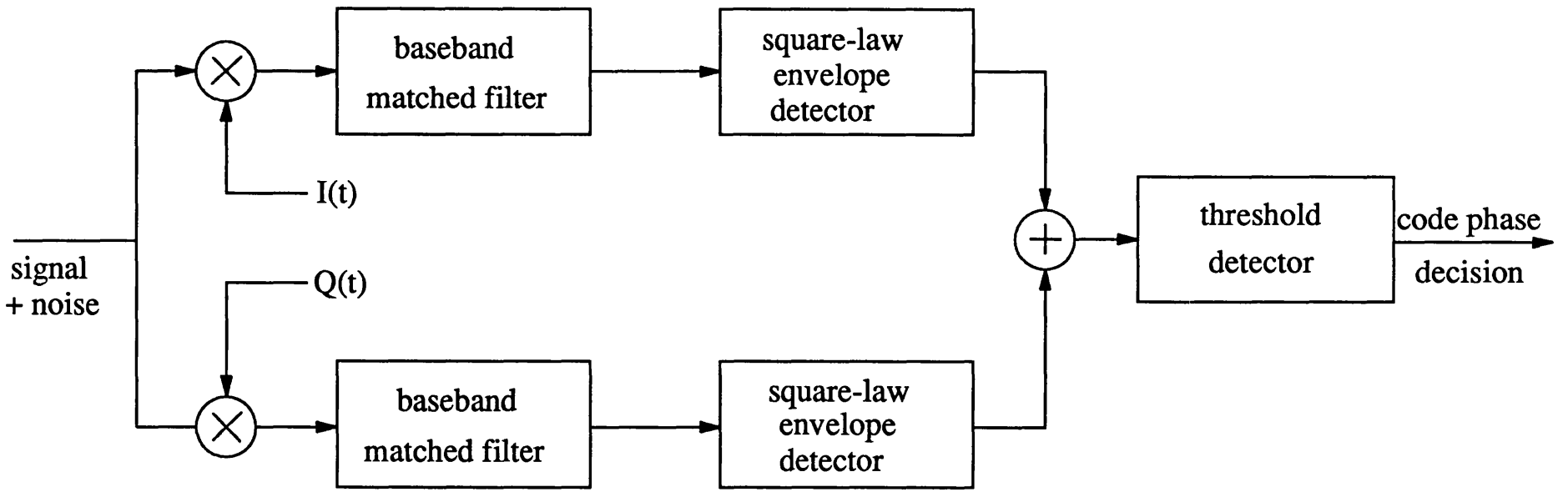

Figure 2.13 Schematic diagram of a matched filter: low-pass version

Glisic has proposed an *automatic decision threshold level control* (ADTLC) for DS spread-spectrum system based on matched filtering [39,40]. Fischer *et al* have described a wideband packet radio for multipath environment using DS spread-spectrum incorporating SAW convolvers as programmable matched filters coupled with binary post processing [41]. Recently, Su has suggested four rapid code acquisition algorithms with parallel and/or serial search using fixed/sequential detection employing PN matched filters [42].

Polydoros and Weber have presented a rapid acquisition scheme using matched filters [43] and have also analyzed the performance of matched filter acquisition using their unified approach [17]. A simple expression for the PN matched filter acquisition time has been presented by Pandit [10] which is given by:

$$T_{acq} = \frac{L}{2f_c}\left[P_{d1} + \sum_{v=1}^{\infty}(2v+1)P_{dv+1}\prod_{\mu=1}^{v}(1-P_{d\mu})\right] \tag{2.45}$$

where P_{dv} and T_v are given by

$$P_{dv} = P_d \exp(-n_{fa}T_v) \tag{2.46}$$

$$T_v = \min(T_{vr}, [v+0.5]\,L/f_c) \tag{2.47}$$

where T_v is the duration of the time interval, characterized by the property that a false alarm in the interval $(t_v - T_v, t_v)$ prevents the v^{th} correlation impulse from achieving lock and t_v is the instant of time at which the v^{th} correlation impulse actually occurs. T_{vr} is the false alarm verification time which is same as the penalty time defined earlier.

The quantities P_d and n_{fa} have to be computed from relevant system data or determined experimentally. In this thesis, reported in chapter 7, P_d and n_{fa} are obtained for the digital matched filter by means of a computer simulation. Pandit's analysis (and the simulation results in chapter 7) provide a comparison between the matched filter performance and the single-dwell serial search and shows that *above a certain value of the input SNR the matched filter yields faster acquisition but below this value the single-dwell system is faster.*

Analysis of the matched filter PN code acquisition receiver by Polydoros and Weber [15), using unified theory, assumes a non-coherent correlator/detector followed by a *coincidence detector* (CD). Upon a tentative decision of the *in-sync* condition the signal is passed through a coincidence detector which operates with the local code generator updated by the stored PN segment and repeated threshold tests are carried out over a fixed time. To strengthen the reliability of the verification operation performed by the CD these tests are now conducted over disjoint MT_c sec time intervals of the received waveform and are thus statistically independent. Upon successful completion of a *majority logic decision* on these

tests, the tracking loop is activated, whereas upon unsuccessful completion, the local code segment is again held fixed and the search continues. By means of their analysis using *unified theory*, the acquisition performance was derived for uniform and worst case *a priori* probabilities for both the non-coherent correlation detector and the coincidence detector and both exact and approximate results were presented. From the numerical results for typical system parameters, it was found that 2 out of 4 majority logic decisions were the optimal choice of the coincidence detector. Further, it was observed that even for the optimized system there exists a rather sharp *thresholding effect* in the sense that below a certain value of E_c/N_o the performance degrades rapidly.

2.7.1 Parallel and hybrid code acquisition schemes

A natural extension from the serial search techniques is to use two or more paths to search more than one code phase at a time with the hope that by increasing the complexity, the acquisition time might decrease in direct relation to the number of paths used. Though the maximum-likelihood detection represents a complete parallel structure, in recent times a few researchers have proposed and analyzed different forms of parallel and hybrid search acquisition schemes.

Milstein, Gevargiz and Das have proposed an acquisition scheme employing *parallel SAW convolvers* and have analyzed the performance both in search and lock modes [33] to arrive at key performance parameters. Cheng has proposed *a class of parallel and hybrid schemes* and has analyzed their performance in the presence of data modulation [44]. Su has presented performance analysis for *four classes of parallel serial acquisition schemes* employing either fixed dwell or sequential detectors [42] with non-coherent integration technique enabling the operation in the presence of data modulation.

The technique by Milstein *et al* [33] is based upon the parallel processing of the received waveform of DS-SS system with multiple SAW convolvers. In this scheme, the full period of sequence, L, is *divided into subsequences* of lengths M, assuming L/M an integer and the search is carried out using N convolvers each employing one of the subsequences as its reference input. *From the analysis it was shown that the parallel processing results in a reduction of the search time which is proportional to M times N.*

A similar approach using pseudonoise matched filters (PNMF) with *different detectors and hybrid search logics* was considered by Su [42]. Several of the proposals using PNMF fall as

the special cases of these algorithms. Performance analysis for four algorithms using PNMF was presented viz.,

1) *PL-FDD Parallel search with fixed dwell detector*
2) *PL-SD Parallel search with sequential detector*
3) *PS-FDD Parallel-serial search with fixed dwell detector*
4) *PS-SD Parallel-serial search with sequential detector*

All the algorithms use two stage procedures with the difference in the second stage and in the verification mode which employ either single-dwell or sequential detection algorithms. PL-FDD is based on maximum-likelihood estimate and makes a parallel decision which is optimum in the sense of minimizing the error probability. The second stage is the well known serial search algorithm. The PS-FDD algorithm makes a parallel decision within each section and examines each section in series. The PL-SD algorithm follows the steps of PL-FDD but uses sequential detection while the PS-SD algorithm follows the steps of PS-FDD and combines the steps of PL-SD algorithm.

From the numerical results, PS-FDD algorithm was found to be superior to PL-FDD algorithm, although this superiority dwindles as E_c/N_o gets higher. However, PL-FDD algorithm was found to be less insensitive to the variation of E_c/N_o. In the case of smaller uncertainty ranges, PS-FDD algorithm was seen to be less impressive. The performance of SD algorithms could not be obtained in the closed form, but tight bounds were obtained. It was found that the mean acquisition time of the PL-SD algorithm can be reduced to at least 7 to 8 times that of PL-FDD algorithm, for the typical parameters considered.

From a comparison of all four algorithms for an optimized set of system parameters, the PS-FDD algorithm was found to be a better choice when the uncertainty range is large. When the uncertainty range is smaller and/or the E_c/N_o becomes higher, which may result from Doppler rate, effects of large integration length, lower data rate, or an adaptive search algorithm, the superiority of the PS-FDD algorithm might have to be passed on to the PL-SD algorithm.

The approach presented by Cheng [44] partitions the correlation time into subintervals and the integration results of each of these subintervals are then non-coherently combined for detection. Two critical design problems were addressed, viz., the choice of the number of subintervals, J, and the degree of parallelism and consequently a totally parallel acquisition scheme and two hybrid schemes have been considered and analyzed. The trade-off between

non-coherent combining loss and data modulation degradation was found to result in the optimum choice of the number of subintervals, whereas the trade-off between *acquisition speed and hardware complexity* was seen to decide the degree of parallelism. This strategy offers a rich set of schemes, allowing easy trade-off between acquisition time and hardware cost. Two forms of data modulations, viz., the alternate data and random data, were considered and the performance of the schemes was analyzed.

From the analysis using circular state diagrams, it was also observed that a fewer number of subintervals are needed to combat the effect of data modulation which is because of the averaging effect of random data. For *hybrid schemes*, the selection of SNR and the detection threshold was seen to be important to the acquisition performance. The optimum number of coherent integration subintervals was found to be a function of total integration time, and the dependence of mean acquisition time on the number of subintervals decreases as the S/N increases.

2.7.2 Acquisition using partial correlation

A rapid acquisition scheme utilizing *partial correlation* of maximal length sequences has been presented by Mark and Blake [34]. This scheme uses *subsequence matched filtering* (SMF) to acquire the sync with matched filter output which is, in fact, the partial correlation function between the stored subsequence (the matched filter impulse response) and subsequences from either the same PN sequence or a different PN sequence in a multi-user environment. The acquisition characteristics of the scheme was derived and the performance was compared with that of Ward's RASE and RARASE.

$$T_{acq,SMF} = \frac{(M+m)\,T_e}{P_{acq}} \tag{2.48}$$

for $T_e = MT_c$ and P_{acq} the probability of sync acquisition.

It has been observed from the results that the subsequence length m has to be increased as the number of users increases to maintain a constant false alarm rate.

Comparison with RASE and RARASE reveals that in a low SNR environment the SMF technique offers rapid acquisition compared with RARASE. However, the system needs to be designed to operate below a threshold SNR to avoid steep increase in acquisition time.

A *modified two level acquisition scheme* similar to that of Mark and Blake [34] was proposed by Wilson, Rappaport and Vasudevan [45]. The scheme is a modification of the *two level*

coarse code acquisition scheme proposed by Rappaport and Schilling [46]. These schemes were described for use with FH systems and are said to be applicable for alternate spread-spectrum schemes also. Rappaport and Schilling's proposal employs a passive correlator in tandem with a bank of active correlators in which a threshold exceedance of the passive correlator initiates an interval of active correlation if any of the active correlators are idle. The scheme combines the rapid search capability of passive correlator with the decision reliability of (long) active correlation. The modified two level scheme [45] uses a bank of passive correlators followed by a bank of active correlators. By using *multiple passive correlators*, unlike the single passive correlator in the earlier proposal, this scheme reduces the probability of missing the short sync prefixed at the start of the coding (preamble), particularly in a fading environment. Analysis was done, based on queuing and detection theory, using a *Gilbert model* to characterize the fading signal. Performance in the presence of noise and jamming has been treated. The reduction in the miss probability using multiple prefixes as preamble has been compared to a single passive correlator case.

2.8 OTHER RESEARCH WORKS INTO CODE ACQUISTITION TECHNIQUES

In addition to the schemes and analyses reviewed hitherto, techniques suitable for FH, FH/DS, and FH/TH hybrid modulations were proposed by Elhakeem, Takhar and Gupta [47]. These techniques employ autoregressive spectral estimation to recover the FH code, quadrature processing for the DS code and simple threshold tests in conjunction with the adaptive filter (used for spectral estimation) to recover TH gating code.

These techniques require acquisition times only of the order of the shift register generator length whereas other schemes of serial and parallel search schemes require acquisition times of the order of the code lengths.

A comparison of schemes for coarse acquisition of FH signals was presented by Putman, Rappaport and Schilling [48] in which serial search, matched filter and two level schemes are compared. A review of basic acquisition methods and the limitations on the technology to realize them in various forms was presented by Rappaport and Grieco [49]. The mean acquisition time and its statistical moments were obtained by Baer [50] stochastic modelling of the square-law detector for a Bayes and Neyman-Pearson type of detectors. A bound on the acquisition time probability distribution was derived by using Chebyshev's inequality to obtain the variance of the acquisition time for a Hopkins type receiver by Leung and

Donaldson [51]. An all digital acquisition circuit using single-dwell serial search was analyzed and acquisition parameters were obtained for the case of correlated noise by Cherubini and Pupolin [52].

2.9 CONCLUSIONS

The common types of code acquisition technique for a direct-sequence spread-spectrum code acquisition have been reviewed. The general analysis techniques proposed for unifying the analysis of serial search acquisition strategies applicable to both uniform and non-uniform serial searches have been discussed. A variety of parallel and hybrid acquisition schemes using either totally parallel or parallel-serial schemes and their analyses have been described. Parallel search techniques using subsequence matched filters were addressed.

Though parallel architectures using maximum-likelihood techniques and matched filters can provide minimum acquisition time, this improvement needs to be traded against the increased hardware complexity. Simpler but optimum techniques using variable-dwell time and optimized search strategies offer better potential. Hitherto, much of the research in code acquisition has been centered around performance analyses and improvements in the search strategies. The problems relating to the *detector structures* and their optimality have received less attention. In this research the optimum detector is addressed and various realization techniques and their performances are analyzed. This work will be discussed in the subsequent chapters of this thesis.

2.10 REFERENCES

1) D.M. Di Carlo, C.L. Weber, "Multiple Dwell Serial Search Performance and Applications to Direct Sequence Code Acquisition", IEEE Trans. Comm., vol-com-31, no. 5, pp 650-659, May 1983.

2) P.M. Hopkins, "A Unified Analysis of Pseudonoise Synchronization by Envelope Correlation", ibid., vol-com-25, No. 8, pp 770- 777, August 1977.

3) A. Wald, *Sequential Analysis*, John Wiley and Sons, New York, 1947.

4) R.B. Ward, "Acquisition of Pseudonoise Signals by Sequential Estimation", IEEE Trans. Comm. Tech., vol-com-13, no. 4, pp 475- 483, Dec. 1965.

5) R.B. Ward, K.P. Yiu, "Acquisition of Pseudonoise Signals by Recursion- Aided Sequential Estimation", IEEE Trans. Comm., vol-com-25, no. 8, pp 784- 794, August 1977.

6) C.C. Kilgus, "Pseudonoise Code Acquisition using Majority Logic Decoding", ibid., vol-com-21, no. 6, pp 772- 774, June 1973.

7) H.M. Pearce and M.P. Ristenblatt, "The threshold Decoding Estimator for Synchronizationwith Binary Linear Recursive sequences", ICC 1971, Montreal, Canada, pp 43.25-43.30, June 12-14, 1971.

8) W.K. Alem and C.L. Weber, "Acquisition Techniques of PN Sequences", NTC 1977, Vol. II, pp 35:2.1 - 35:2.4, Dec. 5-7, 1977.

9) G.F. Sage, "Serial Synchronization of Pseudonoise Systems", IEEE Trans. Comm. Tech., pp 123-127, Dec. 1964.

10) M. Pandit, "Mean Acquisition Time of Active and Passive Correlation Acquisition Systems for Spread Spectrum Communication Systems", IEE Proc. Pt. F, vol. 128, no. 4, pp 211-214, August 1981.

11) R.F. Ormondroyd, V.E. Comley, "Limits on the Search Rate of a Pseudonoise Sliding Correlator Synchronizer due to Self Noise and Decorrelation", IEE Proc. Pt.F, vol. 131 , no. 7, pp 742- 750, Dec. 1984.

12) J.K. Holmes, C.C. Chen, "Acquisition Time Performance of PN Spread Spectrum Systems", IEEE Trans. Comm., vol-com-25, no. 8, pp 778- 783, August 1977.

13) D.M. Di Carlo, C.L. Weber, "Statistical Performance of Single Dwell Serial Synchronization Systems", ibid., vol-com-28, no. 8, pp 1382-1388, August 1980.

14) M.K. Simon *et al, Spread Spectrum Communications*, Vol III. Computer Science Press, Maryland, 1985.

15) J.I.Marcum, "A statistical theory of target detection by pulsed radar, Mathematical approach", IRE Trans. vol. IT-6, pp 145-267, April 1960.

16) A. Polydoros, C.L. Weber, "A Unified Approach to Serial Search Spread Spectrum Code Acquisition - Part I: General Theory", IEEE Trans. Comm., vol-com-32, no. 5, , pp 542- 549, May 1984.

17) A. Polydoros, C.L. Weber, "A Unified Approach to Serial Search Spread Spectrum Code Acquisition - Part II: A Matched Filter Receiver", ibid., pp 550- 560, May 1984.

18) A. Polydoros, M.K. Simon, "Generalized Serial Search Code Acquisition: The Equivalent Circular State Diagram Approach", ibid., vol-com-32, no. 12, pp 1260-1268, Dec. 1984.

19) A. Weinberg, "Generalized Analysis for the Evaluation of Search Strategy Effects on PN Acquisition Performance", ibid., vol-com-31, no. 1, pp 37-49, Jan. 1983.

20) V.M. Jovanovic, "Analysis of strategies for serial-search spread-spectrum code acquisition- Direct approach", ibid, vol. 36, no. 11, pp 1208-1220, November 1988.

21) S.M.Pan, D.E.Dodds and S.Kumar, "Acquisition time distribution for spread-spectrum receivers", IEEE Jou. on Sel. Areas in comm., vol. 8, no. 5, pp 800-808, June 1990.

22) W.R. Braun, "Performance Analysis for the Expanding Search PN Acquisition Algorithm", IEEE Trans. Comm., vol-com-30, no. 3, pp 424-435, May 1982.

23) H. Meyer, G. Polzer, "Performance Analysis for General PN Spread Spectrum Acquisition Techniques", ibid., vol-com-31, no. 12, pp 1317-1319, Dec. 1983.

24) J.K. Holmes, K.T. Woo, "An Optimum PN Code Search Technique for a Given A Priori Signal Location Density", NTC '78, pp 18.6.1 - 18.6.6, 1978.

25) J.H. Chiu, L.S. Lee, "An Improved Sequential Estimation Scheme for PN Acquisition", IEEE Trans. Comm., vol-com-36, no. 10, pp 1182-1184, Oct. 1988.

26) D.M. Grieco, "The Application of Charge Coupled Devices to Spread Spectrum Systems", ibid., vol-com-28, no. 9, pp 1693-1705, Sept. 1980.

27) D.M. Grieco, "Inherent Signal-to-Noise Ratio Limitations of Charge Coupled Device Pseudonoise Matched Filters", ibid, vol-com-28, no. 5, pp 729-732, May 1980.

28) E.G. Magil *et al*, "Charge Coupled Device Pseudonoise Matched Filter Design", ibid, vol 67, pp 50-60, Jan. 1979.

29) L.B. Milstein, P.K. Das, "Spread Spectrum Receiver using Surface Acoustic Wave Technology", ibid., vol-com-25, no. 8, pp 841-847, Aug. 1977.

30) K. Dostert, M. Pandit, "Performance of a SAW Tapped Delay Line in an Improved Synchronizing Circuit", ibid., vol-com-30, no. 1, pp 219-222, Jan. 1982.

31) J. Hjelmstad, R. Skaug, "Fast Synchronization Modem for Spread Spectrum Communication System using Burst Format Message Signalling", IEE Proc. Pt. F, vol. 128, no. 6, pp 370-378, Nov. 1981.

32) M. Kowatsch, "Application of Surface Acoustic Wave Technology to Burst Format Spread Spectrum Communications", ibid., vol. 131, no. 7, pp 734-741, Dec. 1984.

33) L.B. Milstein, J. Gevaritz and P.K. Das, "Rapid Acquisition for Direct Sequence Spread Spectrum Communications Using Parallel SAW Convolvers", IEEE Trans. Comm., vol-com-33, no. 7, pp 593-600, July 1955.

34) J.W. Mark, I.F. Blake, "Rapid Acquisition Techniques in CDMA Spread Spectrum Systems", IEE Proc. Pt. F, vol. 131, no. 2, pp 223-232, April 1984.

35) A Baier, "A Low Cost Digital Matched Filter for Arbitrary Constant Envelope Spread Spectrum Waveforms", IEEE Trans. Comm., vol-com-32, no. 4, pp 354-361, April 1984.

36) G.L. Turin, "An Introduction to Digital Matched Filters", Proc. IEEE, vol. 64, pp 1092-1112, July 1976.

37) N. Couturier, J. Wight and L. Pearce, "Experimental Results for Four Phase Digital Matched Filtering of Spaced Spectrum Waveform", IEEE Trans. Comm., vol-com-34, no. 8, pp 836-840, August 1986.

38) G. Levita, "The Performance of Digital Matched Filters for Multilevel Signals", ibid., vol-com-31, no. 11, pp 1217-1226, Nov. 1983.

39) S.G. Gilsic, "Automatic Decision Threshold Level Control (ADTLC) in Direct Sequence Spread Spectrum System based on Matched Filtering", ibid., vol. 36, no. 4, pp 519-527, April 1988.

40) S.G. Glisic, "Modified Two Level, Double Search Synchronization of Direct Sequence Spread Spectrum Systems", 1984 Zurich Seminar, Paper H 3.1- H 3.8, pp 143-150.

41) J.H. Fischer *et al*, "Wide Band Pocket Radio for Multipath Environments", IEEE Trans. on Comm., vol-com-36, no. 5, pp 564-576, May 1988.

42) Y.T.Su, "Rapid Code Acquisition Algorithms Employing PN Matched Filters", vol. 36, no. 6, pp 724-733, June 1988.

43) A Polydoros, C.L. Weber, "Rapid Acquisition Techniques for Direct Sequence Spread Spectrum Systems", ICC 1981, pp A7.1.1 - A7.1.5.

44) U. Cheng, "Performance of a Class of Parallel Spread Spectrum Code Acquisition Schemes in the Presence of Data Modulation", IEEE Trans. Comm., no. 5, pp 596-604, May 1988.

45) N.D.Wilson, S.S. Rappaport, M.M. Vasudwan, "Rapid Acquisition Scheme for Spread Spectrum Radio in a Fading Environment", IEE Proc. Pt. F, no. 1, pp 95-103, Feb. 1988.

46) S.S. Rappaport, D.L. Schilling, "A Two Level Coarse Code Acquisition Scheme for Spread Spectrum Radio", IEEE Trans. Comm., vol-com- 28, no. 9, pp 1734-1742, Sept. 1980.

47) A.K. Elhakeem, G.S. Takhar and S.C. Gupta, "New Code Acquisition Techniques in Spread Spectrum Communication", ibid., vol-com-28, no. 2, pp 249-257, Feb. 1980.

48) C.A. Putman, S.S. Rappaport and D.L. Schilling, "A Comparison of Schemes for Coarse Acquisition of Frequency Hopped Spread Spectrum Signals", ibid., vol-com-31, no. 2, pp 183-189, Feb. 1983.

49) S.S. Rappaport, D.M. Grieco, "Spread Spectrum Signal Acquisition: Methods and Technology", IEEE Comm. Soc. Magazine, vol. 22, no. 6, pp 6-21, June 1984.

50) H.P. Baer, "The Calculation of the Statistical Properties of the Synchronization Times in a PN Spread Spectrum System for Minimized Acquisition Time Designs", IEEE Trans. Comm., vol-com-28, no. 5, pp 733-739, May 1980.

51) V.C.M. Leung, R.W. Donaldson, "Confidence Estimates for Acquisition Times and Hold- In Times for PN-SSMA Synchronizer Employing Envelope Correlation", ibid., vol-com-30, no. 1, pp 230- 240, Jan. 1982.

52) G. Cherubini, S. Pupolin, "Performance Analysis of an All Digital Acquisition Circuit", ibid., vol-com-33, no. 8, pp 862-868, August 1985.

CHAPTER 3

SEQUENTIAL DETECTION PN CODE ACQUISITION

3.1 INTRODUCTION

In this chapter the application of statistical decision theory to hypothesis testing is introduced. The application of decision theory to signal detection problems (called detection theory) is described and the signal detection problem is introduced. The elements of a statistical decision problem is identified and the generalized statistical hypothesis testing is then described. The decision criteria and the optimum decision rules of the detection problem are described and the merits and demerits of different decision rules, namely, Bayes decision rule, Neyman-Pearson and the minimax decision rules etc., highlighted. The significance of the receiver operating characteristics (ROC) for the detection problem are also discussed. In addition, the basic differences between parametric detection and non-parametric detection (sub-optimum detection) are also identified and a comparative measure of detector performance namely, asymptotic relative efficiency (ARE) is described.

The fundamental differences between a fixed sample size test and a variable length test are presented and the concept of a sequential test is defined. The advantages of sequential hypothesis testing over a fixed sample size test are brought out and the sequential probability ratio test (SPRT) is described. The major performance criteria of the sequential test viz., the operating characteristic function (OCF) and the average sample number (ASN) function are discussed. The complexities in the analysis of the sequential detection are highlighted and the biased square law detector is introduced together with its low SNR approximations. Finally, the application of sequential detection theory to the acquisition of spread-spectrum PN codes is described and the existing research work in this area reviewed.

3.2 STATISTICAL DECISION THEORY

The reception of signals in real-life channels presents many problems to a communication systems theorist as the waveforms appearing at the channel output may be perturbed and contaminated to such an extent that they only faintly represent the transmitted signal.

Therefore, any reliable communication system must use optimum processing to recover the information, which is embedded in the noise, in the most efficient manner. The reception problem is concerned with finding these strategies for processing the received data to combat the pernicious effects of the channel.

The reception problem can be viewed in two ways. One problem of signal reception is to detect the presence or the absence of the signal, that is, to detect whether the noise corrupted signal represents either the signal or the noise. This is conventionally called *signal detection.* The other problem of signal reception is to estimate the signal as a continuous function of time as accurately as possible which is called *signal estimation.* Signal estimation is a process of signal smoothing and filtering. This is an analog process in which the signal to be estimated can have a continuum of values for each instant of time. The receiver estimates the values of a waveform which may be viewed as a sample function of the random process.

In signal detection, the receiver knows *a priori* the set of symbols and their associated waveforms and makes a decision on which of the symbols was being transmitted during the observation interval. Since these decisions are based on the processing of the corrupted signal, the receiver usually makes errors. Optimum reception of the signal is based on the general theory of statistical inference by means of hypothesis testing which has been expanded into statistical decision theory with the pioneering works of Bayes, Neyman and Pearson, Wald [1-3] and others. Both detection and estimation can be formulated as problems in statistical decision theory. The development and analysis of the optimum methods required to estimate the signal correctly leads to *estimation theory* whereas the analyses of the optimum detection methods form *detection theory.*

3.2.1 Elements of a statistical decision problem

The basic elements of a general statistical decision problem are:

i. a set of hypotheses that characterize the possible true states of the process (ie., *a priori* knowledge about the waveforms/symbols).

ii. a test in which data is obtained from which the truth is to be inferred (ie., sampling).

iii. a decision rule that operates on the data to decide optimally which hypothesis in fact best describes the true hypothesis.

iv. a criterion of optimality that reflects the cost of correct and incorrect decisions.

3.2.2 Statistical hypothesis testing

One of the most important statistical tools for making decisions is *hypothesis testing*. Hypotheses are the statements of possible decisions that are being considered. In the communication detection problem, for example, this corresponds to whether the signal is present or absent. Corresponding to each hypothesis there is a probabilistic description of the possible outcome. This probabilistic description, coupled with a criterion or a measure of goodness that the decision will satisfy on the average, dictates a dichotomy (for two hypotheses) of the sample space over which the outcome of the experiment is defined. This dichotomy represents the best (optimum) decision rule subject to the criterion of goodness.

In a binary communication system which transmits either a pulse $s(t)$ or no pulse in an interval of time T, the hypothesis that the received waveform does not contain a signal has to be tested against the hypothesis that the received waveform does contain a signal. The first hypothesis is called the *null hypothesis* normally denoted by H_0 while the second hypothesis is called the *alternative hypothesis* which is denoted by H_1. If the signal to be detected is deterministic, that is, its structure is completely known, then H_1 is called the *simple alternative*. When the signal to be detected is a member of a finite or infinite set of signals then H_1 is called a *composite hypothesis*. In this case even if the hypothesis H_1 is decided, we can only conclude that one member of the signal class is present whose identity is not revealed by the test.

Figure 3.1 shows a general decision problem in terms of mathematical representation in vector spaces. The vector spaces considered are defined as follow:

Signal space, Ω: This is defined as a space in which the class of possible signals can be represented as points s, with each point in space representing a waveform with a particular combination of the signal parameters such as amplitude, phase, doppler and so on. A probability of occurance is assigned to each combination of signal parameters which is normally contained in a joint *a priori* probability density function $\sigma(s)$ over all the points s in signal space Ω.

Noise space, N: This is defined as a space in which all possible waveform realizations of the noise process within the observation interval are represented as points n. From the statistical and spectral properties of noise, an *a priori* joint probability density function $p(n)$ can be deduced which describes the probability of occurance of waveforms in this space.

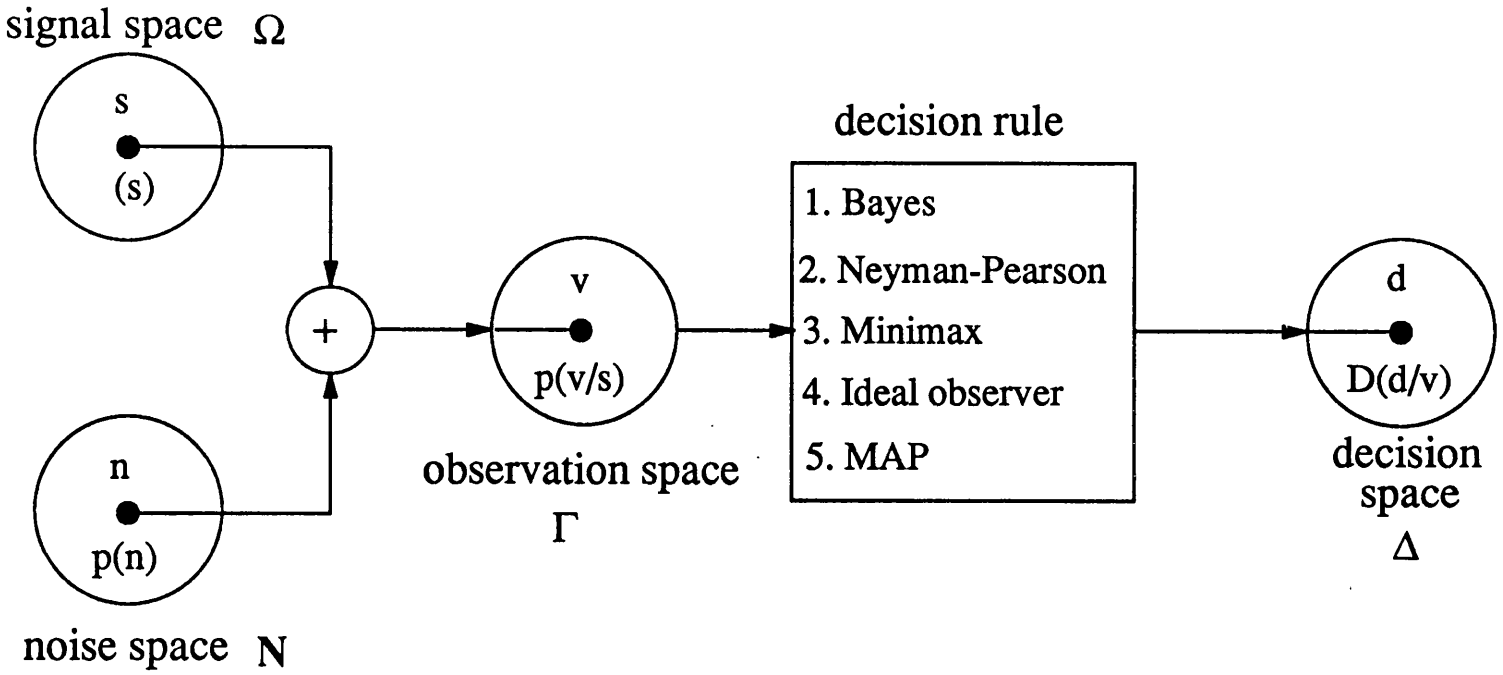

Figure 3.1 General decision problem in vector spaces

Observation space, Γ: This space is defined by means of points v which represent all possible joint combinations of signal plus noise waveforms. The probability of occurance of these waveforms in this space are described by an *a priori* probability density function which is written as a conditional probability $p(v/s)$ and shows explicitly the dependence of the waveform v on the signal s. For convenience, the null hypothesis, $s = 0$, is also included as a point in Γ.

Decision rule: An essential feature of statistical decision theory is the *decision rule* which depends only on the observed waveform v and not on the signal s. A *decision rule* is one that leads to decision d as a result of observation v, and is denoted by $D(d/v)$. The decision rule $D(d/v)$, mathematically describes the conditional probability of deciding d having observed v.

Decision space, Δ: The set of possible decisions d (normally $d_0 = no$ and $d_1 = yes$) in a statistical decision problem can be described as points in a *decision space* Δ with decision rule $D(d/v)$ describing the probability of decision (each point) in the decision space for every possible waveform v. In a signal detection problem, the decision space contains only two points: signal present and signal absent.

With these definitions of the vector spaces, the decision rule can be interpreted as a *mapping* from the observation space Γ into decision space Δ with a preassigned probability $D(d/v)$. Hence, the essence of the decision problem is the *decision rule* that accomplishes this mapping in an optimum way with respect to a particular criterion of excellence.

Signal estimation problems can also be formulated as a statistical decision problem similar to the signal detection problem. However, in this case, the decision space is of the same dimensionality as the signal space unlike the signal detection problem in which the decision space contains only two points.

In the following sections, the optimum decision criterion and various optimum decision rules are described using the above notation.

3.2.2.1 Ratio criterion and Likelihood ratio:

When the samples are submitted to the observer, he employs a certain criterion based on which decision rule is devised. As the *a priori* probability density function of noise is given by $p(v/o)$ and signal plus noise is given by $p(v/s)$ (expressed as conditional probabilities) then a function $\lambda(v)$, defined as:

$$\lambda(v) = \frac{p(v/s)}{p(v/o)} \tag{3.1}$$

represents *the likelihood that the sample is drawn from the signal space relative to the likelihood that it is drawn from the noise space.* Thus, for each sample in the observation space, with a threshold $\eta \geq 0$, a *certain criterion* $A(\eta)$, is selected (eg., minimum average risk or maximum probability of detection etc.,) by using which a list of samples can be chosen satisfying $\lambda(v) \geq \eta$. Hence, if $\lambda(v)$ is sufficiently large it would be reasonable to conclude that the sample is from the signal space. Such a criterion of the form $A(\eta)$ is called the *ratio criterion.* Though a number of definitions are available for a certain criterion being optimum, each of these optimum criteria can be expressed as ratio criterion so that a receiver designed to give a *likelihood ratio* as output could be used with any of them.

3.2.2.2 Optimum decision rule:

An optimum decision rule in a statistical decision problem is the one that gives the best performance when compared to each possible decision rule, normally evaluated on the basis of its relative performance. A method of evaluating such a performance is based on the notion of *a simple cost or loss function* introduced by Wald [3] which associates a quantitative cost $C(s,d)$ with each point s in signal space Ω and each point d in decision space Δ. This function describes the loss incurred by the received system that results in a decision space d for every point s in signal space Ω. One such decision rule that describes a receiver with least average loss is called the *Bayes rule* and the receiver is called a *Bayes Receiver*, however, other decision rules have also been derived based on different performance criteria. Depending upon *the performance criteria* used, the decision rules can be classified as follows:

1) Bayes rule
2) Neyman-Pearson rule
3) Minimax rule
4) Ideal observer criterion
5) MAP decision rule

For a general detection problem when testing hypothesis H_0 (no signal present) against H_1 (signal present) four possible situations arise.

The detector can:

i. accept hypothesis H_0 when hypothesis H_0 is true (correct dismissal)

ii. accept hypothesis H_1 when hypothesis H_0 is true (false alarm)

iii. accept hypothesis H_1 when hypothesis H_1 is true (correct detection)

iv. accept hypothesis H_0 when hypothesis H_1 is true (miss detection)

Decisions i) and iii) are the correct decisions. Error ii) is called a type I error denoted by α and error iv) is called a type II error denoted by β in statistical terminology. α is also referred to as the *level* or *size* of the test whereas $1-\beta$ is referred to as the *power* of the test. In the terminology of communication theory, outcomes ii) and iv) are called the false alarm probability (P_{fa}) and the miss detection probability (P_{md}) respectively. These errors are expressed as:

$$\alpha = \int_{\Gamma} p(v/o)\, D(d_1/v)\, dv \tag{3.2}$$

$$\beta = \int_{\Gamma} p(v/s)\, D(d_o/v)\, dv \tag{3.3}$$

where $p(v/o)$ and $p(v/s)$ are the conditional probability of observing v with signal absent and signal present, and $D(d_1/v)$ and $D(d_o/v)$ are the decision probabilities for decision d_1 and d_o respectively with observation v. The average probability of error denoted by P_e, is often represented as

$$P_e = P(H_o)P(D_1/H_o) + P(H_1)P(D_o/H_1) \tag{3.4}$$

where $P(H_o)$ and $P(H_1)$ are the probability that hypothesis H_o or H_1 are true and $P(D_1/H_o)$ and $P(D_o/H_1)$ are the conditional probability of deciding d_1 or d_o given the hypothesis H_o or H_1 respectively.

3.2.2.2.1 Bayes decision Rule

Bayes criterion is based on the use of a systematic procedure of assigning costs to each decision and then minimizing the total average cost. Defining C_{ij} as the cost associated with choosing hypothesis H_i when actually hypothesis H_j is true, the four possible decisions defined above can be assigned four cost parameters namely C_{00}, C_{10}, C_{11} and C_{01} respectively. The average cost is expressed as:

$$\overline{C} = C_{00}P(H_o)P(D_o/H_o) + C_{10}P(H_o)P(D_1/H_o) + C_{01}P(H_1)P(D_o/H_1) + C_{11}P(H_1)P(D_1/H_1) \tag{3.5}$$

On substituting the probability functions and minimizing the average cost, the Bayes decision rule is derived as:

$$P(H_1)(C_{01}-C_{11})p(v/s) < P(H_o)(C_{10}-C_{00})p(v/o) \tag{3.6}$$

In terms of the likelihood ratio, this can be expressed as:

$$\lambda(v) = \frac{p(v/s)}{p(v/o)} \; >^{H_1}<_{H_o} \; \frac{P(H_o)(C_{10}-C_{00})}{P(H_1)(C_{01}-C_{11})} \tag{3.7}$$

where the symbol $>^{H_1}<_{H_o}$ denotes that the hypothesis H_1 is accepted if the likelihood ratio is greater than the right hand side (R.H.S) of the equation and the hypothesis H_o is accepted if the likelihood ratio is less than the R.H.S. Tests of this kind are also called *likelihood ratio tests* and the right hand side of the equation is called the *threshold* of the test.

3.2.2.2.2 MAP decision rule or a posteriori decision rule

This decision criterion maximizes the *a posteriori* probability $P(H_i/v)$ which is computed after observation v has been made. This decision rule usually leads to a partition of the decision region in to two regions Γ^0 and Γ^1 and H_o or H_1 is chosen depending on a given observation v in either Γ^o or Γ^1 based on the decision rule:

$$\frac{P(H_1)p(v/s)}{P(H_o)p(v/o)} \; >^{H_1}<_{H_o} \; 1 \tag{3.8}$$

$$\frac{p(v/s)}{p(v/o)} \; >^{H_1}<_{H_o} \; \frac{P(H_o)}{P(H_1)} \tag{3.9}$$

Effectively, the MAP decision rule consists of comparing the likelihood ratio with the constant, $P(H_o)/P(H_1)$ which is called the decision threshold. As the decision threshold is purely based on maximizing the *a posteriori* probabilities this is called *maximum a posteriori probability criterion.* This approach has the advantage of getting more information as the observer makes the best possible estimate of the probability of each transmitted message (samples) that his equipment can give him [5].

3.2.2.2.3 Ideal observer criterion or Minimum error probability criterion

The ideal observer criterion originated with Seigert [4] and consists of choosing the dichotomy of decision space into Γ^o and Γ^1 such that the total average probability of error is minimized. This can be used when the cost of correct decisions is assumed or known to be zero and the cost of incorrect decisions is taken to be one (ie., $C_{00} = C_{11} = 0$ and $C_{01} = C_{10} = 1$). This criterion still requires the *a priori* probabilities to be known.

3.2.2.2.4 Neyman-Pearson Rule

Both Bayes and MAP decision rules require the *a priori* probabilities and the relative costs to be known. However, in many circumstances, when neither the cost functions nor the *a priori* probabilities are available, the Neyman-Pearson (N-P) and the minimax criterion are used.

The main advantage of the Neyman-Pearson over the Bayes and ideal observer criteria is that *it yields a detector which keeps the false alarm probability less than or equal to a pre-chosen value and maximizes the probability of detection for the given false alarm probability*. It is based on the Neyman-Pearson lemma of hypothesis testing [2] which is stated as follows:

The necessary and sufficient conditions for a test to be most powerful of level α_o (maximum detectability for a given probability of false alarm) for testing hypothesis H_o against the alternative H_1 are that the test satisfies the conditions:

$$\int_{\Gamma} p(v/o)\, D(d_1/v)\, dv = \alpha_o \tag{3.10}$$

$$\lambda(v) = \frac{p(v/s)}{p(v/o)} \; >^{H_1}<_{H_o} \; \eta \tag{3.11}$$

for the decision threshold η.

This criterion can be shown to be a special case of Bayes criterion with the likelihood test set to maximize the probability of detection, $P(D_1/H_1)$ [45].

3.2.2.2.5 Minimax criterion

The Bayes criterion requires both cost and *a priori* probabilities to be known. For the minimum error probability criterion or the maximum *a posteriori* criterion only the *a priori* probabilities need to be known. For the Neyman-Pearson criterion neither costs nor the *a priori* probabilities are required. The minimax rule is used when the costs are given but the *a priori* probabilities are not known.

This decision rule minimizes the maximum expected cost. When the *a priori* probability is known, the Bayes criterion gives the minimum average cost. If the *a priori* probability is a pure guess then the cost would be always greater than the Bayes cost. However, using the minimax criterion the maximum possible cost when the *a priori* probabilities are unknown is minimized. Therefore, the solution involves finding the least favourable *a priori* probability among the Bayes solutions which is corresponding to the value of *a priori* probability for which the average cost is maximum. The criterion also leads to a decision rule

$$\lambda(v) = \frac{p(v/s)}{p(v/o)} \; >H_1<H_o \; \eta \tag{3.12}$$

As the minimax rule is a Bayes rule relative to a least favourable distribution (the minimax average loss is the maximum of all Bayes losses), it is often criticized as being too conservative and the reasonableness of its use depends on the application.

Thus, in each case, the decision rule leads to a comparison of the likelihood ratio with different threshold values. A receiver that computes the likelihood ratio $\lambda(v)$ for all possible v compares this value with an adjustable threshold can realize any of these tests.

3.2.3 Receiver Operating Characteristics (ROC)

The performance of the decision rules are normally displayed in terms of the probability of detection versus the probability of false alarm for various values of the threshold. These curves are called ROC curves. If the type of criterion chosen for a particular application is a ratio criterion then the complete description of the detector system performance can be read off from the ROC curves [7]. From the definition of the ROC curves, the false alarm probability P_{fa} is shown as the abscissa (x-coordinate) and the probability of detection P_d as the ordinate (y-coordinate) as shown in figure 3.2. The operating point or the operating level of the detector can be derived from the ROC curve as a slope at the point given by $Q_d(X,Y) = \{[P_{fa}[A(\eta)], P_d[A(\eta)]\}$ where the probabilities are for the selected criterion $A(\eta)$ with η as operating level (or threshold). Since most proposed kinds of optimum criteria can be reduced to the ratio criteria, the ROC curve assumes considerable importance in the understanding of detector characteristics. However, in some of the statistical hypothesis tests the operating characteristic function (OCF) is used which is the characteristic of $(1 - P_d)$ *vs* θ with P_{fa} varied, as shown in figure 3.3, where θ normally represents the signal parameter eg., mean or SNR.

3.3 PARAMETRIC AND NON-PARAMETRIC DETECTION

Detection theory is often concerned with the determination of optimum detection utilizing the Neyman-Pearson hypothesis test or the Bayesian approach to hypothesis testing. These methods require the statistical description of the interfering noise process which may be assumed or obtained by the actual measurements. However, the resulting optimum detector using these hypothesis is often difficult to implement.

Another class of detectors called *adaptive or learning detectors* operate in *a near optimum sense* without even a complete statistical description of the background noise. This can be achieved by allowing the system parameters or structure to change as a function of the input. Due to their continually varying structure, adaptive detectors are difficult to analyze mathematically and must be simulated on a computer. Additionally, since the detector structure is a function of the input, it is also dependent on the operating environment and as a

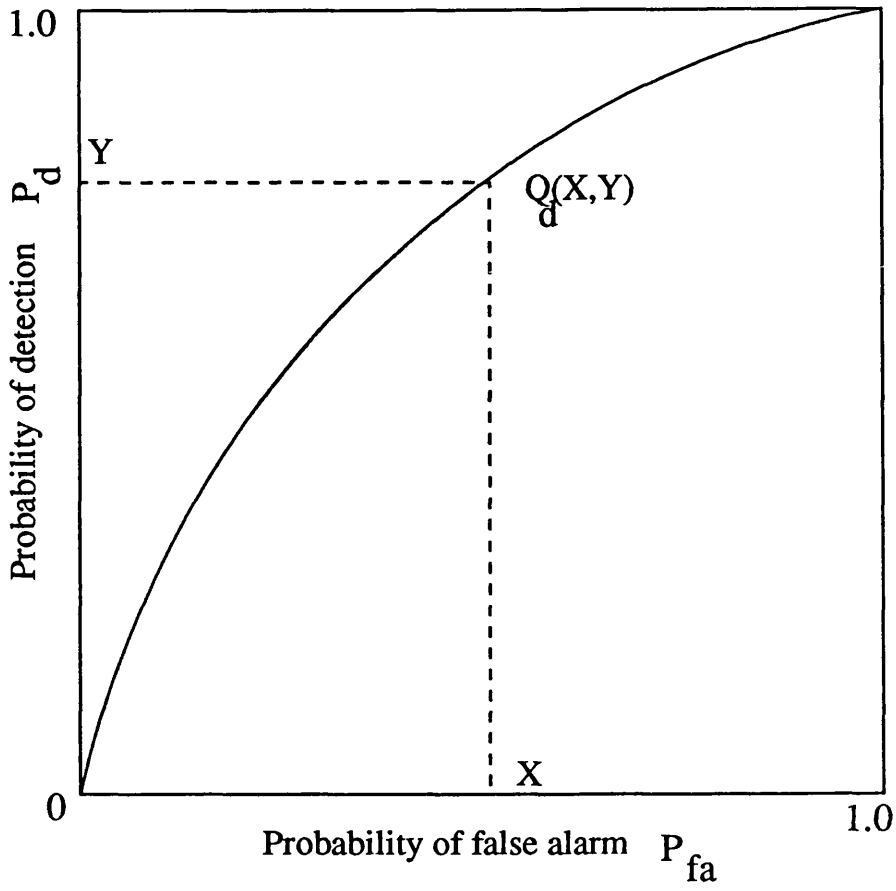

Figure 3.2 Typical ROC curve

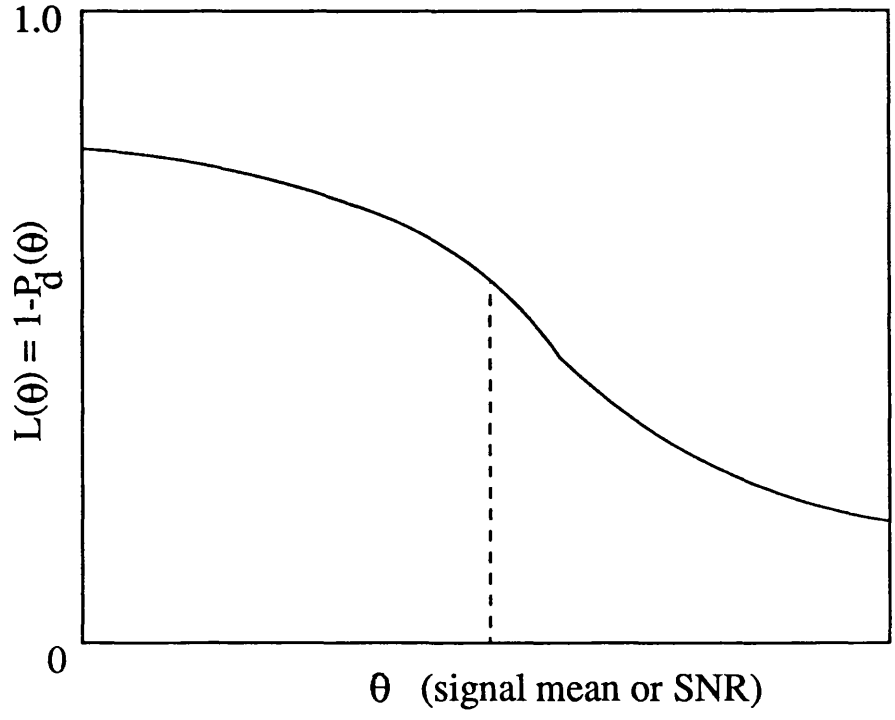

Figure 3.3 Typical OCF curve

result they are generally complex to implement.

When the statistical description of the input noise process is not available, or when the optimum or the adaptive detector is too complex to implement, a non-optimum detector often provides a satisfactory performance. A class of non-optimum detectors called *non-parametric* or *distribution-free* detectors exists which is simple to implement and requires little knowledge of the underlying noise distribution. *Non-parametric* refers to a class of detectors where the input distribution has a specified shape or form but still cannot be classified by a finite number of real parameters. The *distribution-free* detector refers to a class of detectors which makes no assumptions at all concerning the form of the input distributions [8].

3.3.1 Non-parametric versus parametric detection

The differences between non-parametric and parametric detectors can be well described by considering the binary detection problem. Parametric detection utilizes the known form of the probability density function, pdf, of the random observation samples to arrive at the form of the detector D. If the actual pdf's of the observed input signal v are the same as those assumed in determining the detector D, then the performance of the detector in terms of the probability of detection and false alarm is quite good. However, if the densities are significantly different from those assumed , then the performance of the parametric detector may be poor. On the other hand, non-parametric detectors do not assume that the input pdf's are completely known but only make general assumptions about the input, such as the symmetry of the pdf and continuity of the cumulative distribution function. Since a large number of density functions satisfy these assumptions, the pdf's of the input observation v may vary over a wide range without altering the performance of the non-parametric detector. Thus, the performance of a parametric detector depends on the actual input pdf while the non-parametric detector, however, maintains a fairly constant level of performance due to its general assumptions on the form of input pdf.

When applied to the same problem, the performance of the parametric and the non-parametric detectors depends on how well the assumptions of the two detectors are met with. For instance, if the parametric detector is based on the Gaussian assumption and the non-parametric detector on the symmetry of the input pdf and the continuous cumulative distribution function, then for Gaussian inputs the parametric detector will be significantly better than the non-parametric detector. However, if the input densities are non Gaussian but

still symmetric, then the non-parametric detector performs better than the parametric detector.

Another important property is their relative ease of implementation when compared with parametric detectors. For example, an optimum parametric detector for detecting a known signal of positive amplitude in additive white noise on the basis of a set of observations $v = \{v_1, v_2, v_3, \ldots\ldots, v_n\}$ with the noise of zero mean Gaussian density with known variance σ^2 is:

$$D(v) = \begin{cases} 0 & \text{if} \quad \sum_{k=1}^{n} v_k < \eta_o \\ 1 & \text{if} \quad \sum_{k=1}^{n} v_k > \eta_o \end{cases} \tag{3.13}$$

where $\sum_{k=1}^{n} v_k$ is known as test statistic and η_o is known as the threshold of the test.

The simplest non-parametric detector is called the *sign test* and bases its decision only on the signs of the input observations. The sign detector has the form:

$$D(v) = \begin{cases} 0 & \text{if} \quad \sum_{k=1}^{n} u(v_k) < \eta_1 \\ 1 & \text{if} \quad \sum_{k=1}^{n} u(v_k) > \eta_1 \end{cases} \tag{3.14}$$

where $u(v_k)$ is the unit step function, whose value is 0 if $v < 0$ and 1 if $v \geq 0$, and η_1 is the threshold. Clearly, the parametric detector compares the sum of observations against the threshold η_o whereas the non-parametric detector simply determines the polarity of each observation, counts the number of positive observations and compares the total against the threshold η_1. Since the parametric detector requires the observations to be summed and the non-parametric detector requires only the positive observations to be found, the non-parametric detector is considerably simpler to implement. However, the most important property of the non-parametric detectors is the maintenance of a constant level of performance even for wide variations in the input noise density.

3.3.2 Asymptotic Relative Efficiency (ARE)

If two detectors D_1, D_2 using the same hypothesis and the same significance level α (or P_{fa}), and for the same power $1-\beta$ (or P_d) with respect to the same alternative, one detector requires a sample size N_1 and the other detector requires a sample size N_2 then the *relative efficiency* of the first detector D_1 with respect to the second detector D_2 is given by the ratio

$$e_{1,2} = N_2/N_1 \tag{3.15}$$

Since the relative efficiency is a function of the significance level, α, alternative H_1 and the sample size of the two detectors (ie., α, H_1, N_1 and N_2), it is highly dependent on the experimental procedures used while taking the data. It also requires all possible values of α, H_1, N_1 and N_2 to be computed to find a suitable N_2 particularly for a small value of N_1, such that the powers of the two detectors are exactly equal. Some kind of interpolation methods have been employed in the past, but found to be inconsistent [8,9]. Thus, the *finite sample relative efficiency* is difficult to compute as it is highly dependent on experimental methods and even peculiar to the mathematical techniques.

However, a simpler expression can be obtained by holding the significance level and the power constant while the two sample sizes approach infinity and the alternative approaches null hypothesis. This leads to the concept of *asymptotic relative efficiency* (ARE).

The ARE of the detector D_1 with respect to the detector D_2 can be written as

$$E_{1,2} = \underset{\substack{n_1 \to \infty \\ n_2 \to \infty \\ H_1 \to H_o}}{Lt} \frac{n_2}{n_1} \tag{3.16}$$

where n_1 and n_2 are the smallest number of samples necessary for the two detectors to achieve a power of $1-\beta$, for the same hypothesis, alternative and the significance level.

3.3.3 Historical development of signal detection

Decision theory was first studied by Thomas Bayes [1] in the middle of the eighteenth century. However, significant contributions to classical decision theory were made by Neyman and Pearson (1933) [2] who proposed tests that minimize the chances of error. The notions of cost and risk were introduced by Wald (1939) [3]. Seigert, Lawson and Uhlenbeck (1950) [4] applied these ideas to the problem of radar detection. Later Woodward and Davies (1952) [5] used the concept of inverse probability in the study of signal detection. The analysis of signal detection in terms of statistical decision theory was developed by Middleton (1953) [6] while the design of receivers on the basis of the likelihood ratio was advanced by Peterson, Birdsall and Fox (1954) [7].

3.4 FIXED SAMPLE TEST AND SEQUENTIAL TESTING

The statistical decision theory so far discussed assumes that a decision is rendered after a fixed observation interval in which the data is collected. The observations made during this interval may consist of, in general, discrete or sampled (continuous) waveforms. However, in some systems, the observation interval is of variable length instead of being fixed and is dependent on the input data. This is advantageous when the observation interval is needed to be as small as possible.

A test procedure with a variable length observation period was developed by Wald [10] which is known as the *sequential test.* A similar concept was considered by Neyman and Pearson [5] in 1933 as an extension of their theory of hypothesis testing. Their test contained three possible decisions which are: accept hypothesis H_o, reject H_o and no decision. In Wald's sequential test, it is decided whether to make a decision based upon the data already taken or to continue taking more data to improve the decision. The length of the observation interval depends on the quality of the available data. Although it is theoretically possible for a test to continue indefinitely, it has been shown that on average the observation interval is shorter in a sequential test than in a fixed test [10]. Furthermore, in practice, the sequential test is usually truncated after some predetermined number of observations. Though significant work has been done in the application of decision theory to nonsequential tests, with the availability of improved signal processing techniques the sequential tests have gained greater significance.

3.5 SEQUENTIAL DETECTION

Bayes' methods of statistical inference are optimum in the sense that no other hypothesis test can achieve a smaller average risk. However, this test assumes that the number of samples are fixed and determined in advance. If this constraint is relaxed then it is possible to construct hypotheses tests which are superior to Bayes' tests in the sense that, on average, a substantially smaller number of observations is required to achieve the same type I and type II error probabilities. These tests are called *sequential tests* and the application of these tests to detection problems is usually called *sequential detection* and a receiver that performs the sequential test is called a *sequential receiver or a sequential detector.*

In the sequential tests for each sample taken, if the evidence is strong enough, then the decision is taken as to whether the received signal is drawn from the signal space or from the

noise space. If the evidence is not strong then the next sample is taken and the evidence is rechecked. The process is continued until the resulting evidence persuades in favour of the one of the spaces. Thus, an essential feature of a sequential test as distinguished from the fixed sample size test procedure is that the number of observations (samples) required depends on the outcome of previous observations and is, therefore, not a predetermined, but a random number.

3.5.1 Notion of a Sequential test

In a sequential test, a rule is given for making one of the three decisions, namely,

i. accept hypothesis, H

ii. reject hypothesis, H

iii. continue the experiment by making an additional observation.

This test is carried out sequentially and depending upon the outcome of the test at each stage, the test is terminated if the decision is i) or ii). If the third decision is made then the next sample is taken and the test is continued. This process is continued until the first or second decision is made. The number of samples required for terminating the test is a random variable, say m. For each positive integer value m; we can denote the *totality of all possible samples*, say $(v_1, v_2, v_3, \ldots\ldots, v_m)$, with an *m-dimensional* sample space Γ_m. A decision rule can be selected that subdivides the sample space into three mutually exclusive decision regions $\Gamma_m{}^0$, $\Gamma_m{}^1$ and $\Gamma_m{}^2$. After the first observation v_1, hypothesis H is rejected if v_1 lies in region $\Gamma_1{}^o$; H is accepted if it lies in the region $\Gamma_1{}^1$; or a second observation is made if v_1 lies in the region $\Gamma_1{}^2$. On drawing the second sample v_2, H is rejected or accepted or a third observation is made according to the observed sample (v_1, v_2) lying in $\Gamma_2{}^o$, $\Gamma_2{}^1$ or $\Gamma_2{}^2$ respectively. The test terminates only when the sample points fall in either $\Gamma_m{}^o$ or $\Gamma_m{}^1$. A proper choice of sets $\Gamma_m{}^o$, $\Gamma_m{}^1$ and $\Gamma_m{}^2$ ($m = 1,2,\ldots\ldots$) is a fundamental problem in the theory of sequential detection and depends on the consequences of the test.

Two major consequences of a sequential test are:

i. Operating Characteristic Function (OCF)

ii. Average Sample Number (ASN)

3.5.2 Sequential Probability Ratio Test (SPRT)

Let $p_m(v/\theta)$ denote the conditional probability density function of m data samples $v_1, v_2, ..., v_m$ given j signal parameters $\theta_1, \theta_2, ..., \theta_j$ and let $p_m(v/o)$ denote the probability density function of m observed samples given that the signal is absent.

The likelihood ratio function,for m samples, is defined as

$$\Lambda_m(v/\theta) = \frac{p_m(v/\theta)}{p_m(v/o)} \tag{3.17}$$

which is a conditional probability ratio for testing the null hypothesis H_o, against a simple hypothesis H_1 that the signal plus noise is present. Two positive constants A_t and $B_t (B_t < A_t)$ are selected such that at each stage of the experiment, if $B_t < \Lambda_m(v/\theta) < A_t$ the test is continued with the next observation; if $\Lambda_m(v/\theta) \leq B_t$ the test terminates with the acceptance of hypothesis H_o and if $\Lambda_m(v/\theta) \geq A_t$ the test terminates with the acceptance of hypothesis H_1.

The sequential probability ratio test can be summarized as follows:

i) if $B_t < \Lambda_m(v/\theta) < A_t$ continue test

ii) if $B_t \geq \Lambda_m(v/\theta)$ accept hypothesis H_o

iii) if $A_t \leq \Lambda_m(v/\theta)$ accept hypothesis H_1

The threshold values A_t and B_t can be related to the probability of false alarm α and the probability of miss detection $\beta(\theta)$ over the regions $\Gamma_m{}^o$ and $\Gamma_m{}^1$ respectively and yields [10]

$$B_t(1-\alpha) \geq \beta(\theta) \tag{3.18}$$

$$1 - \beta(\theta) \geq A_t\, \alpha \tag{3.19}$$

3.5.2.1 Excess over boundary problem

The above inequalities can be used to establish thresholds A_t and B_t, given the error probabilities α and $\beta(\theta)$. However, since the likelihood function varies discretely as a function of m, exact equality may never occur. This is called the *excess over boundaries* problem which was discussed at length by Wald [10]. Usually, it is assumed that the boundaries are not exceeded by a significant amount especially when the value of m is large ie., signal-to-noise very low.

When the excess is neglected

$$A_t = \frac{1 - \beta(\theta)}{\alpha} \tag{3.20}$$

$$B_t = \frac{\beta(\theta)}{1-\alpha} \tag{3.21}$$

Error probabilities in terms of A_t and B_t can then be expressed as

$$\alpha = \frac{1-B_t}{A_t - B_t} \tag{3.22}$$

$$\beta(\theta) = \frac{B_t(A_t - 1)}{A_t - B_t} \tag{3.23}$$

3.5.3 Operating Characteristic Function (OCF)

It was proved by Wald that the probability of a sequential test terminating is unity if the set of observations v_m are independent [10]. It was also proved that the sequential test will terminate with unit probability for a large class of distributions when the observations v_m are not independent. The operating characteristic function (OCF) denoted by $L(\theta)$ is required for loss computations and evaluation of the average sample number (ASN). The OCF is defined as the conditional probability of accepting hypothesis H_o at the end of the test with the given parameter θ. From this definition

$$L(0) = 1-\alpha \tag{3.24}$$

$$L(\theta) = \beta(\theta) \tag{3.25}$$

The probability that the hypothesis H_1 is accepted at the end of the test (all tests are considered to terminate) is:

$$1 - L(0) = \alpha \tag{3.26}$$

$$1 - L(\theta) = P_d(\theta) \tag{3.27}$$

If the SNR, denoted by γ, is the only parameter involved, then the OCF when plotted appears as shown in figure 3.3. Normally, the sequential ratio test is designed for a specific set of parameters denoted by design parameters θ_d in the parameter space θ. However, the entire OCF is required in order to compute the ASN for all values of θ. Wald has developed an approximate method for computing $L(\theta)$ using a parametric equation which *neglects the excess over boundaries* problem.

For the purpose of computing $L(\theta)$, let us consider the expression

$$\left[\frac{p_m(v/\theta_d)}{p_m(v/o)}\right]^h \tag{3.28}$$

where $h = h(\theta, \theta_d)$ is a real number, such that, the expected value of this expression (3.28) with $h \neq 0$ is given by:

$$\int_{-\infty}^{\infty} \left[\frac{p_m(v/\theta_d)}{p_m(v/o)} \right]^h p_m(v/\theta)\, dv = 1 \tag{3.29}$$

The integrand in this equation is:

$$f_m^*(v) = \left[\frac{p_m(v/\theta_d)}{p_m(v/o)} \right]^h p_m(v/\theta) \tag{3.30}$$

which is a distribution of v.

For the case with $h > 0$, let us denote H as the hypothesis that $p_m(v/\theta)$ is the distribution of v and H^* as the hypothesis that $f_m^*(v)$ is the distribution of v.

Now, consider the sequential probability ratio test with the following rules:

i) continue the test if

$$B_t^h < \frac{f_m^*(v)}{p_m(v/\theta)} < A_t^h \tag{3.31}$$

ii) accept hypothesis H^* when the ratio is equal to or greater than A_t^h

iii) accept hypothesis H when the ratio is equal to or greater than B_t^h

The ratio considered in (3.31) can be written as:

$$\frac{f_m^*(v)}{p_m(v/\theta)} = \left[\frac{p_m(v/\theta_d)}{p_m(v/o)} \right]^h \tag{3.32}$$

Therefore, in the above sequential probability ratio test, equation (3.31) can be rewritten as:

$$B_t < \frac{p_m(v/\theta_d)}{p_m(v/o)} < A_t \tag{3.33}$$

If the test between H^* and H results in the acceptance of H^*, it implies the acceptance of H_1, likewise the acceptance of H corresponds to the acceptance of H_o. From this it follows that $L(0)$, the probability of accepting H_0 given $\theta = 0$, is the same as $L(\theta)$, the probability of accepting H when f_m^* is the true distribution.

From this, $L(\theta)$ can be calculated by using α' and β' which represent the error probabilities for test H^* versus H as follow:

$$A_t^h = \frac{1 - \beta'(\theta)}{\alpha'} \tag{3.34}$$

$$B_t^h = \frac{\beta'(\theta)}{1 - \alpha'} \tag{3.35}$$

$$\alpha' = \frac{1 - B_t^h}{A_t^h - B_t^h} \tag{3.36}$$

$$\beta'(\theta) = \frac{B_t^h (A_t^h - 1)}{A_t^h - B_t^h} \tag{3.37}$$

$$L(\theta) = 1 - \alpha' \tag{3.38}$$

$$L(\theta) = \frac{(A_t^h - 1)}{A_t^h - B_t^h} \tag{3.39}$$

$$L(\theta) = \frac{\dfrac{1-\beta'(\theta)}{\alpha'} - 1}{\dfrac{1-\beta'(\theta)}{\alpha'} - \dfrac{\beta'(\theta)}{1-\alpha'}} \tag{3.40}$$

$L(\theta)$ is the desired operating characteristic function subject to the above condition for h given by equation 3.29. The case for $h < 0$ can also be treated in the similar manner and results in the same expression for $L(\theta)$.

3.5.4 The Average Sample Number (ASN)

The average sample number (ASN) is the average of the number of samples required for the termination of each sequential test. The computation of likelihood ratio for a series of m samples, $v = v_1, v_2, ..., v_m$, as given by (3.17) requires a multiplication of the likelihood ratio's of individual samples. However, in practice, it can be simplified by taking the logarithm of the likelihood ratio's which will result in a summation rather than a multiplication. The ASN of the sequential ratio test assuming the logarithm of the likelihood ratio can be derived using indirect methods and shown below.

The log-likelihood ratio for m samples, with $\theta = \theta_d$, is denoted by Z_m and given by:

$$Z_m = \log \frac{p_m(v/\theta_d)}{p_m(v/o)} \tag{3.41}$$

The sequential test procedure in terms of Z_m is:

i) continue taking samples if $\log B_t < Z_m < \log A_t$

ii) accept H_o when $Z_m \leq \log B_t$

iii) accept H_1 when $Z_m \geq \log A_t$

The average value of Z_m at test termination is approximately given by (neglecting the excess over boundaries) $\log B_t$ times the probability of accepting H_o plus $\log A_t$ times the probability of not accepting H_o. Thus for a terminated test of length n, given θ,

$$E(Z_n/\theta) = L(\theta) \log B_t + [1 - L(\theta)] \log A_t \tag{3.42}$$

where $E(Z_n/\theta)$ is the expectation of the logarithm of the likelihood ratio conditioned on θ.

The average sample number of the sequential ratio test is derived as

$$ASN = \frac{L(\theta)\log B_t + [1-L(\theta)]\log A_t}{E(z/\theta)} \tag{3.43}$$

where $E(z/\theta)$ is the expectation of the logarithm of the likelihood ratio for k^{th} sample (v_k) conditioned on θ.

3.5.5 Low SNR approximations and the Biased Square Law detector (BSD)

A generalized scquential test (possibly randomized) which is more general than the usual sequential probability ratio test of Wald and includes non-optimum as well as Wald's optimum sequential tests was considered by G.E.Albert [16] from which a biased square law detector was obtained as a low SNR model of the sequential detector by Kendall [17]. The sequential test and its approximations are described below.

Let $\{x_i\}$ represent a sequentially observable discrete stationary Markov process with transitions governed by the probability distribution function $F(x_i/x_{i-1})$. The pair of decisions to be made about $F(x_i/x_{i-1})$ are denoted by $d_i = 0,1$ and d_2 is the decision to defer making either d_o or d_1.

Choosing an arbitrary point x_o, the test is carried out by making one of the decisions d_i with probability $\pi_i(x_o)$, i = 0,1,2. If either d_o or d_1 is made then the test continues and the next sample x_1 is drawn using the distribution $F(x_1/x_o)$. Once again, one of the decisions d_i is made and the test either terminates or continues to draw x_2 using the distribution $F(x_2/x_1)$. The process is continued until either d_o or d_1 is made. To guarantee that this occurs with unit probability in a finite number of trials, it is assumed that there is some integer M and some $\rho < 1$ such that for all $m \geq M$ the inequality

$$\int_{-\infty}^{\infty}\int_{-\infty}^{\infty}\cdots\int_{-\infty}^{\infty}\prod_{i=1}^{m}\pi_o(x_i)dF(x_i/x_{i-1}) \leq \rho \leq 1 \tag{3.44}$$

is satisfied for all x_o.

Albert [16] has derived a set of integral equations whose solutions give the most interesting parameters of the test, namely, the probability of test truncation and the average sample number (ASN).

The probability that the test ends with decision d_o or d_1 ie., $P_i(x_o)$ satisfies the integral equation

$$P_i(x_o) = \pi_o(x_o) + \pi_o(x_o) \int_{-\infty}^{\infty} P_i(y)\, dF(y/x_o) \tag{3.45}$$

and the average sample number (ASN) is given by average test duration, $M_1(x_o)$ which also satisfies a similar integral equation

$$M_1(x_o) = \pi_o(x_o) + \pi_o(x_o) \int_{-\infty}^{\infty} M_1(y)\, dF(y/x_o) \tag{3.46}$$

This formulation has the advantage that it gives exact results for a general class of sequential tests which need not be probability ratio tests. Furthermore, any *excess over the boundaries* which might occur is not neglected. However, a serious disadvantage is that the integral equations, for most cases of interest, are difficult (if not impossible) to solve, and the solutions are unwieldy for many situations. Kendall [17] was able to obtain exact solutions for the *non-coherent sequential detection of a sine wave in Gaussian noise* using a biased square-law detector (BSD).

3.5.5.1 Probability of false alarm and ASN for the BSD

The biased square-law detector applied to the spread-spectrum code acquisition (which will be described in detail in the next section) is shown in figure 3.4. If y_k is the k^{th} sample from the square-law envelope detector, which is taken sufficiently apart, then the biased square law detector sample, Y_k, can be obtained by:

$$Y_k = y_k - b \tag{3.47}$$

where b is the bias, given by $b = N_o B(1+\gamma/2)$ with γ as the predetection SNR, B as the predetection filter bandwidth and N_o as the single-sided noise spectral density [46].

These samples are statistically independent and hence, the sample sums (accumulator output), denoted Z_i, are given by:

$$Z_i = \sum_{k=1}^{i} Y_k \tag{3.48}$$

which represent a Markov process. Since the sample sum $Z_i = Z_{i-1} + Y_i$, it follows that

$$dF(Z_i/Z_{i-1}) = \frac{1}{2\sigma^2} \exp\left[-\left(\frac{Z_i - Z_{i-1} + b}{2\sigma^2}\right)\right] dZ_i \qquad Z_i - Z_{i-1} \geq b \tag{3.49}$$

$$= 0 \qquad \textit{otherwise}$$

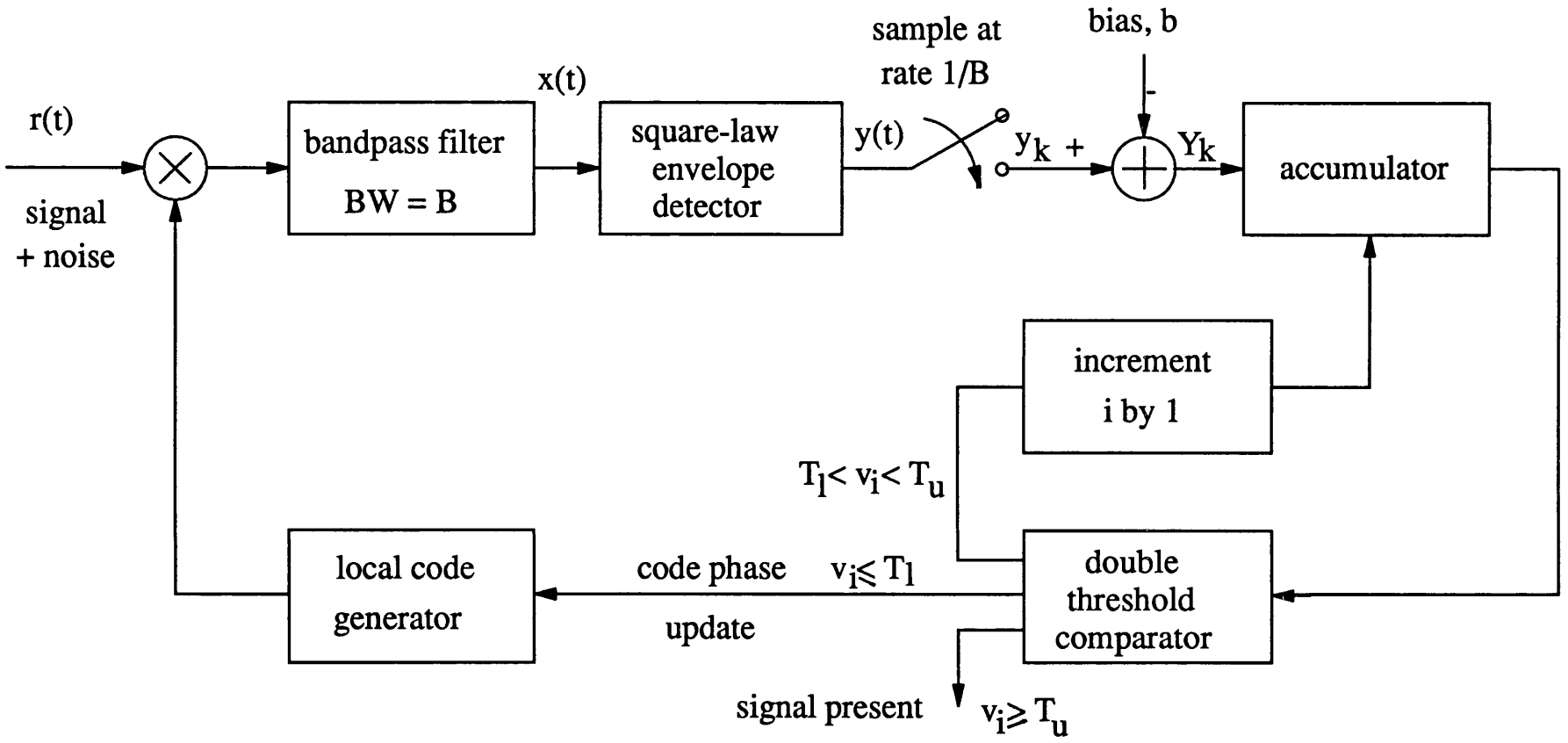

Figure 3.4 Schematic diagram of a biased square-law sequential detection system

Decisions d_o and d_1 correspond to d_o = dismissal, d_1 = alarm, and the set of decision probabilities $\pi_i(Z_k)$, i = 0,1,2 is stationary (ie., independent of k) and given by the following relationships:

$$\pi_o(Z) = \begin{cases} 1 & \eta_2 \le Z \\ 0 & Z < \eta_2 \end{cases} \tag{3.50}$$

$$\pi_1(Z) = \begin{cases} 1 & \eta_1 \le Z \\ 0 & Z < \eta_1 \end{cases} \tag{3.51}$$

$$\pi_2(Z) = \begin{cases} 1 & \eta_2 < Z < \eta_1 \\ 0 & otherwise \end{cases} \tag{3.52}$$

where η_1 and η_2 are the thresholds. Letting $Z_o = 0$ and for $\eta_2 < 0 < \eta_1$, the P_{fa} can be obtained from (3.45) as:

$$P_{fa} = \frac{\exp(-\eta'_2/\gamma)\, G(-D\eta'_2 ; Db')}{\exp[(\eta'_1 - \eta'_2 + b')/\gamma)]\, G[D(\eta'_1 - \eta'_2 + b') ; Db']} \tag{3.53}$$

with the normalizations as follow:

$$b' = \frac{\gamma b}{2\sigma^2} = \frac{\gamma b}{N_o B} \tag{3.54}$$

$$\eta'_i = \frac{\gamma \eta_i}{2\sigma^2} = \frac{\gamma \eta_i}{N_o B} \quad ; \quad i = 1,2 \tag{3.55}$$

$$D = \frac{1}{\gamma} \exp(-b'/\gamma) \tag{3.56}$$

and function G(x;c) is defined as

$$G(x;c) = 1 + \sum_{n=1}^{N} \frac{(nc - x)^n}{n!} \tag{3.57}$$

where N is an integer chosen to satisfy the inequality

$$c \le Nc \le x \le (N+1)c \tag{3.58}$$

Similarly the ASN can be obtained from (3.46) as:

$$ASN = M_1(0) = \exp(-\eta'_2/\gamma)\, H(-D\eta'_2 ; Db') \tag{3.59}$$
$$+ P_2(0) \left\{ 1 - \exp\left[(\eta'_1 - \eta'_2 + b')/\gamma)\right] H\left[D(\eta'_1 - \eta'_2 + b') ; Db'\right] \right\}$$

with the function H(x;c) defined as

$$H(x;c) = (N+1)\exp(-x/\gamma D) - \sum_{n=1}^{N} \sum_{i=0}^{n-1} \frac{(nc - x)^i}{i!(\gamma D)^{i-n}} \tag{3.60}$$

The average test duration for the case of noise only is given by

$$\tau_d = ASN / B \tag{3.61}$$

where Z_i represent samples taken at rate $1/B$.

A similar analysis for the case where the signal is present, is extremely difficult and is not available in the literature. Also for the truncated sequential tests, Albert's approach can not be applied.

3.6 SEQUENTIAL DETECTION APPLIED TO SPREAD-SPECTRUM CODE ACQUISITION

Acquisition of pseudo-noise codes plays a vital role in the detection of direct-sequence spread-spectrum signals. Recently, emphasis has been placed on the need for faster code acquisition in low input signal to noise ratio (SNR) conditions, particularly in certain satellite communication and navigation applications. Commonly, a serial search is employed to acquire initial synchronization of the PN codes, using the correlation between the incoming signal and the locally generated code replica, by searching through all possible code epochs to indicate coarse lock. This works well in low SNRs but the acquisition time can be unacceptably long. Various detectors have been used with the serial search synchronizer to detect the correlation signal, including single or multiple dwell time detectors and matched filters. However, all these detectors have disadvantages and the problems associated with these detectors have been discussed in the previous chapter.

The single and multiple dwell detectors take as long to dismiss each *incorrect* code epoch as to detect the *correct* code epoch while the matched filter, even though faster in detection/dismissal of the correct/incorrect code epoch, suffers from an increase in hardware complexity which is proportional to the length of the PN code. Sequential detectors, however, employ a serial search strategy but use a variable dwell time integration. These detectors are relatively easy to implement and are capable of dismissing the large number of incorrect code epochs quickly, allowing for longer integration of the correct code epoch resulting in reliable and faster code acquisition. For this reason, sequential detectors are the optimum in the sense of minimum dismissal time of the wrong code epoch for a given probability of detection and false alarm [12].

The schematic diagram of the sequential detection PN code acquisition is shown in figure 3.5. As shown in the figure, the sequential detector is used to check the output of the discrete-step serial-search correlator for the presence of a correlation signal representing the coarse in-lock condition. Because of the large noise levels encountered in spread-spectrum systems, this correlation signal is often heavily corrupted by noise. Sequential detection employs the ratio of the *a priori* probabilities of the incoming samples (at the output of the

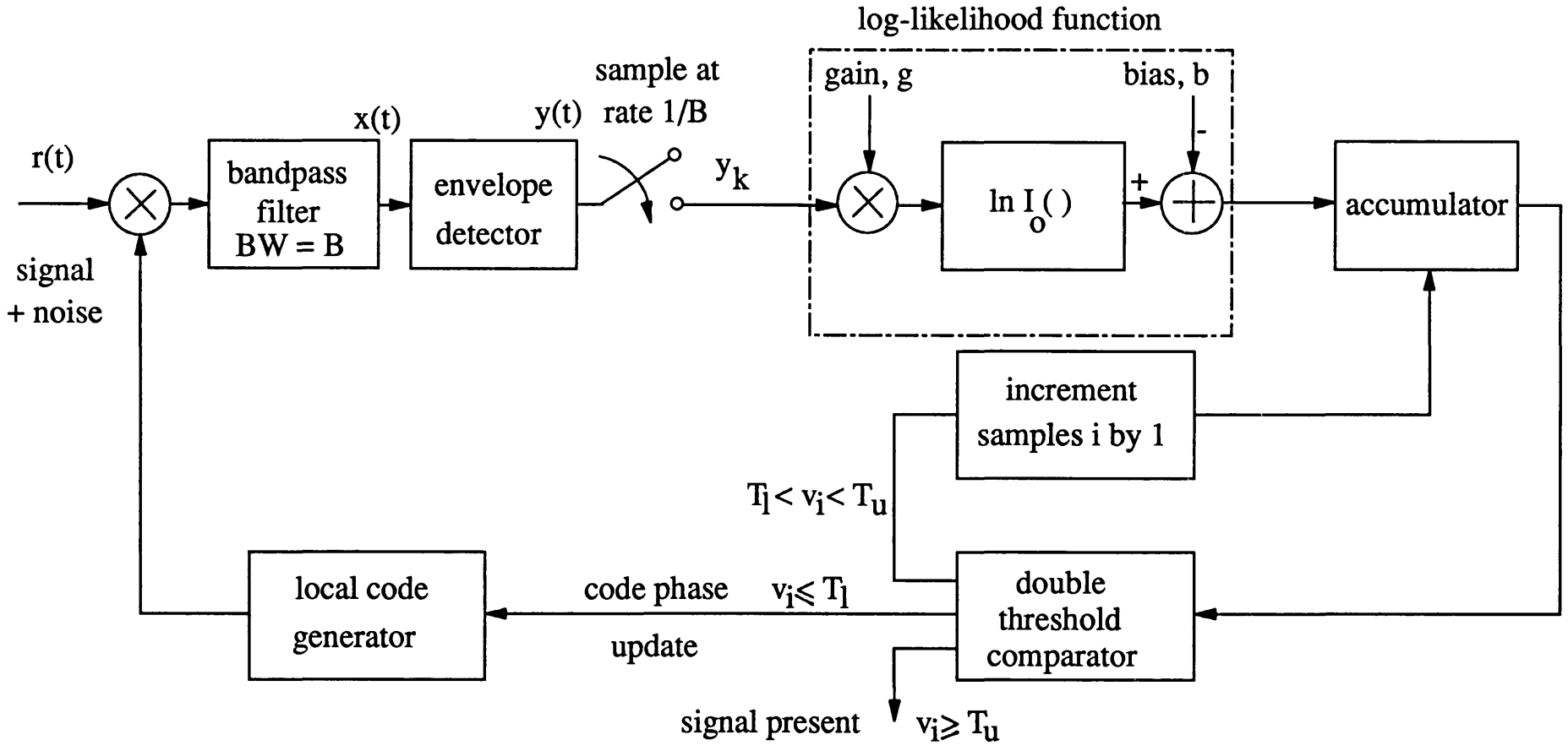

Figure 3.5 Schematic diagram of a sequential detection PN acquisition system.

envelope detector) as a measure of the likelihood of the samples belonging to the wanted correlation signal plus noise (corresponding to the in-lock condition) or noise only (corresponding to the out-of-lock condition). The n ratios of n samples are multiplied to give the likelihood that the envelope detector output is signal or noise averaged over n samples. This likelihood ratio is tested against two thresholds. If the ratio lies between the thresholds, a new sample of the correlator output is taken and the likelihood of it being signal or noise is found. Exceeding either threshold indicates the presence or absence of the correlation signal, respectively.

Let the input signal from the correlator (without data modulation), $x(t)$ be represented as:

$$x(t) = \sqrt{2}A\cos(\omega_o t + \theta_c) + n(t) \tag{3.62}$$

where A is the rms signal amplitude, ω_o is the carrier frequency, θ_c is the random phase of the carrier and $n(t)$ is the noise which is an independent white Gaussian process with a variance, $\sigma^2 = N_o B/2$ where B is the predetection filter bandwidth which, in this case, is equivalent to the data bandwidth and N_o is the single-sided noise spectral density. The actual signal amplitude, however, depends on the degree of correlation between the codes and thus is dependant on the actual code phase misalignment. If the code phase offset is ΔT, then the correlator output is given by $a(A, \Delta T) = A(1-\Delta T/LT_c)$. Thus the correlator output is a random variable, a(t), contributing to the correlation loss. The worstcase correlation loss is estimated to be 2.5dB (SNR loss) for serial search with a step size of half a chip per code cell [32,46].

When the signal $x(t)$ is passed through an envelope detector as shown in figure 3.5, the samples at the output of the envelope detector, y_k, follow a Rayleigh distribution, $p_0(y_k)$, for the case of noise only; and a Rician distribution, $p_1(y_k)$ for the case of signal plus noise. These are given by:

$$p_1(y_k) = \frac{y_k}{2\sigma^2}\exp\left[-\left(\frac{y_k^2}{2\sigma^2}+\gamma\right)\right] I_o\left(2y_k\sqrt{\frac{\gamma}{2\sigma^2}}\right); \quad y_k \geq 0 \tag{3.63}$$

$$= 0 \qquad \textit{otherwise}$$

$$p_o(y_k) = \frac{y_k}{2\sigma^2}\exp\left(-\frac{y_k^2}{2\sigma^2}\right); \quad y_k \geq 0 \tag{3.64}$$

$$= 0 \qquad \textit{otherwise}$$

for the cases of signal present and absent respectively where γ is the predetection SNR given by

$$\gamma = A^2/2\sigma^2 \tag{3.65}$$

and I_o [ ] represents the modified Bessel function of the first kind and zeroth order.

The individual samples of the envelope detector output are assumed to be sufficiently decorrelated by sampling at an interval $T \geq 1/B$. Following the earlier definition, the likelihood function of the k^{th} sample which is the ratio of the *a priori* probability distributions, can be given by:

$$\lambda(k) = \frac{p_1(y_k)}{p_0(y_k)} \tag{3.66}$$

The likelihood ratio after i samples, which is denoted here as Λ_i becomes:

$$\Lambda_i = \frac{\prod_{k=1}^{i} p_1(y_k)}{\prod_{k=1}^{i} p_0(y_k)} \tag{3.67}$$

The sequential probability ratio test (SPRT) is carried out by comparing Λ_i with the two thresholds, an upper threshold, A_t and a lower threshold B_t.

If $\Lambda_i \geq A_t$ hypothesis H_1(*signal present*) is decided and the search is stopped.

If $\Lambda_i \leq B_t$ hypothesis H_0(*signal absent*) is decided and the code epoch is updated.

If $B_t < \Lambda_i < A_t$ sample Λ_{i+1} is taken and the test is repeated for the same relative phase between the codes.

However, in practice, the computational complexity can be reduced significantly by using logarithm of the likelihood function as described in section 3.5.4. Hence, by taking the logarithm of (3.67) and substituting the density functions the sequential test can now be conducted on the accumulated log-likelihood samples with the thresholds replaced by the logarithm of the original thresholds. The accumulated log-likelihood function over i samples, denoted here as v_i, can then be simplified to:

$$v_i = \sum_{k=1}^{i} (-\gamma + \ln[I_o(2y_k\sqrt{\gamma/2\sigma^2})]) \tag{3.68}$$

This accumulator output is tested against the two thresholds which are now denoted by $T_u = \ln(A_t)$, the upper threshold and $T_l = \ln(B_t)$, the lower threshold and the outcomes of the test determine whether the coarse-lock between the codes is achieved or not.

3.6.1 Biased square law detector

The biased square-law detector (BSD) which is a low SNR approximation of the ideal log-likelihood sequential detector as described in section 3.5.5, normally employs a square-law envelope detector for ease of implementation as the square of the envelope of the received

waveform can be easily formed in a receiver and thus it has been of considerable importance. Figure 3.4 shows the BSD employing square-law envelope detector. Following the steps of the ideal sequential detector, the log-likelihood function can be derived as the ratio of the *a priori* probabilities and can be shown to be similar to that of the ideal sequential detector as in (3.68) except that the argument of the $\ln I_o$ [ ] function is replaced by '$2\sqrt{y_k\gamma/2\sigma^2}$' as the *a priori* probabilities are now represented by non-central and central chi-square distributions in the presence and the absence of signal respectively [46].

For low SNRs, however, the $\ln I_o[x]$ function in this log-likelihood function can be approximated by the first two terms of a power series expansion:

$$\ln I_o[x] \approx \frac{x^2}{4} - \frac{x^4}{64} \tag{3.69}$$

and this leads to a biased square law sequential detector (BSD) whose accumulated log-likelihood function, on substitution, becomes [46]:

$$v_i = \sum_{k=1}^{i} \left(-\gamma + \gamma \frac{y_k}{2\sigma^2} - \frac{1}{4}\gamma^2 \left(\frac{y_k}{2\sigma^2} \right)^2 \right) \tag{3.70}$$

$$v_i = \sum_{k=1}^{i} \left(-\gamma + \gamma \frac{y_k}{2\sigma^2} - \frac{\gamma^2}{2} \right) \tag{3.71}$$

$$v_i = \sum_{k=1}^{i} (y_k - b) \tag{3.72}$$

where (3.72) represents the normalized accumulator output with b as the bias of log-likelihood function given by $b = N_o B(1 + \gamma/2)$, and N_o is the single-sided noise spectral density.

Using this simplified log-likelihood function the BSD can be implemented with a simple square law device as shown in figure 3.5 and this represents the low SNR version of the sequential detection for PN code acquisition.

3.7 RECENT DEVELOPMENTS IN RESEARCH WORK INTO SEQUENTIAL DETECTION

The theory of sequential analysis was developed by A.Wald [10] in response to the demands of efficient statistical sampling procedures. Wald and Wolfowitz [12] have also proved the optimality of the sequential probability ratio test between the simple hypothesis that it requires on average fewest number of samples for a given probability of detection (ie., power of the test). Wald has also derived approximate expressions for the decision probabilities and the average sample number neglecting the excess over boundaries problem. These analyses

are valid for a large average sample number or low SNRs [10,13]. Kemperman [14] has exploited the connection between the theory of random walks and Wald's theory and obtained integral equations for the determination of the decision probabilities and the expected sample size of Wald's sequential test. As the solutions for these integral equations are quite difficult, Kemperman and Snyder [15] have also obtained bounds for the solutions which may be used to obtain substantial improvements over the bounds given by Wald. Albert [16] has generalized Kemperman's integral equations to apply to a fairly extensive class of sequential decision problems and has also derived methods to obtain practical results from such integral equations. These methods yield definitive improvements over Wald's approximate methods for setting the decision boundaries and estimating the sample size moments. Kendall [17] has obtained solutions for the generalized integral equations of Albert for a specific case of incoherent detection of a sine wave in Gaussian noise for a biased square law detector when no signal is present and has derived relationships for the probability of false alarm and the average sample number.

The *dissatisfactions associated to Wald's sequential probability ratio test* and Wald's analysis of it were summarized by Siegmund [18] as follow:

i. the open ended continuation region with concomitant possibility of taking an arbitrarily large number of samples is intolerable in practice.

ii. Wald's elegant approximations based on neglecting the excess of the log-likelihood ratio over the stopping boundaries are not especially accurate and do not allow one to study the effect of taking the observations in groups rather one at a time.

iii. the beautiful optimality property of the sequential probability ratio test applies only to the artificial problem of testing a simple hypothesis against a simple alternative.

These issues have received greater attention in statistical decision theory over the past decades and numerous modifications to the sequential probability ratio test have been proposed and their properties studied, often by simulation or lengthy numerical computations and complete theoretical analyses of many such proposals have been carried out [19,20]. The outcome of these investigations has given rise to closed sequential tests or truncated sequential tests defined by nonlinear stopping boundaries and often applied to grouped data. The truncated sequential tests have been proposed by Anderson [19] whereas Goode [20]

has suggested deferred decision theory for the general problem of accelerating the decision.

The *application of sequential tests to the problem of signal detection* (called sequential detection) was first applied by Middleton and Van Meter [21]. Bussgang and Middleton [22] have studied the sequential detection of radar echoes. In their work, the problem of simple binary (ie., two-decision) detection using sequential tests has been extended to the case of optimum detection of pulsed carrier signals in normal noise. Coherent sequential detection of causal signals in normal noise and sequential detection of random signals have also been treated with an important feature of handling of correlated samples and continuous sampling process. Helstrom [23] has presented work on sequential detection theory applied to the detection of unknown range by sampling the receiver output for a radar target detection. Marcus and Swerling [24] have extended the sequential analysis to multiple-resolution-element sequential radars and presented simulation results showing the improvement obtained by sequential procedures. Kendall and Reed [25] have extended the sequential test for radar detection to include multiple targets. Finn [26] has proposed an approach to sequential detection of phased array radars using a two-step approximation called energy variant sequential detection whereas Brennan and Hill [27] called the same procedure a two-step detection. The truncated sequential tests have also been applied to pulsed radar detection and radar surviellance by Bussgang and Marcus [28] and Bussgang and Johnson [29]. In an application of binary sequential detection using uncertainty feedback in which the detector constantly feeds back its state of uncertainty concerning what is being sent, Turin [30] has shown that the sequential detection system when compared to a nonsequential detection system with similar uncertainty feedback, has i) 6dB average power advantage when the prescribed peak-to-average power ratio is too small, and ii) 6dB peak power advantage when the prescribed peak-to-average power ratio is large [31].

Sequential detection has also been applied to spread-spectrum code acquisition by a few researchers in the recent past. Cobb and Darby [32] have presented the computer simulation of sequential detection of spread-spectrum signals by using specific hardware implementations of simplified detector configurations, namely, the ideal detector, envelope detector, biased square law detector and the absolute value detector. The simulation has been carried out in the moderate SNR range of -3dB to +3dB in the IF bandwidth. However, this simulation does not model the presence of data modulation on the carrier and simulates a CW signal after PN despreading. The model also assumes that the clock frequencies are

close enough that the signal level does not change significantly over the length of the test. In a recent work on spread-spectrum code acquisition using sequential detection, Carson [33] has presented a microprocessor based implementation of a sequential detection algorithm together with a search rate control algorithm. Effects of both linear and square law detectors have also been characterized and experimental results when the average sample number is large (corresponding to a design SNR of -6dB to +6dB) has been presented.

The variable dwell time PN search algorithm and its relation to the optimum sequential detector has been presented by Braun [34] who has used a numerical approach to show the optimality of the sequential detector at low SNRs. Meyr and Polzer [35] have presented a method of recursively computing the probability density function of the sample number for the optimum sequential detector with the envelope correlator samples assumed to be statistically independent. Comparatto [36] has analyzed a dual threshold sequential detection receiver and derived a general expression which addresses the probability that the sequential detection procedure ceases after an arbitrary number of samples. This analysis is based on the approximation in which the final expression is conditioned on the previous two samples which was shown to be conservative by Weinberg [37].

The application of sequential detection to the interception of unknown noncoherent frequency hopped waveforms has also been presented by Snelling and Geraniotis [38]. The optimality of the sequential test has also been demonstrated and a truncated sequential test has been derived which shows improvement in the number of samples needed for a decision when the input SNR differs greatly from that assumed in the derivation of the test. Numerical results based on this analysis and the simulation of the interceptor's performance have also been presented. The analysis of the sequential test with asymptotically correct approximations for the operating characteristic function (OCF) and the average sample number (ASN) has been presented by Tantaratana and Poor [39]. Tantaratana and Thomas [40] have considered a class of non-parametric sequential rank tests and derived an approximate analysis. Tantaratana [41] has also presented analysis of a sequential constant false alarm rate (CFAR) detector employing dead zone limiter. Lee and Thomas [42] have presented performance analysis of sequential dead-zone limiter detector and the sequential four-level sign detector. Recently, Lee and Tantaratana [43] have presented analysis of a direct-sequence spread-spectrum system using truncated sequential probability ratio test (TSPRT). In this analysis, approximate worst values of the partial correlation were used to

set up the hypotheses and was shown that the maximum ASN required for the TSPRT is always smaller than that for the fixed dwell scheme. Their results were also compared with simulation results and shown to be in close agreement. Su and Weber [44] have also recently presented two iterative algorithms which are applicable only to limited regions of Wald's approximations for evaluating sequential detector's performance.

In the present research, the analysis of the sequential detection PN code acquisition system has been carried out for various channel impairments in the presence of data modulation and Doppler shift [47-51]. Performance in the presence of two types of jammer signals, namely, the CW jammer and the pulsed jammer has also been considered. Three variants of the sequential detector have been examined and their acquisition performances for all these situations have been compared. Optimization of the sequential detectors with respect to the thresholds, bias and the input SNR has also been carried out and the performance of the sequential detector is compared with that of the more usual fixed-dwell serial search code acquisition techniques, namely, the single-dwell detector and the matched filter.

3.8 REFERENCES

1) Thomas Bayes, "An essay towards solving a problem in the doctrine of chances", Phil. Trans, 53, pp 370-418, 1764.

2) J.Neyman and E.Pearson, "On the problem of the most efficient tests of statistical hypotheses", Phil. Trans. Roy. Soc., A 231, p289 , 1933.

3) A.Wald, " Contributions to the theory of statistical estimation and testing of hypotheses", Ann. Math. Stat., 10, p299 , 1939.

4) A.J.F.Seigert, J.L.Lawson and G.E.Uhlenbeck, *Threshold Signals*, Radiation Laboratory Series (Mc Graw-Hill, New York, 1950), vol.24, Ch. 7.

5) P.M.Woodward and I.L.Davies, "Information theory and inverse probability in telecommunication", Proc IEE, Pt. III, 99(58), pp 37-44, 1952.

6) D.Middleton, *An introduction to statistical decision theory*, McGraw-Hill, New York, 1960.

7) W.W.Peterson, T.G.Birdsall and W.C.Fox, "The theory of signal detectability", 1954 Symposium on Inform. Theory, (also) IRE Tran. (PGIT), vol. 4, pp 179-182, Sep 1954.

8) S.A.Kassam and J.B.Thomas, (ed) *Non-parametric detection-Theory and applications*, Dowden, Hutchinson & Ross, Inc. Pennsylvania, 1980.

9) J.D.Gibson and J.L.Melsa, *Introduction to non-parametric detection with applications*, Academic Press Inc, New York, 1975.

10) A.Wald, *Sequential Analysis*, John Wiley,New York, 1947.

11) J.Neyman and E.Pearson, "The testing of statistical hypotheses in relation to probability a priori", Proc. Cambridge Phil. Soc., 29, 1933.

12) A.Wald and J.Wolfowitz, "Optimum character of the Sequential Probability Ratio Test", Annals of Math. Stat., vol.19, pp 326-339, 1948.

13) A.Wald, *Statistical decision functions*, John Wiley,New York, 1950.

14) Kemperman, H.H.B., *The general one-dimensional random walk with absorbing barriers with applications to sequential analysis*, University of Amsterdam, These de Doctorat, 1950.

15) W.S.Snyder, "Calculations for maximum permissible exposure to thermal neutrons", Nucleonics, vol. 6, pp 46-50, 1950.

16) G.E.Albert, "On the computation of the sampling characteristics of a general class of sequential decision problems", Ann. Math. Stat. vol.25, pp 340-356, 1954.

17) W.B.Kendall, "Performance of the Biased Square Law Sequential Detector in the absence of signal", IEEE Trans. Inform. Theory, IT-11, pp 83-90, January 1965.

18) D.Siegmund, *Sequential analysis, Tests and confidence intervals*, Springer-Verlag, New York, 1985.

19) T.W.Anderson, "A modification of the sequential probability ratio test to reduce the sample size", Ann. Math. Stat. vol.31, pp 165-197, 1960.

20) H.H.Good, "Deferred decision theory", in *Recent developments in Information and decision processes*, R.E.Machol and P.Gray, Eds. New York, Macmillan,1962.

21) D.Middleton and D.Van Meter, "Detection and Extraction of Signals in noise from the viewpoint of statistical decision theory", Soc. for Ind. and Appl. Math., vol. 4, no. 4 , Dec 1955 and vol. 5, no. 1, Mar 1956.

22) J.J.Bussgang and D. Middleton, "Optimum sequential detection of signals in

noise", IRE Trans. on Infor. Theory, vol. IT-1, pp5-18, December 1955.

23) C.W.Helstrom, "A range sampled sequential detection system", IRE Trans. Inform. Theory, vol. IT-8, pp 43-47, Jan 1962.

24) M.B.Marcus and P.Swerling, "Sequential detection in radar with multiple resolution bins", IRE Trans. Inform. Theory, pp 237-245, Apr 1962.

25) W.B.Kendall and I.S.Reed, "A sequential test for radar detection of multiple targets", IRE Trans. Inform. Theory, IT-9, pp 51-53, Jan 1963.

26) H.M.Finn, "A new approach to sequential detection in phased array radars", Proc. 1963 National Winter Convention on Military Electronics (1963).

27) L.E.Brennan and F.S.Hill.Jr, "A two-step sequential procedure for improving the cumulative probability of detection of radars", IEEE Trans. Military Electronics, mil-9, pp 278-287, Jul/Oct 1965.

28) J.J.Bussgang and M.Marcus, "Truncated sequential hypothesis tests", IEEE Trans. on Infor. Theory, vol. IT-13, pp 512-516, Jul 1967.

29) J.J.Bussgang and N.Johnson, *A monograph on truncated sequential tests*, Rome Air Development Centre, Griffiths Air Force Base, Rome, N.Y., RADC-TR-66-705, Jan 1967.

30) G.L.Turin, "Signal design for sequential detection systems with feedback", IEEE Trans. Inform. Theory, pp 401-408, Jul 1965.

31) G.L.Turin, "Comparison of sequential and nonsequential detection systems with uncertainty feedback", IEEE Trans. Inform. Theory, vol. 12, no. 1, pp 5-8, Jan 1966.

32) R.F.Cobb and A.D.Darby, "Acquisition performance of simplified implementations of the sequential detection algorithm", NTC Conference Record,pp 43.4.1-43.4.7, December 4-6, 1978, Birmingham, AL.

33) L.M.Carson, "A microprocessor based spread-spectrum processor for low signal-to-noise ratios", ICC'82 Conference Record, pp 230-234, 1982.

34) W.R.Braun, "Comparison between variable and fixed dwell-time PN acquisition algorithm", ICC'81 Conference Record, pp 59.5.1-59.5.5, Denver, CO, Jun 1981.

35) H.Meyr and G.Polzer, "A simple method for evaluating the probability density function of the sample number for the optimum sequential detector", IEEE Trans. Comm, vol. com-35, no. 1, pp 99-103, Jan 1987.

36) G.M.Comparetto, "A generalized analysis for a dual threshold sequential detection PN acquisition receiver", IEEE Trans. Comm, vol. com-35, no.9, pp 956-960, Sep 1987.

37) A.Weinberg, "Generalized analysis for the evaluation of search strategy effects on PN acquisition performance", IEEE Trans. Comm, vol. com-31, pp 37-49, Jan 1983.

38) W.E.Snelling and E.Geraniotis, "Sequential detection of unknown frequency-hopped waveforms", IEEE Jou. on Sel. Areas in Comm. vol. 7, no. 4, pp 602-617, May 1989.

39) S.Tantaratana and H.V.Poor, "Asymptotic efficiencies of truncated sequential tests", IEEE Trans. Inform. Theory, vol. IT-28, pp 911-923, Nov 1982.

40) S.Tantaratana and J.B.Thomas, "Truncated sequential probability ratio test", Inform. Sci., vol. 13, pp 283-300, 1977.

41) S.Tantaratana, "Sequential CFAR detectors using a dead-zone limiter", IEEE Trans. com., vol. 38, no.9, pp 1375-1383, Sep 1990.

42) C.C.Lee and J.B. Thomas, "Sequential detection based on simple quantization", Jou. of the Franklin Institute, Pergamon Press plc., vol. 312, no. 2, pp 119-135, August 1981.

43) Y.H. Lee and S.Tantaratana, "Acquisition of PN sequences for DS/SS systems using truncated sequential probability ratio test", Jou. of the Franklin Institute, Pergamon Press plc., vol. 328, no. 2/3, pp 231-248, 1991.

44) Y.T.Su and C.L.Weber, "A class of sequential tests and its applications", IEEE Trans. Comm, vol. 38, no. 2, pp 165-171, Feb 1990.

45) A.D. Whalen, *Detection of signals in noise*, Academic Press Inc., New York, 1971.

46) M.K. Simon *et al*, *Spread Spectrum Communications*, Vol III. Computer Science Press, Maryland, 1985.

47) K.V.Ravi and R.F.Ormondroyd, "Computer simulation of a quantized log-likelihood sequential detector for faster acquisition of spread-spectrum pseudo-noise signals." 5th International Conference on Radio Receivers and associated systems, IEE Conference publication No. 325, pp 207-211, July 24-26,1990, Cambridge, UK.

48) K.V.Ravi and R.F.Ormondroyd, "Comparison of the acquisition performance of biased square law and quantized log-likelihood sequential detectors for PN acquisition" IEEE International Symposium on Spread Spectrum Techniques and Applications, Symposium Proceedings, pp 53-58, September 24-26,1990, London, UK.

49) K.V.Ravi and R.F.Ormondroyd, "Performance of sequential detectors for the acquisition of data modulated spread-spectrum pseudo noise signals", IEEE International Conference on Communications, ICC'91, June 23-26, 1991, Denver, Colorado, USA.

50) K.V.Ravi and R.F.Ormondroyd, "Simulation performance of a quantized log-likelihood sequential detector for PN code acquisition the presence of data modulation and Doppler shift", MILCOM'91, November 4-7, 1991, McLean, USA (to be presented).

51) R.F.Ormondroyd and K.V.Ravi, "Performance of the serial-search PN code acquisition techniques using Monte-Carlo simulation - A comparative evaluation", MILCOM'91, November 4-7, 1991, McLean, USA (to be presented).

CHAPTER 4

COMPUTER MODELS, SIGNAL MODELS AND THE MONTE-CARLO SIMULATION PROCEDURES

4.1 INTRODUCTION

In this chapter the computer models used to simulate the three variants of sequential detector for the acquisition of direct-sequence spread-spectrum signals are described. The signal models employed to simulate various types of received signal structures in the presence and the absence of data modulation including the effects of code rate and the residual carrier Doppler frequency offsets are presented. The channel model employed to simulate the various channel impairments viz., Gaussian noise, jamming and the interference are also described. In addition, the analytical description of each of the functions required in the system model for both the transmit and the receive sides has been presented and the software techniques used to realize various functional blocks representing all received signal models employed to analyze the performance of the detectors are described.

In order to assess the relative performance of PN code acquisition using the sequential detector, a single-dwell detector and a digital matched filter detector were also simulated and their performances for the equivalent system parameters were also obtained. The system models used for both these detectors and the software realization of their functional blocks are also presented. Finally, the Monte-Carlo computer simulation procedure employed to assess the statistical performance of each of these detectors is explained.

4.2 COMPUTER MODELS

The transmitted and the received signals are assumed to be at baseband and consequently, a baseband direct-sequence spread-spectrum transmitter with a non-coherent receiver using various detection systems was simulated. Various serial-search detector algorithms using their equivalent baseband models were employed. The serial-search technique using sequential detection algorithms corresponding to three variants of the sequential detector

were simulated. The three variants of the sequential detector considered for simulation are:

i. ideal log-likelihood sequential detector (LLD)

ii. quantized log-likelihood sequential detector (QLD)

iii. biased square law sequential detector (BSD)

In addition, two common serial-search techniques with a single-dwell detector and a digital matched filter detector were also realized in software. Both the transmitter and the receiver were simulated as the finite state machines with the state of the machine depending upon the the shift registers of the PN code generators. The simulation was carried out on the Gould-Unix main frame computer and HP 9000 Series 835 mini computer using Fortran-77 as a primary programming language. Various functional blocks of the transmitter, channel and the receiver models are described in detail in the following sections.

4.2.1 Transmitter model

The schematic block diagram of a direct-sequence spread-spectrum transmission system is shown in figure 4.1a. The spread-spectrum transmitter consists of a PN code generator and a data generator whose outputs are modulo-2 added together to represent a simple BPSK modulated direct-sequence spread-spectrum signal in the baseband. In the simulation, the transmitter spreading sequence was assumed to be a maximal-length pseudo-random noise (PN) code clocked at a rate R_c = 100 Kb/s with a code length L = 127 chips. A pseudo-random sequence of length 15 was used as a data sequence with the data transitions synchronized with the PN code clock, however, the occurance of each bit was chosen to occur randomly with respect to the start of the PN code (incoherently added). The data bit duration was made equal to the PN code length resulting in a data rate $R_d = R_c/L$ = 100/127 Kb/s = 787 b/s and a provision to select or deselect the data was also provided. This choice of code parameters allows the spread-spectrum system to provide a *processing gain* of 21dB assuming ideal filtering and 0dB implementation loss.

The code rate and the code length were chosen to keep the computer simulation time within a manageable limit in order to obtain a sufficiently large number of runs needed for the Monte-Carlo simulation technique. For the code rate of 100 Kb/s chosen, a sampling rate of 200 Kb/s was used which represents each PN code bit with two samples. As the local code phase was slide past in steps of half a chip and the random initial code phase uncertainty was always set to be a multiple of a cell (half a chip) duration this provides sufficient accuracy.

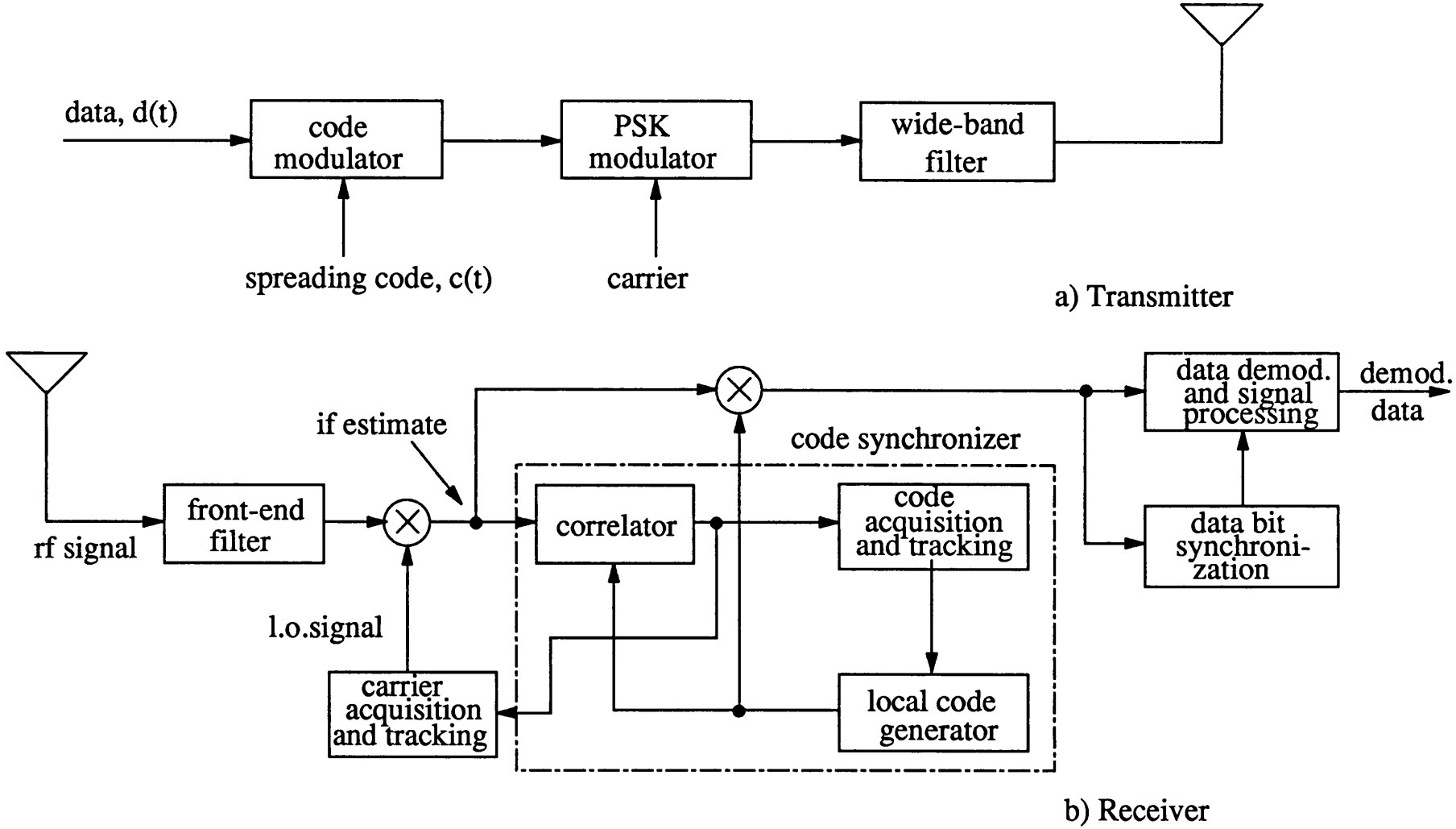

Figure 4.1 Schematic diagram of a direct-sequence spread-spectrum system.

The case of continuously random initial code phase uncertainty has not been modelled to keep the simulation time in practical limits.

4.2.2 Channel model

The transmission characteristics of the channel were simulated under the assumption of additive white Gaussian noise (AWGN) using a Gaussian random number generator routine with zero mean and a controllable variance. A random number generator with uniform distribution was generated using the linear congruents method and from this distribution the Gaussian distribution was obtained using the Box-Muller method [1]. The randomness of this distribution was verified by conducting many runs and plotting the probability density function as well as the cumulative density function and from this it was found that the distribution was *tightly normal* over the range $\pm 3\sigma$. This was also found to be as good as a distribution obtained by the direct application of central limit theorem with fairly a large number of samples drawn from the same uniform distribution. Since this functional block was particularly important in the simulation process, several sources of random numbers were also used and the resulting Gaussian distributions were compared. Figure 4.2 shows the cumulative frequency plotted against the bin number on a *normal probability paper* for three distributions generated by using the following methods.

i. Box-Muller method using uniform distribution by linear congruents method [1].

ii. Box-Muller method using Prospero uniform distribution [2].

iii. Direct application of central-limit theorem using Prospero uniform distribution.

For all three methods, the cumulative probability lies approximately on a straight line, as expected for the Gaussian distribution. The mean and variance can also be seen to be closely in agreement for all three distributions (for a zero-mean, unit variance in the range $\pm 3\sigma$). The mean was verified by obtaining the bin number corresponding to 50% cumulative frequency which is also 50 for 100 bins considered. The standard deviation was obtained by the difference in the number of bins corresponding to the 50% and 84% cumulative frequency which is close to 17 for a $\pm 3\sigma$ over 100 bins. However, based on the best agreement of data with the straight line fit, the Box-Muller method using the uniform distribution generated by linear congruents method was chosen for the present research.

The continuous-wave (CW) interference and the pulsed tone jamming which were used to model the typical spread-spectrum interference (intentional/unintentional) and jamming

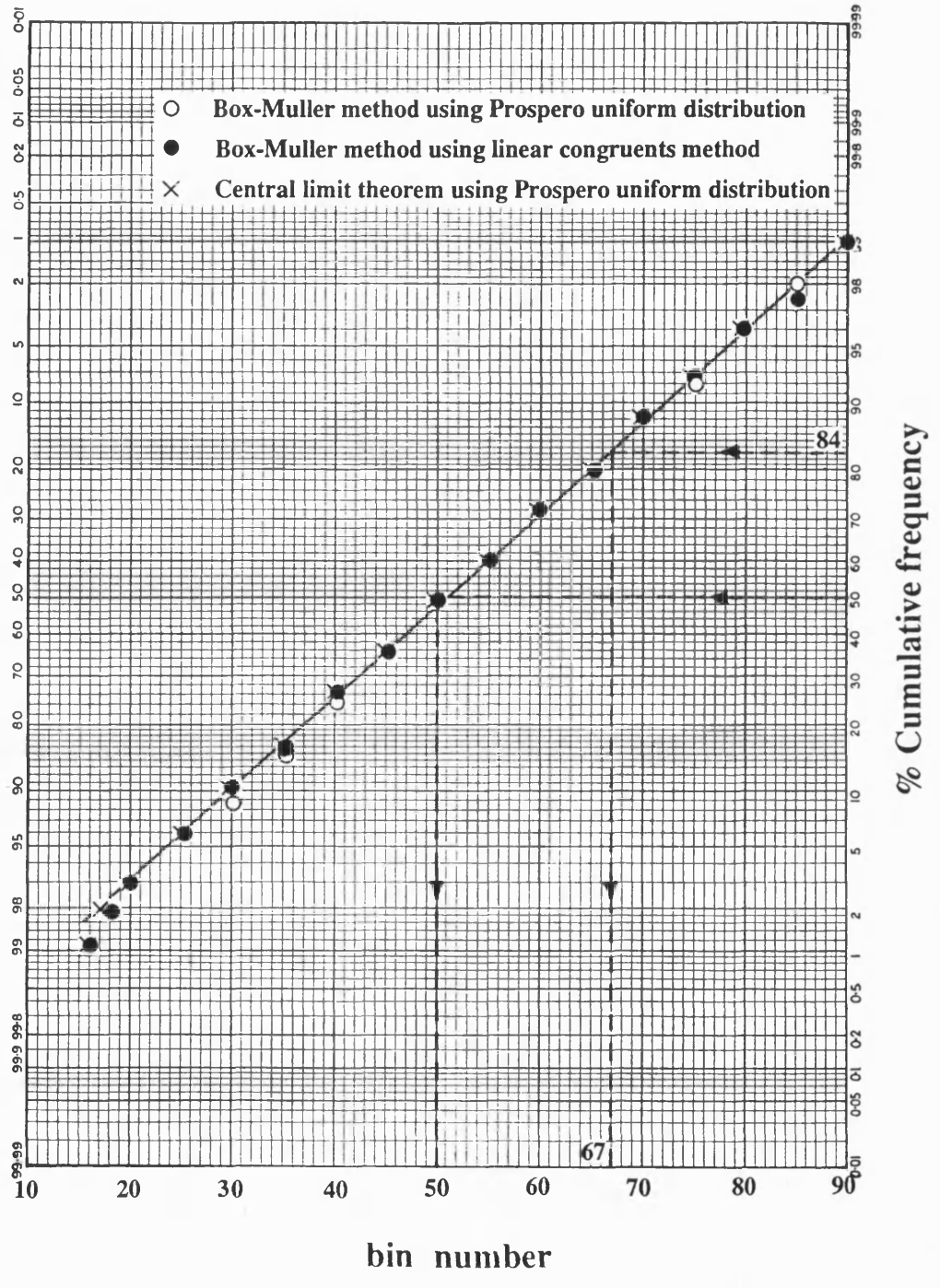

Figure 4.2 Cumulative frequency Vs bin number for Gaussian distributions.

strategies were also generated and used together with the Gaussian noise. Both these jammer waveforms and their mathematical models are discussed in section 4.4.

4.2.3 Receiver model

The schematic diagram of a spread-spectrum receiver is shown in figure 4.1b. As the main emphasis is on the initial acquisition, the code acquisition aspects of the receiver were simulated and consequently the acquisition models employed are described in this section. Figure 4.3 shows a schematic diagram of the generalized PN code synchronization in the spread-spectrum receiver with the code acquisition system explicitly shown.

Both the serial-search techniques using the sequential detection and the single-dwell detection simulated, use common signal processing during the signal correlation phase and then the correlator samples are processed according to the each type of detector. Therefore, the receiver model employs common functional blocks until the envelope detector/sampler and these samples are then processed according to its specific sequential detection algorithm corresponding to each of its variants or the fixed-dwell serial-search algorithm as appropriate. However, the serial-search using the digital matched filter employs a slightly different model which will be described subsequently.

4.2.4 Common signal processing modules

The functional blocks common to all the variants of sequential detector and the single-dwell detector are:

i. Correlator/multiplier

ii. Predetection filter

iii. Local code generator

iv. Envelope detector

v. Sampler

The software techniques employed in realizing all these functional blocks are described below:

4.2.4.1 Correlator

The correlator is the first functional block in the receiver modules and was simulated as a simple multiplier of the corrupted received samples with a locally generated code chips or code cells. In the present simulation, cells of half a code chip duration are assumed and

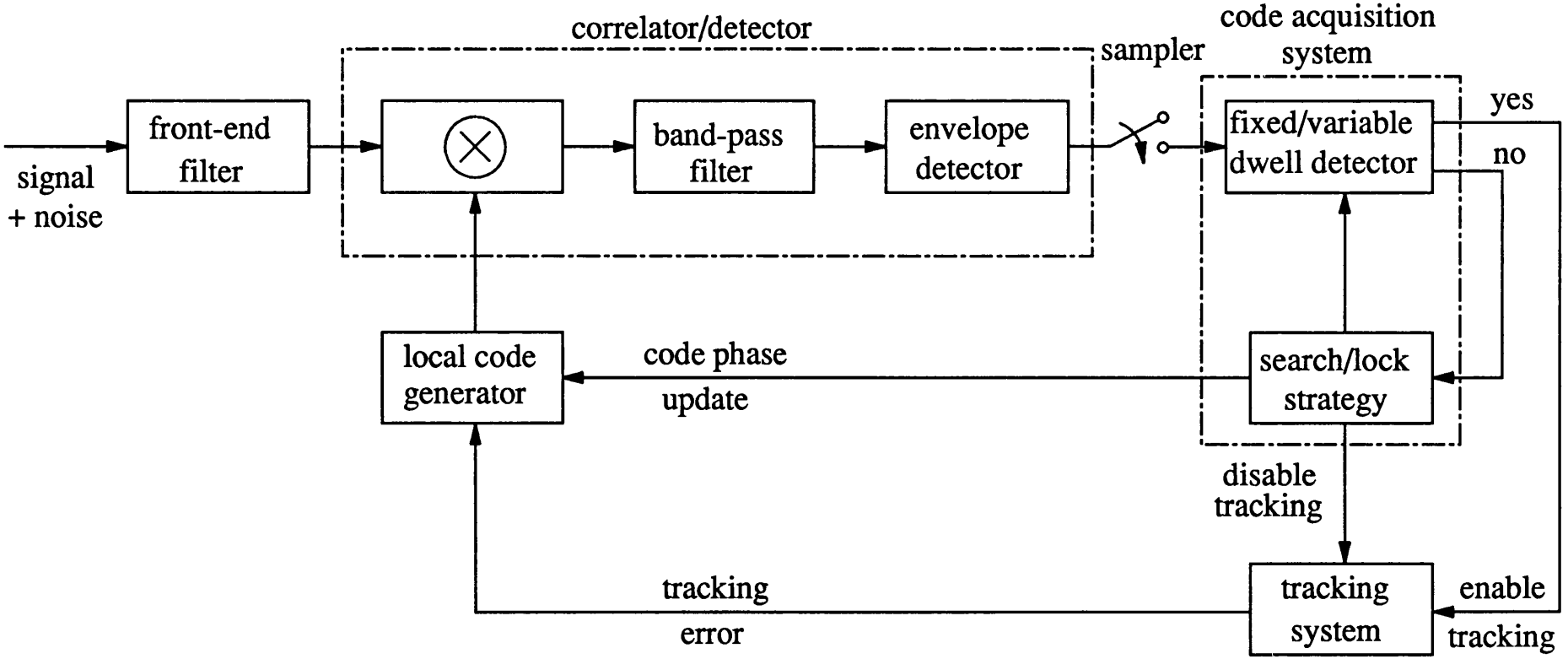

Figure 4.3 Schematic diagram of the generalized code synchronization in a direct-sequence spread-spectrum receiver.

consequently coarse acquisition is achieved to an accuracy of better than half a code chip. The output of this multiplier was then filtered by the predetection filter to extract the correlated signal which will provide a measure of synchronization between the incoming signal and the local code replica.

4.2.4.2 Local code generator

The local code generator works at the same code rate and the code length as the transmit code generator using the same code polynomial with the known starting state but is asynchronous to the transmit code as the code phase is unknown in the beginning. The local code phase could be incremented in steps of one cell relative to the transmit code phase whenever the test failed. The sliding of code was carried out by keeping track of the code states as well as the cell under comparison and updating the contents of the local code generator. Both transmit and receive code generators were each assigned a flag to monitor which cell was being processing. The flag was toggled whenever the cell was incremented. This method allows a simple realization of local code delay of one cell whenever the test fails, by simply holding the local code flag from being toggled.

4.2.4.3 Predetection filter

This filter plays an important role as the detector performance critically depends on the filter bandwidth and the predetection SNR. A digital low pass filter realization was employed to simulate this filter. Infinite impulse response (IIR) techniques using the bilinear transformation method were used to realize a third order Butterworth configuration [4,5]. This filter was found to provide satisfactory performance compared to a first order Butterworth filter whose cut-off characteristics are not sharp enough or a third order Chebyshev configuration which shows poor phase characteristics. The design of the predetection filter is discussed in the appendix 4.1 in some detail.

4.2.4.4 Envelope detector and Sampler

In practical spread-spectrum acquisition systems it is common to use square-law envelope detectors to remove the effects of data modulation on the correlation signal. However, this presents the designer with serious problem as the correlation signal is distorted due to the non-linearity of the squaring process (which is commonly known as squaring loss) resulting in a reduced predetection SNR. The linear envelope detectors are a better solution, however, realization of such a detector with wide dynamic range is quite difficult. The absolute value

detectors are sometimes a good choice as it is easy to realize digitally. In this work absolute-value detector is assumed and realized by simply removing the sign bit of each sample.

The filter output was passed through an absolute-value detector whose output was then fed to the sampler. The envelope detector output need to be sampled at a rate $R_s \leq B$ where B is the predetection filter bandwidth which is, in this simulation, equal to the data rate R_d. This is required to ensure sufficient decorrelation of the samples to the sequential detector as the detector works on the assumption of uncorrelated samples. Consequently, a sampling time equal to $T = 2/R_d$ was employed in the simulation.

4.2.5 Sequential detector models

4.2.5.1 Ideal log-likelihood sequential detector (LLD)

The LLD, as shown earlier in figure 3.5 (chapter 3), was simulated by using the ideal values of the '$\ln I_o$ [ ]' transformation required in the computation of the log-likelihood function as given by equation (3.68) in chapter 3 which is reproduced here for convenience.

$$v_i = \sum_{k=1}^{i} (-\gamma + \ln[I_o(2y_k\sqrt{\gamma/2\sigma^2})]) \tag{4.1}$$

where

$$\gamma = A^2/2\sigma^2 \tag{4.2}$$

and γ is the predetection SNR.

$$v_i = \sum_{k=1}^{i} (-b + \ln [I_o\ (g \times y_k)]) \tag{4.3}$$

where b is the bias and g is the gain of the log-likelihood function.

The log-likelihood value corresponding to each k^{th} sample output y_k was computed by using the sample value which was weighted by the gain, g in the argument of the '$\ln I_o$ [ ]' transformation and then adding a bias, b to this transformed value. These log-likelihood values were accumulated and the accumulated value v_i was compared against the upper and lower thresholds T_u and T_l. Depending on the outcome of these comparisons the test was either terminated or continued by taking a new sample until either the presence or the absence of the signal was detected. On detecting the presence of the correlator signal an *in-sync* condition was declared, however, if the test indicated the absence of signal, then the *out-of-sync* condition was declared and the local code was stepped up by one cell to search for the next code phase, and the test was repeated.

4.2.5.2 Quantized log-likelihood sequential detector (QLD)

For the QLD, the signal from the sampler was passed through a uniform quantizer as shown in figure 4.4, in which the number of levels Q was a variable. The quantized sample was then passed through '$\ln I_o$ [ ]' transformation as in the case of the LLD and the quantized value of the sample was transformed using which the log-likelihood function was computed.

This provides the flexibility of testing the performance of the QLD with various quantization levels namely, Q=10,16,32,40,50,100 to determine the minimum number of quantization levels required for a practical realization. In effect, the QLD models an implementation of a log-likelihood detector using a look-up table (possibly stored in a ROM).

4.2.5.3 Biased square law sequential detector (BSD)

The log-likelihood function of the BSD as shown earlier in figure 3.4, was derived in chapter 3 and the result is reproduced below:

$$v_i = \sum_{k=1}^{i}\left(-\gamma+\gamma\frac{y_k}{2\sigma^2}-\frac{1}{4}\gamma^2\left(\frac{y_k}{2\sigma^2}\right)^2\right) \tag{4.4}$$

$$= \sum_{k=1}^{i}\left(-\gamma+\gamma\frac{y_k}{2\sigma^2}-\frac{\gamma^2}{2}\right) \tag{4.5}$$

$$= \sum_{k=1}^{i}(y_k-b) \tag{4.6}$$

where (4.6) represents the normalized accumulator output with b as the bias of the log-likelihood function, given by $b = N_o B(1+\gamma/2)$, and N_o is the single-sided noise spectral density.

In the case of the BSD, the square-law envelope detected samples were directly used and the bias, b was added to it. This approximate likelihood measure was accumulated and the sequential test was carried out.

For all the three sequential detector models the thresholds and the bias can be fixed at any desired value to achieve the optimization of the detector.

4.3 SIGNAL MODELS

A baseband PN modulated signal in the presence and absence of data modulation and Doppler shift was generated and corrupted by Gaussian noise. The Doppler frequency offsets on both the code clock and/or the carrier frequency were simulated to examine the performance of all the detectors in various channel conditions. The received signals were also assumed to have been jammed by an intentional/unintentional jammer/interferer and the

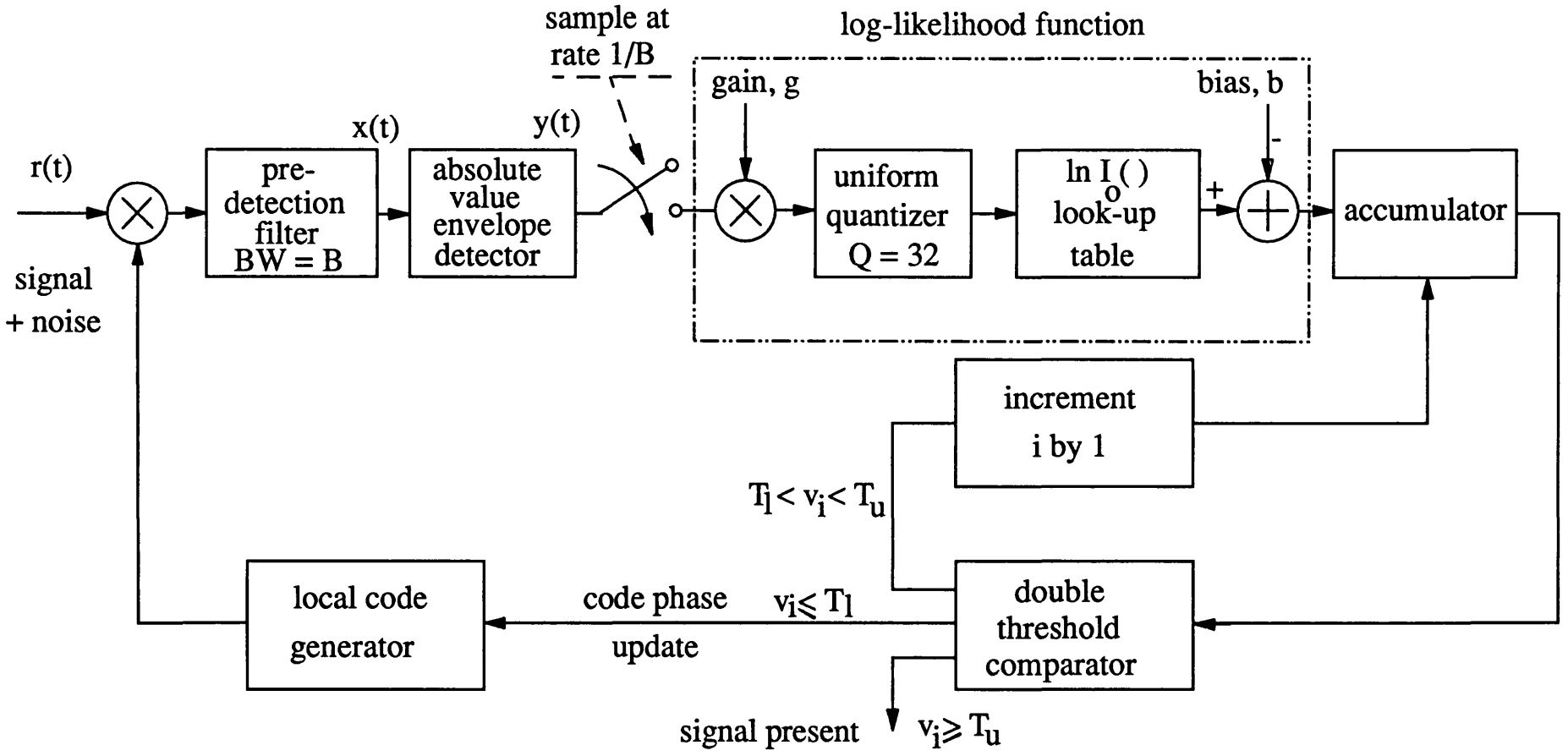

Figure 4.4 Schematic diagram of a quantized log-likelihood sequential detector.

performance of the detectors was obtained in the presence of a CW jammer and a pulsed tone jammer. The models employed for generating the signal structures represent each of the various combinations of these features.

The transmitted signal with BPSK data modulation can be represented simply by:

$$s(t) = \sqrt{2S}\, c(t)\, d(t)\, \cos \omega_c t \tag{4.7}$$

where c(t) is the PN binary waveform and d(t) is the data waveform given by

$$c(t) = C_k \qquad kT_c \le t \le (k+1)T_c \tag{4.8}$$
$$C_k \in -1,1 \qquad k \text{ an integer}$$

and C_k is the PN code sequence with T_c as the code chip interval.

$$d(t) = d_n \qquad nT_o \le t \le (n+1)T_o \tag{4.9}$$
$$d_n \in -1,1 \qquad n \text{ an integer}$$

and d_n is the PN code sequence with T_o as the data bit interval.

The data and the PN code clocks are assumed to be coincident such that $N = T_o/T_c$, where N is the processing gain which is 127 in the present simulation.

At the receiver, the received signal is a composite structure after Doppler shift and channel impairments and can be viewed as being from two classes (for the purpose of clarity), one containing data modulation and the other with no data modulation. Six types of composite received signal structures were thus considered in the simulations (without considering the cases of jamming which will be discussed in the subsequent sections) and their mathematical models are shown below:

Signal type 1: DS spread-spectrum signal without data modulation.

$$r_1(t) = \sqrt{2S}\, c(t - \zeta T_c) \cos(\omega_c t + \theta_c) + n(t) \tag{4.10}$$

This is the simplest form of signal with no data modulation and Doppler shift which is used as the reference signal to establish the comparative degradations when the data modulation and/or Doppler shift are present.

Signal type 2: DS spread-spectrum signal with code Doppler frequency offset without data modulation.

$$r_2(t) = S_2(t) \cos(\omega_c t + \theta_c) + n(t) \tag{4.11}$$

$$S_2(t) = \sqrt{2S}\, c\left(\frac{t}{1-\zeta'} - \zeta T_c\right) \tag{4.12}$$

This signal represents the code rate Doppler shift, ζ'/T_c, by incorporating the change in the code duration caused by the Doppler shift as a translation in the time of occurance, proportional to the Doppler shift under the assumption of an ideal code rate Doppler.

However, in practice, the non-uniform Doppler shift on various spectral components can lead to the distortion of the original spectrum as well as the waveform. This signal type prevails in practice when the carrier Doppler is well compensated and the residual carrier Doppler is quite negligible, however, the residual code Doppler is still considerably harmful.

Signal type 3: DS spread-spectrum signal with code and carrier Doppler frequency offset without data modulation.

$$r_3(t) = S_3(t)\cos(\omega_c t) + n(t) \tag{4.13}$$

$$S_3(t) = \sqrt{2S}\, c\left(\frac{t}{1-\zeta'} - \zeta T_c\right)\cos(\omega_d t + \theta_c) \tag{4.14}$$

This signal provides both code rate Doppler offset and carrier Doppler frequency offset. Even though, in many applications such as satellite communications the carrier Doppler shift is generally well compensated the residual carrier Doppler shift is still considerable and this model addresses these issues.

Signal type 4: DS spread-spectrum signal with data modulation.

$$r_4(t) = \sqrt{2S}\, d(t - \xi T_o - \zeta T_c)\, c(t - \zeta T_c)\cos(\omega_c t + \theta_c) + n(t) \tag{4.15}$$

This signal models the random data modulation which is synchronous to PN code clock.

Signal type 5: DS spread-spectrum signal with code Doppler frequency offset and data modulation.

$$r_5(t) = S_5(t)\cos(\omega_c t + \theta_c) + n(t) \tag{4.16}$$

$$S_5(t) = \sqrt{2S}\, c\left(\frac{t}{1-\zeta'} - \zeta T_c\right) d\left(\frac{t - T_i}{1-\zeta'} - \xi T_o\right) \tag{4.17}$$

This signal models the data modulation and the code rate Doppler shift assuming the situations in which the carrier Doppler is fully compensated and the residual Doppler on the carrier is negligible.

Signal type 6: DS spread-spectrum signal with code and carrier Doppler frequency offset with data modulation.

$$r_6(t) = S_6(t)\cos(\omega_c t) + n(t) \tag{4.18}$$

$$S_6(t) = \sqrt{2S}\, c\left(\frac{t}{1-\zeta'} - \zeta T_c\right) d\left(\frac{t - T_i}{1-\zeta'} - \xi T_o\right)\cos(\omega_d t + \theta_c) \tag{4.19}$$

This signal represents the worst case situation with the data modulation and both code rate Doppler and the residual carrier Doppler shift.

The symbols used in the above equations are defined as: S is the rms signal power, $d(t)$ and $c(t)$ are the data and code sequences with T_c the chip time of the PN code, T_o is the data bit

duration which is assumed to be an integral multiple of T_c, ζT_c the received code phase offset, $\xi T_o + \zeta T_c$ the received data bit phase offset assuming that the data stream timing is synchronized to the code chip time, ζ'/T_c is the received code frequency offset, ω_d is the received carrier radian frequency offset, T_i represents the beginning of the integration interval, ω_c and θ_c are the carrier radian frequency and random phase, and $n(t)$ is the additive white Gaussian noise with one-sided power spectral density N_o.

For the purpose of simulating these signals at baseband, the carrier frequency was assumed to be zero. The output of the correlator at baseband representing a sample value on the correlator curve for the case with data modulation and both code and carrier Doppler frequency offsets (signal type 6) can be given by

$$x(t) = u(t)\cos(\theta_c) + n(t) \tag{4.20}$$

$$u(t) = \sqrt{2}A\, c\left(\frac{t}{1-\zeta'} - \zeta T_c\right) d\left(\frac{t-T_i}{1-\zeta'} - \xi T_o\right) c\left(\frac{t}{1-\tau'} - \tau T_c\right) \tag{4.21}$$

where τT_c represents the local code phase offset and τ' represents the local code frequency error with $\zeta' - \tau' \ll 1$.

It is this correlator signal which is envelope detected and whose samples are directly emphasized by the nonlinearity function 'ln $I_o[\ ]$' of the sequential detector or fed to the single-dwell detector.

4.4 JAMMER MODELS

Two types of jammer signals were considered; namely, the CW jammer and the pulse jammer. In case of the CW jammer, the baseband equivalent of the jammer at the exact centre frequency of the spread-spectrum signal (carrier frequency) was assumed with the jammer-to-carrier power ratio, J/S varied. In case of the pulse jammer, the fraction of time that the pulse jammer was present (pulse duty factor) was varied for each value of J/S assuming that the average pulse power is constrained. The noise component contributed by the jamming signals can be derived as follow:

The received signal $r(t)$ in the presence of the jamming signal $J(t)$ is represented (assuming noiseless situation) as:

$$r(t) = s(t) + J(t) \tag{4.22}$$

where $s(t)$ is the transmitted direct-sequence BPSK signal given by (4.8). The receiver multiplies this signal by the PN waveform $c(t)$ to obtain the correlator signal $x(t)$, which is given by:

$$x(t) = c(t)\,[\,s(t) + J(t)\,] \tag{4.23}$$

$$x(t) = \sqrt{2}A\,d(t)\cos\omega_c t + c(t)\,J(t) \tag{4.24}$$

since $c^2(t) = 1$ the first component in the above equation represents the unspread BPSK signal and the second component $c(t)\,J(t)$ represents the *effective noise waveform due to jamming.*

However, the *noise term* contributed by the *jammer after correlation* clearly depends upon the number of PN chips over which the integration is carried out. For BPSK modulation, the equivalent noise component after correlator is given by:

$$n = \sqrt{\frac{2}{T_o}} \int_0^{T_o} c(t)\,J(t)\cos\omega_c t\,dt \tag{4.25}$$

$$n = \sqrt{\frac{2}{T_o}} \sum_{k=0}^{N-1} C_k \int_{kT_c}^{(k+1)T_c} J(t)\cos\omega_c t\,dt \tag{4.26}$$

where $C_0, C_1, \ldots\ldots, C_{N-1}$ are the N PN code chips with chip duration T_c and T_o is the data bit duration. The *jamming component* can then be defined as:

$$J_k = \sqrt{\frac{2}{T_c}} \int_{kT_c}^{(k+1)T_c} J(t)\cos\omega_c t\,dt \tag{4.27}$$

The resultant noise component in terms of jammer component can be written as

$$n = \sqrt{\frac{1}{N}} \sum_{k=0}^{N-1} J_k\,C_k \tag{4.28}$$

As the PN sequence can be approximated as an independent identically distributed binary sequence with (probability of occurance, $p = 1/2$), the noise component for any fixed jammer sequence $\mathbf{J} = (J_0, J_1, \ldots\ldots, J_{N-1})$ is a sum of independent random variables.

4.4.1 CW Jammer model

The most harmful jammer waveform is the one that maximizes J_k (jammer component) for each value of k. The jammer does not know the PN sequence $\{C_k\}$ and therefore, it should place as much energy as possible in the cosine coordinate of the signal to cause maximum damage which can be achieved by a CW signal. Generally, the jammer does not know the transmitted carrier phase also, thus, a deterministic CW jammer waveform model normally employs a random phase which is given by:

$$J(t) = \sqrt{2J}\cos(\omega_c t + \theta_j) \tag{4.29}$$

with J as the jammer power and θ_j as the phase parameter. The jammer component, thus, becomes

$$J_k = \sqrt{JT_c}\cos(\theta_j) \tag{4.30}$$

for all k, which is maximized when $\theta_j = 0$.

The received signal in the presence of CW jammer (in Gaussian noise) representing the worst case jammer with its entire power being placed in the exact signal coordinates viz., the carrier

frequency and the phase, can be given by

$$r(t) = \sqrt{2S}\, c(t+\zeta T_c)\cos(\omega_c t + \theta_c) + \sqrt{2J}\cos(\omega_c t + \theta_c) + n(t) \tag{4.31}$$

The correlator signal at baseband becomes:

$$x(t) = [\sqrt{2}A\, c(t+\zeta T_c) + \sqrt{2J}\,]\, c(t+\tau T_c)\cos\theta_c + n(t) \tag{4.32}$$

4.4.2 Pulse Jammer model

The pulse jammer with a time-averaged power of J is assumed to have the peak power J_p during the pulse interval given by

$$J_p = J/\rho \quad ; \rho < 1 \tag{4.33}$$

where ρ is the pulse duty factor which is the fraction of time the jammer is on.

The performance in the presence of any arbitrary jammer is normally expressed relative to the performance in the presence of a wideband jammer with uniform power spectral density, which is referred to as its *base line performance.* In the case of a pulse jammer, the jammer power spectral density, N_j/ρ where $N_j = J/W_{ss}$ with W_{ss} as the spread bandwidth, is used to compare its performance with an equivalent base line jammer with spectral power density N_J. The pulse jammer is normally expected to prevail over an interval of a few data bit durations with the assumption that the cases where the jammer might be on only for a small fraction of the transmitted data bit duration are ignored.

The received signal in the presence of a pulsed tone jammer waveform for the case of no data modulation can be represented as

$$r(t) = \sqrt{2S}\, c(t+\zeta T_c)\cos(\omega_c t + \theta_c) + \sqrt{J_p}\sum_{k=-\infty}^{\infty} P_J(t-kT_J)\cos(\omega_J t + \theta_J) + n(t) \tag{4.34}$$

where

$P_J(t) = 1 \qquad 0 \le t \le \tau_J$

$= 0 \qquad$ otherwise

τ_J = pulse width

T_J = time between successive pulses

with the rest of the symbols defined as earlier.

When the frequency difference between the desired spread-spectrum signal and the tone of the pulsed jammer is small enough ie., $\Delta\omega = |\omega_c - \omega_J| \approx 0$, then any bandlimiting of the jammer is considered negligible and the jammer carrier is assumed to be phase-locked to the desired signal. The received phase-locked jammer signal is thus given by

$$r(t) = \left[\sqrt{2S}\, c(t+\zeta T_c) + \sqrt{J/\rho}\sum_{k=-\infty}^{\infty} P_J(t-kT_J-\Delta_J)\right]\cos(\omega_c t + \theta_c) + n(t) \tag{4.35}$$

with $0 \le \Delta_J \le T_J$ which is the random pulse delay. The correlator output with the pulse jammer can be represented as

$$x(t) = \left[\sqrt{2}A\, c(t+\zeta T_c) + \sqrt{J/\rho} \sum_{k=-\infty}^{\infty} P_J(t-kT_J-\Delta_J) \right] c(t+\tau T_c)\cos(\theta_c) + n(t) \qquad (4.36)$$

The correlator outputs in (4.32) and (4.36) contain the equivalent noise components contributed by the jammer signals. This signal is envelope detected and the sampled output is passed to the sequential detector.

The signal-to-jammer power ratio S/J and the bit energy to jammer spectral power density E_b/N_j of a pulse jammer are related by:

$$\frac{E_b}{N_j} = \frac{S/R_b}{J/W_{ss}} = \frac{W_{ss}/R_b}{J/S} = \frac{N}{J/S} \qquad (4.37)$$

$$= PG + S/J \quad (in\ dB) \qquad (4.38)$$

where N and PG represent the processing gain in number of PN chips and in dB respectively. The rest of the symbols are as defined earlier.

A critical fraction of time the pulse jammer is on $\rho = \rho^*$ (the critical duty factor) exists that leads to the worst case bit error probability P_b as the E_b/N_j is varied and defined as [3]

$$\rho^* = \frac{0.709}{E_b/N_j} \qquad E_b/N_j > 0.709 \qquad (4.39)$$

$$= 1 \qquad E_b/N_j \le 0.709$$

This critical duty factor was also employed to observe the acquisition performance with E_b/N_j.

4.5 THE MONTE-CARLO SIMULATION PROCEDURES

The Monte-Carlo simulation is generally used to obtain the statistical behaviour of the detectors by counting the number of detections and false alarms for several runs of the detector [6-10]. This has been recognized as a well known adjunct to the analysis of communication systems when the analysis through closed form solutions is either very difficult or the solutions are unwieldy. Further, it provides a more realistic and complete understanding of the system behaviour for a practical range of system parameters. Even though the methods cannot be easily applied to provide generalized solutions, the applicability can be extended using quasi-analytic methods based on the observations for the limited ranges of interest. In the present work, the Monte-Carlo simulation procedure has been employed to obtain the performance of serial-search detectors for spread-spectrum code acquisition in various conditions.

4.5.1 Simulation of the sequential test procedure

The sequential test was simulated with the incoming sequence of a random starting phase and the search was carried out by examining the correlator output corresponding to each code cell. The correlator samples were accumulated after the appropriate log-likelihood transformation depending upon the each variant of the sequential detector and one of the three decisions namely; i) in-sync, ii) out-of-sync and iii) no decision (indeterminate) was made. The test was terminated on the decisions i) and ii) while continued by taking a new sample whenever the decision (iii) was made. At the end of each test, if the out-of-sync was detected (decision ii) then the local code phase was updated by one cell and the next test was carried out with the same incoming signal. If the in-sync was detected (decision i), then the input signal with a new arbitrary random phase was taken and a new sequential test was carried out.

At least 100 such trials, each with a different starting code phase, were employed and the number of detections and miss detections were determined. For every sequential test the number of false alarms and the successful dismissals were also obtained. At the end of 100 trials, using these results, the probability of detection and the probability of false alarm were computed. For every sequential test the number of samples needed for each out-of-sync decision was also obtained and the average sample number (ASN) over the 100 tests was computed.

All these observations were carried out for a range of system parameters by varying the upper threshold T_u, lower threshold T_l, bias b, design SNR and the input SNR in the appropriate ranges of interest. Usually, the input SNR was varied from -10dB to -25dB corresponding to a predetection SNR range +10dB to -4dB (as the process gain is 21dB) and the performance with different thresholds and bias values were obtained. With the PN code length of 127 and a total of 100 tests, each with an arbitrary code phase, these tests achieve P_d with an accuracy of 1×10^{-2} and P_{fa} with an accuracy better than 1×10^{-4} [11-13]. However, from the statistical confidence level, these accuracies are one order less.

4.5.2 Computer model of the single-dwell detector

The schematic diagram of a single-dwell detector is shown in figure 4.5. As shown in figure the single-dwell detector uses a similar computer model as the sequential detector until the envelope detector/sampler and the sampled output is then, fed to a single-dwell serial search algorithm. This detector accumulates (integrates) the sampled outputs of the envelope

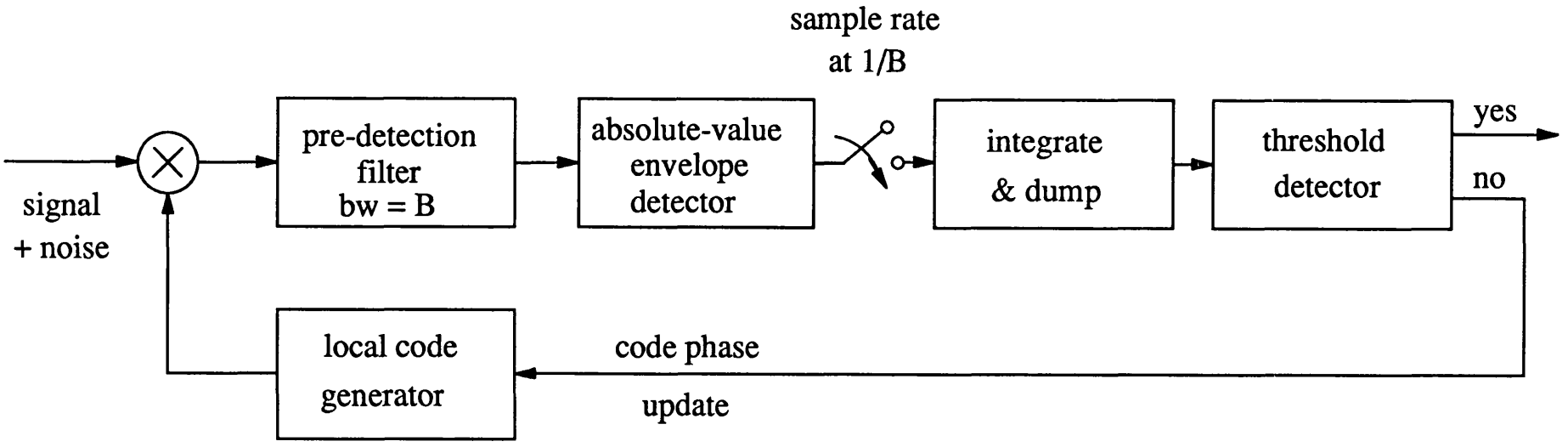

Figure 4.5 Schematic diagram of a non-coherent single-dwell detector at baseband.

detector for a fixed duration which is called the *dwell time* and compares the sample sum with a threshold at the end of the dwell time. If the integrator output crosses the threshold, then the coarse in-sync is declared else the out-of-sync is declared and the search continued.

As with the sequential detector, 100 tests were carried out with each fixed-dwell test starting with the incoming code sequence of an arbitrary random phase and the P_d and P_{fa} were obtained from which the mean acquisition time was computed. The simulation was carried out for a range of threshold and the dwell time and the optimization of the detector performance over these parameter ranges was performed.

4.5.3 Computer model of the digital matched filter

The simulation of a digital matched filter employs the same transmit model as the single-dwell and sequential detectors. However, the receiver employs a digital matched filter model for code acquisition which is quite different from both the sequential detector and the single-dwell detector.

The schematic diagram of the digital matched filter is shown in figure 4.6. It consists of:

i. a hard limiter or 1-bit A/D converter

ii. a digital correlator

iii. a replica code register

iv. a threshold detector

As shown in figure the digital matched filter uses a hard quantizer or a 1-bit A/D converter which converts the corrupted received baseband signal into a bipolar signal which was then fed to the digital correlator. The length of the correlator is same as the code length $L = 127$. The correlator compares the incoming signal with a stored local replica and computes the correlation between the two codes using the autocorrelation function computed as:

$$acf = \frac{2\, n_{agr}}{L} - 1 \tag{4.40}$$

where n_{agr} is the number of agreements over a code length and acf is the auto correlation value for a given code delay.

The correlation value was tested against a threshold to decide whether the synchronization was achieved or not. If the threshold was not crossed, then a new incoming chip was loaded into the correlator and the comparison was carried out. The decisions were made at a rate equal to the code rate (or a multiple of the code rate) and hence, for each comparison, $L-1$

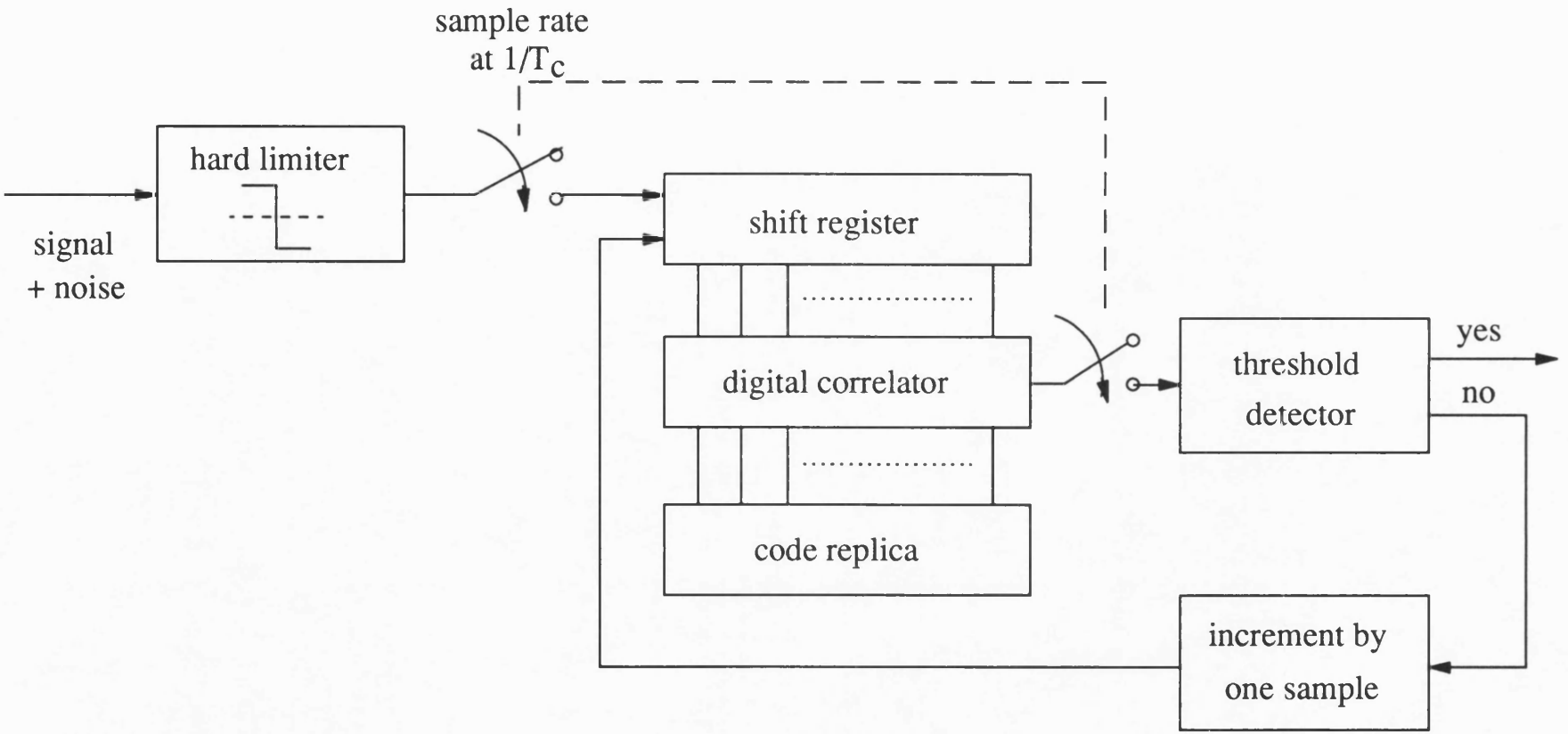

Figure 4.6 Schematic diagram of a digital matched filter at baseband.

previous data bits participate along with the received data bit. For each comparison, a parallel comparison with the uncorrupted version of the received signal (clean transmit signal) was also carried out and the uncorrupted correlator output (ideal case) was generated. This ideal correlator signal was employed to check either the in-sync or the out-of-sync conditions to decide the number of miss detections and false alarms (or equivalently the correct detections and correct dismissals).

For each test, the number of false alarms and the successful dismissals were obtained and the search was carried out until the synchronization was achieved. For each set of system parameters, 100 such tests were carried out and the P_d and P_{fa} were obtained from which the mean acquisition time was computed. The tests were repeated by varying the input SNR in the range -10dB to -30dB for a range of threshold values and various performance characteristics of the digital matched filter were obtained, and the optimization of the detector was achieved.

4.6 REFERENCES

1) W.H.Press *et al*, *Numerical recipes - The art of scientific computing*, Cambridge University Press, Cambridge, 1986.

2) *Prospero Fortran for GEM version*, Prospero Software, London 1987.

3) M.K.Simon, J.K.Omura, R.A.Scholtz and B.K.Levitt, *Spread spectrum communications*, vol. 1, Computer Science Press, Maryland, USA, 1985.

4) L.R.Rabiner and B.Gold, *Theory and applications of digital signal processing*, Prentice Hall Inc, NJ, 1975.

5) R.D.Strum and D.E.Kirk, *First principles of discrete systems and digital signal processing*, Addison-Wesley Publishing Company, USA, 1988.

6) R.Y.Rubinstein, *Simulation and the Monte-Carlo method*, John Wiley & Sons, 1981.

7) H.A.Meyer (Ed), *Symposium on Monte-Carlo methods*, John Wiley & Sons, 1956.

8) L.C.Palmer, P.Y.Chang, "Simulating spread spectrum systems" COMSAT Technical Review, vol. 19, no. 2, pp 163-194, Fall 1989.

9) U.R.Krieger, B.Muller-Clostermann and M.Sczittnick, "Modeling and analysis of communication systems based on computational methods for Markov chains"

IEEE Jou. on Sel. Areas in Comm. vol. 8, no. 9, pp 1630-1648, December 1990.

10) R.F.W.Coates, G.J.Janacek and K.V.Lever, "Monte Carlo simulation and random number generation" IEEE Jou. on Sel. Areas in Comm. vol. 6, no. 1, pp 58-66, January 1988.

11) K.V.Ravi and R.F.Ormondroyd, "Computer simulation of a quantized log-likelihood sequential detector for faster acquisition of spread-spectrum pseudo-noise signals." 5th International Conference on Radio Receivers and associated systems, IEE Conference publication No. 325, pp 207-211, July 24-26,1990, Cambridge, UK.

12) K.V.Ravi and R.F.Ormondroyd, "Comparison of the acquisition performance of biased square law and quantized log-likelihood sequential detectors for PN acquisition" IEEE International Symposium on Spread Spectrum Techniques and Applications, Symposium Proceedings, pp 53-58, September 24-26,1990, London, UK.

13) K.V.Ravi and R.F.Ormondroyd, "Performance of sequential detectors for the acquisition of data modulated spread-spectrum pseudo noise signals", IEEE International Conference on Communications, ICC'91, June 23-26, 1991, Denver, Colorado, USA.

APPENDIX 4.1

Design of a third-order Butterworth low-pass filter

The third order Butterworth low-pass filter has been designed as an infinite impulse response (IIR) filter using bilinear transform method.

The transfer function of the analog filter in the transform domain is

$$G(s) = (s^2+s+1)(s+1) \tag{A.1}$$

On denormalizing the transfer function using $s \rightarrow s/\omega_{ca}$ where ω_{ca} is the cut-off frequency of the analog filter, G(s) becomes

$$G(s) = \frac{1}{\left[\left(\frac{s}{\omega_{ca}}\right)^2+\frac{s}{\omega_{ca}}+1\right]\left[\left(\frac{s}{\omega_{ca}}\right)+1\right]} \tag{A.2}$$

$$G(s) = \frac{\omega_{ca}^3}{\left(s^2+\omega_{ca}s+\omega_{ca}^2\right)\left(s+\omega_{ca}\right)} \tag{A.3}$$

By using prewarping, ω_{ca} can be expressed in terms of the cut-off frequency of the digital filter ω_{cd} and the sampling frequency f_s with a sampling time, $T = 1/f_s$.

$$\omega_{ca} = \frac{2}{T}\tan\left(\frac{\omega_{cd}T}{2}\right) = 2f_s\tan\left(\frac{\omega_{cd}}{2f_s}\right) \tag{A.4}$$

Using bilinear transform

$$s = \frac{2}{T}\frac{(z-1)}{(z+1)} = \frac{2}{T}\frac{(1-z^{-1})}{(1+z^{-1})} \tag{A.5}$$

The transfer function of the digital filter can thus be expressed as

$$G(z) = \frac{\omega_{ca}^3}{\left(\frac{2}{T}\right)^3\left(\frac{1-z^{-1}}{1+z^{-1}}\right)^3 + 2\omega_{ca}\left(\frac{2}{T}\right)^2\left(\frac{1-z^{-1}}{1+z^{-1}}\right)^2 + 2\omega_{ca}^2\left(\frac{2}{T}\right)\left(\frac{1-z^{-1}}{1+z^{-1}}\right) + \omega_{ca}^3} \tag{A.6}$$

$$\frac{Y(z)}{X(z)} = \frac{\omega_{ca}^3(1+z^{-1})^3}{\left(\frac{2}{T}\right)^3(1-z^{-1})^3 + 2\omega_{ca}\left(\frac{2}{T}\right)^2(1-z^{-1})^2(1+z^{-1}) + 2\omega_{ca}^2\left(\frac{2}{T}\right)(1-z^{-1})(1+z^{-1})^2 + \omega_{ca}^3(1+z^{-1})^3} \tag{A.7}$$

Let

$$a = \left(\frac{2}{T}\right)^3 \tag{A.8}$$

$$b = 2\omega_{ca}\left(\frac{2}{T}\right)^2 \tag{A.9}$$

$$c = 2\omega_{ca}^2\left(\frac{2}{T}\right) \tag{A.10}$$

$$d = \omega^{ca^3} \tag{A.11}$$

On substituting in (A.7) and simplification the transfer function becomes

$$\frac{Y(z)}{X(z)} = \frac{d(1+3z^{-1}+3z^{-2}+z^{-3})}{(a+b+c+d)+(3d+c-b-3a)z^{-1}+(3a+3d-b-c)z^{-2}+(d+b-a-c)z^{-3}} \tag{A.12}$$

$$Y(z)(a+b+c+d) = d(1+3z^{-1}+3z^{-2}+z^{-3})X(z) - (3d+c-b-3a)z^{-1}Y(z) \tag{A.13}$$
$$-(3a+3d-b-c)z^{-2}Y(z) - (d+b-a-c)z^{-3}Y(z)$$

$$Y(z) = P(1+3z^{-1}+3z^{-2}+z^{-3})X(z) - Qz^{-1}Y(z) - Rz^{-2}Y(z) - Sz^{-3}Y(z) \tag{A.14}$$

where

$$P = \frac{d}{(a+b+c+d)} \tag{A.15}$$

$$Q = \frac{(3d+c-b-3a)}{(a+b+c+d)} \tag{A.16}$$

$$R = \frac{(3a+3d-b-c)}{(a+b+c+d)} \tag{A.17}$$

$$S = \frac{(d+b-a-c)}{(a+b+c+d)} \tag{A.18}$$

By retransforming into time domain the sampled output of the digital filter becomes

$$y(n) = P[x(n)+3x(n-1)+3x(n-2)+x(n-3)] - Qy(n-1) - Ry(n-2) - Sy(n-3) \tag{A.19}$$

The filter output y(n) can be easily realized for a given cut-off frequency and sampling frequency by computing the coefficients P,Q,R and S and using the recursive equation (A.19) with an appropriately set initial conditions for the realization of a causal filter. In the present simulation, f_s = 200 kHz and f_c = 787 Hz were employed and the filter frequency response was first verified for various known sinusoids in the passband and cut-off region. The impulse response was also verified by using an input sequence '100000.....' and the stability of the filter was assessed.

CHAPTER 5

PERFORMANCE OPTIMIZATION OF THE SEQUENTIAL DETECTOR IN THE ABSENCE OF DATA MODULATION

5.1 INTRODUCTION

In this chapter, the sequential detector is applied to the problem of initial acquisition of direct-sequence spread-spectrum pseudo-noise signals in the absence of data modulation and the performance of three variants of the sequential detector is presented. The optimization of the three variants with respect to various critical system parameters is also presented and the optimum performances of each variant are compared.

In the subsequent sections, the acquisition performance is presented in two parts. In the first part, the performance of an ideal log-likelihood sequential detector (LLD) is obtained by means of a Monte-Carlo simulation. The ideal log-likelihood function is very difficult to implement. However, it is possible to implement the function digitally using a look-up table approach. Consequently, a variant of the sequential detector called the quantized log-likelihood sequential detector (QLD) was considered. The principal parameter of interest, in the first instance, is the number of quantization levels by the quantized log-likelihood function to provide a comparable performance with the ideal log-likelihood function. Hence, the effect of the number of quantization levels of the uniform quantizer Q, on the acquisition performance of the quantized log-likelihood sequential detector was obtained and compared with the performance of an ideal log-likelihood sequential detector. From these results, the minimum number of quantization levels for the QLD yielding an acquisition performance close to the ideal sequential detector LLD, has been determined.

The log-likelihood function can also be realized employing an approximate model to the ideal log-likelihood function, suitable at *low SNR* conditions, and this results in another variant called the biased square law sequential detector (BSD) which was described in chapter 3. The acquisition performance of the BSD was also determined for the identical

system parameters. The acquisition performances of the three variants are presented and compared for two bias values, namely, the Wald's optimum bias (defined in chapter 3) and a non-optimum bias value.

In the second part of this chapter, two stages of optimization employed for all three variants of sequential detector are presented and discussed. In order to obtain the optimum performance of the three variants, in the first phase, optimization was carried out with respect to both the upper and lower thresholds of the detectors. In a second stage, the detectors were also optimized with respect to the input SNR and the design SNR. The three dimensional acquisition characteristics pertaining to both the stages of optimization are presented and the optimization of the detectors is then discussed.

PART I: PERFORMANCE OF THE SEQUENTIAL DETECTORS

5.2.1 System Parameters

The critical system parameters determining the performance of the sequential detector system are: i) the upper threshold, T_u ii) the lower threshold, T_l iii) the bias value, b and iv) the input SNR or equivalently the predetection SNR, γ. For most of the time, the SNR at the input to the sequential detector is more appropriate than the SNR obtained at the input to the spread-spectrum receiver. Consequently, in all the characteristics presented, the *predetection SNR* denoted by γ is used. This is the SNR at the output of the predetection filter after the spread-spectrum correlation and is therefore larger than the receiver input SNR by the spread-spectrum processing gain. In order to obtain a valid simulated performance of the detector, the loop gain of the sequential detector also needs to be carefully optimized to achieve acceptable probabilities of detection and false alarm over the input SNR range of interest.

5.2.2 Performance Parameters

The major performance parameters of the sequential detector considered are: i) average sample number (ASN), ii) probability of detection (P_d) and iii) probability of false alarm (P_{fa}). The performance of the sequential detector is generally characterized by its *Average Sample Number* (ASN) which is the number of samples required to terminate the test. Assuming that the samples occur at a rate of $1/T \leq B$, where B is the predetection filter bandwidth, the mean dismissal time is given by:

$$T_{dis} = ASN/B \tag{5.1}$$

The performance is also characterized by the probability of detection P_d and the probability of false alarm P_{fa} for a given input SNR. However, when applied to the acquisition of spread-spectrum signals, the total mean acquisition time, T_{acq}, plays a significant role than the ASN and consequently major emphasis is placed on the acquisition time characteristics.

5.2.3 Total mean acquisition time

The mean acquisition time of a sequential detector depends on a combination of ASN, P_d and P_{fa}. While the occurance of false alarms cause a false alarm penalty time to be added to the acquisition time, miss detection (or a non-unity P_d) increases the number of passes of the search through the uncertainty region, depending on the required probability of overall acquisition P_{acq}. The total mean acquisition time is the sum of the search times required to search that part of the uncertainty region where the signal is *not* present and the search time for the cell where the signal *is* present. However, normally the time for the latter is neglected due to the large number of cells where the signal is not present. The time for verification of a false alarm (T_{vr}) and the time to reach truncation to declare the signal present (T_{tr}) are typically assumed to be $50ms$ each. Thus the mean acquisition time T_{acq} with the overall probability of acquisition $P_{acq} = 0.9$ (assumed for the present simulation) is given by:

$$T_{acq} = T_{dis}\left[1 + \frac{P_{fa}(T_{tr} + T_{vr})}{T_{dis}}\right] q \left[\frac{\ln(1 - P_{acq})}{\ln(1 - P_d)}\right] \tag{5.2}$$

where q is the total number of code cells to be searched.

5.2.4 Performance of the quantized log-likelihood detector

To assess the acquisition performance of the sequential detector, the ASN, P_d and P_{fa} were obtained by means of a computer simulation of the sequential detector for the predetection SNR, γ, ranging from -4dB to +10dB for various thresholds and bias values. Generally, it was observed that P_d is decided mainly by both the lower threshold and the bias while P_{fa} is mainly controlled by the upper threshold and the bias level. The effect of the other threshold seems to be minor in both cases. For the purpose of the initial evaluation of the QLD to obtain the minimum number of quantization levels, the upper threshold was fixed at 5.0 and three lower threshold values equal to -5.0, -2.0 and -0.5 were chosen. These values are in the range of the near-optimum values observed in the optimization of the detectors which will be presented in the subsequent sections. For each set of thresholds, two different bias levels, b, were also employed, which are at the normalized Wald's optimum, $b_1 = \gamma(1+\gamma/2)$ and a non-

optimum bias equal to $b_2 = \gamma$ [1-3]. The bias in this case is directly derived from the predetection SNR and provides the ideal realization of the log-likelihood function for each value of the input SNR. The choice of these values allows the performance variation with a sub-optimum bias as well as the near-optimum thresholds to be analyzed more completely.

5.2.5 Effect of the number of quantization levels

The effect of the number of quantization levels, Q, on the performance of the QLD were obtained for Q = 10,16,32,40,50 and 100 with the upper and lower thresholds at 5.0 and -5.0 respectively. The characteristics of the ASN versus predetection SNR and the mean acquisition time versus predetection SNR, as a function of Q, are presented in figures 5.1 and 5.2. The ASN and the acquisition characteristics for both the QLD with number of quantization levels $Q = 32$ and the LLD are also shown in figures 5.3 and 5.4 at both bias values with the upper threshold at 5.0 and the lower threshold at -5.0.

5.2.5.1 ASN versus Predetection SNR

The ASN for the sequential detection system is seen to depend on the lower threshold, the bias value and the predetection SNR. From the characteristics shown in figure 5.3, it is observed that the ASN increases with the decreasing predetection SNR. For example, for the ideal LLD with the optimum bias, the ASN is 6.25 at SNR = 0dB for the lower threshold at -5.0 while the ASN is 15.54 at SNR = -3dB for the same threshold. With the non-optimum bias, the ASN is slightly higher than that with the optimum bias ie., 10.2 at SNR = 0dB and 21.1 at SNR = -3dB for the same threshold. The ASN for the QLD with Q = 32 closely agrees with the LLD at SNR = 0dB. However, at SNR = -3dB, the QLD appears to be overshooting the LLD showing a sharp increase in the ASN with the decreasing SNR which can be attributed to the effect of quantization at low SNRs. This effect of coarse quantization on the ASN at lower predetection SNRs can be seen in figure 5.1. The effect of quantization noise on the ASN for $Q > 50$ is seen to be minimal even at lower SNRs.

As the lower threshold is increased the ASN reduces, however, the false alarm probability also starts increasing, and this starts to control the mean acquisition time. This factor limits the choice of the lower threshold to moderate values. With the optimum bias, the ASN is seen to be always lower than with the non-optimum bias.

5.2.5.2 Mean Acquisition Time versus Predetection SNR

Figure 5.4 shows the minimum mean acquisition time for two biases with the upper

threshold at 5.0 and the lower threshold at -5.0. The mean acquisition time as a function of the predetection SNR has been plotted for both the LLD and the QLD (for Q = 10,16,32,40,50 and 100), and the results are shown in figure 5.2. Typically, the mean acquisition time reduces as the predetection SNR increases from -4dB, passes through a minimum and then increases. At the lower predetection SNR = -4dB, the ASN and the P_{fa} are both at their maximum and these are the dominant terms which cause a higher acquisition time even though the P_d is also at its maximum value. As the SNR is increased, the initial fall in the mean acquisition time is due to decreases in both the ASN and the P_{fa}. A further increase in the SNR, even though causes the ASN and P_{fa} to be reduced, increases the mean acquisition time. This is because of the significant reduction in P_d, causing the number of passes through the uncertainty region to rise sharply. The reason for this is not immediately obvious, because it seems logical that increasing the SNR would increase P_d. However, in the case of sequential detector the detector bias, b, is determined by the predetection SNR. As the SNR is improved, the bias level *falls* relative to the upper threshold and the likelihood of the samples exceeding the upper threshold thus *decreases*.

The minimum mean acquisition time and the optimum predetection SNR at which it occurs vary with the thresholds, the biases and the type of the detector. The optimum SNR with the non-optimum bias is seen to be broader than that with the optimum bias while the minimum mean acquisition time with the optimum bias is always less than that with the non-optimum bias as seen from figure 5.4.

The mean acquisition time for QLD with Q = 32 closely agrees with the LLD for most part of the SNR region of interest. For the QLD with the number of quantization levels set at Q = 10 and 16, although the acquisition time still shows a minimum, it is higher than the minimum achievable and rises very sharply with varying SNR. However, for Q = 32 and above, this minimum almost merges with that of the LLD and the characteristic closely agrees with that of the LLD throughout the SNR range of interest. The optimum SNR occurs around 7dB for both the LLD and the QLD with a minimum achievable acquisition time of approximately *0.5 sec* for the given system parameters.

The minimum mean acquisition time obtainable from the QLD appears to be considerably less than for fixed-dwell serial search systems with the same system parameters (which will be shown in chapter 7). However, the input SNR necessary to achieve this minimum mean acquisition time is higher. This is due to the fact that the simulation, employs a bias which

depends on the predetection SNR. A sequential detector designed with this input SNR as the optimum, with the bias derived from its predetection SNR, can provide the optimum performance for an input SNR of around -15dB for a 127 chip sequence. However, as seen from figure 5.4, the bias of the sequential detector plays an important part in determining the optimum input SNR, and hence, on the choice of the design SNR. As Wald's optimum bias is valid only for the lower input SNRs and the exact expressions for the decision probabilities and the average test duration do not require the bias to correspond to Wald's optimum bias [3], changing the bias independently from the predetection SNR would allow the choice of a design SNR suitable for a wider range of input SNRs. The effects of the bias variation (sub-optimum bias) and the design SNR, on the acquisition performance will be fully examined in the subsequent sections and the optimum detector performance will be derived.

Thus, the QLD with 32 quantization levels is seen to have a performance close to that of the ideal log-likelihood sequential detector. With this number of quantization levels, a simple realization of the QLD using a look-up table approach can be implemented digitally with an easily manageable size of ROM (read only memory), thus reducing the hardware complexity and consequently the QLD with 32 quantization levels has been employed for all further analyses.

5.3 COMPARISON OF THE ACQUISITION PERFORMANCE OF BSD AND QLD

This part compares the acquisition performance of the quantized log-likelihood sequential detector (QLD) with the biased square law sequential detector (BSD). The BSD was also simulated with the same system parameters as the QLD and its acquisition performance was obtained. The performance of the QLD with $Q = 32$ and the BSD have been compared both at Wald's optimum bias and at a non-optimum bias for a predetection SNR ranging from -4dB to +10dB.

5.3.1 Comparison of the acquisition performance

From equation (5.2) it was observed that the total mean acquisition time is not only directly related to the mean dismissal time but also to P_d and P_{fa}. Consequently, the simulation results have been presented to facilitate the comparisons of ASN as well as the mean acquisition time. It has been observed that, for both types of detector, P_d is mainly decided by the lower threshold T_l, and the bias value b, whereas P_{fa} is mainly decided by the upper threshold, T_u, and the bias value; with the other thresholds showing a minor influence on

both P_{fa} and P_d.

For the purpose of comparison, the upper threshold was fixed at 5.0 and the lower threshold was set to -5.0,-2.0 and -0.5 with the two bias values b, viz: normalized Wald's optimum, $b_1 = \gamma(1 + \gamma/2)$ and the non-optimum, $b_2 = \gamma$ and the simulation was repeated for each set of values. The ASN, P_d and P_{fa} for the QLD with $Q = 32$ and the BSD for both bias values with different threshold settings was obtained, and the variation of ASN with predetection SNR are shown in figures 5.5-5.6 for both types of detector.

5.3.2 ASN characteristics

The ASN of the sequential detector depends both on the lower threshold and the bias value and is always seen to be less when optimally biased than when non-optimally biased. From the characteristics shown in figure 5.5 and 5.6 , it can be seen that the ASN increases with decreasing predetection SNR. For the QLD, the ASN is lower than the BSD at an SNR = 0dB and almost as good as the LLD (figure 5.3). The difference is mainly due to the effect of the coarse approximation employed in the BSD by truncating the power series expansion of the $\ln I_o[\ ]$ function to the fourth power. However, at an SNR = -3dB the QLD overshoots the BSD and shows a sharp increase in the ASN when the SNR is further decreased. This rise is seen to be due to the effect of quantization at low SNRs. Nevertheless, when the quantization levels are increased to $Q > 100$ this rise in the ASN is seen to be minimal as shown in figure 5.1.

5.3.3 Acquisition characteristics

The mean acquisition time for both the detectors as a function of the predetection SNR in the range of -4dB to 10dB is shown in figures 5.7 and 5.8 for both the optimum and the non-optimum bias points. For both the QLD and the BSD, the mean acquisition time initially decreases with increase in SNR from -4dB and passes through a minimum. As in the case of LLD and the QLD (discussed earlier), for the case of BSD also the initial fall in T_{acq} is attributed to decreases in the ASN and the P_{fa} with an increasing SNR. The increase in T_{acq} is also because of the significant reduction in P_d at higher SNRs which increases the number of passes required.

For the case of the QLD, the minimum T_{acq} is always less with the optimum bias than with the non-optimum bias. However, for the BSD the minimum occurs with the *non-optimum* bias. This leads to the observation that the truncation error in the $\ln I_o[\ ]$ function when

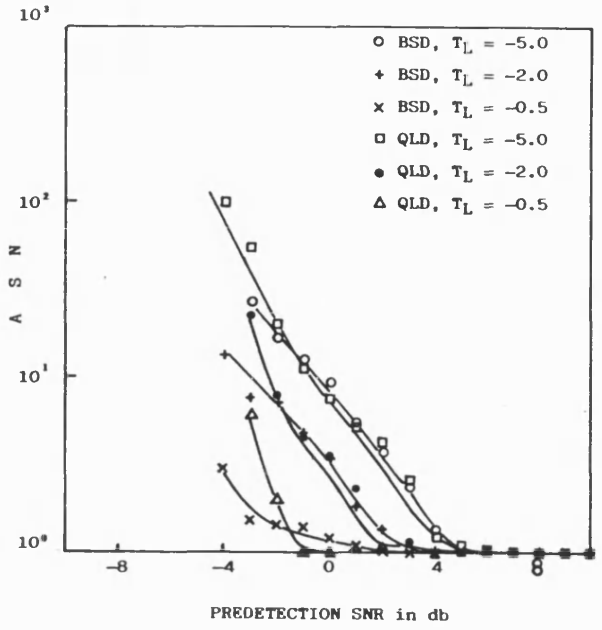

Figure 5.5 A S N vs γ for BSD and QLD at $b = b_1$.

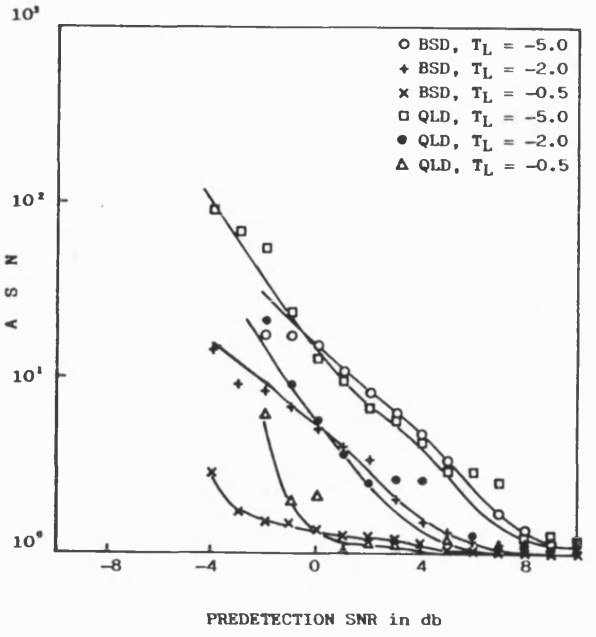

Figure 5.6 A S N vs γ for BSD and QLD at $b = b_2$.

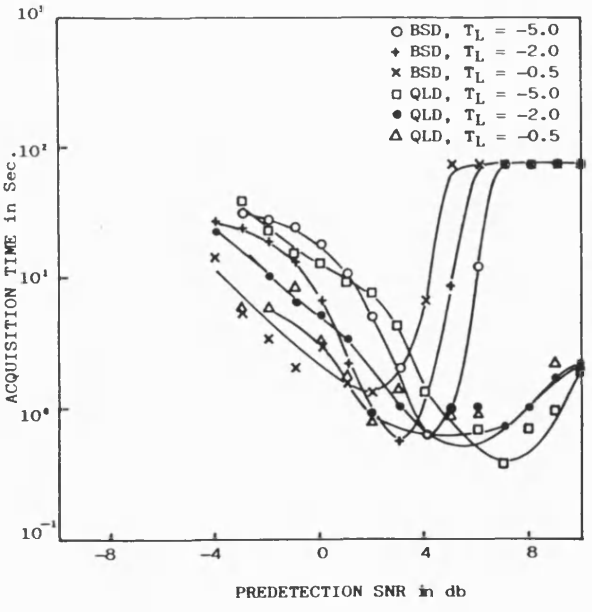

Figure 5.7 T_{acq} vs γ for BSD and QLD at $b = b_1$.

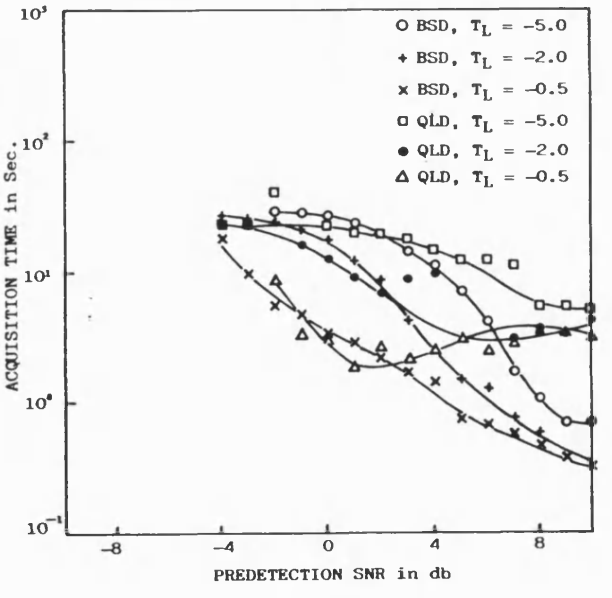

Figure 5.8 T_{acq} vs γ for BSD and QLD at $b = b_2$.

approximated with the BSD, requires that the bias needs to be carefully tuned for optimum performance. The optimum predetection SNR is higher in the case of the non-optimum bias than with the optimum bias. For the QLD, the optimum SNR occurs around 7dB (with normalized Wald's optimum bias) whereas for the BSD, the optimum SNR occurs around 10dB (with non-optimum bias) and is higher than either the LLD or the QLD, thus limiting its use to operation in high SNRs. The corresponding input SNRs at which this minimum occurs are -14dB for the QLD and -11dB for the BSD. In all the cases, minimum mean acquisition times of around 0.5*sec* are achieved.

Thus, the QLD is found to perform better with the optimum bias at low SNRs than the BSD. The mean acquisition time of the BSD at the optimum bias rises rapidly with the increasing SNR and is also highly sensitive to the predetection SNR whereas the QLD has a relatively robust performance at the optimum SNR. The BSD achieves the minimum mean acquisition time for the non-optimum bias at a higher predetection SNR. Performance of the BSD is found to be worse than the QLD, in particular, for achieving minimum mean acquisition time at lower predetection SNR. The exact realization of a square law detector is also quite difficult whereas the realization of the QLD (for example, using a look-up table approach for 32 quantization levels) can be implemented easily with a relatively small ROM size.

Even though certain conclusions have been drawn from these results, the exact realization of the sequential detector requires the optimum or near-optimum system parameters to be used to achieve the best performance. As seen from the above comparisons, the lower threshold, the bias value and the predetection SNR play critical role in determining the performance of the detector. Normally, as the bias is derived from the SNR, the variation in the input SNR ideally causes a change in the bias. However, it is also an engineering requirement to design a sequential detector at a fixed design SNR which can work for a wide range of input SNRs without much degradation. All these considerations lead to the investigation of the optimum design SNR and the associated system parameters for an optimum sequential detector. These optimizations were carried out for all three variants and their optimum performance is discussed in the following sections.

PART II: OPTIMIZATION OF SEQUENTIAL DETECTOR

5.4.1 Optimization procedure

As the mean acquisition time is critically related to all the system parameters, two stages of optimization were carried out to determine the optimum acquisition performance of the sequential detector. In stage one, both the upper and lower thresholds were varied over the practical range of interest at a fixed predetection SNR and the acquisition performance was obtained. In the second stage, both the predetection SNR and the design SNR were varied using the near-optimum thresholds obtained from stage one and the acquisition performance was then obtained. The bias was then set as a function of the design SNR and the input SNR (predetection SNR) was varied to obtain the required performance characteristics. For all the characteristics, two bias values related to the design SNR were employed, the first was the normalized Wald's optimum bias, $b = b_1$ and the second was a non-optimum bias, $b = b_2$, both defined in section 5.2.4. The characteristics for both these stages have been plotted as three dimensional (3-d) curves with the logarithm of T_{acq} on the vertical axis and their characteristics are discussed in the following sections.

5.4.2 Acquisition time characteristics

The mean acquisition time T_{acq}, ASN, P_d and P_{fa} were determined by varying the thresholds (stage I optimization) and by varying the input SNR and the design SNR (stage II optimization) and the optimization curves are shown separately for both stages of optimization.

5.4.3 Threshold optimization curves

Figures 5.9a through 5.14a show the optimization curves with respect to the upper and lower thresholds for both bias values. For all the variants, both the input SNR and the design SNR were chosen to result in the T_{acq} close to the minimum acquisition time observed from the results of the previous section. For both the LLD and the QLD, all the curves were obtained at a fixed input SNR of -13dB (corresponding to a predetection SNR = 8 dB) for a design SNR also at 8dB and the lower threshold was varied from -1.0 to -15.0 whilst the upper threshold was varied from 0.0 to 10.0. In case of the BSD, the design SNR was set at 4dB whereas the corresponding input SNR was at -17dB (predetection SNR = 4dB). The same range of thresholds as for the LLD and QLD were used. For ease of interpretation, the

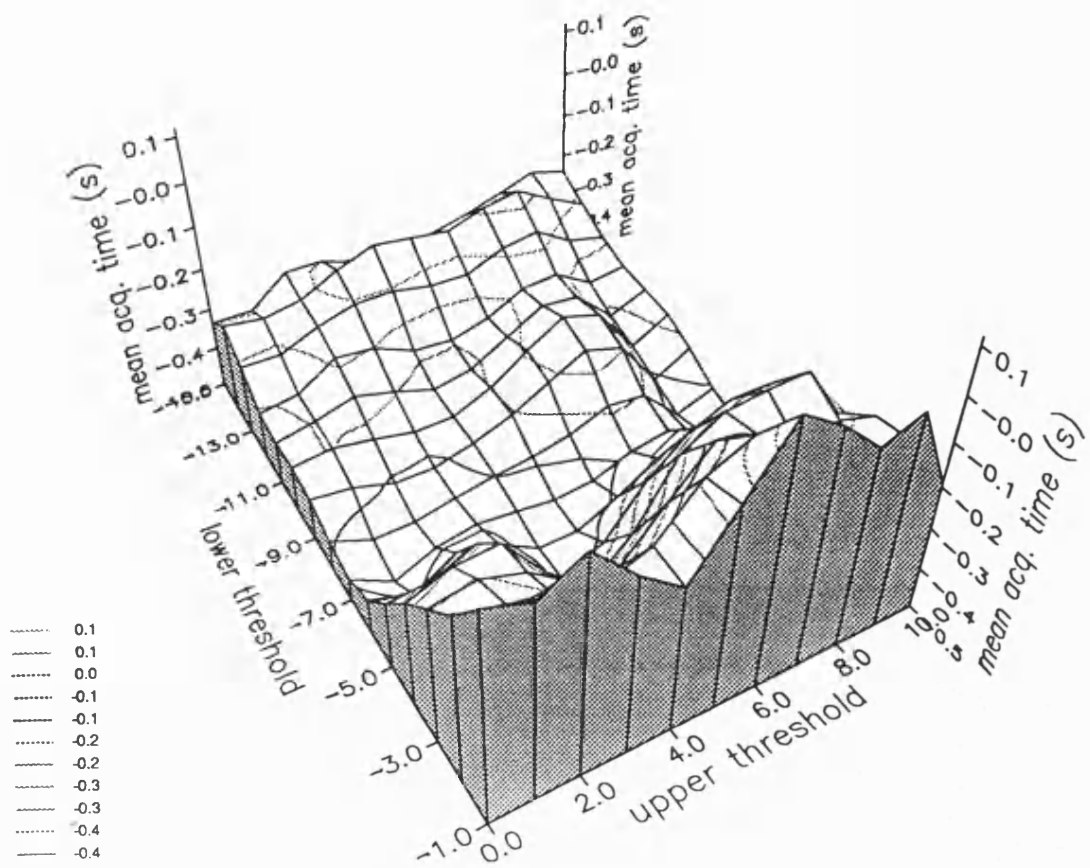

a) 3-d representation

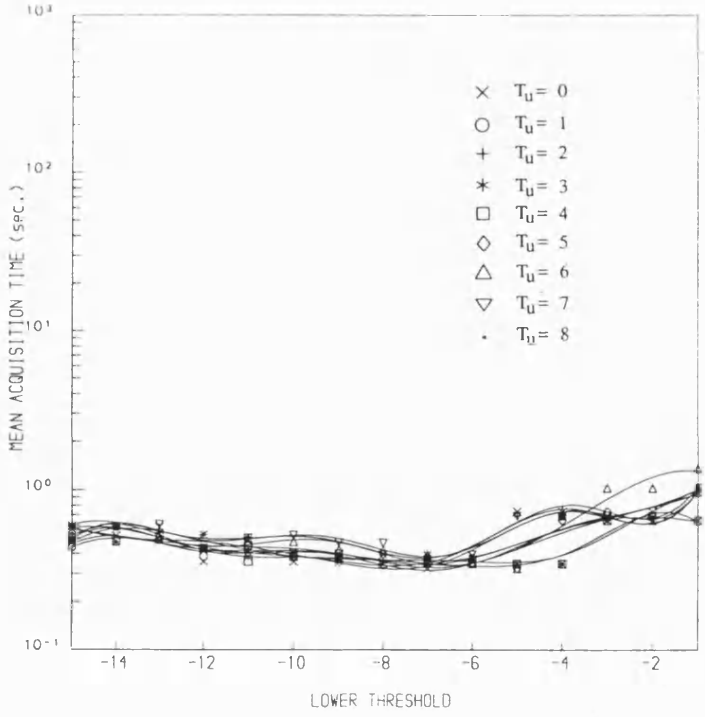

b) 2-d representation

Figure 5.9 T_{acq} vs T_u and T_l for LLD at $b = b_1$.

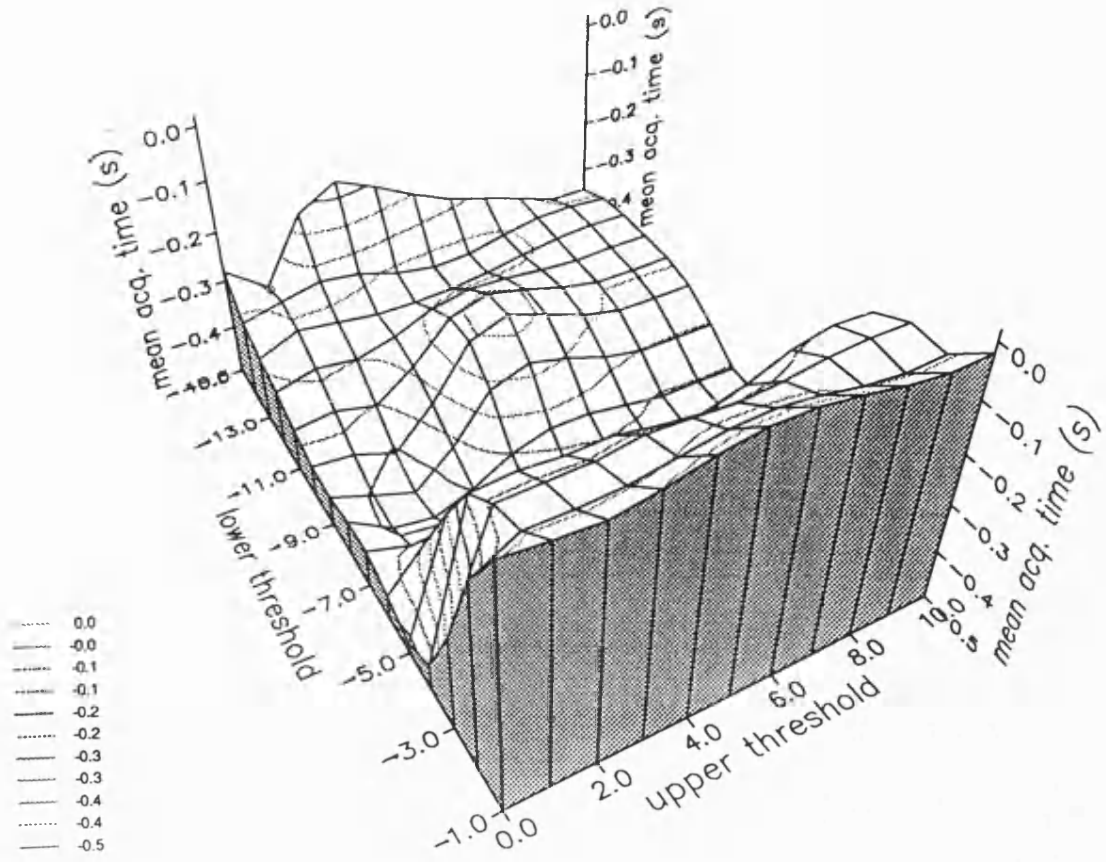

a) 3-d representation

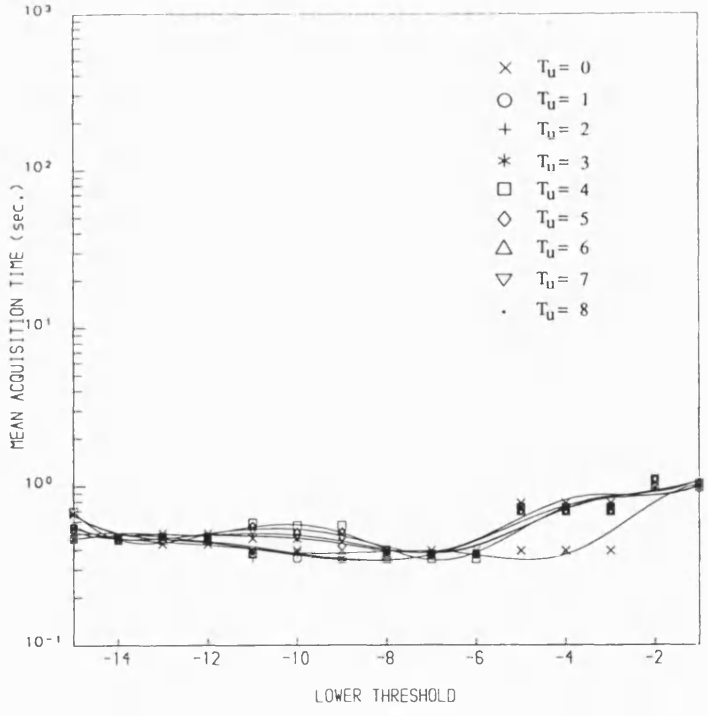

b) 2-d representation

Figure 5.10 T_{acq} vs T_u and T_l for QLD at $b = b_1$.

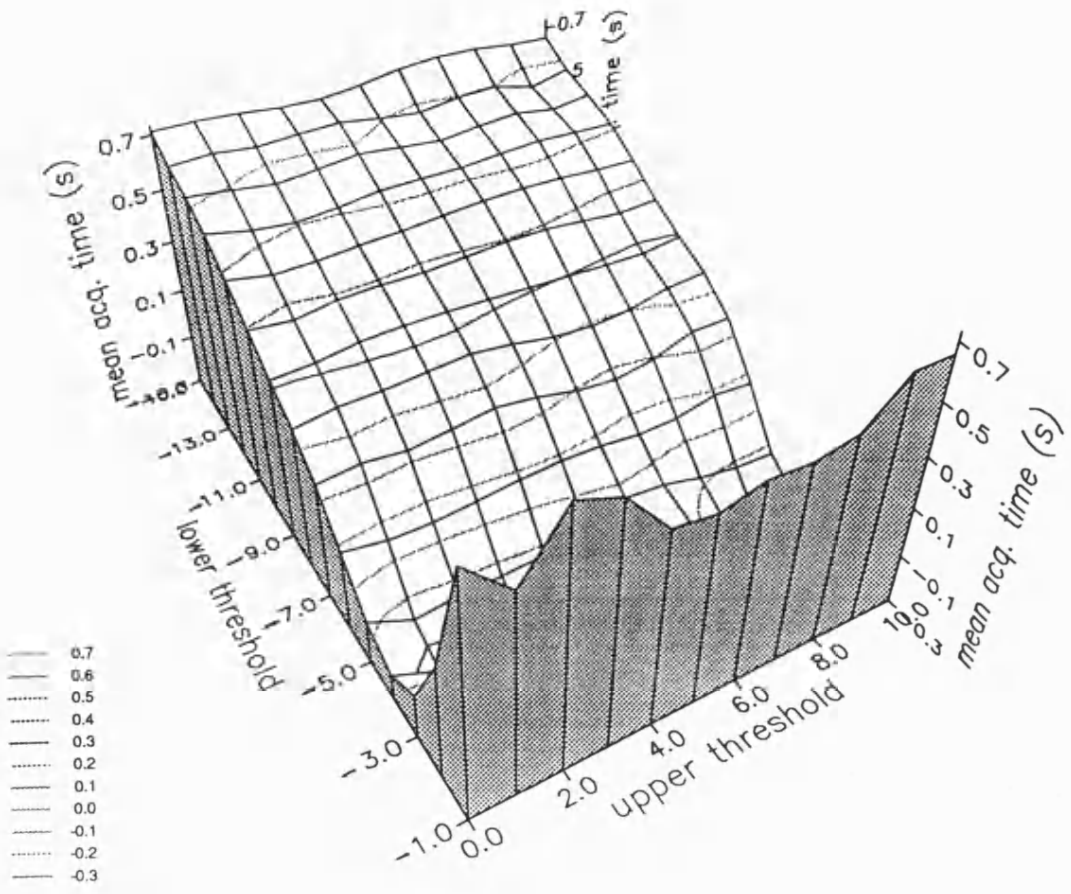

a) 3-d representation

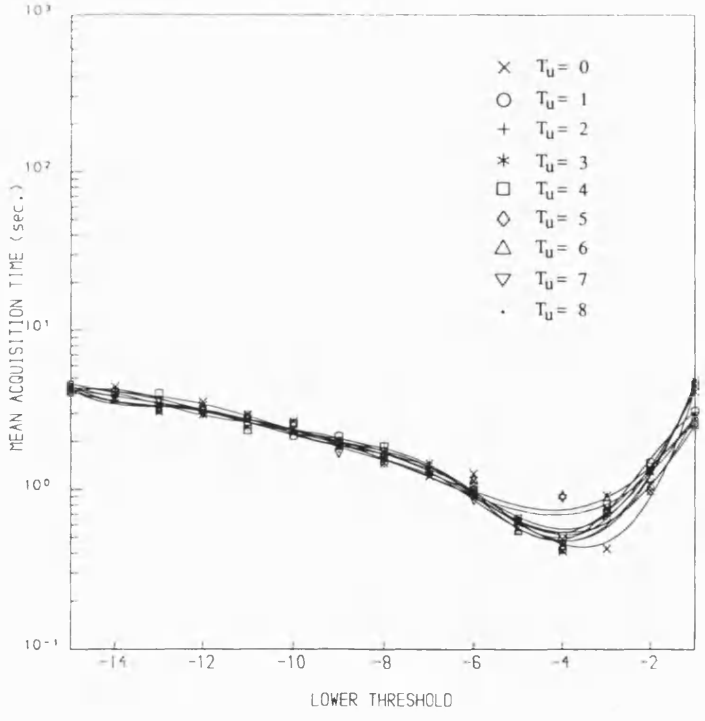

b) 2-d representation

Figure 5.11 T_{acq} vs T_u and T_l for BSD at $b = b_1$.

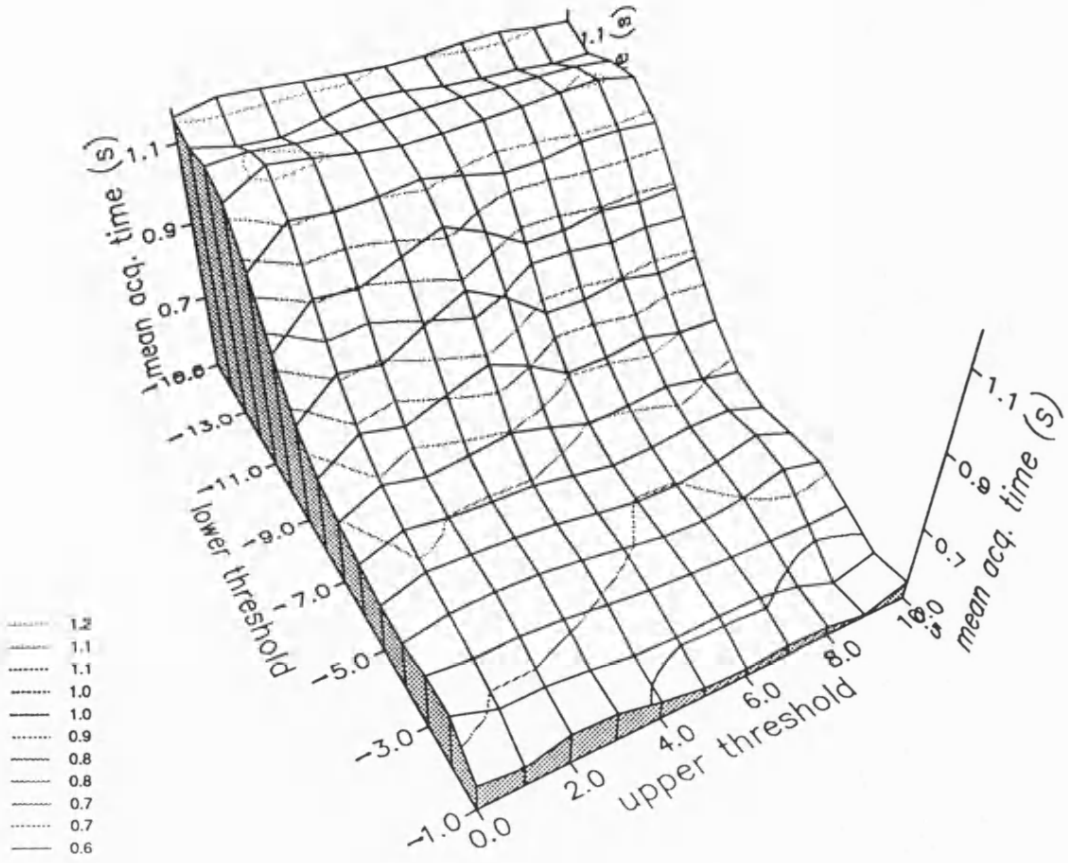

a) 3-d representation

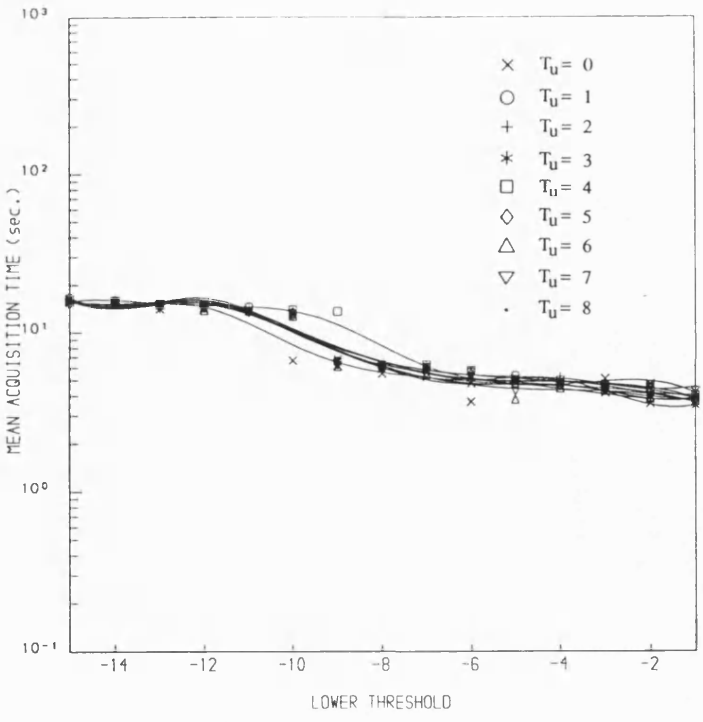

b) 2-d representation

Figure 5.12 T_{acq} vs T_u and T_l for LLD at $b = b_2$.

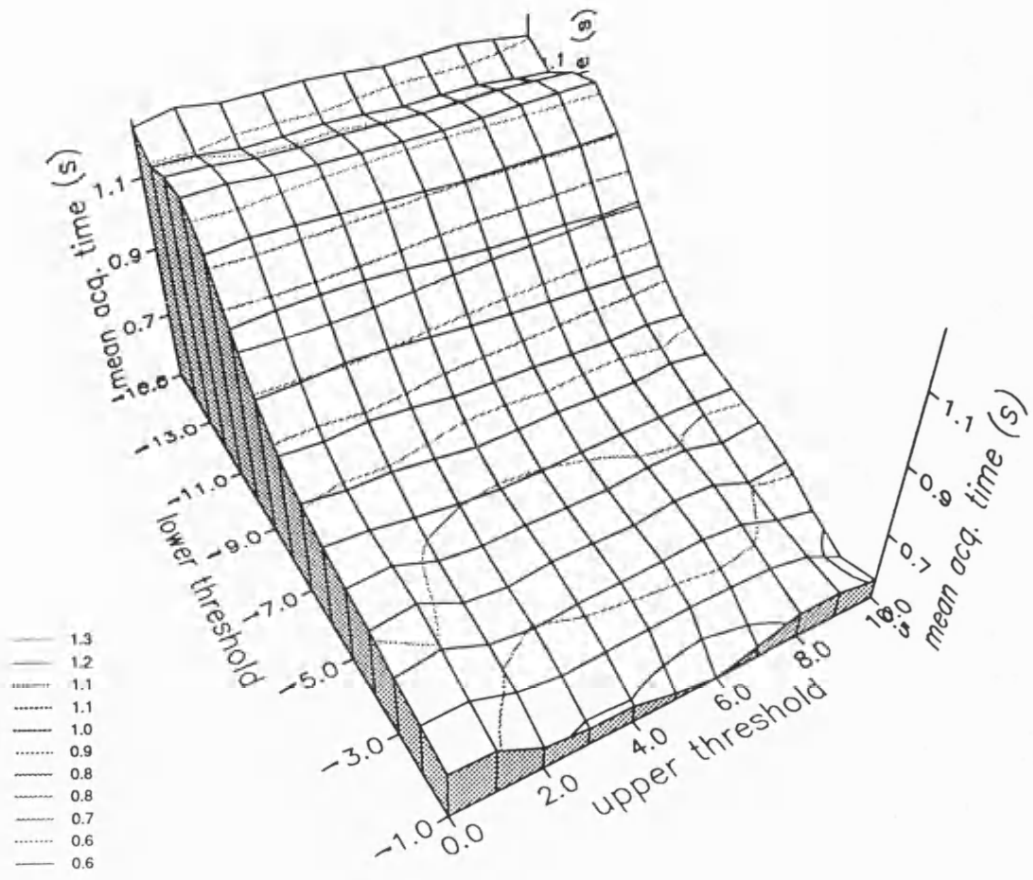

a) 3-d representation

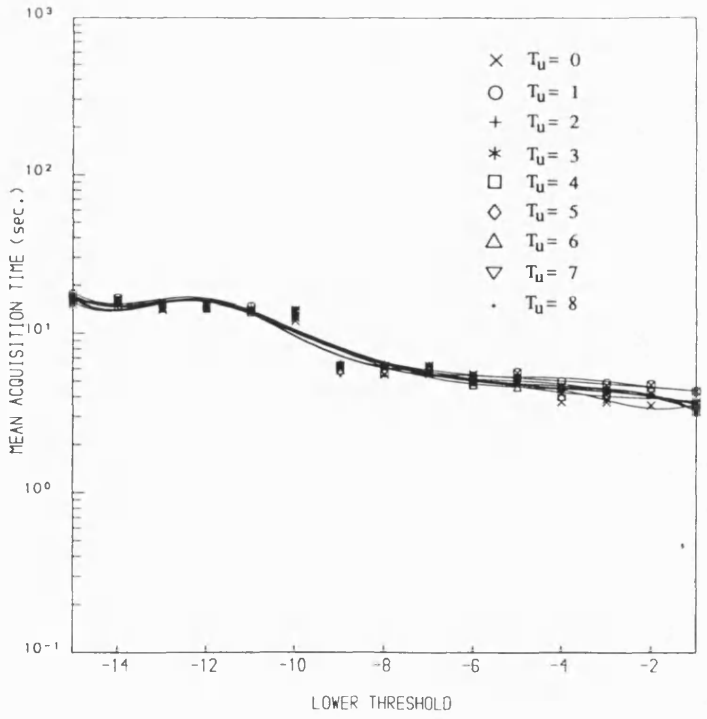

b) 2-d representation

Figure 5.13 T_{acq} vs T_u and T_l for QLD at $b = b_2$.

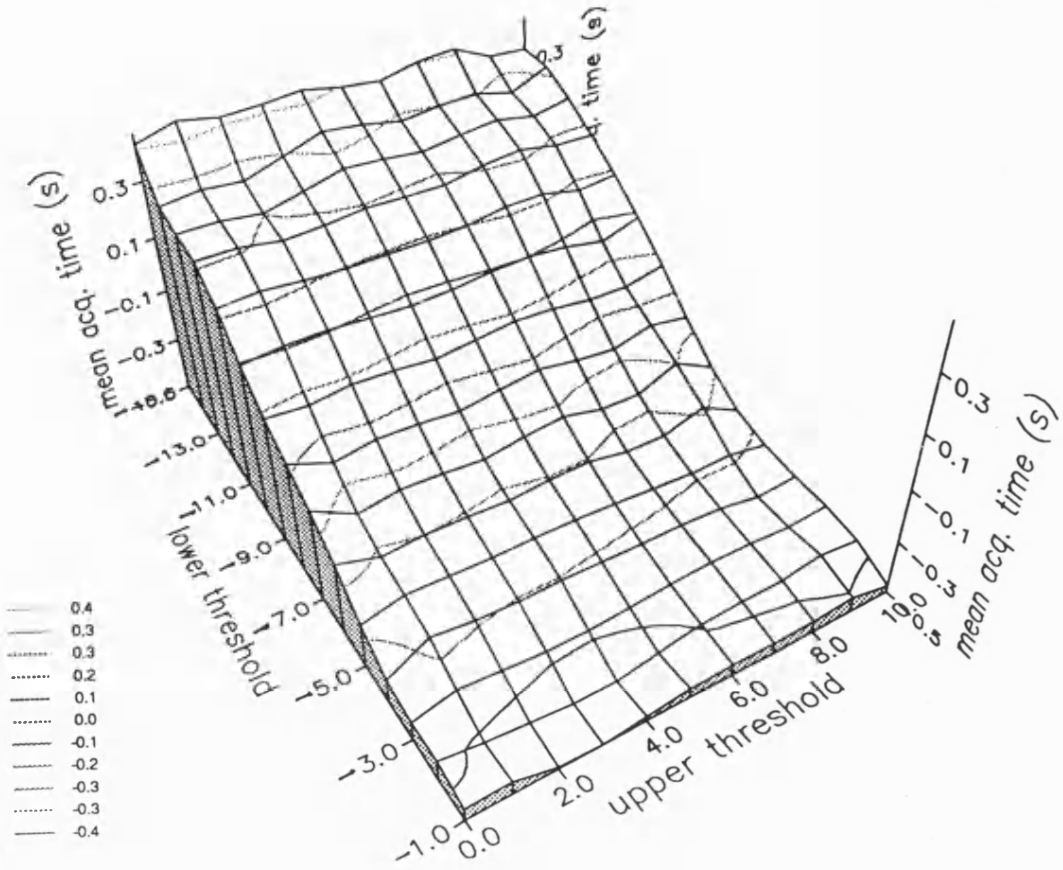

a) 3-d representation

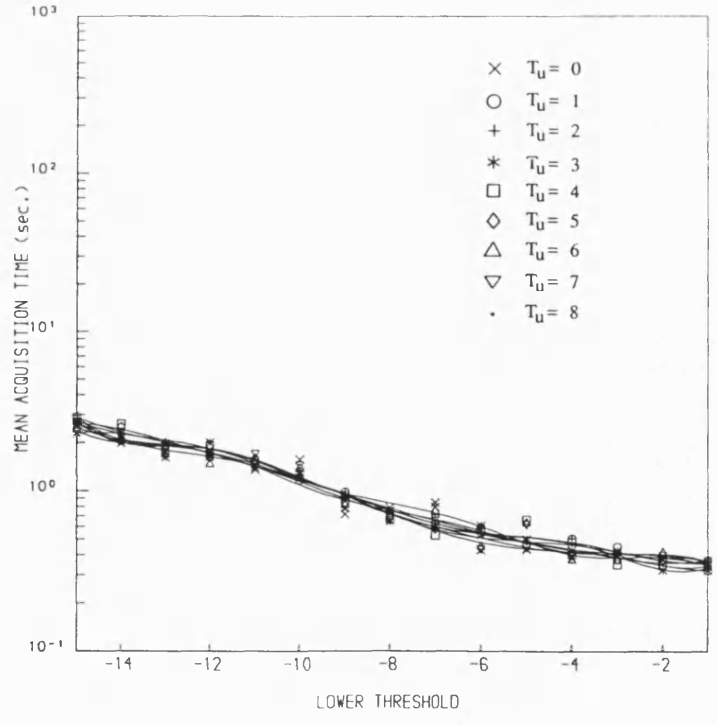

b) 2-d representation

Figure 5.14 T_{acq} vs T_u and T_l for BSD at $b = b_2$.

corresponding two-dimensional (2-d) plot for each characteristics, with T_{acq} plotted against the lower threshold when the upper threshold was varied in steps, is also presented in figures 5.9b - 5.14b.

From these figures it is observed that as the lower threshold is decreased, the mean acquisition time also decreases and passes through a minimum for each value of the upper threshold. However, the characteristics of all three variants at both the bias values are least affected with the change in the upper threshold (for the given range of parameters used). For the case of optimum bias, the minimum mean acquisition time occurs at a lower threshold generally around -5.0 (close to -4 for the BSD and -7 for the LLD and QLD) for most values of the upper threshold. However, the minimum is seen to be broader for both the LLD and the QLD than the BSD. The BSD has a minimum which is quite sharp and stable with the upper threshold whereas both the LLD and the QLD show broader minima. Both the LLD and the QLD also exhibit local minima unlike the BSD which shows a sharper global minimum. Although the minimum drifts around the lower threshold = -5.0 for the LLD and the QLD with different upper thresholds, it shows a stronger dependence on the bias value for all detectors.

In case of the non-optimum bias b_2 as shown in figures 5.12 through 5.14, the minimum T_{acq} is found to occur at a much higher value of the lower threshold which is around -1.0 and remains to be almost constant with the upper threshold. With this bias, all three variants show a similar trend, but the BSD has a lower minimum acquisition time than either the LLD or the QLD throughout the range of lower threshold.

Thus, the typical values of thresholds namely T_u = 5.0 and T_l = -5.0 for $b = b_1$ and T_l = -0.5 for $b = b_2$ were chosen from these observations and used in the stage II optimization.

5.4.3.1 ASN characteristics

The ASN for both the LLD and the QLD has been seen to be close to 1.0 and increases with the decreasing lower threshold. However, the change has been seen to be minimal for both the variants as ASN changes from 1.0 (at higher values of T_l) to 1.05 (at lower values of T_l). This is due to the fact that the bias and the input SNR are set to be constant which largely determine the ASN while both the thresholds in the range of interest show less influence. However, in case of the BSD, although the upper threshold still has least effect, both the bias and the lower threshold influence the ASN more. In this case, with the Wald's optimum bias, the ASN varies from 1.0 - 4.0 with the decreasing lower threshold whilst this variation is

from 1.0 - 2.5 for the non-optimum bias. This significant change in the ASN is caused due to the fact that the bias and the input SNR of the BSD are much lower than the LLD and the QLD which reduces their dominance allowing the thresholds to influence more.

5.4.3.2 Probabilities of detection and false alarm

The probability of detection and probability of false alarm with lower threshold for various values of the upper threshold are also shown in figures 5.15 through 5.23, for all the three variants. It is found that both P_d and P_{fa} decrease as the lower threshold is increased for all values of the upper threshold at Wald's optimum bias shown in figures 5.15 - 5.20. This is because the higher values of lower threshold forces the sequential test to be terminated quickly, causing increased miss detections. However, the upper threshold has very little influence on P_d for all three variants of the sequential detector which is the principal reason for the insensitivity of T_{acq} with the upper threshold (as ASN is almost constant).

Nevertheless, the bias value is found to have more influence on both P_d and P_{fa} rather than the upper threshold. At the non-optimum bias $b = b_2$, P_d becomes saturated to a value of P_d = 0.99 throughout the range of lower threshold for all values of upper threshold considered. The P_{fa} with this bias as shown in figures 5.21 - 5.23, shows a sharp rise for both the LLD and the QLD (notice the change in the scale on y-axis) when compared to that with Wald's optimum bias, eventhough it is reduced with the increasing lower threshold. The P_{fa} for the BSD, however, is relatively unchanged at this bias.

As the ASN is relatively unchanged for the LLD and the QLD, it is the fall in the detector probabilities with the increasing lower threshold which causes the T_{acq} to be reduced as observed in figures 5.12 - 5.14. In case of BSD, both the reducing ASN and the fall in detector probabilities influence the minimum mean acquisition time.

5.4.4 SNR optimization curves

Figures 5.24a through 5.29a show the effect on the mean acquisition time when operating the sequential detector at a predetection SNR which is different from the design value. The curves show T_{acq} plotted with respect to the predetection SNR and the design SNR for an upper threshold at 5.0 and a lower threshold at -5.0 and -0.5 for the bias value at b_1 and b_2 respectively (which were chosen from the stage I optimization). Figures 5.24b - 5.29b show the corresponding characteristics plotted as two-dimensional (2-d) curves with the design SNR varied in steps.

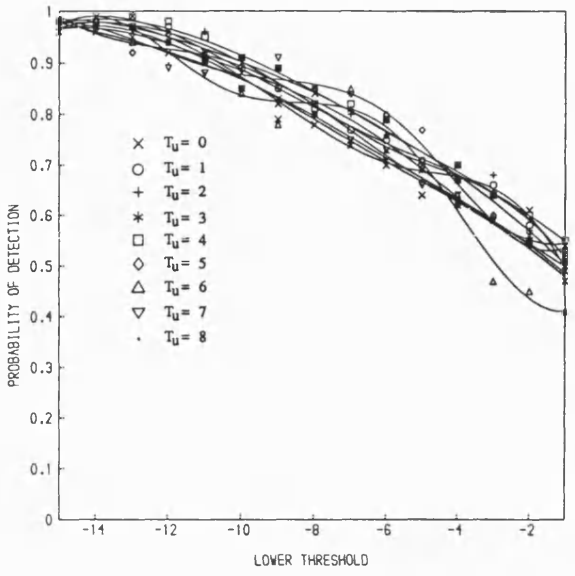

Figure 5.15 P_d vs T_u and T_l for LLD at $b = b_1$.

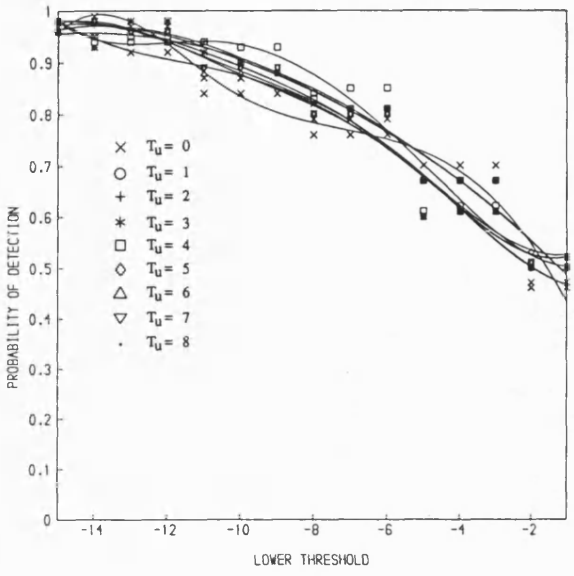

Figure 5.16 P_d vs T_u and T_l for QLD at $b = b_1$.

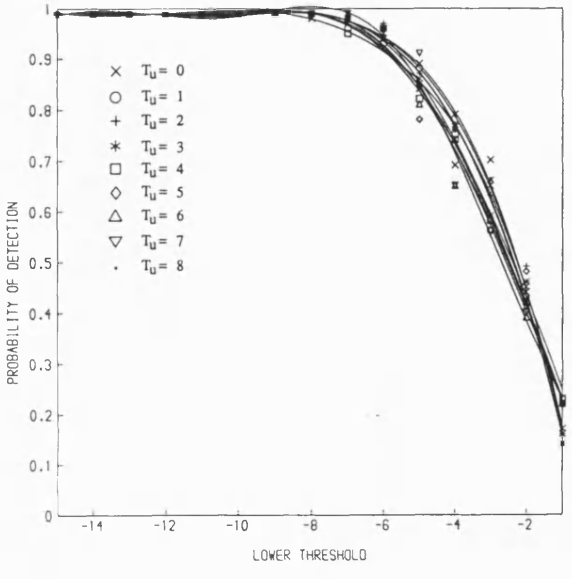

Figure 5.17 P_d vs T_u and T_l for BSD at $b = b_1$.

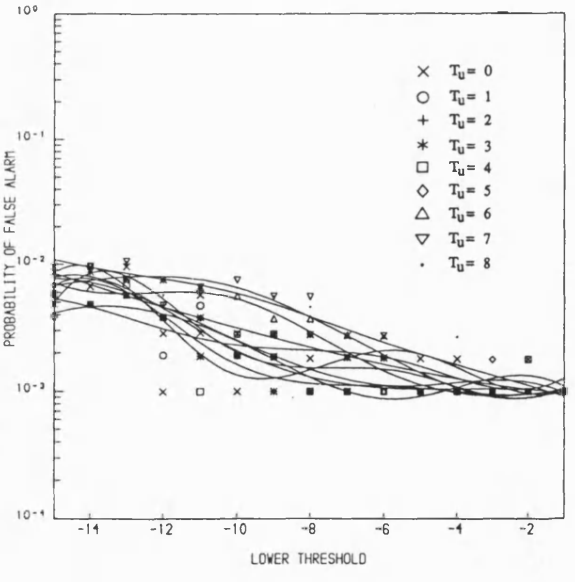

Figure 5.18 P_{fa} vs T_u and T_l for LLD at $b = b_1$.

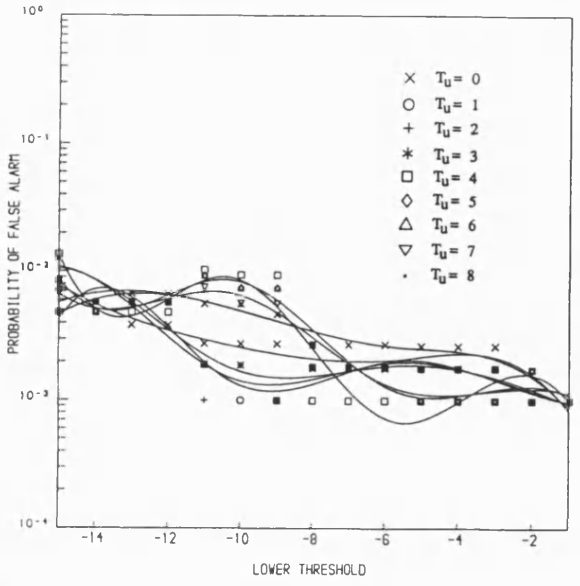

Figure 5.19 P_{fa} vs T_u and T_l for QLD at $b = b_1$.

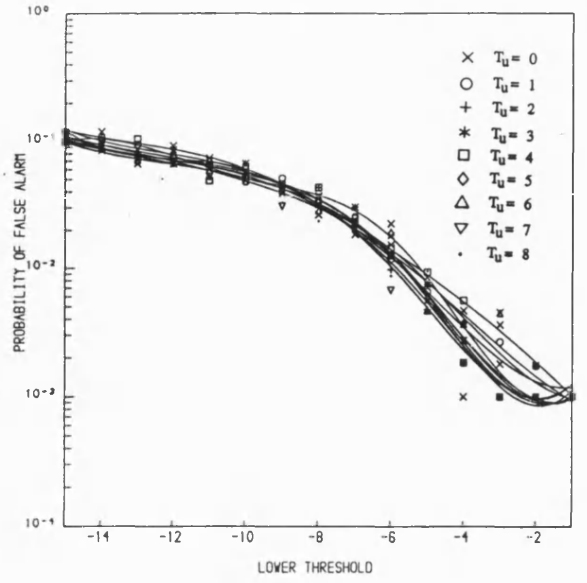

Figure 5.20 P_{fa} vs T_u and T_l for BSD at $b = b_1$.

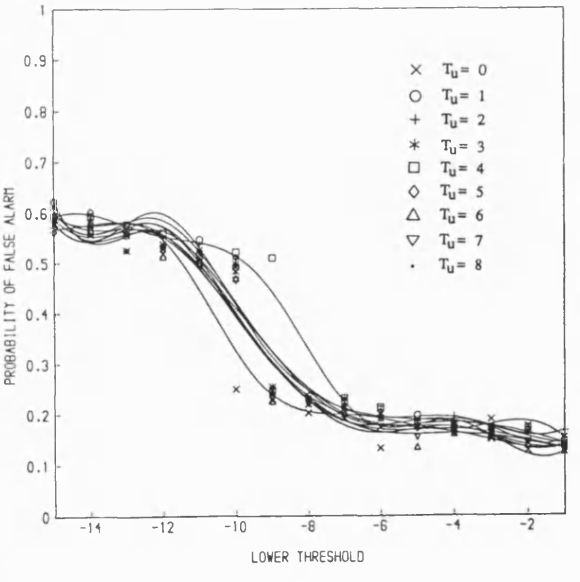

Figure 5.21 P_{fa} vs T_u and T_l for LLD at $b = b_2$.

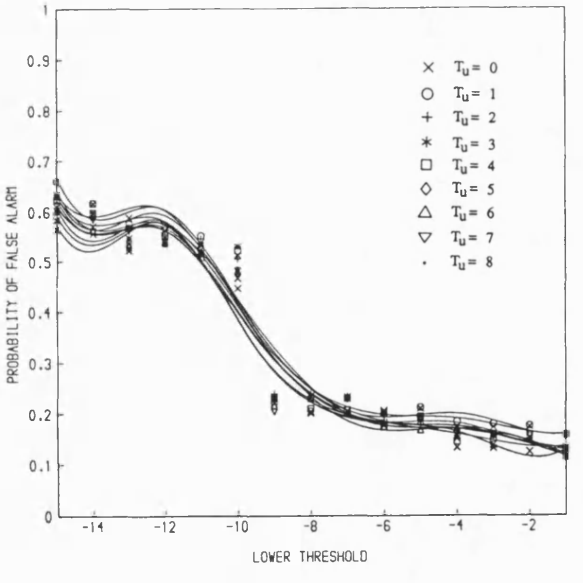

Figure 5.22 P_{fa} vs T_u and T_l for QLD at $b = b_2$.

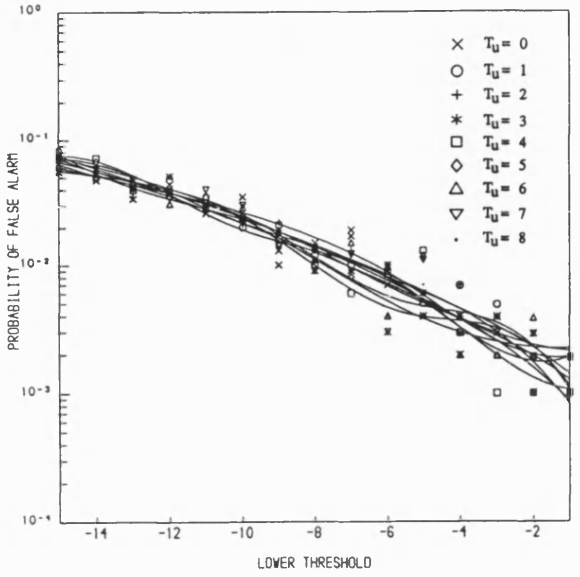

Figure 5.23 P_{fa} vs T_u and T_l for BSD at $b = b_2$.

From these figures, when the predetection SNR is varied from -4dB to 10dB, the mean acquisition time is observed to be strongly dependent on the design SNR. It is also seen that the mean acquisition time passes through a minimum for a range of design SNRs and predetection SNRs and these ranges depend on the bias value and the detector type. For the LLD, as shown in figure 5.24 this minimum occurs for design SNRs from 2dB to 10dB with the predetection SNR ranging -2dB to 8dB. However, the global minimum for the LLD occurs when the actual predetection SNR of 8dB matches the design SNR. Alternatively, it can also be observed that there is an optimum design SNR for each value of the predetection SNR.

In figure 5.25 the characteristics for the QLD are shown and the optimum behaviour is seen to be close to that of the LLD with the global minimum also occurring for both the predetection SNR and the design SNR around 8dB.

For the case of BSD as shown in figure 5.26, the minima are sharply defined, particularly at the higher predetection SNRs. The optimum design SNR ranges from 2dB to 6dB only and the global minimum occurs at a predetection SNR of 8dB for a design SNR at 6dB corresponding to an equivalent input SNR of -15dB.

The characteristics for the non-optimum bias b_2 are presented in figures 5.27 through 5.29. These curves show a shift in the minimum when compared with the case of Wald's optimum bias for all three variants of the detector. All three variants show a minimum at higher design SNRs. However, in case of both the LLD and the QLD, the predetection SNR required is much less than that with Wald's optimum bias which is now at 5-6 dB. For the BSD, both the design SNR and the predetection SNR at which the global minimum occurs are increased to 10dB. Nevertheless, the performance of the BSD at lower SNRs is still superior to that with the Wald's optimum bias. In fact, all the detectors tend to show clear minima (local minima) at lower predetection SNRs also even though the global minimum occurs at higher design SNRs.

In order to assess the various contributing factors for the above behaviour of the detectors the ASN and the detector probabilities for the corresponding system parameters have also been plotted (for stage II optimization) and shown in figures 5.30 through 5.38.

5.4.4.1 ASN characteristics

For most of the cases discussed, the ASN remains constant as the predetection SNR is varied

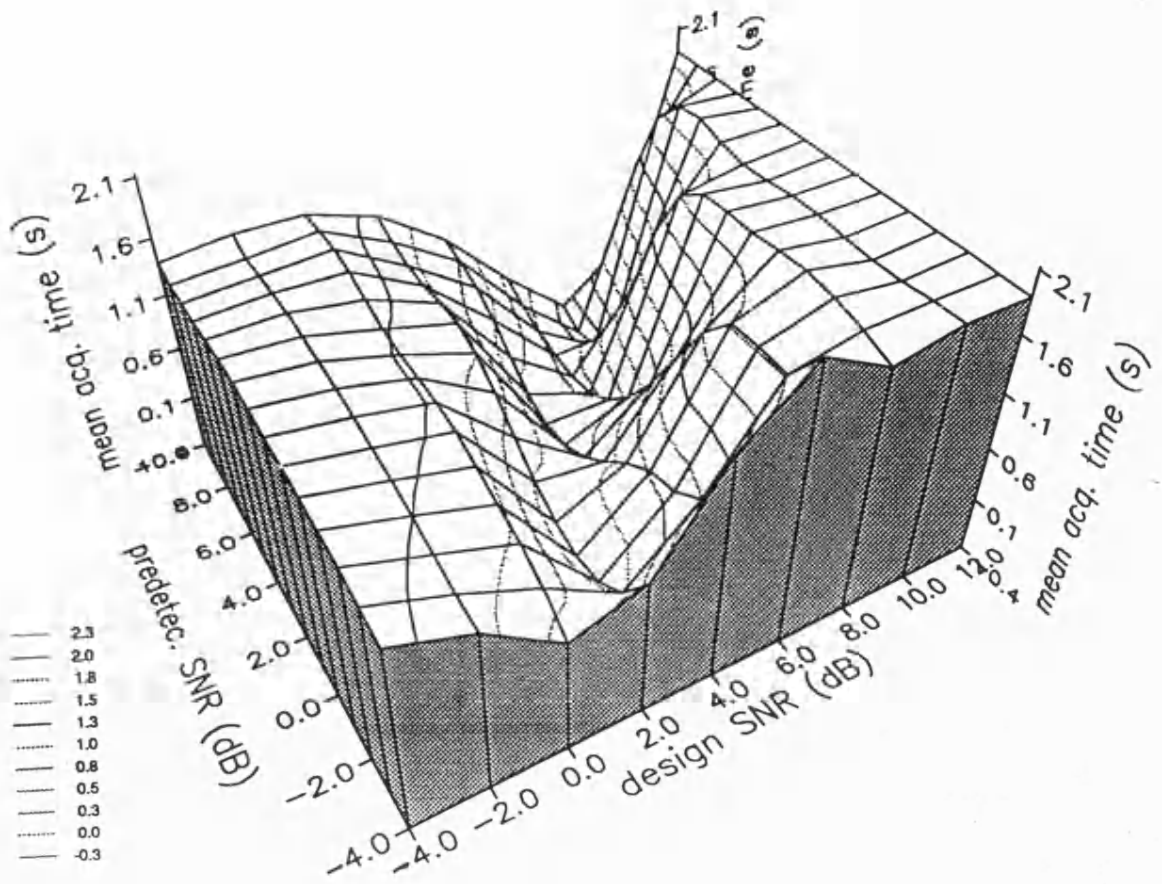

a) 3-d representation

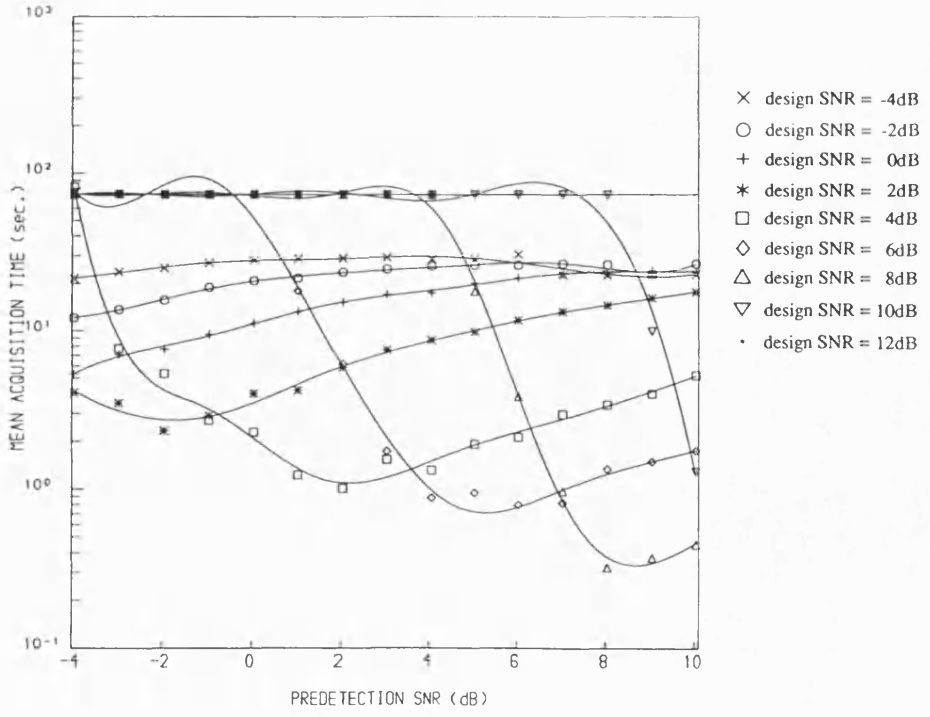

b) 2-d representation

Figure 5.24 T_{acq} vs γ and γ_{dsn} for LLD at $b = b_1$.

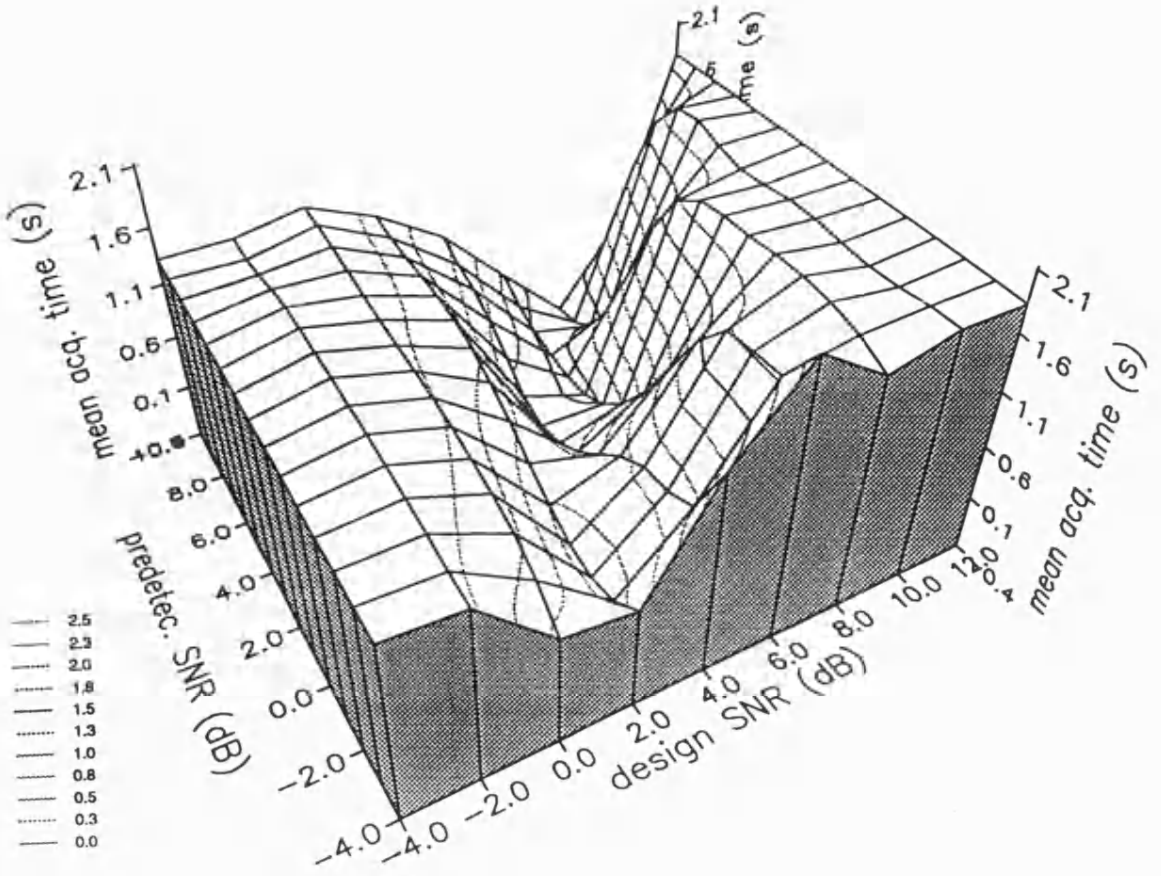

a) 3-d representation

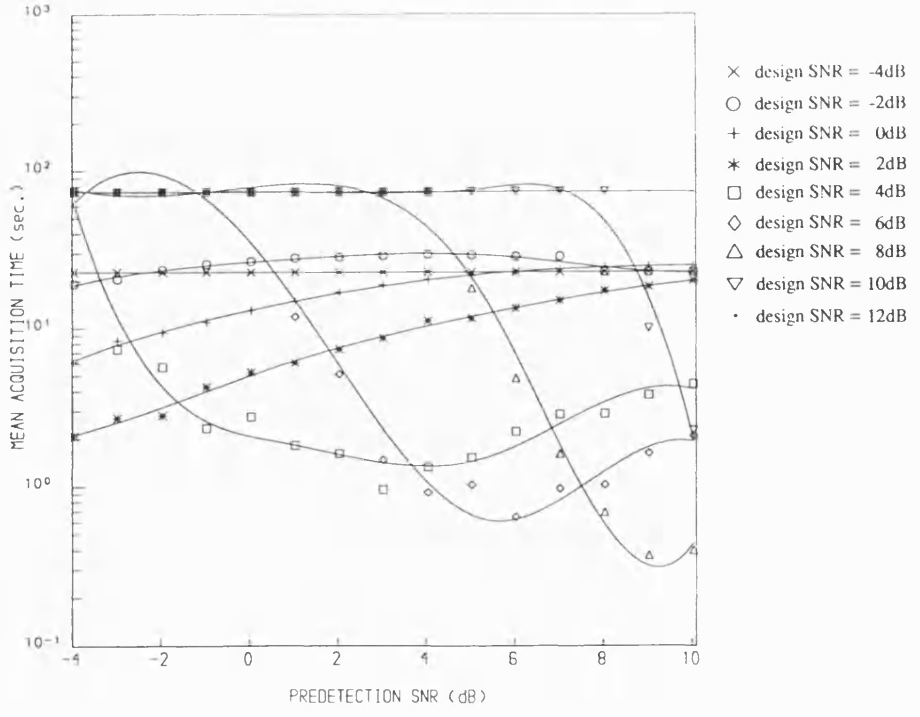

b) 2-d representation

Figure 5.25 T_{acq} vs γ and γ_{dsn} for QLD at $b = b_1$.

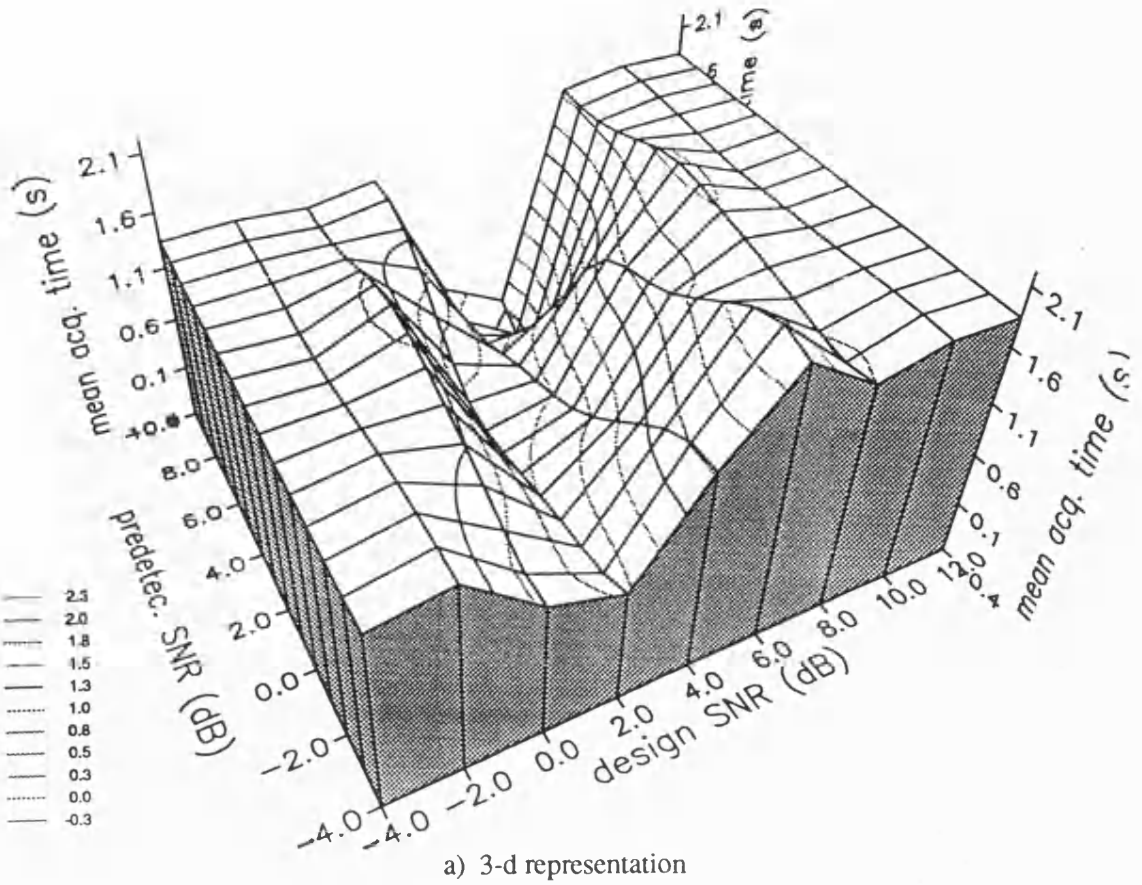

a) 3-d representation

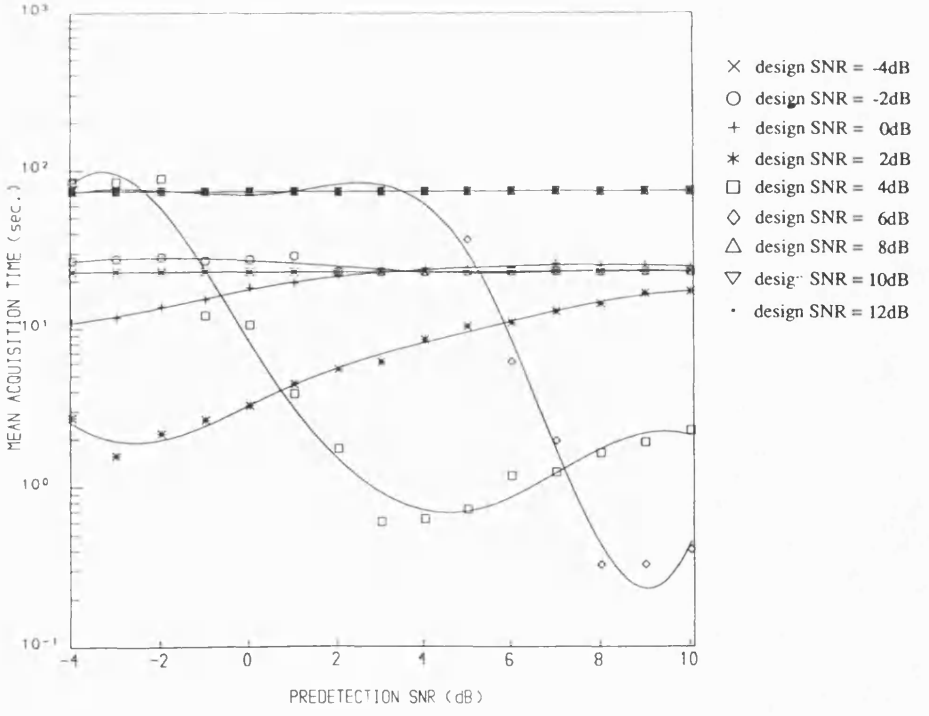

b) 2-d representation

Figure 5.26 T_{acq} vs γ and γ_{dsn} for BSD at $b = b_1$.

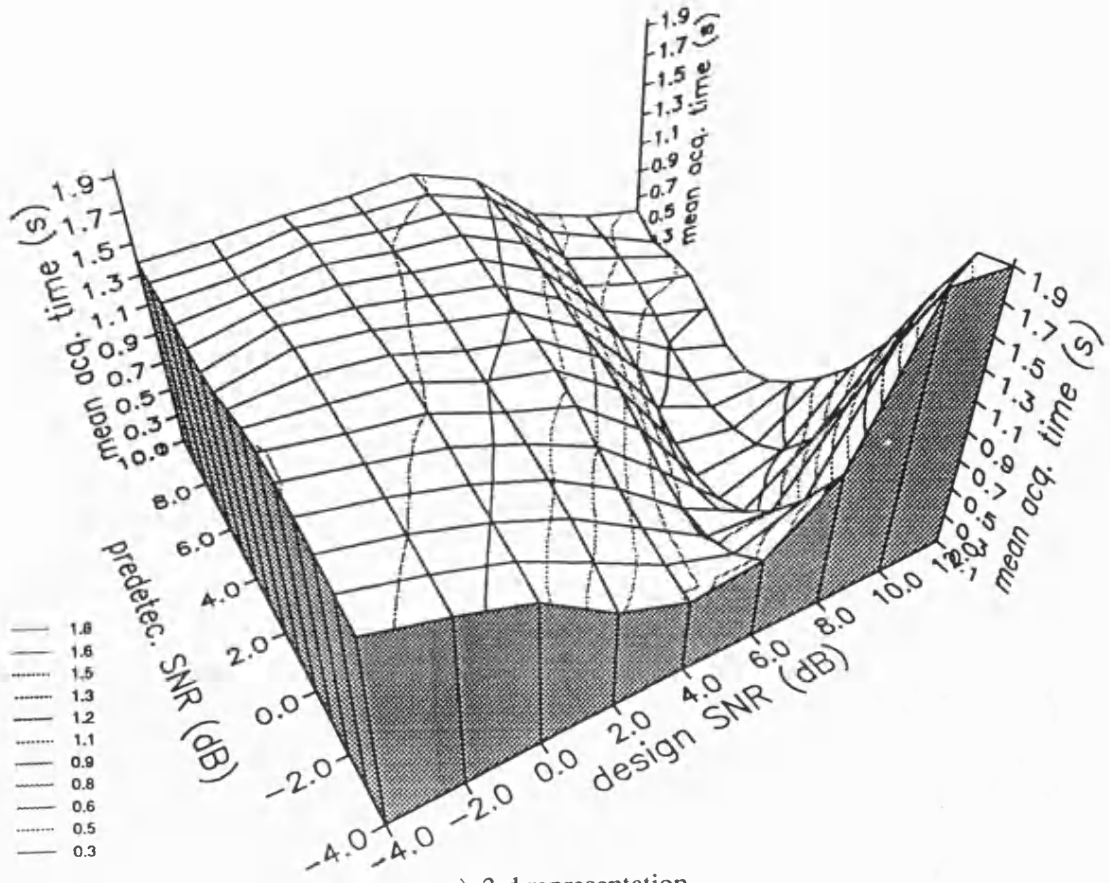

a) 3-d representation

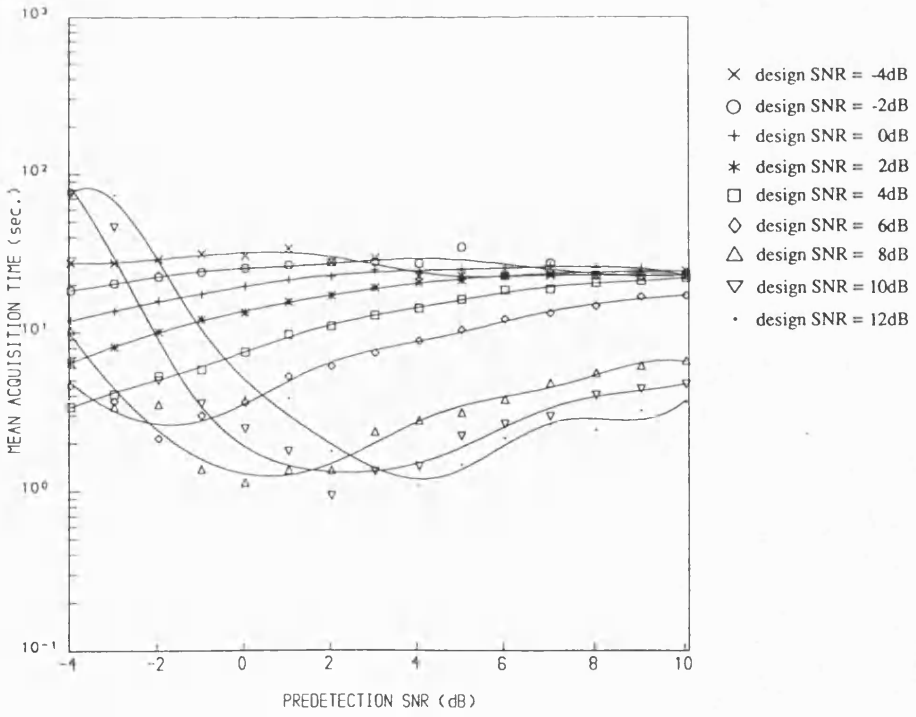

b) 2-d representation

Figure 5.27 T_{acq} vs γ and γ_{dsn} for LLD at $b = b_2$.

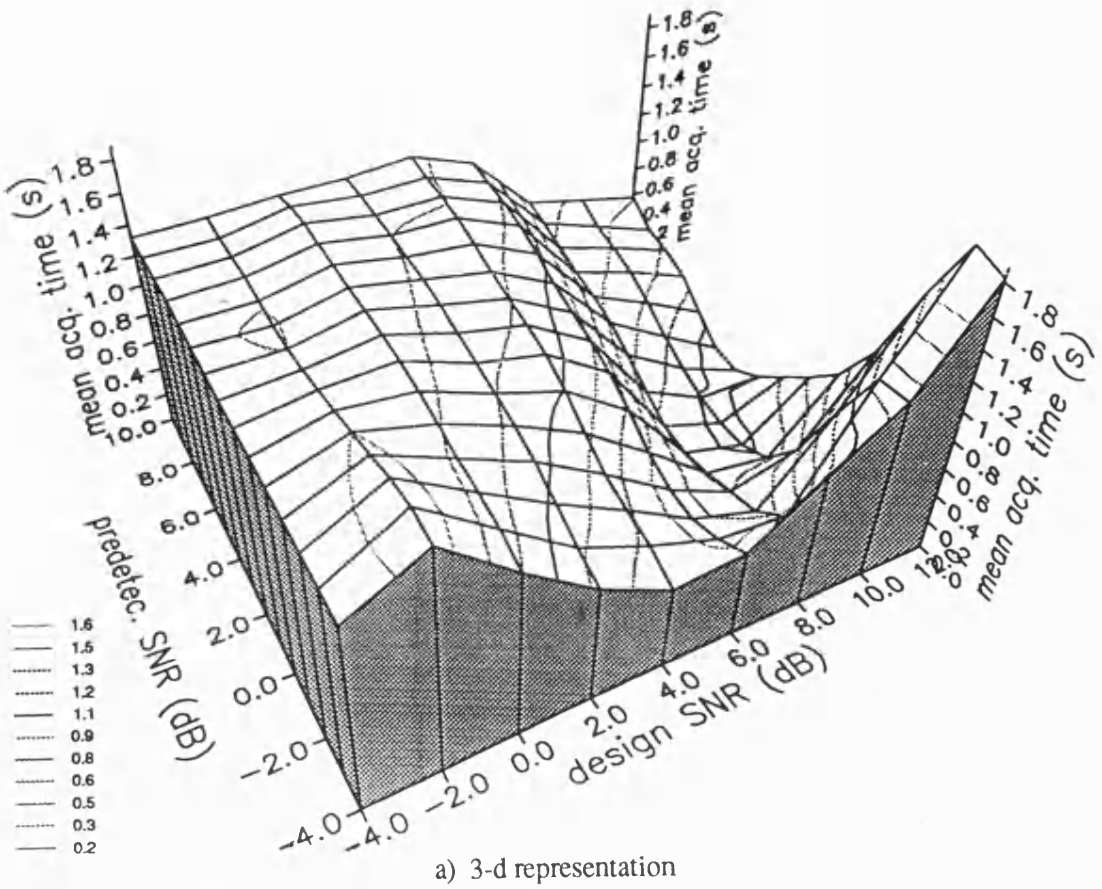

a) 3-d representation

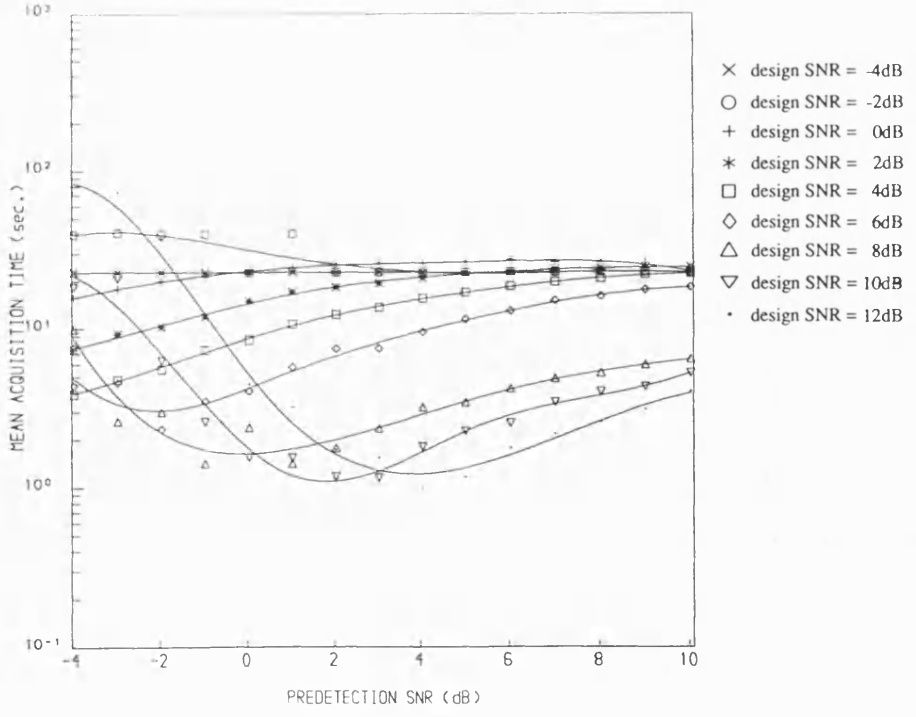

b) 2-d representation

Figure 5.28 T_{acq} vs γ and γ_{dsn} for QLD at $b = b_2$.

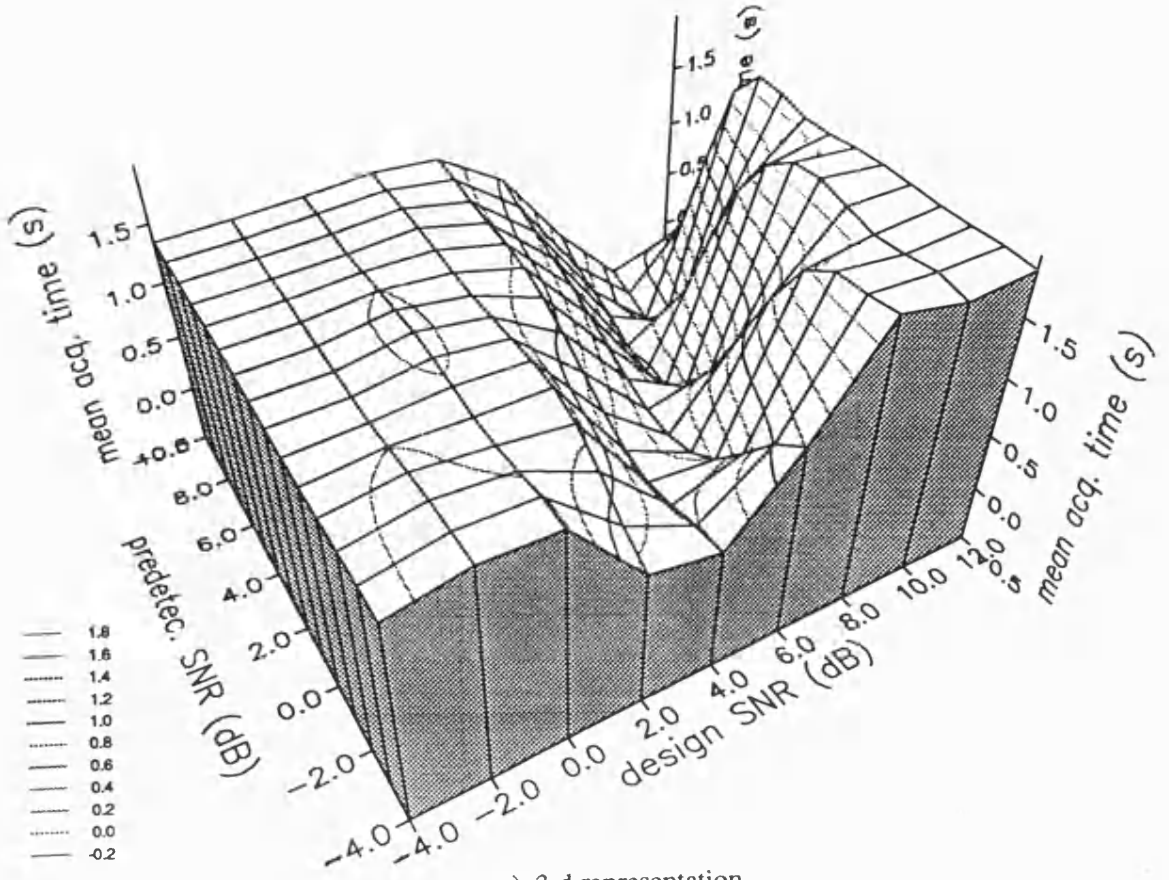

a) 3-d representation

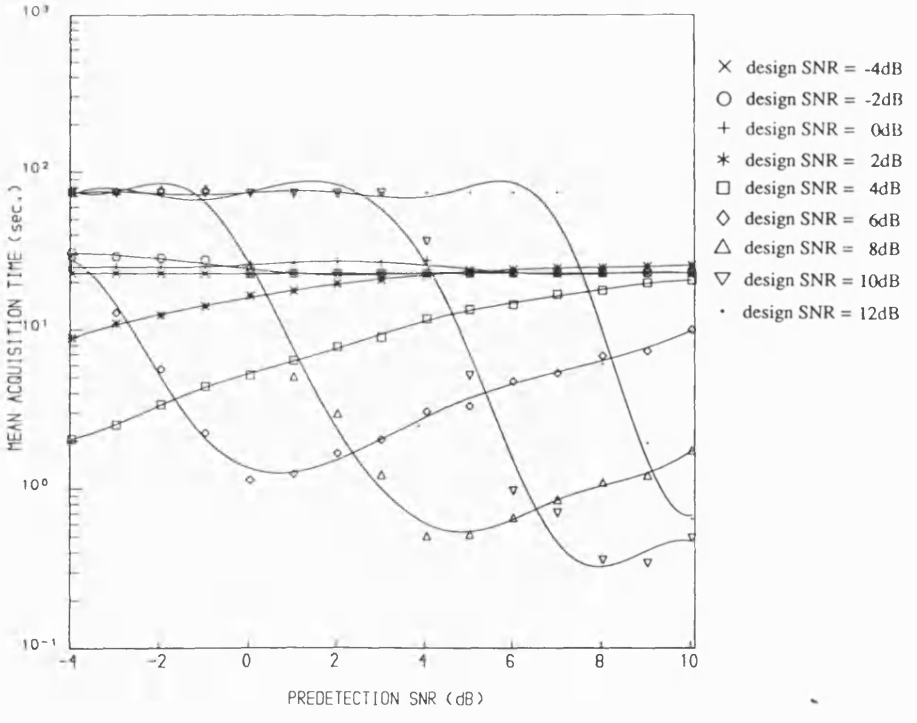

b) 2-d representation

Figure 5.29 T_{acq} vs γ and γ_{dsn} for BSD at $b = b_2$.

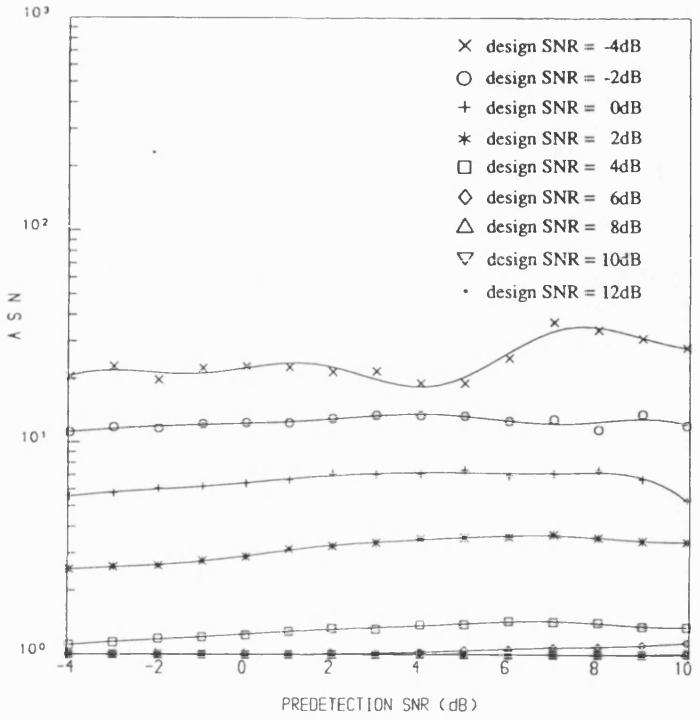

Figure 5.30 A S N vs γ and γ_{dsn} for LLD at $b = b_1$.

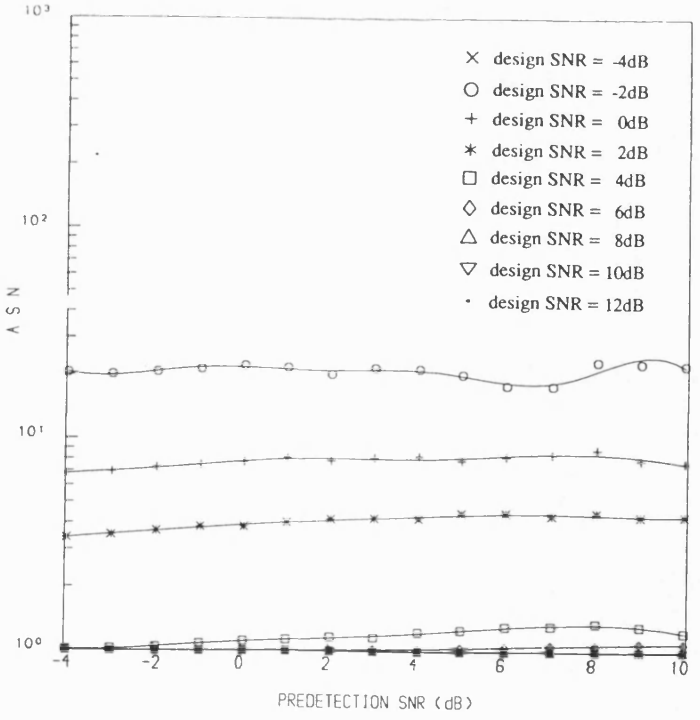

Figure 5.31 A S N vs γ and γ_{dsn} for QLD at $b = b_1$.

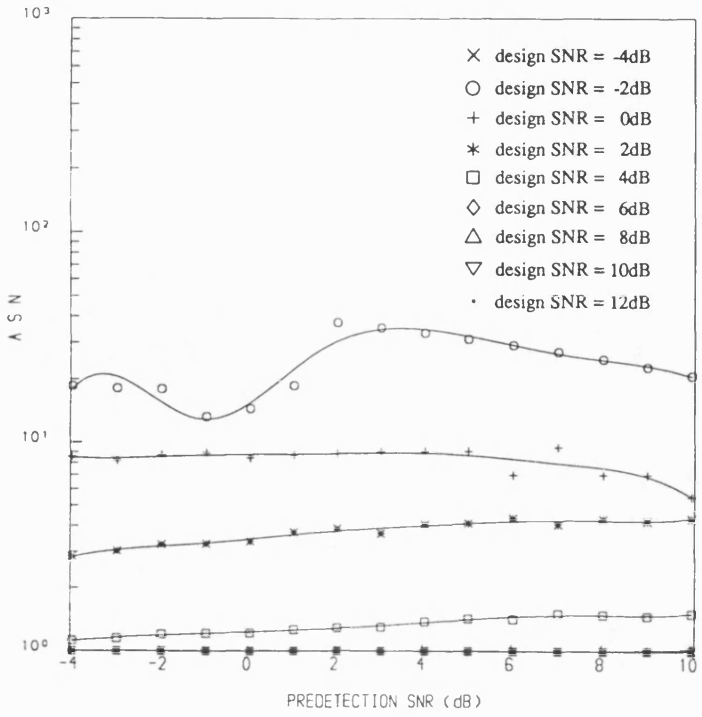

Figure 5.32 A S N vs γ and γ_{dsn} for BSD at $b = b_1$.

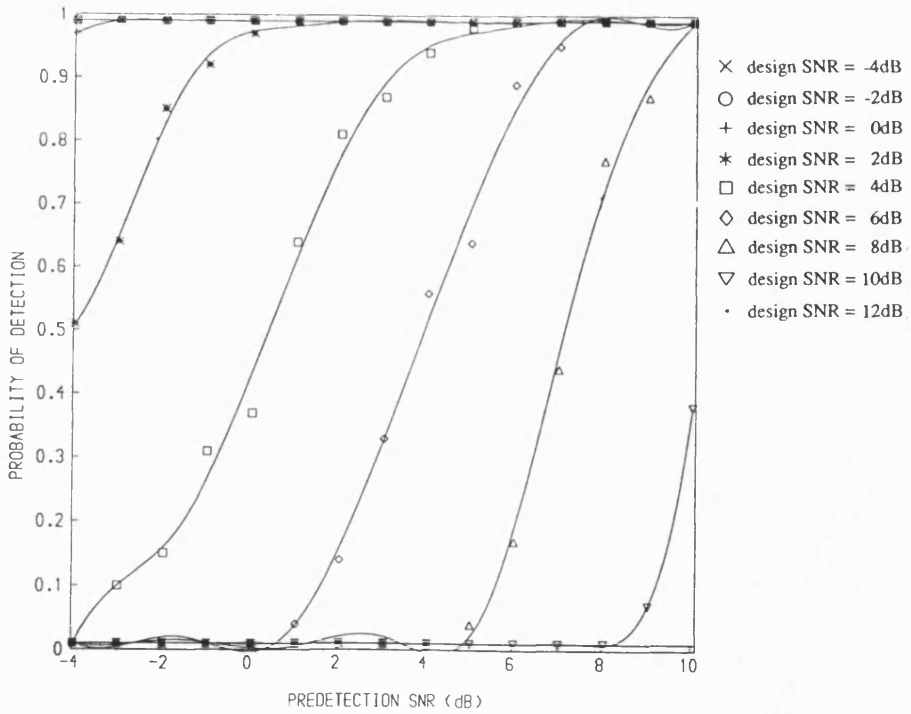

Figure 5.33 P_d vs γ and γ_{dsn} for LLD at $b = b_1$.

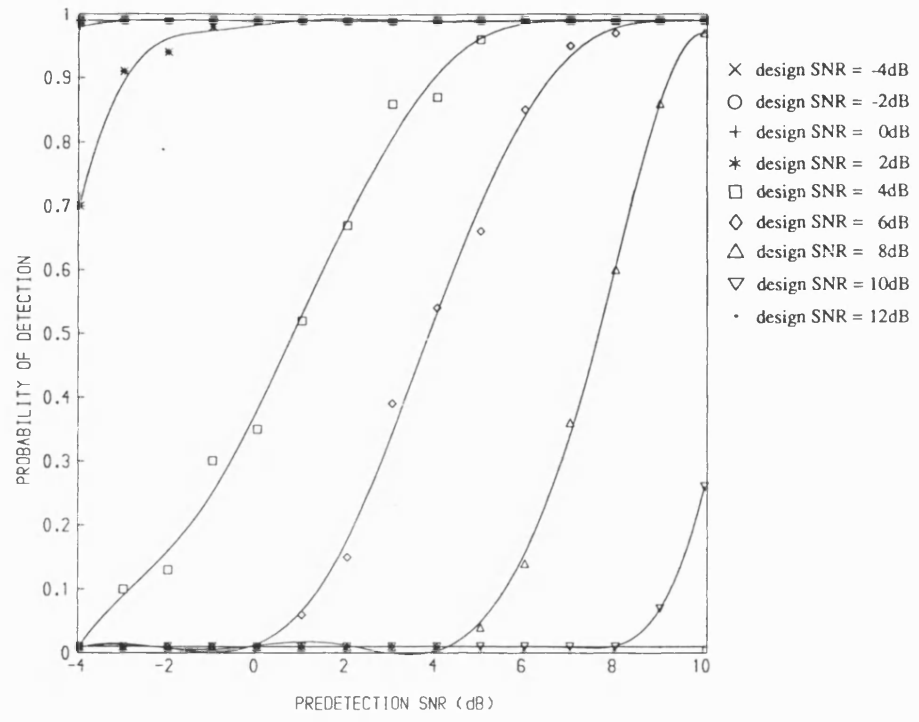

Figure 5.34 P_d vs γ and γ_{dsn} for QLD at $b = b_1$.

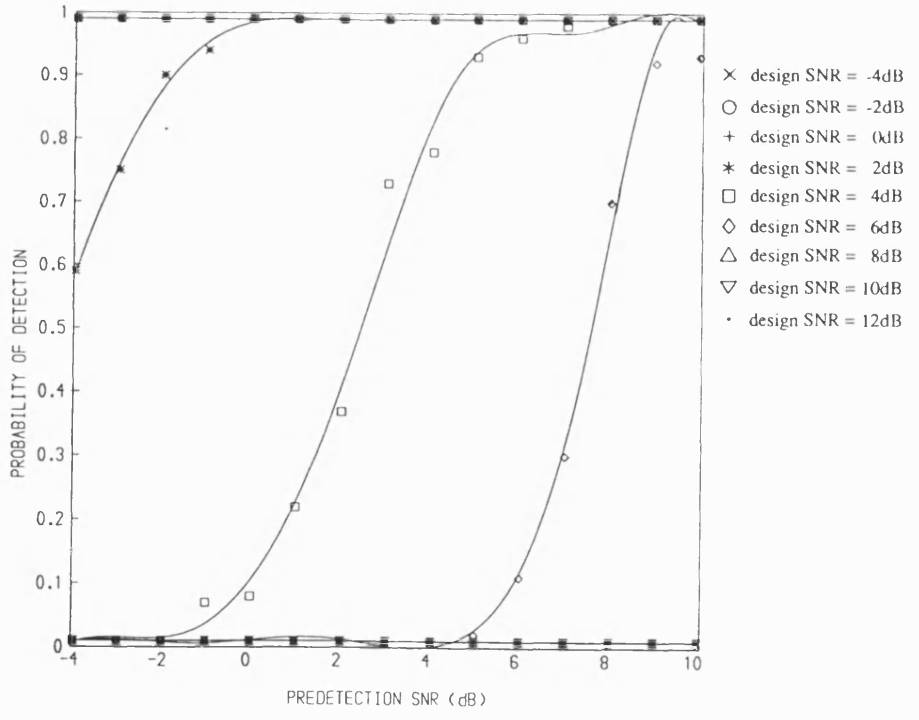

Figure 5.35 P_d vs γ and γ_{dsn} for BSD at $b = b_1$.

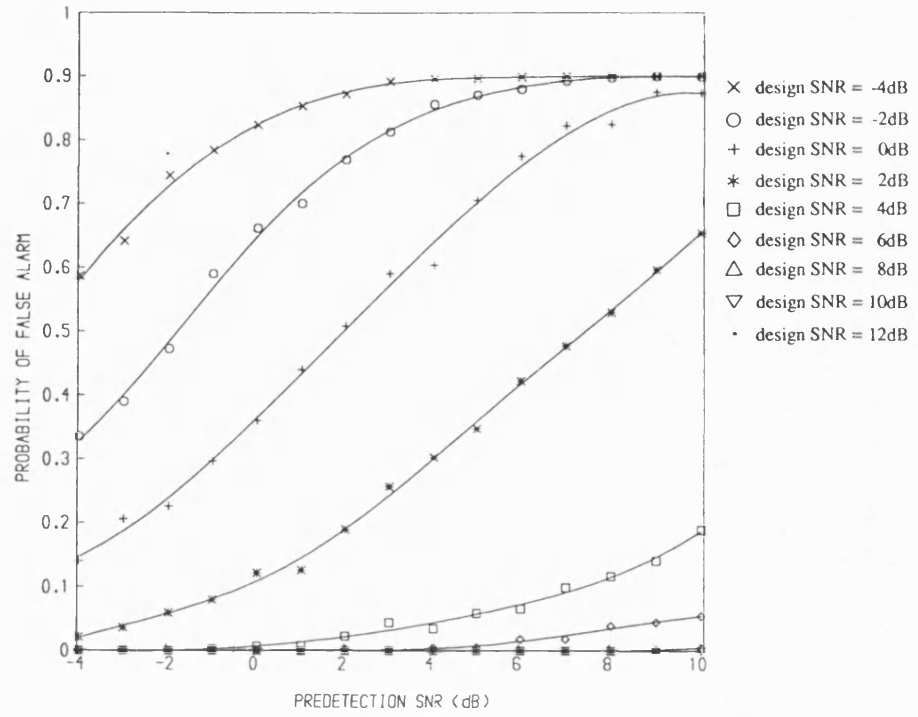

Figure 5.36 P_{fa} vs γ and γ_{dsn} for LLD at $b = b_1$.

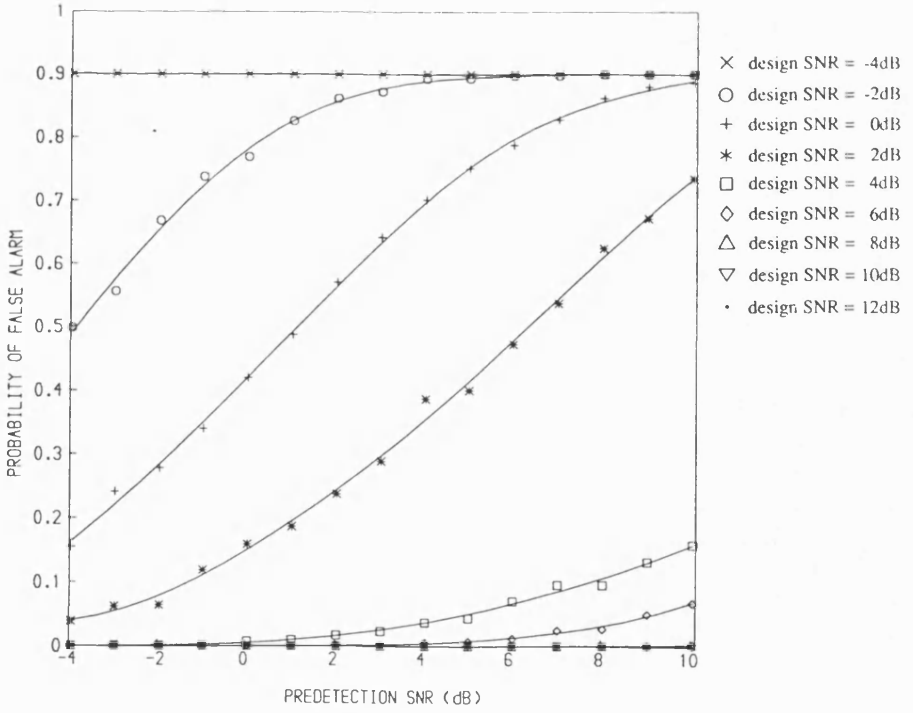

Figure 5.37 P_{fa} vs γ and γ_{dsn} for QLD at $b = b_1$.

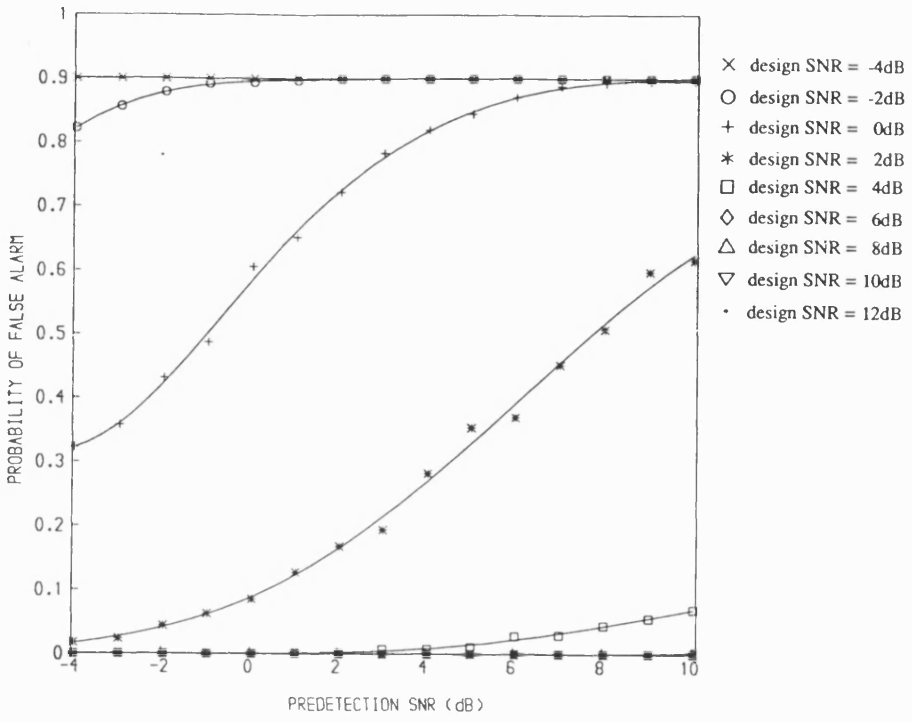

Figure 5.38 P_{fa} vs γ and γ_{dsn} for BSD at $b = b_1$.

CHAPTER 6

PERFORMANCE OF SEQUENTIAL DETECTORS IN THE PRESENCE OF DATA MODULATION AND DOPPLER SHIFT

6.1 INTRODUCTION

In the first part of this chapter, the effect of data modulation on the acquisition performance of the quantized log-likelihood sequential detector (QLD) and the biased square law detector (BSD) are compared with the ideal log-likelihood sequential detector (LLD) for predetection SNRs in the range -4dB to 10dB. The degradation in the acquisition performance due to the presence of random BPSK data modulation was assessed for each variant of the sequential detector and new results on the acquisition performance of sequential detectors in the presence of data modulation are presented and compared with the performance without data modulation. In the second part, the problem of initial acquisition of direct-sequence spread-spectrum PN codes under low SNR conditions is extended to include the presence of carrier and code Doppler frequency offsets. This analysis also examines, for the first time, the effect of both carrier and code Doppler on the mean acquisition time of a sequential detector.

In an earlier paper, Cobb and Darby characterized the acquisition performance of a sequential detector using a computer simulation [1]. However, their simulation did not include the presence of the data modulation and also employed various simplifications, and only the results of the miss detection probability for a given ASN and the probability of false alarm were presented. As a part of this research work, recently results on the computer simulation of more complete implementations of the biased square law and a quantized log-likelihood sequential detector in the absence of data modulation were presented by Ravi and Ormondroyd [2]-[3] which were discussed at length in the previous chapters.

In this chapter, new results on the acquisition performance of three variants of sequential detector in the presence of random BPSK data modulation and/or Doppler shift are presented and these are compared with the performance in the absence of data modulation and/or

Doppler shift [5].

PART I: ACQUISITION PERFORMANCE IN THE PRESENCE OF DATA MODULATION

In this part, the effect of data modulation on the quantized log-likelihood sequential detector, the biased square law sequential detector and the ideal log-likelihood sequential detector is presented and their performances compared. The effect of data modulation on the acquisition performance is analyzed for each variant of the sequential detector for identical system parameters and presented for both the Wald's optimum and the non-optimum bias values for predetection SNRs in the range -4dB to 10dB. The analysis is carried out with each detector operating at its optimum design SNR in the predetection SNR range from -4dB to 10dB (which are obtained from the previous optimization results). The ASN and the acquisition time characteristics are also compared both in the presence and absence of data modulation. Additionally, the variation of detector probabilities is presented and the effect of data modulation on these probabilities discussed.

6.2.1 EFFECT OF DATA MODULATION ON THE CORRELATION FUNCTION

The log-likelihood function defined earlier which is given by (3.68) does not model the loss of correlation due to the data modulation present on the carrier. When the data is added, the received signal with data modulation, $r(t)$ can be written as:

$$r(t) = \sqrt{2S}\, d(t+\xi T_o + \zeta T_c)\, c(t+\zeta T_c) \cos(\omega_c t + \theta_c) + n(t) \tag{6.1}$$

where all the symbols have been defined in chapter 4.

The correlator signal at baseband in the presence of data modulation (representing a sample value on the correlator curve), $x(t)$, is given by:

$$x(t) = u \cos(\theta_c) + n(t) \tag{6.2}$$

$$u = \sqrt{2}A\, d(t+\xi T_o + \zeta T_c)\, c(t+\zeta T_c)\, c(t+\tau T_c) \tag{6.3}$$

When $x(t)$ is passed through the envelope detector, the presence of data on the carrier causes degradation in the output of the correlator since the correlation across the data bit boundaries can result in the loss of the wanted signal when the data bit changes polarity. Furthermore, if the square law detector is used to remove the data modulation effects, this would add a squaring loss term due to the rectification of the noise signal.

Normally, the data modulation distortion effect can be reduced by using a combined output from a bank of parallel I-Q detectors, each matched to a different pattern which the data sequence can assume within the correlation interval. However, the number of such detectors could be quite high as it depends on the number of data bits to be integrated and the resolution of the data epoch uncertainty. Another method is to employ square law noncoherent combining detection in which the correlation time is partitioned into a number of subintervals. The integration results in these subintervals can then be combined noncoherently for detection. Recently, such a scheme has been analyzed by Cheng [4]. Using this method, the effect of data modulation is reduced but at the cost of combining loss. Although this is not as efficient as the parallel bank of I-Q detectors, it does not suffer from the penalty of complexity.

In the sequential detectors simulated here, the envelope detector samples are directly emphasized by the nonlinearity function 'ln $I_o[\ ]$' and the result is accumulated for the threshold comparisons. Therefore, the correlation interval cannot be partitioned into subintervals for combining directly. However, a parallel implementation is possible, whereby a bank of detectors, each with its own sequential detection algorithm can be matched to a different data pattern. In this work, no parallel implementation was assumed and hence, a sequential detector operating serially to search entire uncertainty region was simulated and its acquisition performance with data modulated PN signals was evaluated.

6.2.2 SIMULATION OF DATA MODULATED SIGNALS

The three variants of sequential detector were simulated by means of the Monte-Carlo computer simulation, described earlier. However, the incoming pseudo-noise (PN) code sequence, which is of length $L = 127$ and chip rate $R_c = 1/T_c = 100Kb/s$, was modulated by a random binary data sequence at a rate, $1/T_o = R_c/L = 1/LT_c$ with random data transitions. A pseudo-noise (PN) code of length 15 was used as a data sequence and each time the test was repeated, a new data sequence was generated with an arbitrary data transition.

With these data modulated PN signals, the simulation was carried out to obtain various performance characteristics. As the acquisition performance of the sequential detectors depends critically on the bias, SNR and the threshold settings of the log-likelihood function, the bias, in this case, was set to be a function of the predetection SNR (to enable comparison with the ideal behaviour). For each detector, three lower threshold values T_l = -5.0, -2.0, -0.5 (in the range of their near-optimum thresholds) and an upper threshold T_u = 5.0 were

employed and the acquisition performance was obtained for the bias values b_1 and b_2. The signal gain after envelope detection was optimized to result in maximum probability of detection for a given probability of false alarm and predetection SNR.

6.2.3 ACQUISITION PERFORMANCE

For each detector, with each set of system parameters, the *ASN*, P_d, P_{fa} were obtained. The ASN and the acquisition time characteristics are plotted for the cases with data modulation and no data modulation. The variation of the detector probabilities have also been plotted with predetection SNR and the performances are compared subsequently.

6.2.4 ASN characteristics

The variation of ASN with predetection SNR has been plotted for each detector for all three lower thresholds at each bias value and is shown in figures 6.1 through 6.6. For all the detectors, the ASN decreases with increasing predetection SNR both in the absence and the presence of data modulation. This is attributed to the fact that increasing predetection SNR increases the bias value which in turn reduces the value of log-likelihood function and this causes the lower threshold to be exceeded more frequently. As for the earlier cases, the value of ASN depends strongly on the lower threshold and the bias. With the further reduction in the level of the lower threshold, a rapid fall in the ASN with the predetection SNR is observed for both cases. The ASN in the presence of data modulation does not change significantly when compared to the case of no data modulation, particularly at higher predetection SNRs. However, a slight increase in the ASN at lower predetection SNRs is observed for all the detectors. Thus, the presence of data does not significantly degrade the ASN performance.

6.2.5 Probability of detection and Probability of false alarm

The probability of detection and the probability of false alarm are shown in figures 6.7 through 6.18. Both the predetection SNR and the lower threshold are seen to have a strong influence on the detector probabilities P_d and P_{fa} for both cases with data modulation and no data modulation. At lower predetection SNRs, with the lower threshold set at -5.0, both the probability of detection and the probability of false alarm are at their maximum. With increasing predetection SNR, both these probabilities are observed to decrease both with and without data for all three detectors when biased at Wald's optimum bias, $b = b_1$. This is due to the fact that as the predetection SNR improves, the log-likelihood function falls due the

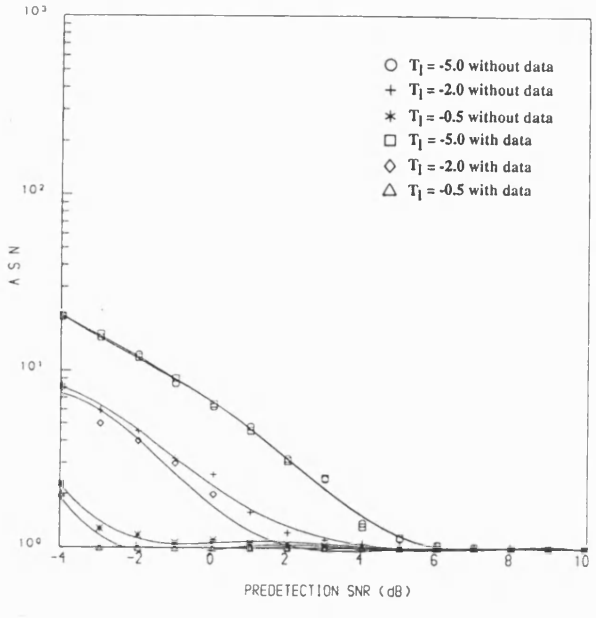

Figure 6.1 A S N vs γ for LLD at $b = b_1$ in the presence and the absence of data modulation.

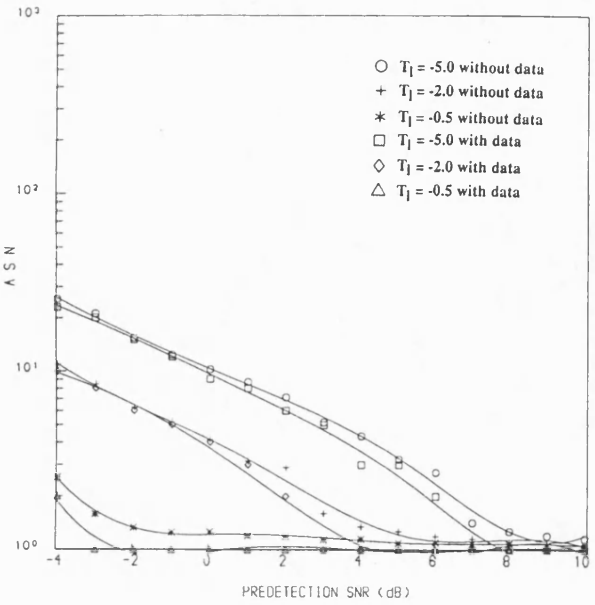

Figure 6.2 A S N vs γ for LLD at $b = b_2$ in the presence and the absence of data modulation.

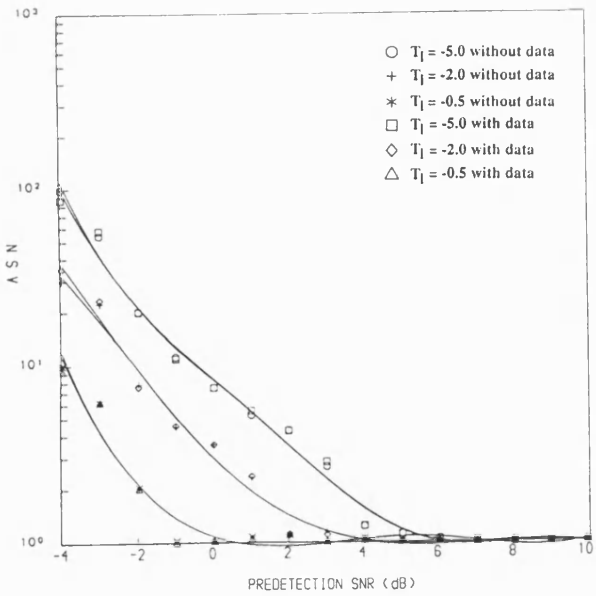

Figure 6.3 A S N vs γ for QLD at $b = b_1$ in the presence and the absence of data modulation.

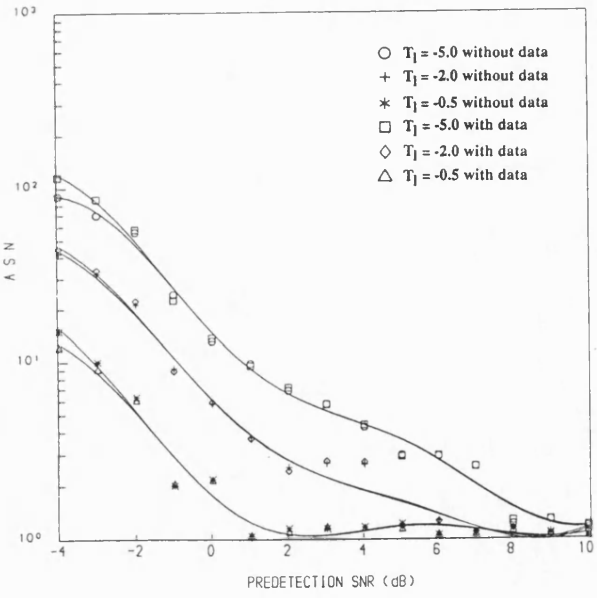

Figure 6.4 A S N vs γ for QLD at $b = b_2$ in the presence and the absence of data modulation.

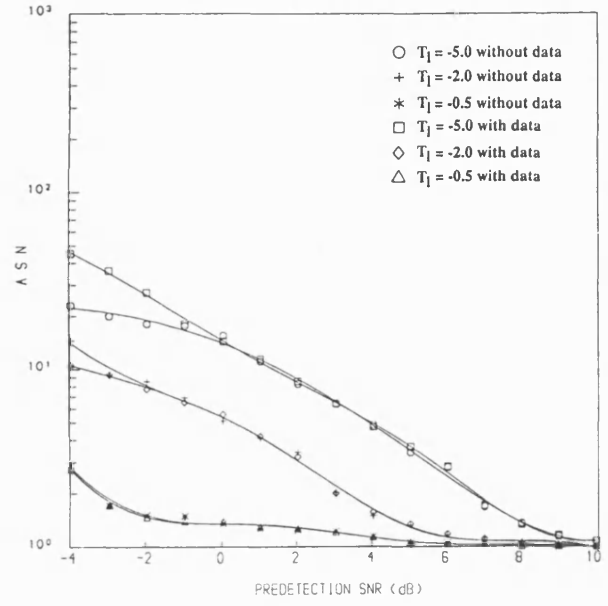

Figure 6.5 A S N vs γ for BSD at $b = b_1$ in the presence and the absence of data modulation.

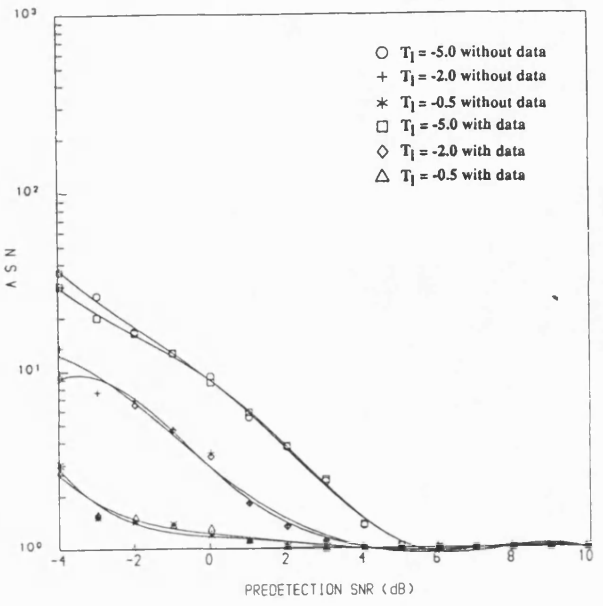

Figure 6.6 A S N vs γ for BSD at $b = b_2$ in the presence and the absence of data modulation.

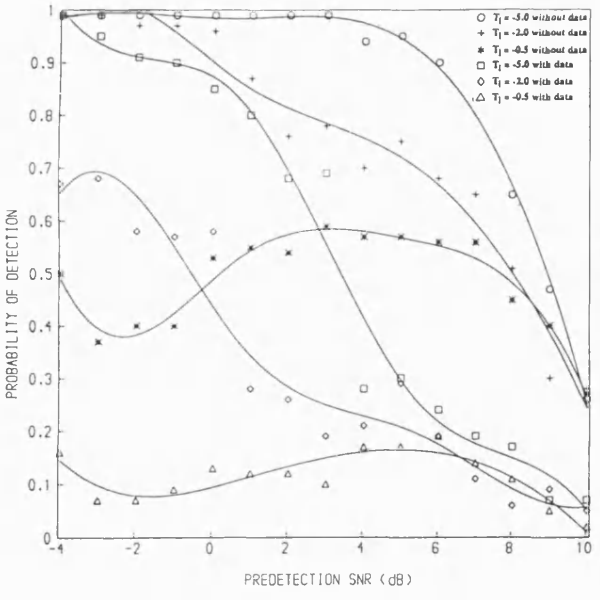

Figure 6.7 P_d vs γ for LLD at $b = b_1$ in the presence and the absence of data modulation.

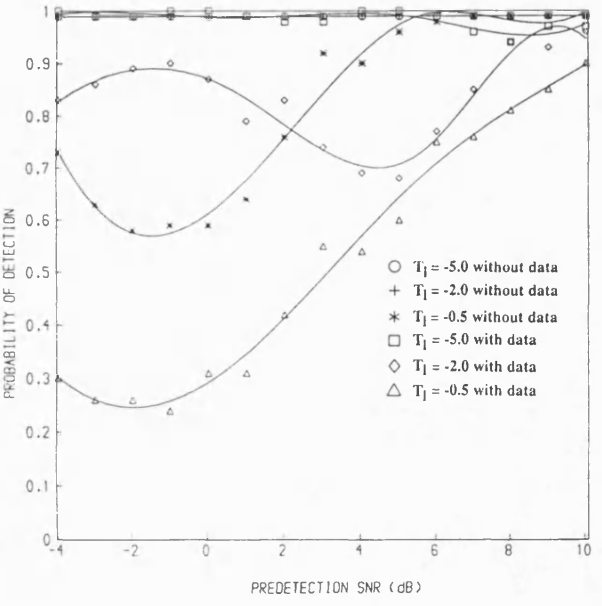

Figure 6.8 P_d vs γ for LLD at $b = b_2$ in the presence and the absence of data modulation.

high bias value and the probability of the wanted signal crossing the upper threshold falls. It can also be seen that increasing the lower threshold has also the effect of reducing both P_d and P_{fa} as the lower threshold is crossed too frequently thus reducing the decision reliability. With further increase in predetection SNR, P_d tends to the same value for all the lower thresholds and for both bias values.

However, with the non-optimum bias, both the LLD and QLD as shown in figures 6.8 and 6.10 show an increase in the P_d at higher predetection SNRs, particularly at higher values of T_l. At the lower values of T_l the P_d is seen to be saturated. This is due to the non-optimum behaviour of the detectors when the relationship between the bias and predetection SNR changes. As the log-likelihood function at this bias is less dependent on the bias ($b_2 = \gamma$) compared to when biased at Wald's optimum bias ($b_1 = \gamma(1+\gamma/2)$, the predetection SNR influences the P_d more. However, at lower predetection SNRs, the bias is still dominant and this produces minima in the P_d (at T_l = -0.5) in the medium predetection SNRs. Similar tendency is seen in case of P_{fa} for the QLD at T_l = -0.5, however, it is not pronounced. The BSD, however, shows decreasing probabilities for both biases at all three values of lower threshold which can be attributed to the approximations employed, giving the likelihood function a closer dependence on the predetection SNR rather than the bias.

For all detectors, although the detector probabilities both with and without data modulation change in a similar way with respect to the variation of the lower threshold and the predetection SNR. However, a significant degradation in P_d with data modulation is observed. Nevertheless, for all the situations shown in figures 6.13 through 6.18, P_{fa} is not seriously affected for the case with data modulation.

Thus, the presence of data modulation is seen to affect P_d more than the P_{fa} and the ASN, and hence it is the change in P_d which is dominant in affecting the mean acquisition time.

6.2.6 Mean acquisition time

Figures 6.19 through 6.24 show the acquisition time characteristics of each detector, with and without data modulation and at both values of bias. As the ASN, P_d and P_{fa} change with the increasing predetection SNR, this causes the mean acquisition time to pass through a minimum. The increase in the ASN is responsible for the initial increase in the mean acquisition time at lower predetection SNRs whereas the reduction in P_d causes the mean acquisition time to increase after passing through the optimum SNR. The optimum SNR and the minimum mean acquisition time are also observed to change with the bias for all the

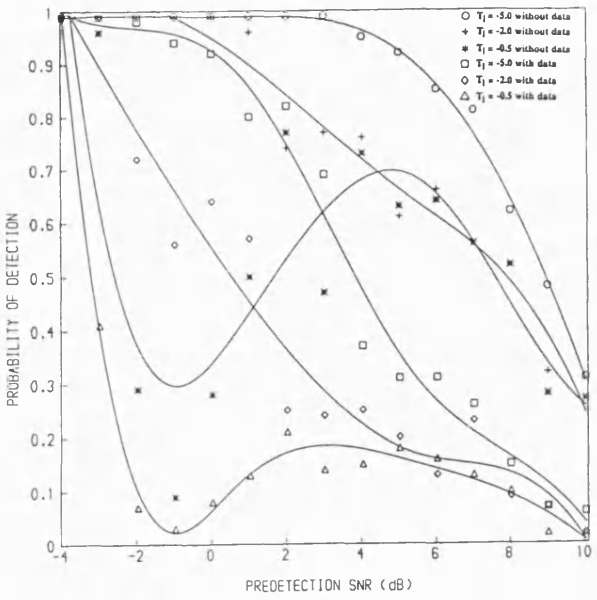

Figure 6.9 P_d vs γ for QLD at $b = b_1$ in the presence and the absence of data modulation.

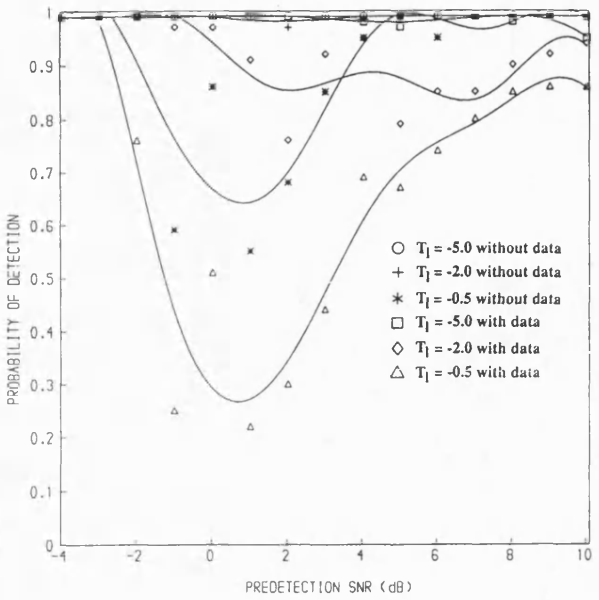

Figure 6.10 P_d vs γ for QLD at $b = b_2$ in the presence and the absence of data modulation.

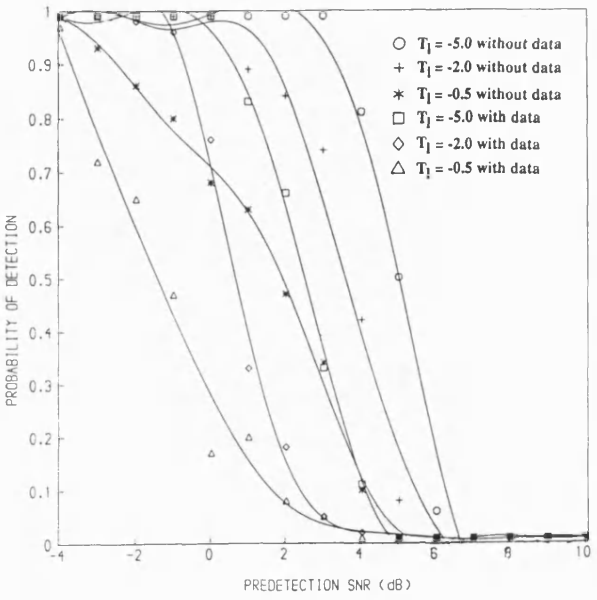

Figure 6.11 P_d vs γ for BSD at $b = b_1$ in the presence and the absence of data modulation.

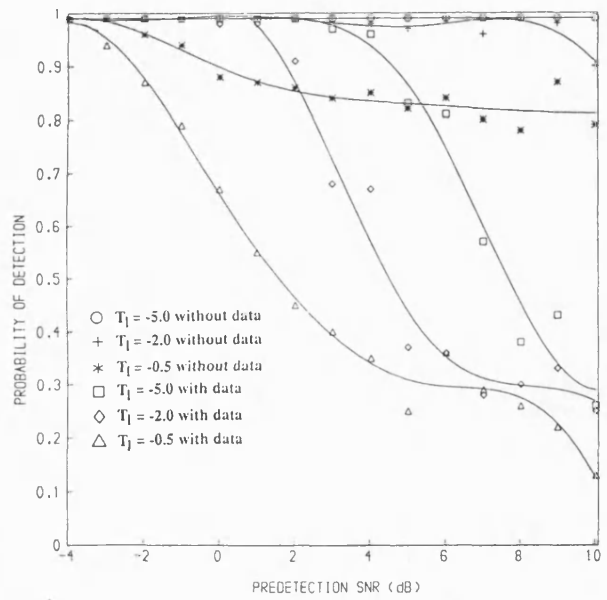

Figure 6.12 P_d vs γ for BSD at $b = b_2$ in the presence and the absence of data modulation.

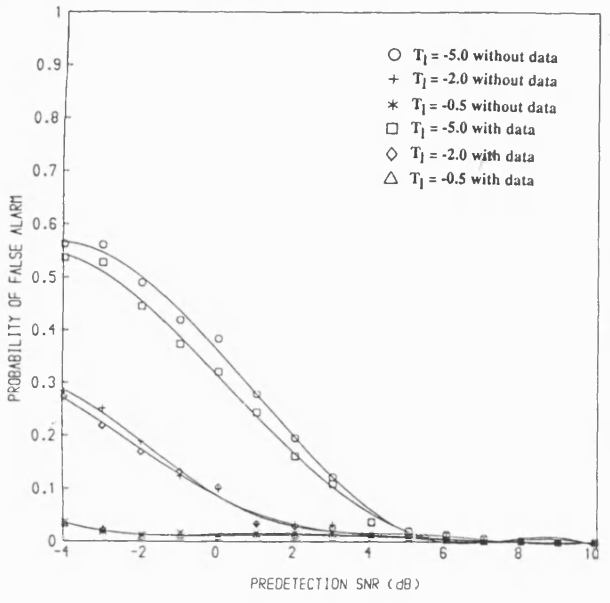

Figure 6.13 P_{fa} vs γ for LLD at $b = b_1$ in the presence and the absence of data modulation.

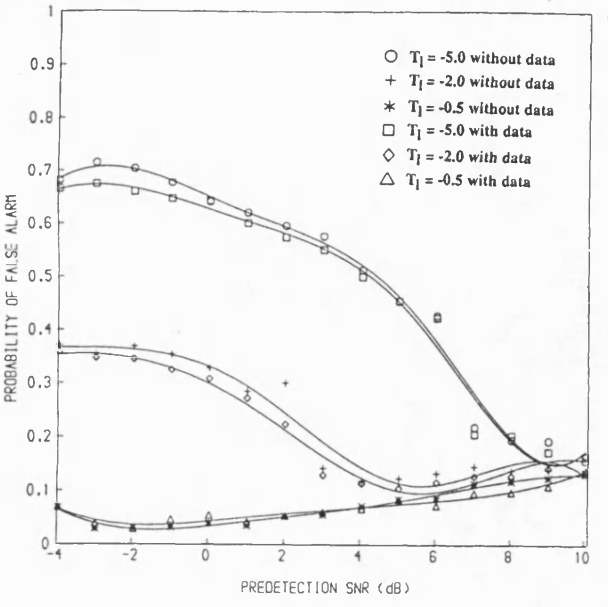

Figure 6.14 P_{fa} vs γ for LLD at $b = b_2$ in the presence and the absence of data modulation.

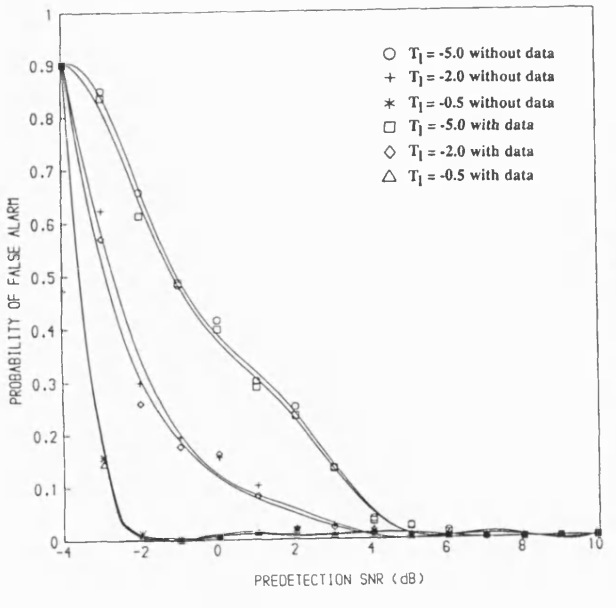

Figure 6.15 P_{fa} vs γ for QLD at $b = b_1$ in the presence and the absence of data modulation.

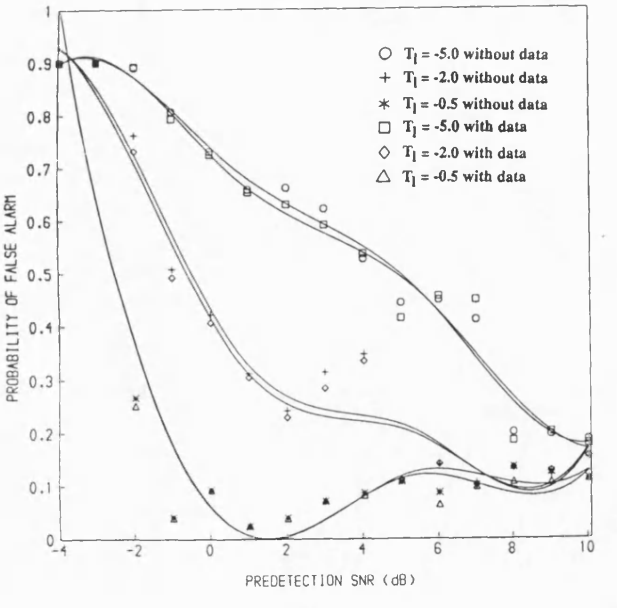

Figure 6.16 P_{fa} vs γ for QLD at $b = b_2$ in the presence and the absence of data modulation.

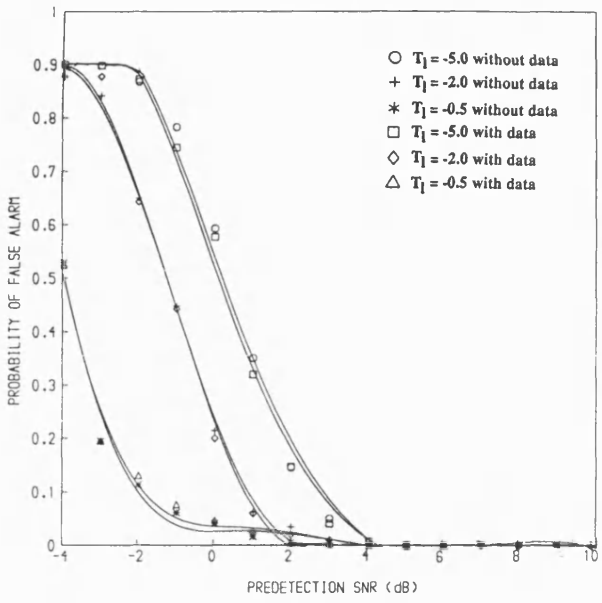

Figure 6.17 P_{fa} vs γ for BSD at $b = b_1$ in the presence and the absence of data modulation.

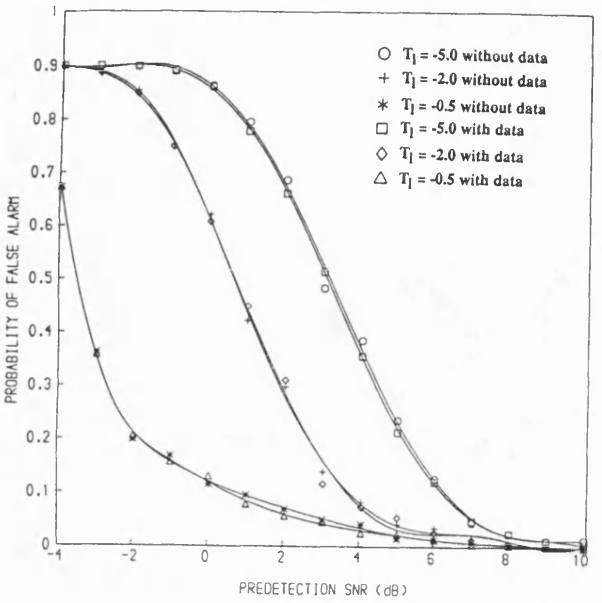

Figure 6.18 P_{fa} vs γ for BSD at $b = b_2$ in the presence and the absence of data modulation.

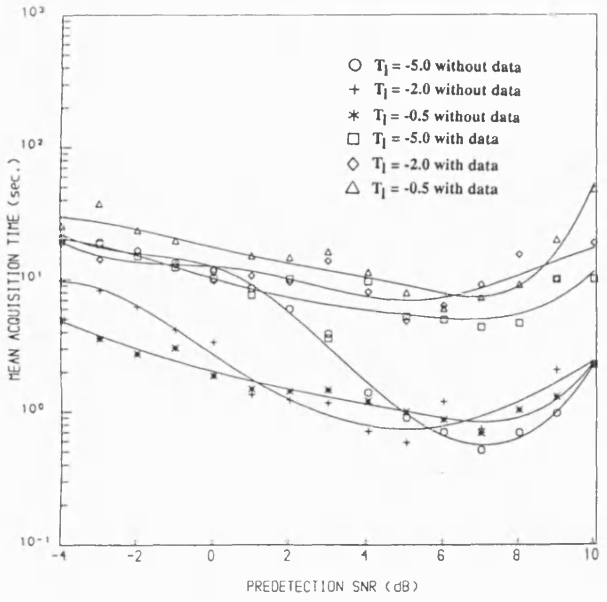

Figure 6.19 T_{acq} vs γ for LLD at $b = b_1$ in the presence and the absence of data modulation.

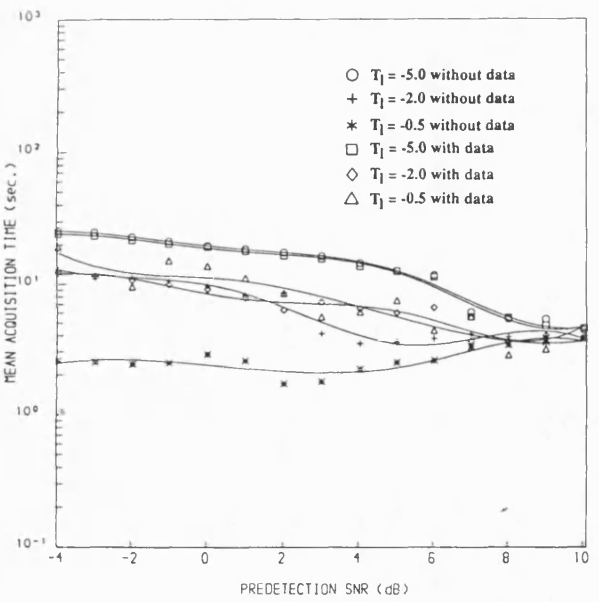

Figure 6.20 T_{acq} vs γ for LLD at $b = b_2$ in the presence and the absence of data modulation.

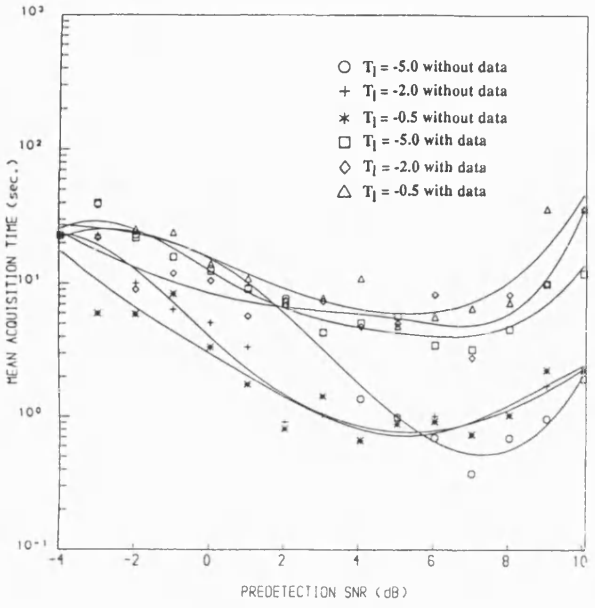

Figure 6.21 T_{acq} vs γ for QLD at $b = b_1$ in the presence and the absence of data modulation.

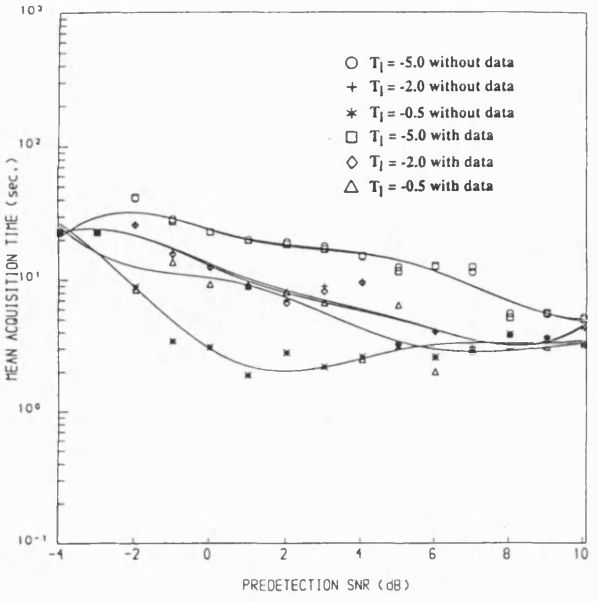

Figure 6.22 T_{acq} vs γ for QLD at $b = b_2$ in the presence and the absence of data modulation.

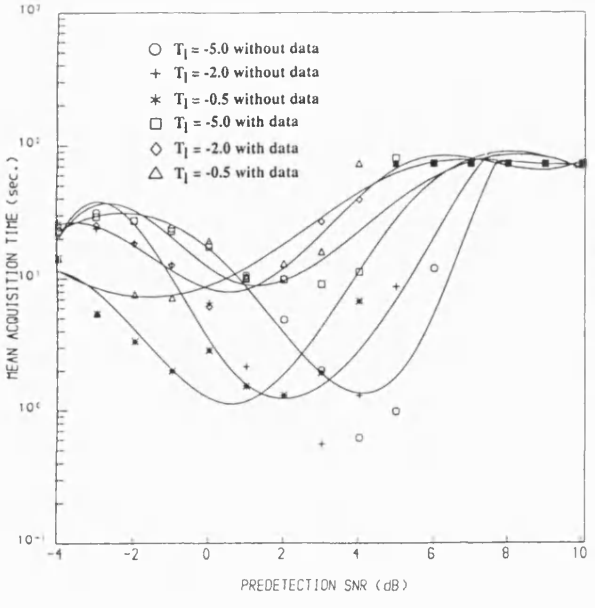

Figure 6.23 T_{acq} vs γ for BSD at $b = b_1$ in the presence and the absence of data modulation.

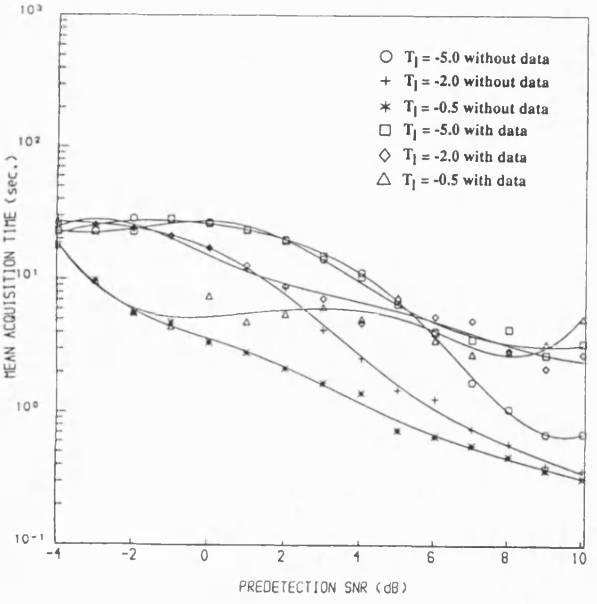

Figure 6.24 T_{acq} vs γ for BSD at $b = b_2$ in the presence and the absence of data modulation.

detectors.

The presence of data modulation is seen to affect both the minimum mean acquisition time and the optimum SNR. For all variants, the curves are found to shift upwards, showing a general degradation in the minimum mean acquisition time. This is due mainly to the degradation of P_d caused by the loss of correlation signal which is due to the filtering and envelope detection loss at the data bit transitions caused by polarity changes.

For the LLD and the QLD, when operated at the optimum bias point, the degradation in acquisition performance is virtually the same at all three lower thresholds for higher values of γ (say, $\gamma > 4$dB). However, for values of $\gamma < 4$dB, the degradation is minimized for T_l = -5.0 whereas it is still substantial when the lower threshold is either -2.0 or -0.5. When operated under non-optimum bias conditions, the degradation is reduced and uniform throughout the range of γ except for T_l = -0.5 which shows a significant degradation at lower values of γ. At higher values of γ, the degradation is observed to tend to a same value. For the BSD with optimum bias, the degradation is greater at the lower values of γ and decreases at higher values of γ as the characteristic becomes saturated. At the non optimum bias, the BSD shows more degradation at higher values of γ while the degradation at the lower values of γ seems to be quite negligible.

The acquisition performance of the QLD closely agrees with that of the LLD both with and without data modulation. For example, at the optimum bias the optimum SNR for the LLD and the QLD without data modulation is around 5-7dB with the minimum mean acquisition time ranging from 0.5-1.0sec (depending upon the value of the lower threshold) and 4-8sec for the same range of optimum SNR with data modulation. When the bias is changed, both the LLD and the QLD show similar changes in the performance both with and without data modulation. The minimum mean acquisition time without data has now increased to 2-5sec whereas with data it does not show significant change.

For the BSD without data when biased at Wald's optimum bias, the SNR at which the the mean acquisition time is minimum, occurs around 3-4dB. In this case, the minimum mean acquisition time is typically 0.5-1.0sec. However with data, the optimum SNR reduces to between -1dB and 2dB with an increase in the minimum mean acquisition time of approximately 10sec. The actual minimum for the BSD occurs with a *non-optimum* bias around 10dB without data and around 8dB with data. Thus, the actual input SNR required for the operation of the BSD with data modulated signals is 2-3dB less than that with no data

modulation, however, minimum mean acquisition time attainable is increased. In case of the LLD and the QLD, although the optimum SNR does not change significantly, the minimum mean acquisition time is increased by 5-10 times.

PART II: ACQUISITION PERFORMANCE IN THE PRESENCE OF DATA MODULATION AND DOPPLER SHIFT

In this part, the problem of initial acquisition of direct-sequence spread-spectrum PN codes under low SNR conditions in the presence of carrier and code Doppler frequency offsets is addressed. As before, the analysis is carried out by means of a Monte-Carlo simulation. First, the effect of various code Doppler offsets was simulated for an LLD without data modulation and the degradation in the mean acquisition time for three different code Doppler offsets was compared. Later, the degradation in the acquisition performance due to the presence of data modulation with a typical Doppler shift of 100chips/s in a code rate of 100kchips/s was assessed for all three detectors; with each detector operating at its optimum design SNR in the predetection SNR range from -4dB to 10dB. New results for the acquisition performance, as the input SNR is varied about the optimum design value, are presented for the LLD, QLD and BSD.

For many practical applications, such as satellite communication systems, a particular problem is that of Doppler frequency offset, both with respect to the carrier frequency and the clock frequency of the incoming PN codes. Carrier Doppler frequency offset has an effect because the IF bandwidth (and hence noise bandwidth) must be wider to accommodate the frequency offset and hence this has an effect of increasing P_{fa} and also decreases P_d due to long-term decorrelation. Code rate Doppler offset causes the two codes to be decorrelated, which reduces the probability of correctly detecting the wanted code epoch and also causes the generation of *self-noise* [6]. The purpose of this work is to establish by how much these frequency offsets can have detrimental effect on the mean acquisition time of the code synchronizer.

Though the code acquisition problem has attracted considerable research attention recently, very few published analyses have considered both data modulation and Doppler effects. Of these, Holmes [7] has presented an approximate analysis of the performance degradation of a single dwell serial search scheme due to Doppler offsets on the code rate, but this analysis

did not include the effect of the change in detection probability. Davisson and Flikkema presented performance results of a parallel acquisition scheme using maximum likelihood detectors for signals carrying data and affected by Doppler [8], whilst Cheng *et al* [9] have considered the effect of code and carrier Doppler on the spread spectrum acquisition problem using square law non-coherent combining detection with parallel/hybrid architectures.

The purpose of this analysis is to examine, for the first time, the effect of both carrier and code Doppler on the mean acquisition time of a sequential detector. The degradation in the mean acquisition time due to both Doppler effects in the presence and absence of random binary data modulation for the three variants of sequential detector are analyzed at the two values of bias employed in the previous analyses.

6.3.1 DOPPLER EFFECTS ON PN CODE CORRELATION

Doppler shift affects the acquisition performance in two ways, namely, carrier frequency offset and code frequency offset. If the carrier Doppler shift is small then the code frequency offset is so small that it can be ignored. However, in certain applications, such as the high dynamics GPS receiver and TDRSS spread-spectrum links, the Doppler conditions are severe and the resultant code Doppler offsets cannot be ignored.

The presence of code frequency offset causes code chip slipping during the correlation between the received code and the local PN code. This causes decorrelation, resulting in the reduced probability of detection, and the acquisition performance can be degraded significantly [6]. Further, it can reduce the average search rate depending upon the polarity of the Doppler (direction of code slipping) and hence can unusually increase the acquisition time. In fact, the search rate can be reduced to zero if the code phase shift caused by Doppler over a dwell time is same as the mean code phase update and this can cause a drastic increase in the acquisition time.

Often, both carrier and code Doppler can be partially removed by using the known user dynamics. However, the residual Doppler is still normally quite significant. The presence of residual Doppler on a data modulated carrier affects the acquisition in two ways. First, the residual carrier Doppler causes long-term decorrelation between the incoming code and the local PN code through phase rotations of the correlation signal at the residual carrier frequency and secondly, the data modulation causes similar decorrelation due to unpredictable phase shifts due to the data transition.

To combat the effects of decorrelation non-coherent combining using square law detectors is normally employed. Though this does not eliminate the decorrelation completely, it is kept to a minimum depending on the data transition density but does cause squaring loss. Both Doppler effects can also be alleviated by subdividing the correlation interval and the frequency uncertainty region and using a parallel bank of correlators and combiners. However, the degree of parallelism depends on a tradeoff between hardware complexity and the acquisition performance.

6.3.2 SIMULATION OF DOPPLER EFFECTS

The received signal structures at the input to the correlator can be viewed as being from two classes: one, containing data modulation and the other with no data modulation. Consequently, six types of signal model with and without Doppler shift were considered and their mathematical representations have been given in chapter 4. These signal types are:

1. DS spread-spectrum signal without data modulation.
2. DS spread-spectrum signal with code Doppler frequency offset without data modulation.
3. DS spread-spectrum signal with code and carrier Doppler frequency offset without data modulation.
4. DS spread-spectrum signal with data modulation.
5. DS spread-spectrum signal with code Doppler frequency offset and data modulation.
6. DS spread-spectrum signal with code and carrier Doppler frequency offset with data modulation.

When a spread-spectrum signal with data modulation and Doppler shift is received by the spread-spectrum correlator, the output of the correlator at baseband, $x(t)$, can be represented as:

$$x(t) = u(t)\cos(\theta_c) + n(t) \tag{6.4}$$

$$u(t) = \sqrt{2}A\, c\left(\frac{t}{1-\zeta'} - \zeta T_c\right) d\left(\frac{t-T_i}{1-\zeta'} - \xi T_o\right) c\left(\frac{t}{1-\tau'} - \tau T_c\right) \tag{6.5}$$

where τT_c represents the local code phase offset and the rest of the symbols as defined in chapter 4.

The correlator signal is envelope detected, and the samples are then directly emphasized by the nonlinearity function '$\ln I_o[\ ]$' in the sequential detector.

The simulation models these effects by generating the code rate Doppler and the residual carrier Doppler. In order to generate the code rate Doppler, the transmit and receive PN chips are passed through a counter with the next transition of the code chip set according to the count ratio, required to offset the clock rates, as needed by the Doppler shift. This method provides an easy way of simulating the Doppler shift and also scope for extending the simulation to include the Doppler rate by simply varying the count ratio. The residual carrier Doppler offset was generated by modelling its equivalent effect at baseband, using the equivalent amplitude error due to the carrier frequency drift. The Doppler frequency error on the sampled signal, $s(t)'$ at a Doppler radian frequency ω_d was thus simulated as:

$$s(t)' = s(t)\ \cos(\omega_d n T_s) \tag{6.6}$$

where n is the number of the sample taken at an interval $T_s = 1/f_s$ and $s(t)$ is the time varying signal without Doppler shift.

The direct-sequence spread-spectrum signals were simulated, as earlier, with a pseudo noise code of length $L = 127$ and chip rate $R_c = 1/T_c = 100$ kchips/sec. These codes were modulated by a random binary data sequence at a rate, $1/T_o = R_c/L = 1/LT_c$ with random data transitions. A range of Doppler code frequency offsets from 100 chips/sec to 10 kchips/sec were generated and the effect of various code Doppler offsets was obtained for the LLD for the case of no data modulation. A residual carrier frequency offset of 1kHz was also generated and a typical Doppler code frequency offset of 100 chips/sec was then impressed on the transmit PN code clock. An additive white Gaussian noise (AWGN) was added and the composite spread-spectrum signals both with and without data were used to generate the corrupted received signals.

6.3.3 ANALYSIS OF SIMULATION RESULTS

The simulation employs the near-optimum values for the system parameters of the detector: i) T_u, ii) T_l, iii) bias, b and iv) design γ, γ_{dsn}, obtained from the optimization discussed in chapter 5. All the performance parameters namely, i) ASN ii) probability of detection, P_d iii) probability of false alarm, P_{fa} and iv) total mean acquisition time, T_{acq} were examined for the six types of signals considered and the performance degradations assessed.

Thus, three lower threshold values at T_l = -5.0,-2.0,-0.5 and an upper threshold value at T_u = 5.0 were employed with both the bias values b_1 and b_2 for the predetection SNR, range of -4dB to 10dB. The optimum design SNR γ_{dsn} corresponding to each detector, which was obtained through previous optimization results, was employed and the acquisition

characteristics were obtained using this design SNR γ_{dsn} with γ varied about γ_{dsn}.

6.3.4 Mean Acquisition Time

First, the mean acquisition time of the LLD for three different code Doppler offsets was compared with its ideal performance and the degradation due to code Doppler was assessed. Later, the degradation in the acquisition performance of the three variants, when all six signal structures were employed, was obtained for a typical Doppler shift of 100 chips/sec and the results compared.

6.3.5 Effect of code Doppler offset on the mean acquisition time

The mean acquisition time as a function of the predetection SNR for the LLD with three code Doppler offsets is shown in figure 6.25. The three code Doppler offsets employed are 100 chips/sec, 1 kchips/sec and 10 kchips/sec in a code rate of 100 kHz. The curves show that the mean acquisition time is degraded significantly when the Doppler offset is 10 kchips/sec (which is normally considered to be a very high Doppler shift for the code rate of 100 kHz). However, as the Doppler shift is reduced, the degradation reduces particularly at higher predetection SNRs. For a Doppler shift of 1 kchips/sec, the degradation is still quite high, but, it is tolerable when the Doppler shift has fallen to 100 chips/sec. In our further investigations on the effects of both carrier and code Doppler shift, a code rate Doppler offset of 100 chips/sec was employed.

6.3.6 Effect of carrier and code Doppler offset on the mean acquisition time

In figures 6.26 through 6.31, the mean acquisition time is plotted as a function of predetection SNR, γ. The six curves on each graph correspond to the six signal types 1-6 defined earlier. Signal type 1 is used as the reference signal for the purpose of comparison. In all the figures, it is observed that T_{acq} is maximum at low γ and starts to decrease as γ is increased and then passes through a minimum for all signal types. The reasons for this are attributed to the dominance of P_d and P_{fa} which change with γ. At a very low γ both P_d and P_{fa} are very low and it is the reduced P_d that causes a high T_{acq} whereas at a very high γ both P_d and P_{fa} are also very high and it is the false alarm penalty which causes the T_{acq} to increase once again. This is due to the fact that the detector is operated at a fixed design SNR, γ_{dsn}, thus the bias value is fixed even though the predetection SNR changes. At higher γ, the increased signal strength dominates in determining the value of the log-likelihood function rather than the bias value and this causes higher P_d and P_{fa} as the tendency to cross the upper

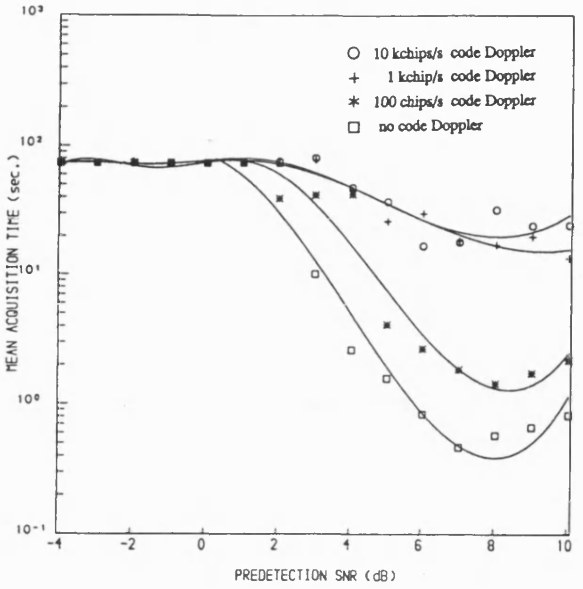

Figure 6.25 T_{acq} vs γ at various Doppler shifts for LLD at $b = b_1$.

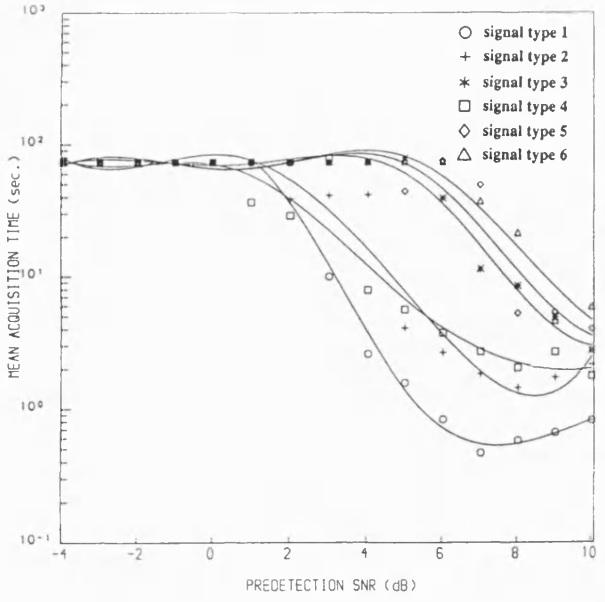

Figure 6.26 T_{acq} vs γ for LLD at $b = b_1$ with data modulation and Doppler shift.

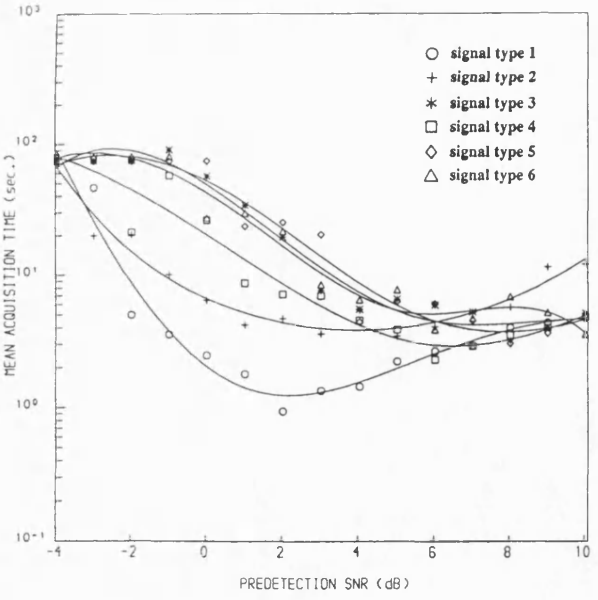

Figure 6.27 T_{acq} vs γ for LLD at $b = b_2$ with data modulation and Doppler shift.

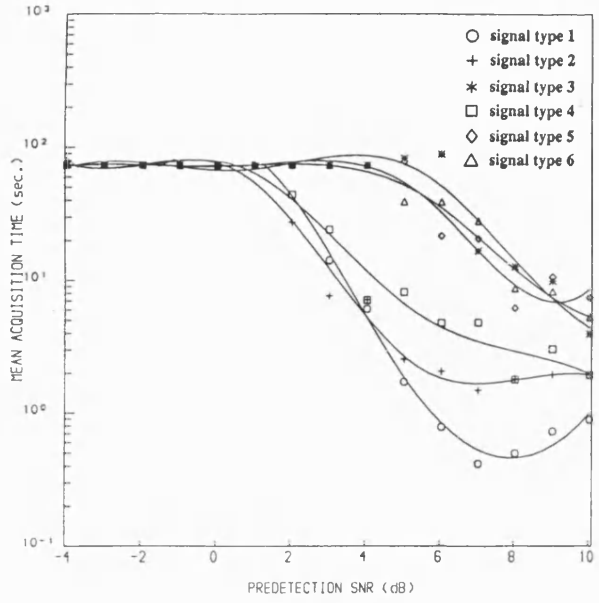

Figure 6.28 T_{acq} vs γ for QLD at $b = b_1$ with data modulation and Doppler shift.

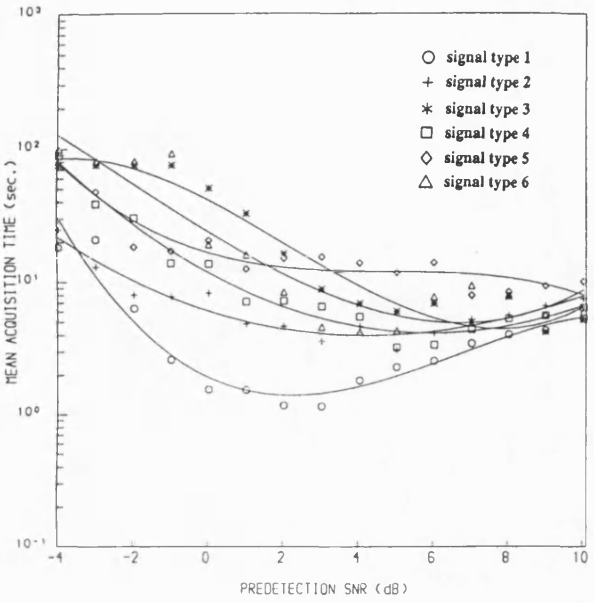

Figure 6.29 T_{acq} vs γ for QLD at $b = b_2$ with data modulation and Doppler shift.

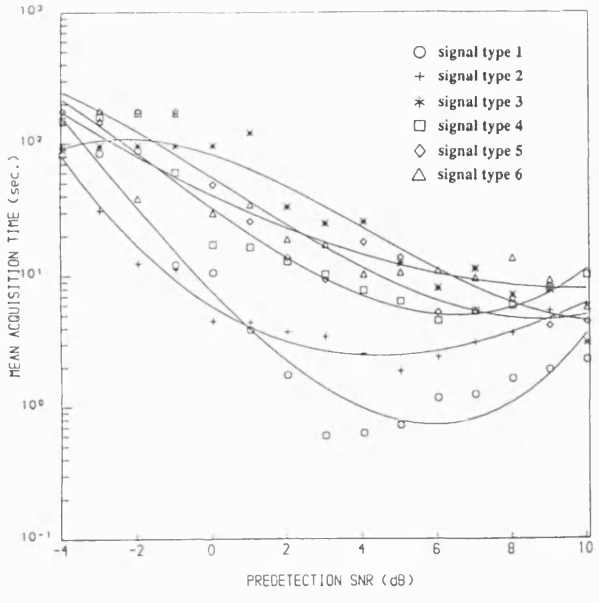

Figure 6.30 T_{acq} vs γ for BSD at $b = b_1$ with data modulation and Doppler shift.

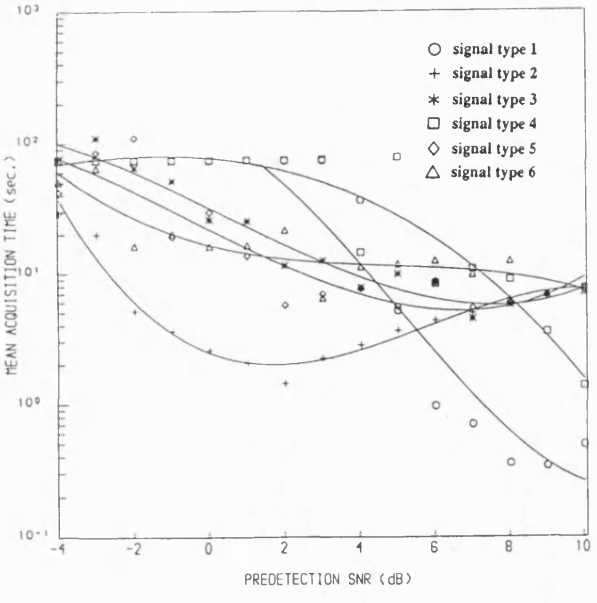

Figure 6.31 T_{acq} vs γ for BSD at $b = b_2$ with data modulation and Doppler shift.

threshold increases (because the bias has the effect of reducing the log-likelihood function whereas the signal strength has the effect of increasing the log-likelihood function). However, at lower γ, the bias term dominates rather than the signal strength causing lower P_d and P_{fa} as the tendency to cross the lower threshold increases. The best combination of P_d and P_{fa} produces the minimum T_{acq} and the γ at which it occurs is the optimum γ which is referred to as γ_{opt} in the further discussion. However, with changing system parameters, the ASN and the rate at which P_d and P_{fa} vary also change and this causes a change in both the minimum T_{acq} and the value of γ_{opt}.

Figures 6.26 and 6.27 show the characteristics of the LLD with bias values b_1 and b_2. At Wald's optimum bias, b_1, signal type 1 produces the minimum T_{acq}. This is approximately 0.5sec and the corresponding γ_{opt} occurs at 7dB. The addition of Doppler shift and/or data modulation is found to degrade both the minimum T_{acq} and γ_{opt}. With the addition of code Doppler only (signal type 2), T_{acq} is found to be degraded slightly whereas with the addition of both Doppler frequency offsets (signal type 3) the degradation is seen to be quite severe. For signal type 2, the minimum T_{acq} is at 1.5sec with a γ_{opt} at 8dB, representing a 1dB degradation in the γ_{opt} and a threefold increase in minimum T_{acq}. Signal type 3 causes 3dB degradation in γ_{opt} and an almost eightfold increase in the minimum T_{acq}.

When data is added, the degradation is seen to be worse still. With the addition of data (signal type 4), the minimum T_{acq} is increased to 2sec whereas with Doppler shift ie., signal types 5 and 6, it is 4sec and 5sec respectively. The degradation in γ_{opt} for these signal types is more than 3dB. When the bias is changed to a non-optimum value, b_2, as shown in figure 6.27 the degradation in the minimum T_{acq} at higher values of γ is quite similar for all the signal types, and the minimum T_{acq} is around 5sec. However, the degradation in T_{acq} is quite different at lower γ's.

In figures 6.28 and 6.29, the performance of the QLD is considered. With the bias values, b_1 and b_2 the QLD has a performance which closely matches with that of the LLD. The worst case minimum T_{acq} for this detector is also found to occur with signal type 6 and it is approximately 6sec and occurs when the γ_{opt} = 10dB.

The performance of the BSD, shown in figures 6.30 and 6.31, is slightly different from the performance of the LLD and the QLD. It has better characteristics at lower γ with Wald's optimum bias, b_1. The minimum T_{acq} varies from 3sec to 5sec for signal types 2-6 resulting in an increase of 3-5 times compared to that of the signal type 1. The γ_{opt} is close to 8dB for

signal types 3-6 which amounts to a degradation of 2dB only, compared to the performance of signal type 1. However, for signal type 2, it is at 4dB, representing an improvement of 2dB in the γ_{opt}. With the non-optimum bias b_2, signal types 1 and 4 show a minimum T_{acq} at higher γ; however, the drift towards lower γ is prominent with the rest of the signal types. The minimum T_{acq} remains to be close to 5sec for signal types 3-6 and 1sec for signal type 2. This drift in γ towards lower values is expected because the BSD has been found to be a good approximation to the log-likelihood function at low SNR's [10].

6.3.7 Comparison of the degradation in the mean acquisition time

At Wald's optimum bias, the LLD and the QLD show a degradation in γ_{opt} of approximately 3dB without data (with reference to signal type 1) and 2dB with data (with reference to signal type 4). The degradation in the value of minimum T_{acq} is close to 10 times compared to that without data. At the nonoptimum bias, b_2, γ_{opt} is degraded by 5dB without data (with reference to signal type 1) and 2dB with data (relative to signal type 4). Though the degradation due to data modulation and Doppler shift is quite high, the addition of data itself causes a significant degradation. For the BSD with the bias b_1, in the absence of data, γ_{opt} suffers by 3dB while the minimum T_{acq} is degraded by 4 times. In the presence of data, even though γ_{opt} suffers by the same degree, the minimum T_{acq} is increased by 5 times. However, at bias b_2, γ_{opt} is reduced by 2dB , with the minimum T_{acq} increased by 5 times in the presence of data and 10 times in the absence of data.

6.3.8 Effect on the ASN characteristics

The ASN curves corresponding to each detector for the T_l = -5.0 are shown in figures 6.32 through 6.37. As the detectors were operated at their corresponding near-optimum design SNR, the ASN for all signal types remains nearly constant for the entire range of predetection SNR. However, in all the cases, the ASN is the lowest for signal type 1 which is the reference signal type and highest for the signal types 4-6 which represent the data modulated signals. The effect of Doppler shift on the ASN has been observed to be minimal.

6.3.9 Effect on Probability of detection and Probability of false alarm

Figures 6.38 through 6.43 represent the variation of P_d with the predetection SNR for each signal type, at both bias values with the lower threshold at -5.0. The probability of detection is quite low at lower predetection SNRs and increases with increasing SNR. This is due to the fact that the detector bias is fixed as it was operated at a near-optimum design SNR and

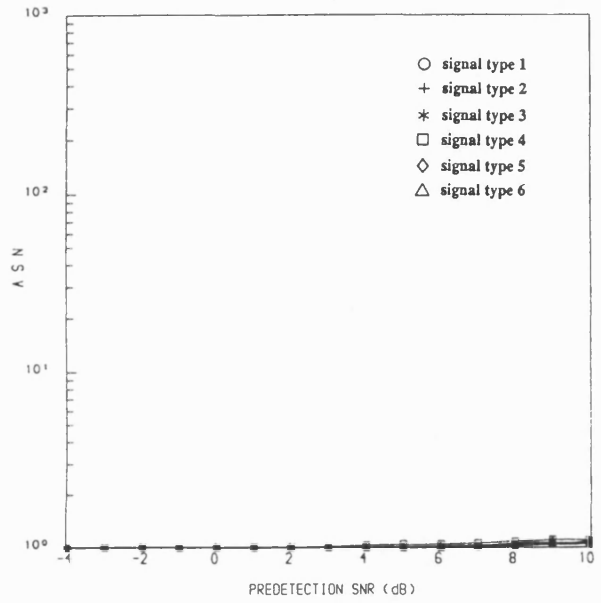

Figure 6.32 A S N vs γ for LLD at $b = b_1$ with data modulation and Doppler shift.

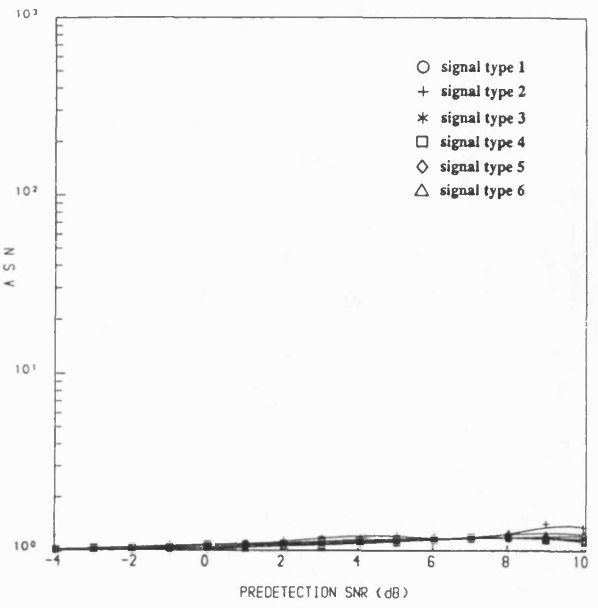

Figure 6.33 A S N vs γ for LLD at $b = b_2$ with data modulation and Doppler shift.

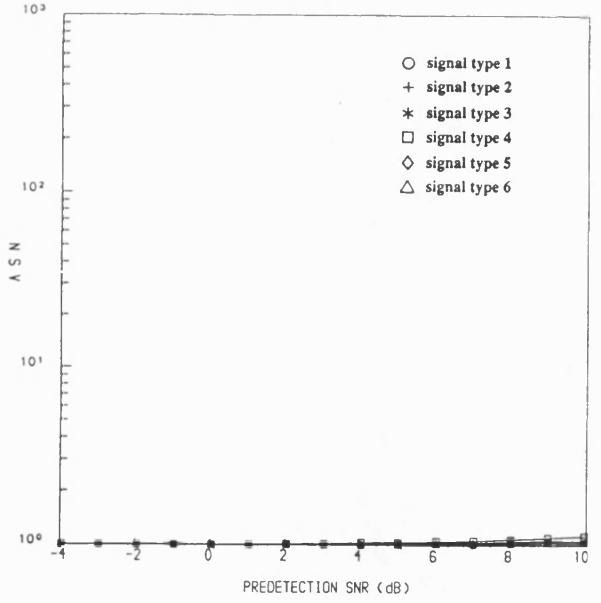

Figure 6.34 A S N vs γ for QLD at $b = b_1$ with data modulation and Doppler shift.

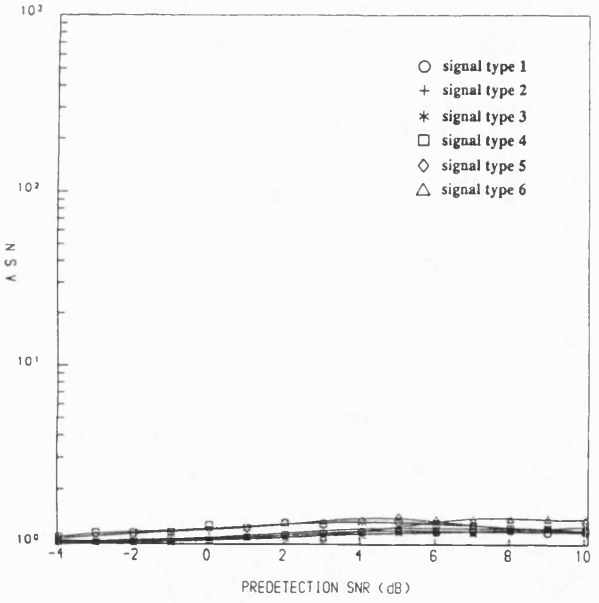

Figure 6.35 A S N vs γ for QLD at $b = b_2$ with data modulation and Doppler shift.

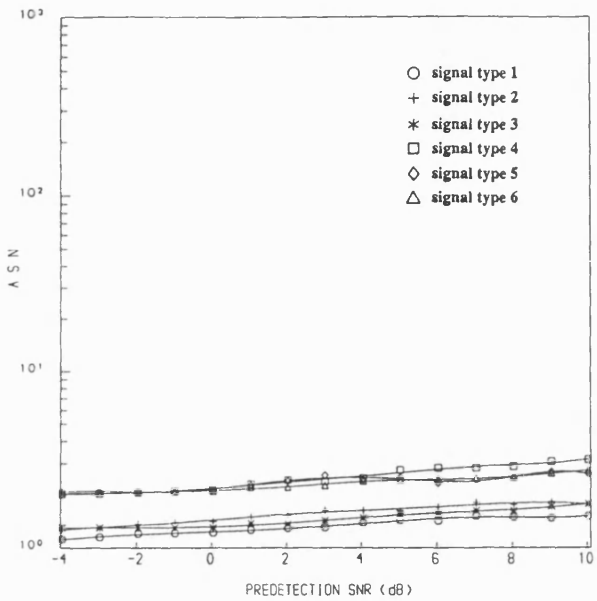

Figure 6.36 A S N vs γ for BSD at $b = b_1$ with data modulation and Doppler shift.

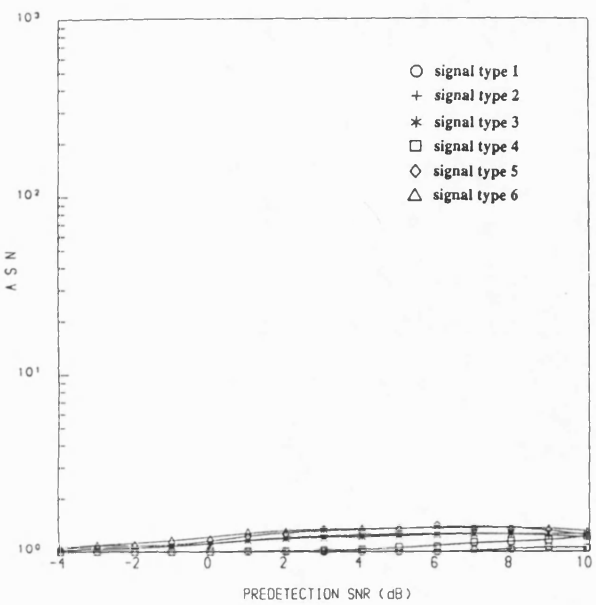

Figure 6.37 A S N vs γ for BSD at $b = b_2$ with data modulation and Doppler shift.

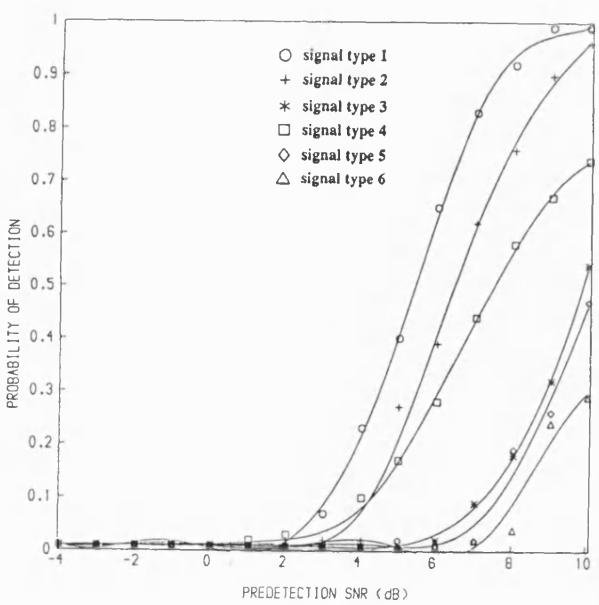

Figure 6.38 P_d vs γ for LLD at $b = b_1$ with data modulation and Doppler shift.

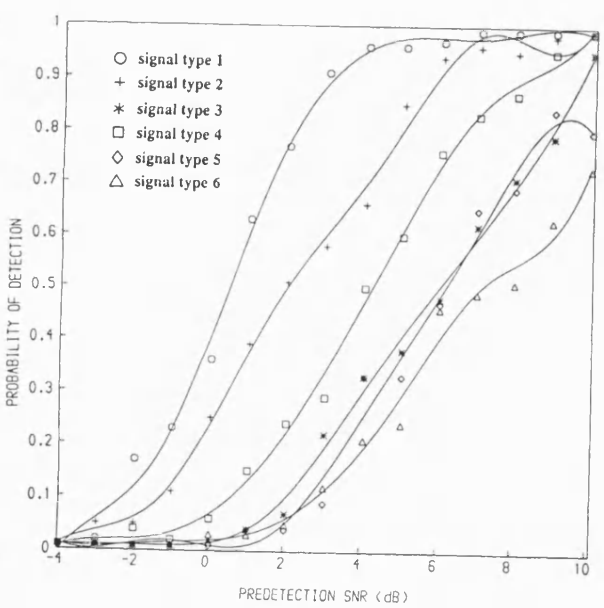

Figure 6.39 P_d vs γ for LLD at $b = b_2$ with data modulation and Doppler shift.

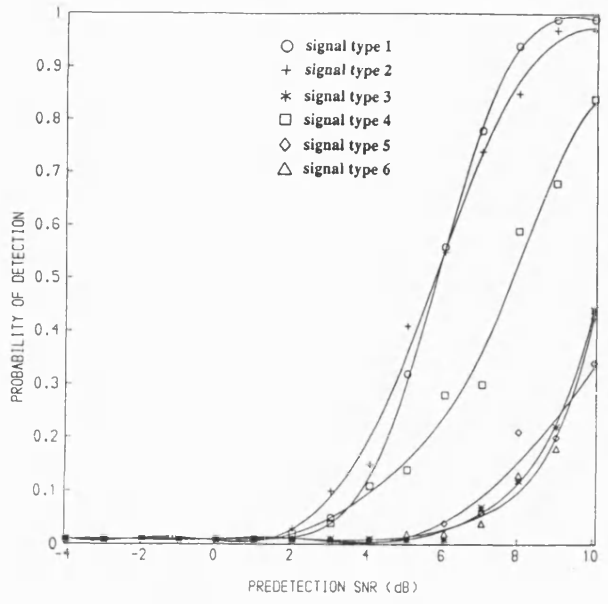

Figure 6.40 P_d vs γ for QLD at $b = b_1$ with data modulation and Doppler shift.

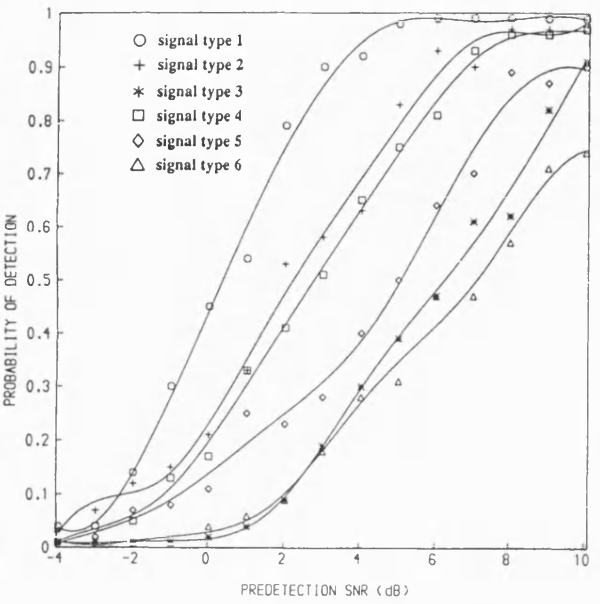

Figure 6.41 P_d vs γ for QLD at $b = b_2$ with data modulation and Doppler shift.

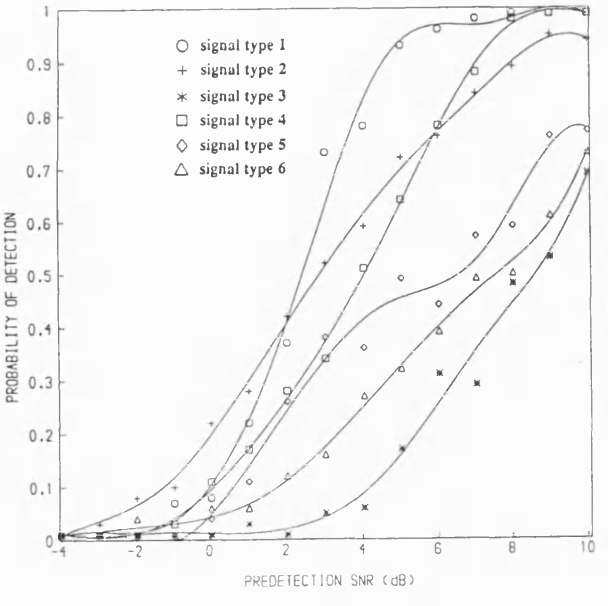

Figure 6.42 P_d vs γ for BSD at $b = b_1$ with data modulation and Doppler shift.

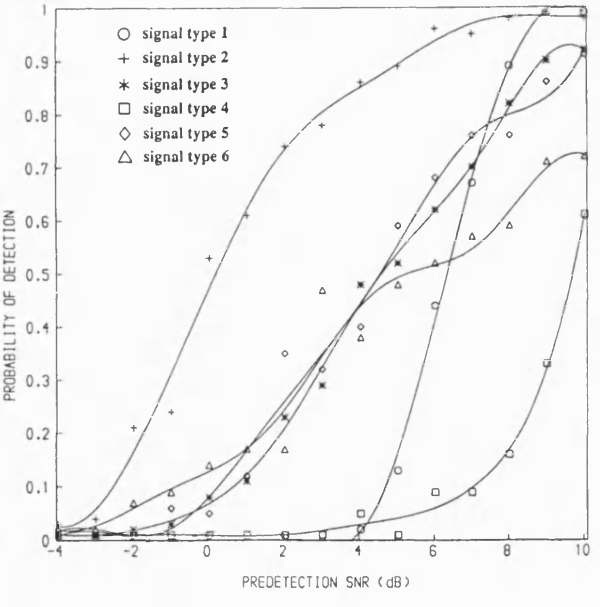

Figure 6.43 P_d vs γ for BSD at $b = b_2$ with data modulation and Doppler shift.

hence, the predetection SNR dominates in the growth of log-likelihood function (as explained earlier). The presence of data modulation degrades P_d for all cases and the signal type 6 is seen to suffer the most in case of both the LLD and QLD. However, for the BSD at b_1, the degradation due to both Doppler offsets without data modulation (signal type 3) is seen to dominate all other signal types whereas for b_2 the data modulation degradation (signal type 4) dominates over its combined effect with the Doppler shifts (signal type 6). The P_d with b_2 is always higher than with b_1 for the LLD and QLD for all signal types. In case of the BSD, the signal type 1 and 3 produce higher P_d with b_1 than with b_2.

The effect of Doppler shift and data modulation on P_{fa} is shown in figures 6.44 through 6.49. For all cases, P_{fa} increases with the increasing predetection SNR which is due to the increased tendency to cross upper threshold as a result of increased correlation noise (as the signal strength increases). For all variants of the detector, the P_{fa} does not change significantly at the lower predetection SNRs for most signal types, however, the data modulation and Doppler shift introduces additional increase in the P_{fa}. In the case of the LLD, the signal type with the code Doppler (signal type 2) suffers the most with both bias values. The QLD undergoes the similar degradation with the b_1, however, with the b_2, the signal type 6 takes over. In case of the BSD, it is the signal type 6 which produces the worst degradation.

6.4 CONCLUSIONS

For all three types of sequential detector, the data modulation has been seen to degrade the minimum mean acquisition time and this is due principally to a reduction in the probability of detection, P_d rather than an increase in the ASN or the P_{fa}. The QLD agrees closely with the LLD, with and without data modulation and has broader optimum SNR characteristics than the BSD which shows a sharp increase in the mean acquisition time with the increase in predetection SNR. Although the LLD and QLD do not show significant changes in the optimum design SNR, the optimum design SNR for the BSD is found to be reduced by approximately 3dB. However, for all detectors the minimum mean acquisition time is found to increase by 5-10 times depending on the lower thresholds and the biases.

The degradation due to both carrier and code Doppler frequency offsets in the presence of data modulation is found to be quite significant for all three types of sequential detector. The degradation in the performance of the QLD is similar to that of the LLD. Both the detectors show a drift of +3dB in the γ_{opt} with the minimum mean acquisition time increased by 10

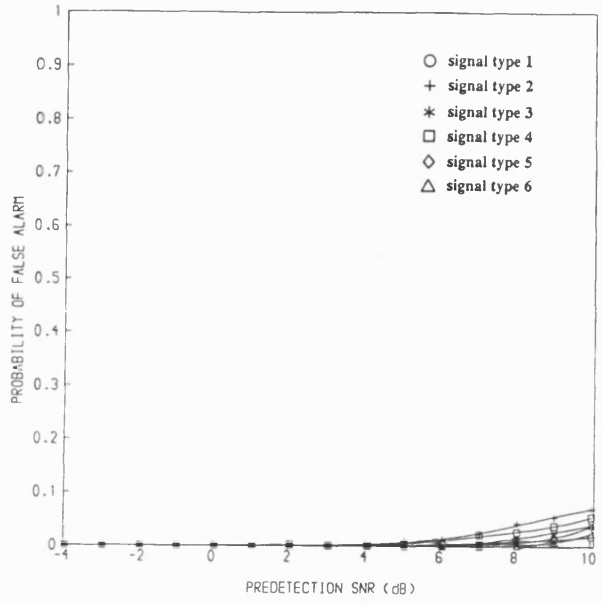

Figure 6.44 P_{fa} vs γ for LLD at $b = b_1$ with data modulation and Doppler shift.

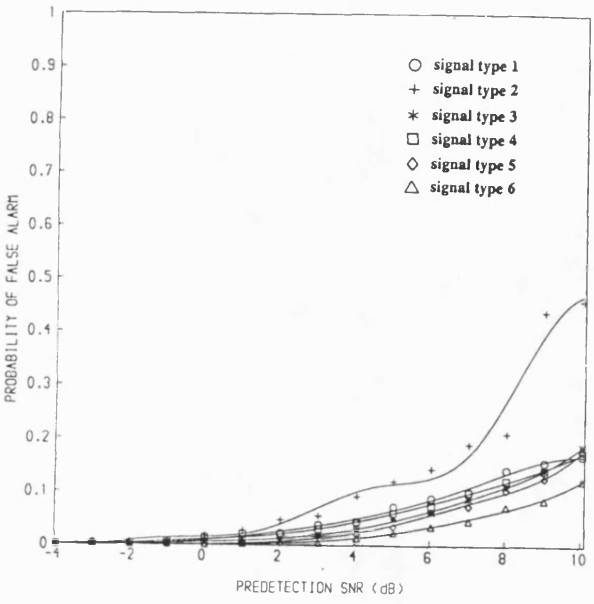

Figure 6.45 P_{fa} vs γ for LLD at $b = b_2$ with data modulation and Doppler shift.

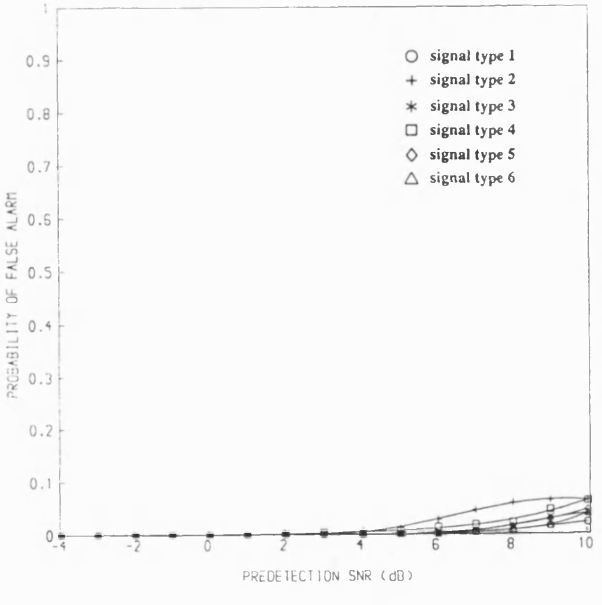

Figure 6.46 P_{fa} vs γ for QLD at $b = b_1$ with data modulation and Doppler shift.

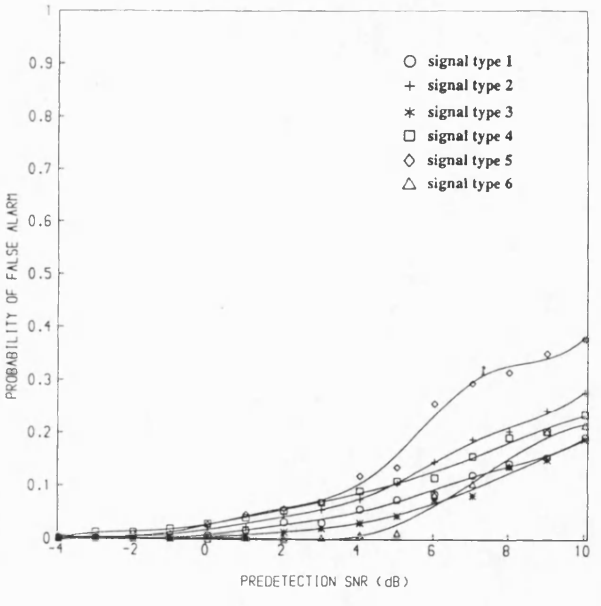

Figure 6.47 P_{fa} vs γ for QLD at $b = b_2$ with data modulation and Doppler shift.

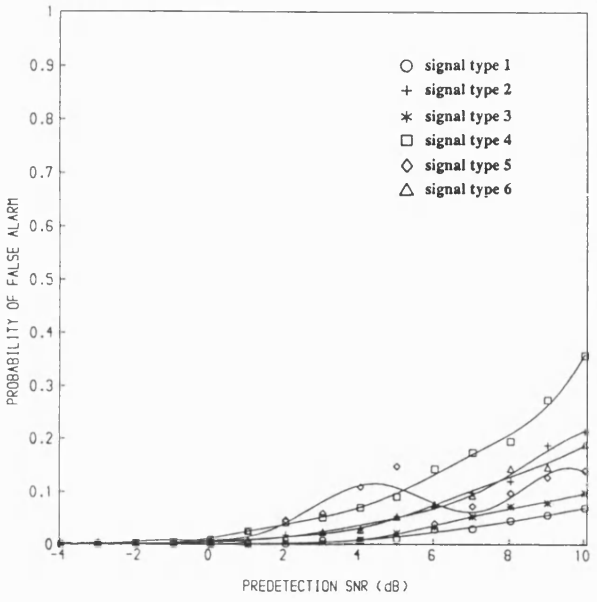

Figure 6.48 P_{fa} vs γ for BSD at $b = b_1$ with data modulation and Doppler shift.

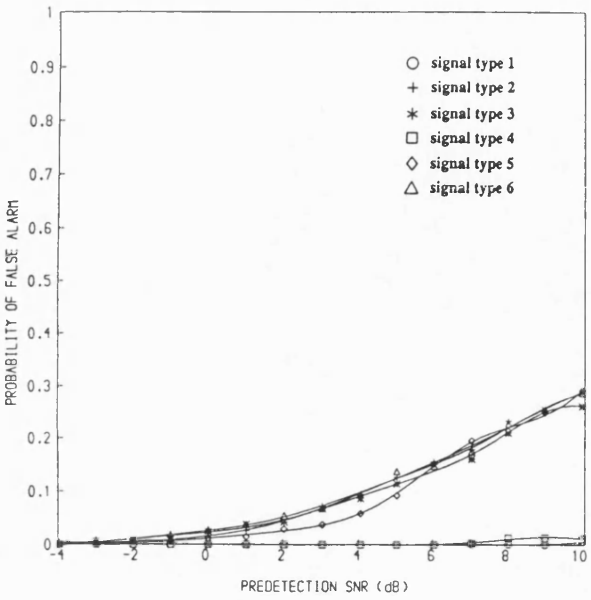

Figure 6.49 P_{fa} vs γ for BSD at $b = b_2$ with data modulation and Doppler shift.

times without data and a drift of +2dB with minimum T_{acq} increased by more than 10 times with data. The performance of the BSD is improved at lower γ compared to that of the QLD and LLD, particularly with Wald's optimum bias. However, the degradation in the γ_{opt} is +3dB and the minimum T_{acq} is increased by 4 times without data; but with the presence of data, the γ is degraded by 3dB and the minimum T_{acq} is increased by 5 times.

Even though degradation due to code and carrier Doppler in the presence of data is quite significant for all the three detectors, when only code Doppler is present the degradation seems to be reasonable. The effect of the code and carrier Doppler with data modulation are seen to degrade the mean acquisition time by 5-10 times and cause a 3-5dB degradation in γ_{opt}. In practice, this means that the system must operate in 3-5dBs less noise to achieve acceptable acquisition performance.

6.5 REFERENCES

1) R.F.Cobb and A.D.Darby, "Acquisition performance of simplified implementations of the sequential detection algorithm", NTC Conference Record, pp 43.4.1-43.4.7, December 4-6, 1978, Birmingham, AL.

2) K.V.Ravi and R.F.Ormondroyd, "Computer simulation of a quantized log-likelihood sequential detector for faster acquisition of spread-spectrum pseudo-noise signals." 5th International Conference on Radio Receivers and associated systems, IEE Conference publication No. 325, pp 207-211, July 24-26,1990, Cambridge, UK.

3) K.V.Ravi and R.F.Ormondroyd, "Comparison of the acquisition performance of biased square law and quantized log-likelihood sequential detectors for PN acquisition" IEEE International Symposium on Spread Spectrum Techniques and Applications, Symposium Proceedings, pp 53-58, September 24-26,1990, London, UK.

4) U.Cheng, "Performance of a class of parallel spread-spectrum code acquisition schemes in the presence of data modulation" IEEE Trans. Comm, vol.36, No.5, pp 596-604, May 1988.

5) K.V.Ravi and R.F.Ormondroyd, "Performance of sequential detectors for the acquisition of data modulated spread spectrum pseudo noise signals", IEEE International Conference on Communications, ICC'91, June 23-26, 1991, Denver, Colorado, USA.

6) R.F.Ormondroyd and V.E.Comley, "Limits on the search rate of a sliding correlator synchronizer due to the effects of self-noise and decorrelation" IEE Proceedings, Part F, vol. 131, no. 7, pp 742-750, December 1984.

7) J.K.Holmes, *Coherent Spread Spectrum Systems*, John Wiley & Sons, New York, 1982.

8) L.D.Davisson and P.G.Flikkema, "Fast single-element PN acquisition for the TDRSS MA system" IEEE Trans. on Communications, vol.36, no. 11, pp 1226-1235, November 1988.

9) U.Cheng, W.J.Hurd and J.I.Statman, "Spread-spectrum code acquisition in the presence of Doppler shift and data modulation" IEEE Trans. on Communications, vol. 38, no. 2, pp 241-250, February 1990.

10) W.B.Kendall, "Performance of the biased square law sequential detector in the absence of signal", IEEE Trans. Inform. Theory, IT-11, pp 83-90, January 1965.

CHAPTER 7

PERFORMANCE OF THE SEQUENTIAL DETECTOR IN THE PRESENCE OF CW INTERFERENCE AND PULSE JAMMING AND A COMPARATIVE EVALUATION OF SERIAL SEARCH TECHNIQUES

7.1 INTRODUCTION

This chapter is organized into two parts. In the first part, the acquisition performance of three variants of sequential detector is analyzed in the presence of CW interference (or an intentional CW jammer) and pulsed jamming for various jammer-to-signal power ratio's (J/S). The performance of the sequential detector in the presence of a CW jammer at various values of J/S is presented for a range of input SNR (due to Gaussian noise) from -10dB to -25dB. The effect of duty factor on the pulse jammer for a noiseless case has been investigated and the acquisition performance for several values of the duty factor (the fraction of time that the pulse is present), with the J/S varied from 10dB to 25dB is presented. The critical duty factor causing maximum bit error probability for each value of J/S has been considered and its effect on the acquisition performance shown. The effect of pulse jamming in Gaussian noise has also been observed for a typical duty factor of $\rho = 0.1$ with J/S varied for the input SNR from -10dB to -25dB and its acquisition performance presented.

In the second part of this chapter, the Monte-Carlo simulation of acquisition systems has been extended to two other common forms of serial search technique namely, a non-coherent single dwell detector and a digital matched filter and their acquisition performances are compared with that of the sequential detector. The detectors have been optimized with respect to their critical system parameters, and the acquisition performance for an equivalent range of input SNRs has been obtained. The optimized acquisition performance has been compared with that of the LLD for the input SNR range from -10dB to -25dB and their relative performance is assessed.

The results of this comparison show that the sequential detector working at its optimized design predetection SNR performs better than both the single-dwell detector and the matched

filter, particularly at low input SNRs. However, as the predetection SNR is increased, the sequential detector is still marginally better than the single-dwell detector, but the matched filter starts showing significant improved performance at high SNRs. The sensitivity of the minimum mean acquisition time with the optimized system parameters for each detector has also been shown and the performances are compared.

PART I: PERFORMANCE OF THE SEQUENTIAL DETECTOR IN THE PRESENCE OF CW INTERFERENCE AND PULSE JAMMING

7.2.1 Interference and jamming

The acquisition performance of a direct-sequence spread spectrum receiver can be degraded significantly in the presence of an interfering signal or a jamming signal as both can deny the acquisition of a correct signal by acting as additional (unpredictable) noise sources which can cause an increase in the probability of false alarm of the detected correlation signal or conversely a reduced probability of detection. Both the interfering signal (intentional or unintentional) and the jammer waveform can be of several forms depending upon the jammer strategy. The optimum jammer strategy for an intentional interferer/jammer, whose main aim is to jeopardize the communication link, is to concentrate the entire jammer power in the exact signal coordinates to jam the signal completely. However, as the jammer has generally no complete knowledge of the signal coordinates it is a random strategy and many forms of jammer strategies can be used depending upon the type of the spread-spectrum signal being jammed. The various forms of jammer waveform are:

i. Broadband and partial-band noise jammers

ii. Tone (CW and multi-tone) jammers

iii. Pulse jammers

iv. Jammers with arbitrary power distributions (random jammer)

v. Repeat-back jammers

vi. Smart jammers

The constant-power broad-band jammer spreads the entire power over total spread bandwidth and hence does not exploit the knowledge of the anti-jam communication system except for

the spread bandwidth. The effect of such a jammer on the spread-spectrum performance is equivalent to white Gaussian noise and its performance is normally referred to as the *baseline performance.* The worst performance (in the sense of bit-error rate) is caused by the partial-band or partial-time (pulsed) jammers. The CW and pulse jammers are effective against direct-sequence spread-spectrum signals whereas the partial-band and multi-tone jammers are more effective against frequency hopping spread-spectrum signals. For direct-sequence spread spectrum signals, the CW jammer is the most harmful as it can place as much energy as possible in the cosine coordinate (as the signal carries maximum power in this coordinate), thus causing maximum degradation to the signal. CW and multi-tone jammers can affect frequency hopping signals more than the partial-band jammers when the tones are distributed over the spread-spectrum bandwidth as they can easily inject energy into the non-coherent detectors. An effective anti-jam system in the presence of such jammers is expected to provide a performance which is close to or better than the baseline performance, regardless of the type of jammer waveform (as its anti-jam strategy is expected to be designed to counter the extra threat caused by the jammer strategy).

A number of researchers have analyzed the effect of these jammers on the bit error rate performance of spread spectrum systems and have also analyzed the methods employed to reduce the effect of jamming on bit error probabilities [1,2]. Coding and interleaving have been found to be most effective to recover most of the performance loss. Other methods to enhance performance in the presence of jamming/interference have also been analyzed which employ various diversity techniques, filtering techniques and signal processing methods (spectral estimation, adaptive techniques etc.,). However, the analysis of the effect of jamming on the acquisition performance of spread spectrum receivers has not yet received significant attention in the literature, particularly for the various acquisition strategies that currently exist. Seiss and Weber [3] have analyzed an I-Q detector used in a serial-search acquisition system in CW and pulsed jamming. They consider this detector to be more effective in the presence of data modulation than the correlator/square-law detector. Their results show that for the case of constrained average pulse jammer power, the jammer's duty factor does not impact acquisition time when the pulse repetition factor (PRF) is quite high, however, for a duty factor of unity, it was found that the acquisition performance was degraded maximally when the PRF was low. The results also imply that the CW jammer causes the worst case jamming and optimal for an effective jammer. Milstein [4] has analyzed the effect of narrow-band interference on the serial search acquisition after an

interference suppression filter using transform domain processing. He has obtained analytical results for the probabilities of error in both the search and lock modes and has shown the improvement that can be gained by the use of an interference suppression filter prior to the acquisition system. In the present research, the effect of CW interference and jamming on the sequential detection code acquisition has been analyzed, for the first time, and the degradation in the acquisition performance is assessed.

7.3 EFFECT OF JAMMING ON THE CORRELATOR OUTPUT

7.3.1 CW jammer

The waveform of the received signal with the additive CW jammer for the case of no data modulation can be represented as:

$$r(t) = \sqrt{2S}\, c(t+\zeta T_c)\cos(\omega_c t + \theta_c) + \sqrt{2J}\cos(\omega_j t + \theta_j) + n(t) \tag{7.1}$$

where ω_j and θ_j are the radian frequency and the phase of the jammer waveform with J as the rms power and the rest of the symbols as defined earlier in chapter 4. The worst case CW jammer occurs when the entire power is placed in the exact coordinates of the wanted signal viz., the carrier frequency and the phase. Thus, in the worst case $\omega_j = \omega_c$ and $\theta_j = \theta_c$ and the received signal becomes:

$$r(t) = [\sqrt{2S}\, c(t+\zeta T_c) + \sqrt{2J}\,]\cos(\omega_c t + \theta_c) + n(t) \tag{7.2}$$

The correlator signal at the baseband in the presence of the CW jammer is:

$$x(t) = [\sqrt{2}A\, c(t+\zeta T_c) + \sqrt{2J}\,]\, c(t+\tau T_c)\cos(\theta_c) + n(t) \tag{7.3}$$

7.3.2 Pulse jammer

The received signal in the presence of a pulsed tone jammer waveform for the case of no data modulation can be represented as

$$r(t) = \sqrt{2S}\, c(t+\zeta T_c)\cos(\omega_c t + \theta_c) + \sqrt{J_p}\sum_{k=-\infty}^{\infty} P_J(t-kT_J)\cos(\omega_J t + \theta_J) + n(t) \tag{7.4}$$

where

J_p = peak jammer power = J/ρ

$P_J(t) = 1 \qquad 0 \le t \le \tau_J$

$= 0 \qquad$ otherwise

J = average jammer power

τ_J = pulse width

T_J = time between successive pulses

ρ = jammer duty factor = τ_J/T_J

with the rest of the symbols defined as earlier.

When the frequency difference between the desired spread-spectrum signal and the tone of the pulsed jammer is small enough ie., $\Delta\omega = |\omega_c - \omega_J| \approx 0$, then any bandlimiting of the jammer is considered negligible and the jammer carrier is assumed to be phase-locked to the desired signal. The received phase-locked jammer signal is thus given by

$$r(t) = \left[\sqrt{2S}\, c(t+\zeta T_c) + \sqrt{J/\rho} \sum_{k=-\infty}^{\infty} P_J(t-kT_J-\Delta_J)\right]\cos(\omega_c t + \theta_c) + n(t) \qquad (7.5)$$

with $0 \le \Delta_J \le T_J$ which is the random pulse delay. The correlator output with the pulse jammer can be represented as

$$x(t) = \left[\sqrt{2}A\, c(t+\zeta T_c) + \sqrt{J/\rho} \sum_{k=-\infty}^{\infty} P_J(t-kT_J-\Delta_J)\right] c(t+\tau T_c)\cos(\theta_c) + n(t) \qquad (7.6)$$

The correlator outputs in (7.3) and (7.6) contain the equivalent noise components contributed by the jammer. This signal is envelope detected and the sampled output is passed to the sequential detector.

7.4 SIMULATION OF THE JAMMERS

The CW interference or jammer was simulated assuming the worst case situation with the exact carrier frequency and phase. Thus, the equivalent additive noise on the baseband spread-spectrum signal to the correlator signal was simulated for each value of J/S. The pulse jammer at the baseband was simulated with the assumption of a constrained average power and hence, the peak power was varied for each value of the duty factor so that the average power was maintained constant. A period of 10 data bits were assumed and the pulse power was spread over the fraction of every 10×127 code chips depending upon the duty factor. For both types of jammer, the additive white Gaussian noise was added to the PN signal along with the jammer and the composite corrupted signal was fed to the correlator.

7.5 SIMULATION PERFORMANCE IN THE PRESENCE OF JAMMERS

The acquisition performance of the three variants of sequential detector has been examined in the presence of both the CW interference and pulse jammer. The mathematical models employed for the simulation of both the jammers have already been described in chapter 4. The received signal representation with jammers has been given in the previous section.

The effect of jamming on the acquisition performance was assessed differently depending

upon the type of jamming employed. For the CW jammer, the jammer-to-signal power ratio (J/S) was set at several values with the input SNR (due to Gaussian noise) varied from -10dB to -25dB. However, for the pulsed jammer, the duty factor was changed for each value of J/S (to maintain a constant average pulse power) and the performance for a range of J/S in the presence and the absence of Gaussian noise was obtained. For the pulse jammer in Gaussian noise, a typical value of $\rho = 0.1$ was chosen and the acquisition performance was obtained with the input SNR varied from -10dB to -25dB with the J/S set at several values as in the case of CW jammer. The effect of the critical duty factor (ρ^*) of the pulse jammer which maximizes the bit error rate as a function of J/S, as defined in chapter 4, was also investigated and its effect on the acquisition performance obtained.

7.5.1 Analysis of the degradation due to a CW jammer

The input SNR due to additive Gaussian noise was varied from -10dB to -25dB for a CW jammer-to-signal power ratio, J/S, which was selected to be one of six different values 5, 10, 20, 30, 40, 50 dB, and the ASN, P_d, and P_{fa} were obtained. From these results, the mean acquisition time was computed for each detector operating at normalized Wald's optimum bias in the usual way. The bias and the design SNR were set as a function of γ (for this purpose, γ was assumed to be numerically equal to the predetection SNR contributed by the Gaussian noise only) and the acquisition characteristics were then obtained. The variation of mean acquisition time, ASN and the probabilities of detection and false alarm are plotted as a function of input SNR and J/S.

7.5.1.1 Mean acquisition time

The characteristics are shown in figures 7.1-7.3 for the three types of detector. In these graphs, the mean acquisition time T_{acq} is plotted against the input SNR (denoted as γ_{in}) for various values of J/S. From these curves, it is seen that the mean acquisition time is little affected when J/S < 20dB. For J/S greater than 30dB the acquisition time starts increasing for each γ_{in}, and the minimum in the mean acquisition time which is normally observed when there is no jamming also starts to disappear. When J/S ≥ 50dB, the mean acquisition time is seen to be almost independent of the input SNR (over the range of interest) and attains a maximum value of T_{acq}. The degradation in the performance of the QLD with $Q = 32$ is also seen to be similar to the LLD (as expected) whereas for the BSD the minimum in T_{acq}, normally observed with no jamming, does not disappear completely as J/S increases but

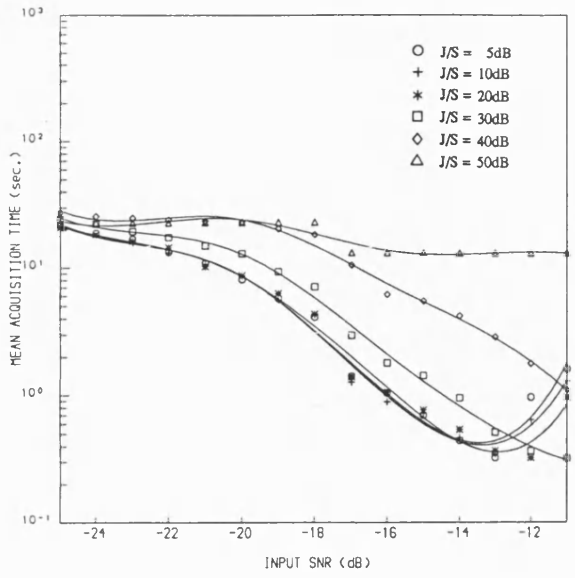

Figure 7.1 T_{acq} vs input SNR for LLD with CW jammer.

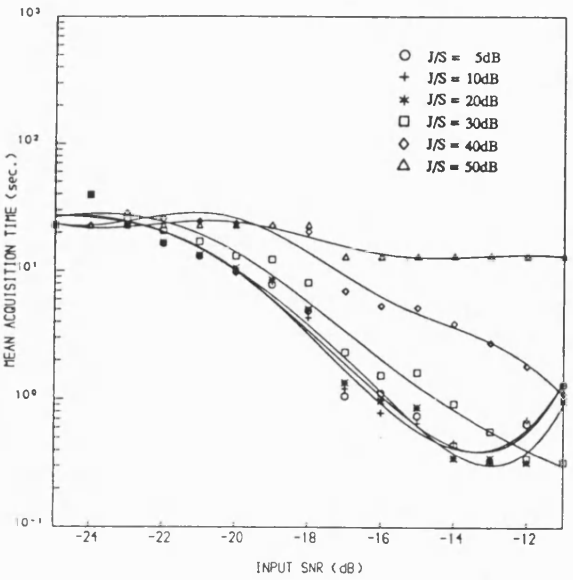

Figure 7.2 T_{acq} vs input SNR for QLD with CW jammer.

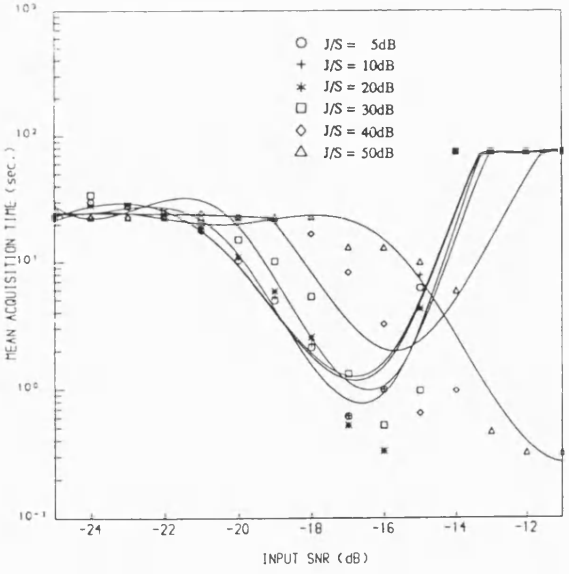

Figure 7.3 T_{acq} vs input SNR for BSD with CW jammer.

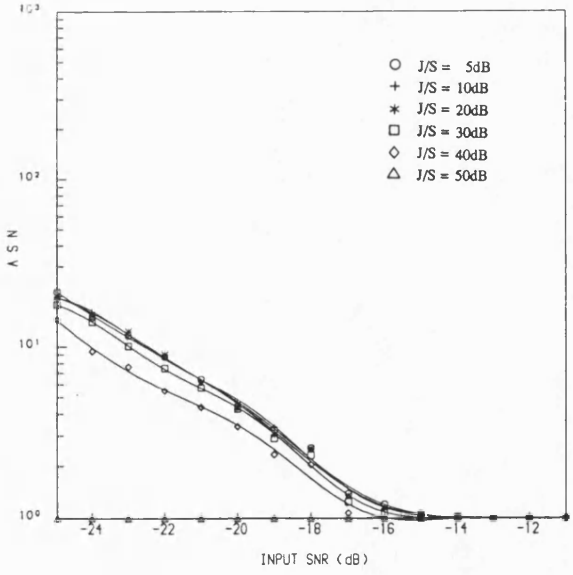

Figure 7.4 A S N vs input SNR for LLD with CW jammer.

moves slowly towards higher values of γ_{in}. At the maximum chosen value of J/S = 50dB, for BSD this minimum is seen to have moved close to γ_{in} = -10dB.

Thus, the effect of the CW jammer is seen to increase the required input SNR of the sequential detector for which the mean acquisition time is minimum, with severe degradation in the minimum mean acquisition time observed, particularly at higher values of J/S.

7.5.1.2 ASN characteristics

The variation of the ASN characteristics with J/S is shown in figures 7.4-7.6. At the lower values of γ_{in} the ASN is seen to be higher and reduces with the increasing J/S showing a systematic fall with increasing γ_{in}, for all values of J/S considered. This explains why the mean acquisition time increases even at relatively low false alarm rate in this region (figure 7.10). For J/S = 50dB, the ASN is seen to be zero which is due mainly to the saturation in the detectability causing maximum false alarms with no correct dismissals (as the computation of the ASN is based on dismissals only). Thus, in this region the reason for the increase in T_{acq} is not due to an increase in the ASN but an increase in the false alarm rate.

7.5.1.3 Probabilities of detection and false alarm

The probability of detection and the probability of false alarm are shown in figures 7.7 through 7.12 for all three detectors. In the case of both the LLD and QLD, shown in figures 7.7 and 7.8, when J/S is below 30dB, P_d is seen to decrease with the increasing γ_{in} particularly at the higher values. This is due to the fact that as the input SNR increases, the bias point of the sequential detector also increases and this has the effect of reducing P_d. However, with J/S above 30dB the P_d is almost saturated and shows no variation with γ_{in}. For the BSD as shown in figure 7.9, the probability of detection falls rapidly for J/S below 40dB and shows saturation for J/S = 50 dB throughout the range of γ_{in}.

The probability of false alarm is shown in figures 7.10-7.12 for all detectors. It is observed to reduce with increasing γ_{in} for all values of J/S. However, it shows a large increase for values of J/S above 20dB and this increase is mainly responsible for the degradation in the acquisition performance inspite of the low ASN and higher P_d in these regions.

7.5.2 Analysis of the degradation due to pulse jammer

The pulsed tone jammer was simulated over a range of duty factors and J/S values. The duty factor is represented as the fraction of time that the pulse is present over an interval of 10 data bit durations, denoted by ρ. It is assumed that the average pulse power is constrained and

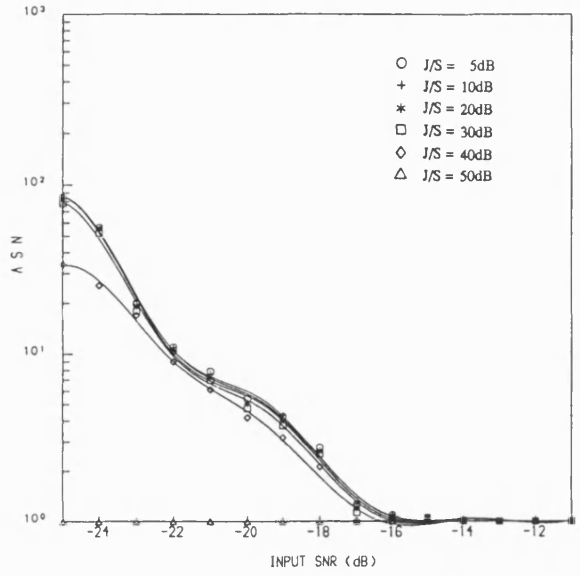

Figure 7.5 A S N vs input SNR for QLD with CW jammer.

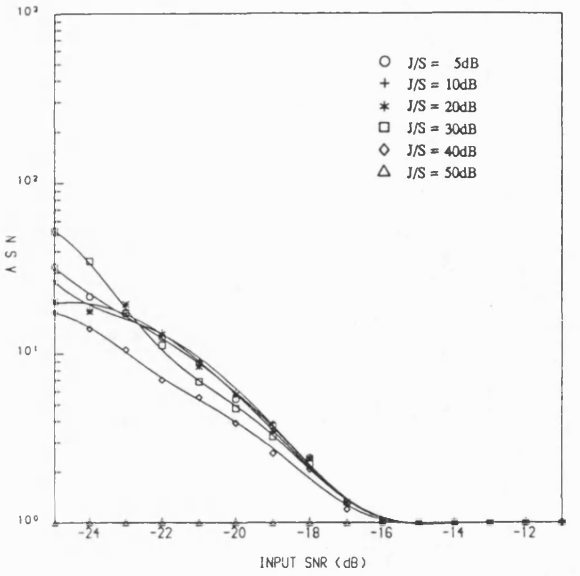

Figure 7.6 A S N vs input SNR for BSD with CW jammer.

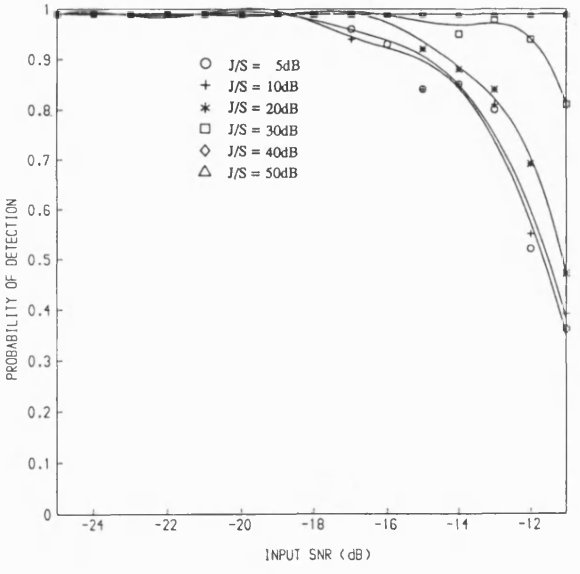

Figure 7.7 P_d vs input SNR for LLD with CW jammer.

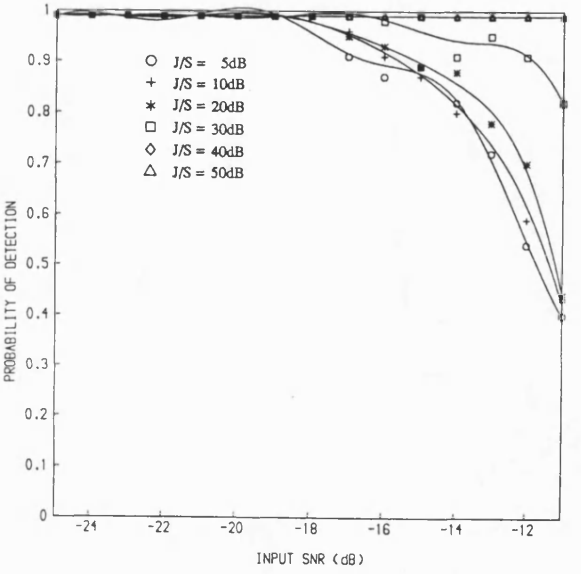

Figure 7.8 P_d vs input SNR for QLD with CW jammer.

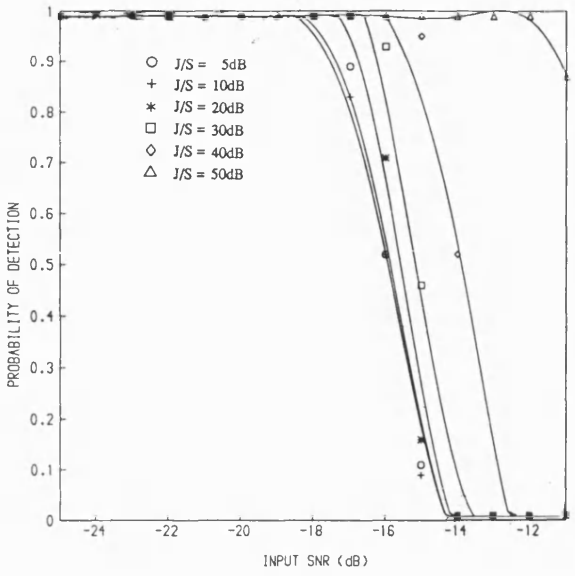

Figure 7.9 P_d vs input SNR for BSD with CW jammer.

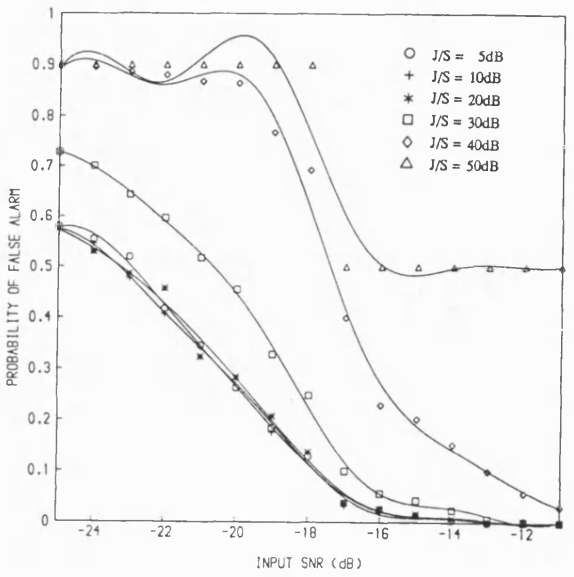

Figure 7.10 P_{fa} vs input SNR for LLD with CW jammer.

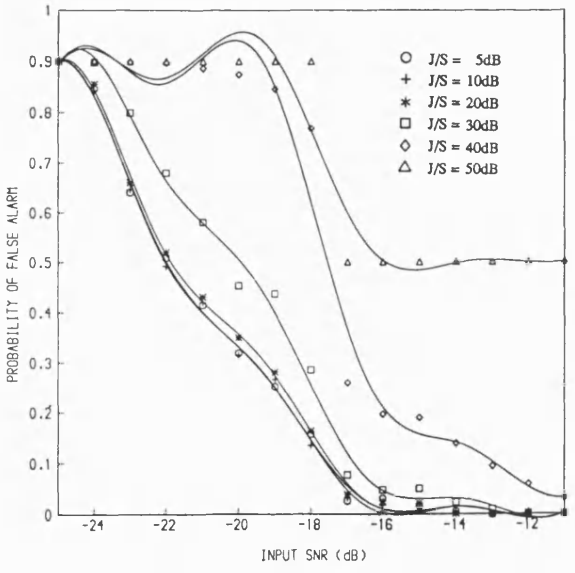

Figure 7.11 P_{fa} vs input SNR for QLD with CW jammer.

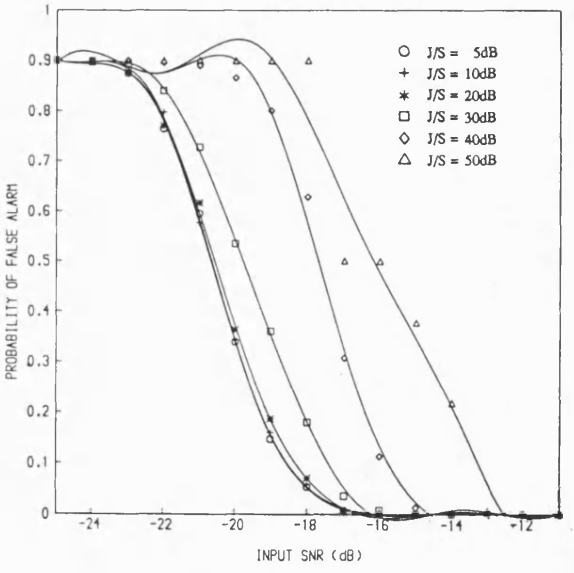

Figure 7.12 P_{fa} vs input SNR for BSD with CW jammer.

consequently the peak pulse power is varied with the duty factor, for each value of the J/S, to give the same average power. Two cases have been investigated with the pulse jammer, one in the noiseless situation and the other in the presence of Gaussian noise. For the noiseless case, the signal-to-average jammer power ratio, S/J was varied from -10dB to -25dB (equivalent to a predetection SNR of -4dB to 10dB) and the acquisition characteristics were obtained for values of ρ at 0.5, 0.1, 0.01 and 0.001. The case of continuous jamming, $\rho = 1.0$, and the critical value of $\rho = \rho^*$ for each S/J which has been defined earlier were also employed, and for all values of ρ the acquisition characteristics were obtained. For the case of the pulse jammer with additive Gaussian noise, J/S was varied for a typical value of ρ = 0.1 and the acquisition characteristics for a range of AWGN input SNR were obtained.

7.5.3 Effect of pulse jammer in noiseless case

For the noiseless case, the mean acquisition time, the ASN and the probabilities of detection and false alarm as a function of J/S and ρ have been presented and the degradation is assessed.

7.5.3.1 Mean acquisition time

The effect of the value of ρ for pulse jamming on the mean acquisition time, for J/S varied from 10dB to 25dB, is shown in figures 7.13 through 7.15 for all three detectors. (For the purpose of convenience S/J rather than J/S is used to plot this set of curves) From these results it is observed that for the case of the LLD and QLD (figures 7.13 and 7.14 respectively), the degradation in T_{acq} for a value of ρ greater than 0.1 is seen to be quite tolerable with continuous jamming ($\rho = 1.0$) showing almost insignificant degradation. However, when the value of ρ is reduced, the degradation is seen to be severe, with the worst case degradation occurring for values of $\rho = 0.01$ and lower. The critical duty factor ρ^* (in the sense of bit-error-rate) is also seen to cause a significant degradation in the minimum mean acquisition time. However, this curve is found to pass in between $\rho = 0.1$ and $\rho = 0.01$ and thus is seen to be no longer critical in the sense of mean acquisition time. For all values of ρ, the input S/J (due to jammer) at which the minimum T_{acq} occurs is observed to be relatively unchanged (which is at S/J = -13dB). For the case of the BSD, the degradation seems to be relatively tolerable even with $\rho = 0.01$ and the worst case degradation occurs with $\rho = 0.001$.

7.5.3.2 ASN characteristics

For all three types of detector, the ASN as shown in figures 7.16-7.18, is seen to fall with S/J

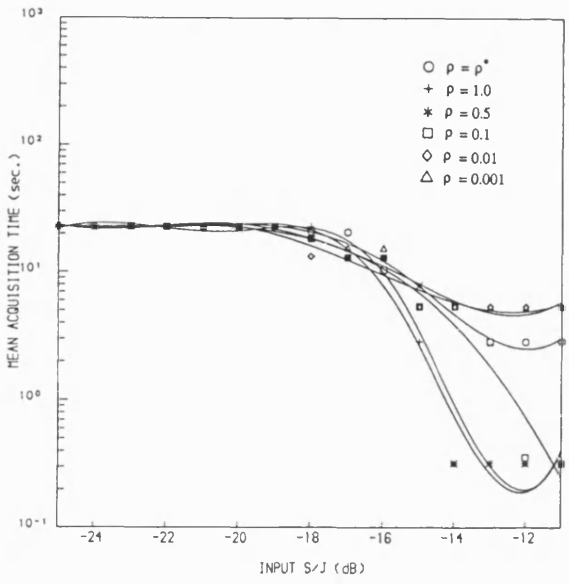

Figure 7.13 T_{acq} vs input SNR for LLD with pulse jammer in noiseless case.

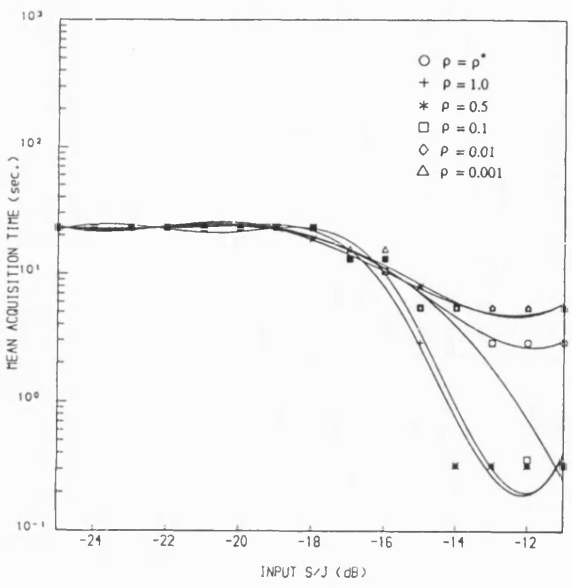

Figure 7.14 T_{acq} vs input SNR for QLD with pulse jammer in noiseless case.

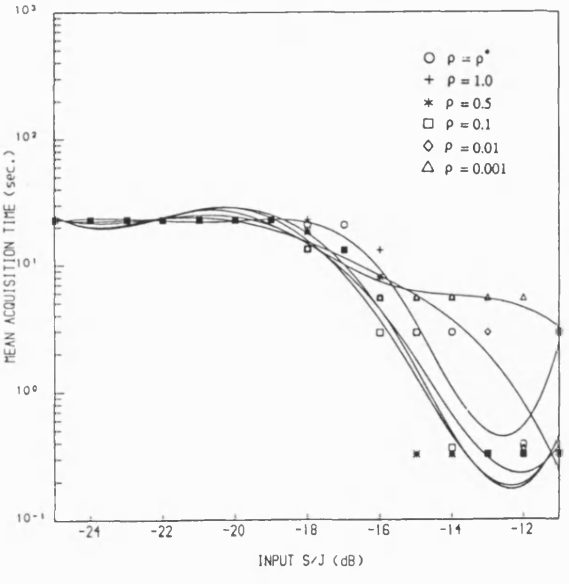

Figure 7.15 T_{acq} vs input SNR for BSD with pulse jammer in noiseless case.

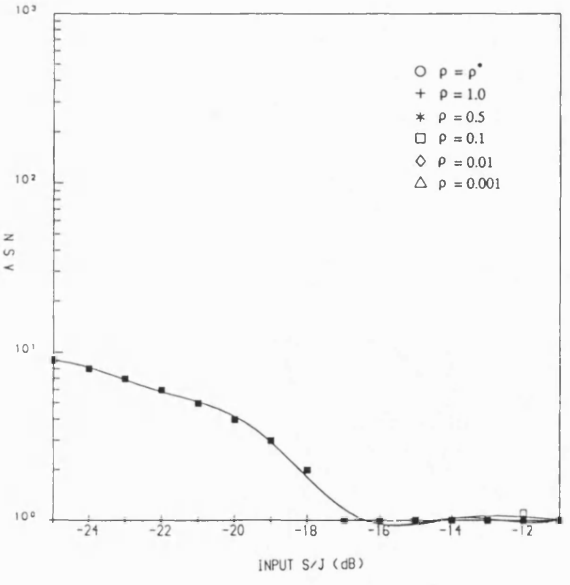

Figure 7.16 A S N vs input SNR for LLD with pulse jammer in noiseless case.

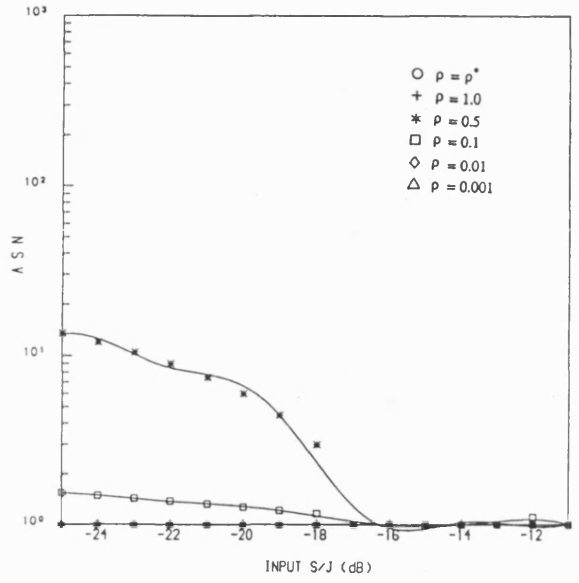

Figure 7.17 A S N vs input SNR for QLD with pulse jammer in noiseless case.

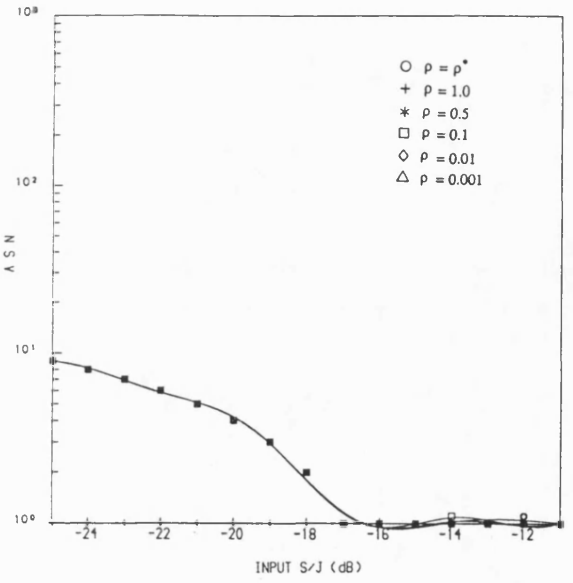

Figure 7.18 A S N vs input SNR for BSD with pulse jammer in noiseless case.

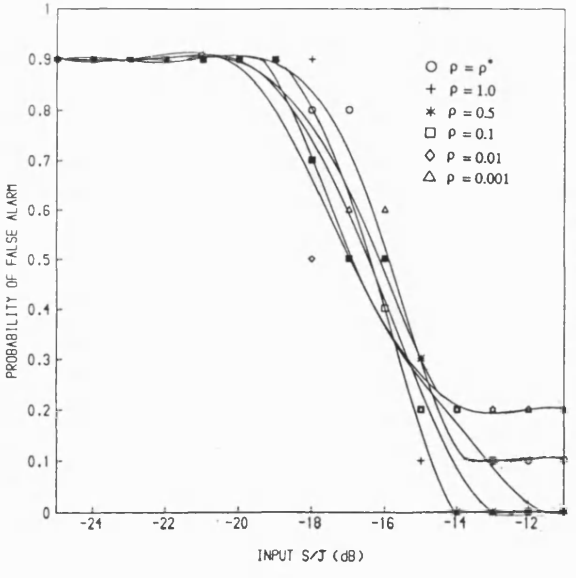

Figure 7.19 P_{fa} vs input SNR for LLD with pulse jammer in noiseless case.

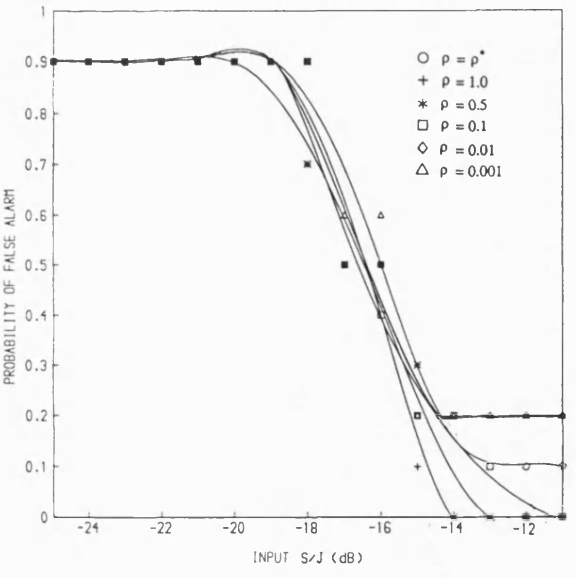

Figure 7.20 P_{fa} vs input SNR for QLD with pulse jammer in noiseless case.

for all values of ρ. However, the ASN with the continuous case (ρ = 1.0) shows zero for all values of S/J which is due to the saturation in detectability, as explained earlier, causing 100% false alarms. In the case of the QLD, for most values of ρ the ASN remains close to zero except for the case where ρ = 0.5.

7.5.3.3 Probabilities of detection and the false alarm

The probability of detection for all cases is seen to have saturated at 0.99 throughout the range of S/J for all three detectors. However, the probability of false alarm as shown in figures 7.19-7.21 show a rapid fall for all cases for the value of S/J below -15dB. When S/J is increased beyond -15dB, the P_{fa} reaches close to zero for the value of ρ less than 0.1, however, for ρ greater than 0.1 it still continues to be around 0.2. This false alarms at higher values of S/J are mainly responsible for the increased mean acquisition time at ρ greater than 0.1.

7.5.4 Effect of pulse jammer in the presence of Gaussian noise

For the case of the pulse jammer in Gaussian noise the duty factor was set at ρ = 0.1 and the input SNR, γ_{in} (due to AWGN) was varied from -10dB to -25dB for five values of J/S = 0.0, 3.0, 5.0, 8.0 and 10.0 dB (corresponding to J/S region considered above) and the acquisition characteristics were obtained. The mean acquisition time, the ASN and the probabilities of detection and false alarm are plotted as a function of input SNR and J/S.

7.5.4.1 Mean acquisition time

The variation of T_{acq} with input SNR due to Gaussian noise at various values of J/S is shown in figures 7.22 - 7.24. For the J/S less than 3dB, the mean acquisition time is found to be unaffected for the entire range of input SNR considered. However, when J/S is increased above this value, the degradation in T_{acq} starts increasing, with minimum T_{acq} reaching its maximum value when J/S is around 8dB and above. Thus, in the presence of Gaussian noise it is found that lower average pulse jammer power is tolerated than for the case with no additive Gaussian noise.

7.5.4.2 ASN Characteristics

The ASN for these cases is shown in 7.25 - 7.27 for the LLD, QLD and BSD respectively. It is observed to increase with increasing J/S, and also seen to fall with increasing input SNR. For the case of J/S around 8dB or more, the ASN is found to be zero which is once again due to the saturation in detectability which leads to all detections of the sequential detector being

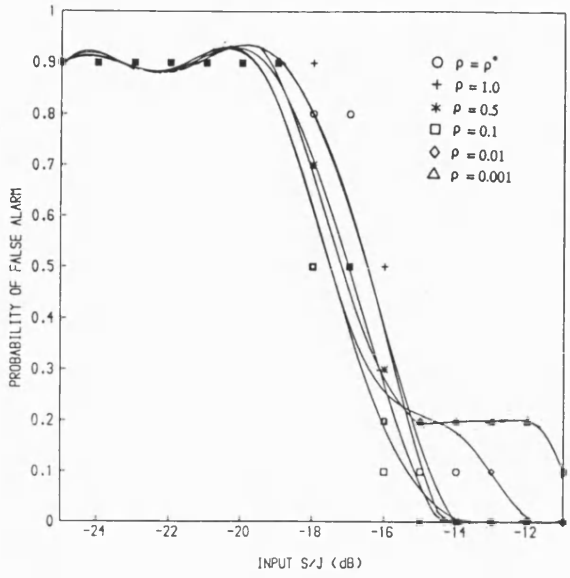

Figure 7.21 P_{fa} vs input SNR for BSD with pulse jammer in noiseless case.

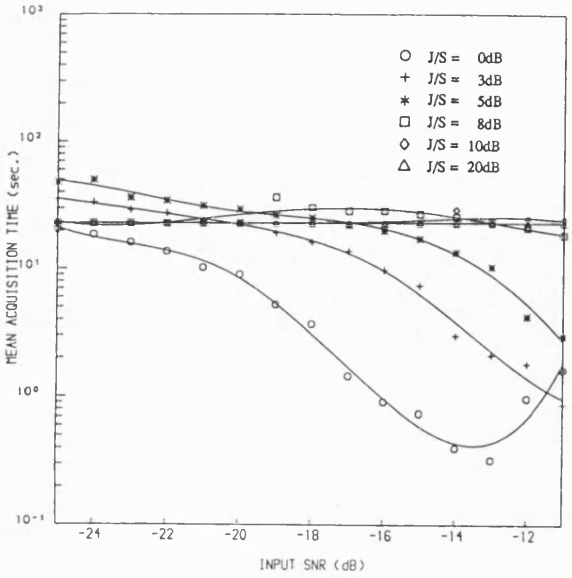

Figure 7.22 T_{acq} vs input SNR for LLD with pulse jammer in Gaussian noise.

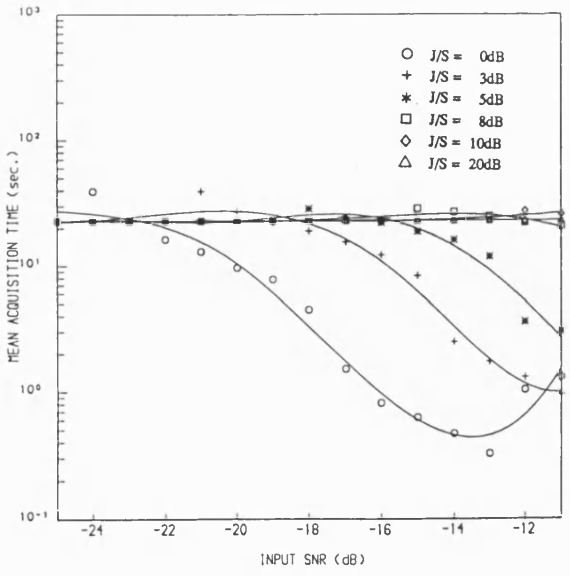

Figure 7.23 T_{acq} vs input SNR for QLD with pulse jammer in Gaussian noise.

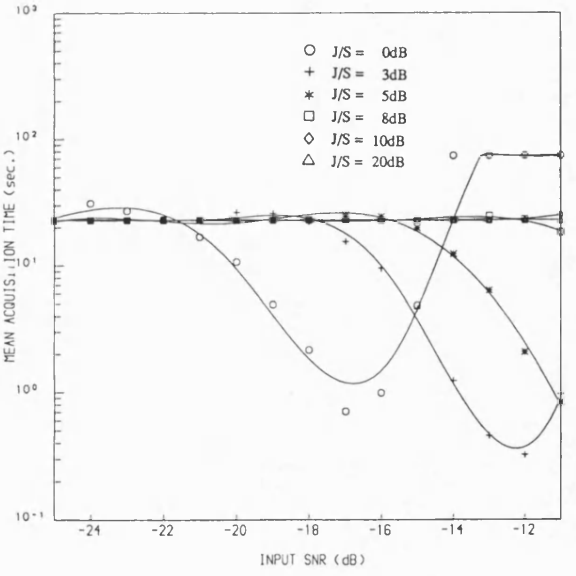

Figure 7.24 T_{acq} vs input SNR for BSD with pulse jammer in Gaussian noise.

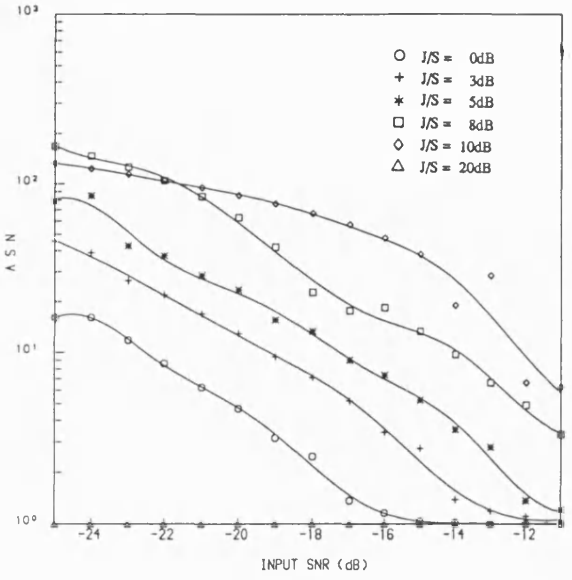

Figure 7.25 A S N vs input SNR for LLD with pulse jammer in Gaussian noise.

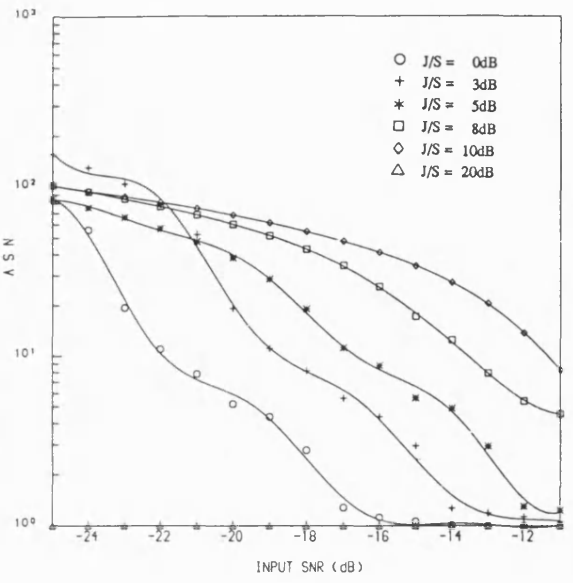

Figure 7.26 A S N vs input SNR for QLD with pulse jammer in Gaussian noise.

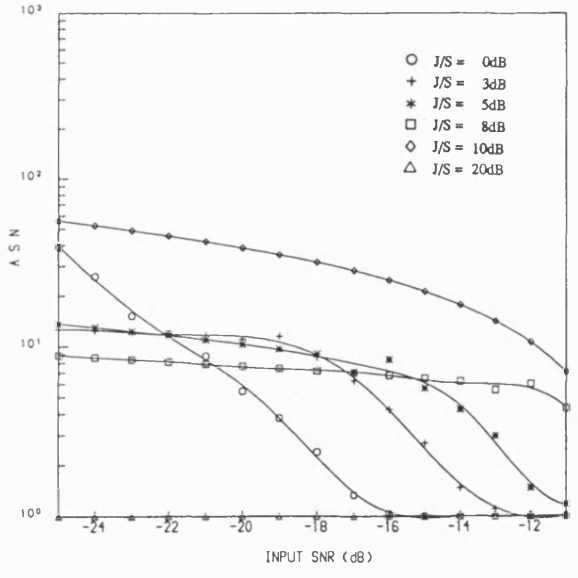

Figure 7.27 A S N vs input SNR for BSD with pulse jammer in Gaussian noise.

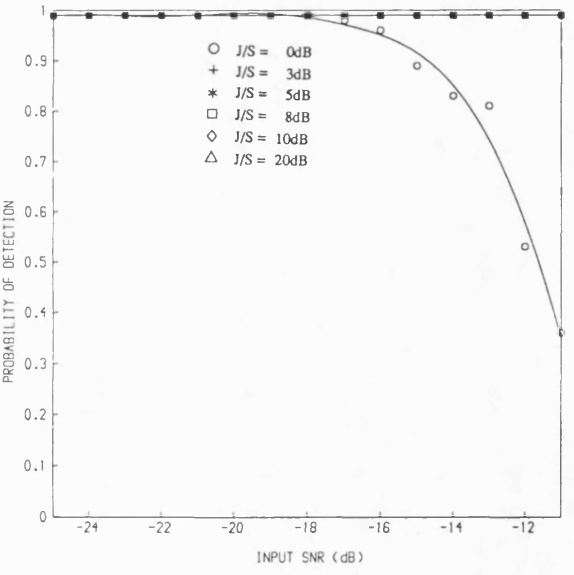

Figure 7.28 P_d vs input SNR for LLD with pulse jammer in Gaussian noise.

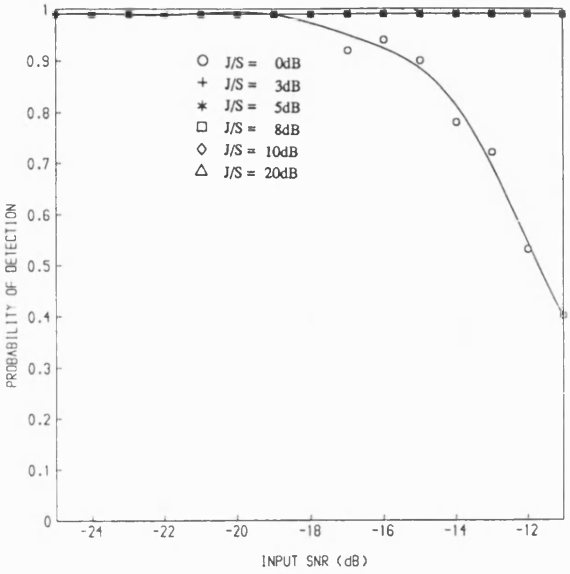

Figure 7.29 P_d vs input SNR for QLD with pulse jammer in Gaussian noise.

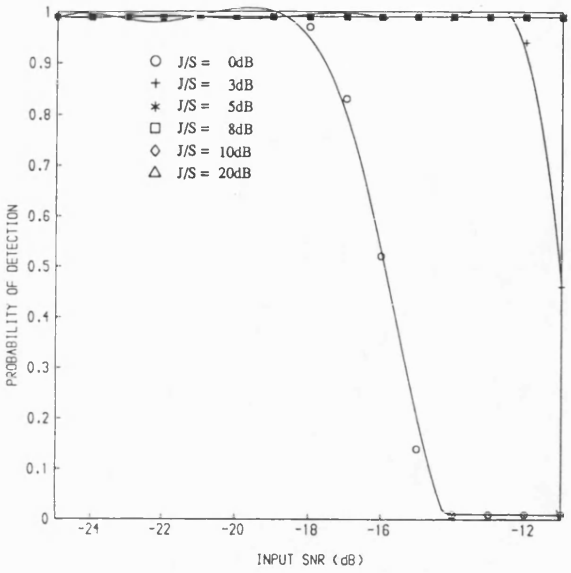

Figure 7.30 P_d vs input SNR for BSD with pulse jammer in Gaussian noise.

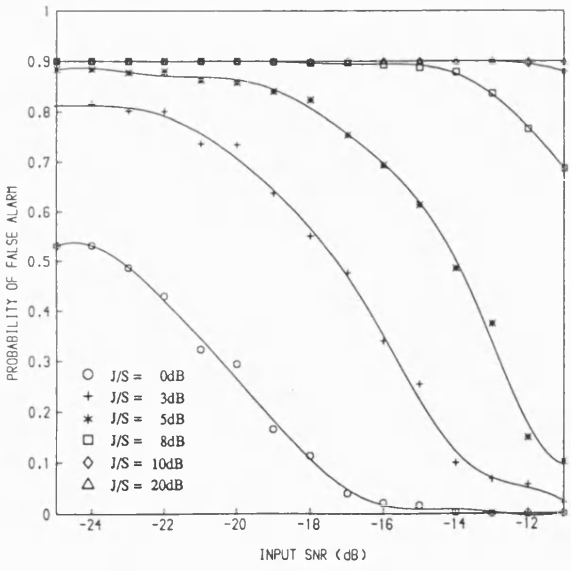

Figure 7.31 P_{fa} vs input SNR for LLD with pulse jammer in Gaussian noise.

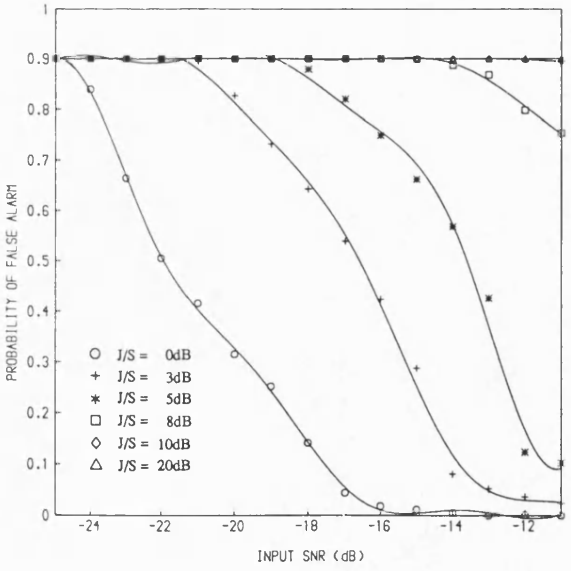

Figure 7.32 P_{fa} vs input SNR for QLD with pulse jammer in Gaussian noise.

false alarms.

7.5.4.3 Probabilities of detection and the false alarm

From figures 7.28 - 7.30 for the LLD, QLD and BSD respectively, P_d is found to saturate for the higher values of J/S. However, when J/S is less than 3dB, there is a systematic fall in P_d particularly at higher values of input SNR. The probability of false alarm is shown in figures 7.31 - 7.33 for all three types of detector. It is found that the increasing S/N reduces P_{fa}. However, it is also observed that the P_{fa} increases significantly with the increasing J/S and this causes the increase in the mean acquisition time as discussed above.

7.5.5 Conclusion

In conclusion, for the case of the CW jammer with J/S < 20dB the T_{acq} is little affected whereas for J/S < 30dB the degradation in T_{acq} is considered to be tolerable, however, when J/S > 30dB the degradation increases monotonically with J/S. The pulse jammer, in the noiseless situation causes a tolerable degradation in T_{acq} when the duty factor ρ is less than 0.1. There is a systematic degradation when ρ is less than 0.1, causing maximum degradation at $\rho = 0.01$ and lower. When Gaussian noise is added to the pulse jammer, the degradation is tolerable as long as J/S < 3dB for $\rho = 0.1$ (compared with 30dB for CW jammer) and increases sharply for J/S > 3dB reaching saturation around 8dB. Thus, in the presence of Gaussian noise, the pulse jammer with a properly chosen duty factor can significantly degrade the acquisition performance compared to the CW jammer. It is also observed that the pulsed jammer with the duty factor approaching 1.0 (which is the case of continuous jamming) behaves similar to the CW jammer at values of J/S less than 5dB.

PART II: PERFORMANCE OF THE SERIAL SEARCH PN CODE ACQUISITION TECHNIQUES - A COMPARATIVE EVALUATION

This part of the chapter, presents a comparative performance analysis of three serial-search PN code acquisition techniques using Monte-Carlo computer simulation method. The three serial-search code acquisition techniques considered are: i) the non-coherent sequential detector ii) a digital matched filter and iii) the non-coherent fixed-dwell detector. The detector operating characteristics for both the single dwell detector and the digital matched filter were obtained through simulation and their acquisition performances were assessed.

The acquisition performance of these detectors was then compared with the sequential detector for the case of no data modulation over a predetection SNR range of -4dB to 10dB.

In chapter five, the dependence of the mean acquisition time and the mean dismissal time on the bias (and the related design SNR) of the log-likelihood function and the detector thresholds was assessed and the acquisition performance of the three configurations of the sequential detector were compared for the same predetection SNR range. In this section of the chapter, the critical dependence of the mean acquisition time on the system parameters is analyzed for both the digital matched filter and the single-dwell detector and the optimization of these parameters to obtain minimum mean acquisition time is obtained. In particular, the optimization of the detector threshold and the dwell-time with the input SNR is obtained for both the digital matched filter and single-dwell detector and their acquisition performance is compared with that of the variable-dwell-time sequential detector with ideal log-likelihood function (LLD) over an equivalent range of input SNR.

In addition, the theoretical performance of a single-dwell-time serial-search acquisition system has also been evaluated numerically using a two-dimensional optimization of the mean acquisition time with the threshold, the dwell-time and the input SNR. The simulated acquisition performance of the single-dwell detector is compared to the theoretical performance, and is shown to be in a close agreement.

7.6 SERIAL SEARCH TECHNIQUES - A GENERIC COMPARISON

Several code acquisition techniques which are commonly used for the acquisition of spread-spectrum signals have been discussed in chapter 2 based on their detector type and the type of search algorithm. The majority of these techniques are identified under the search strategy used, namely, serial-search techniques, maximum-likelihood techniques and sequential estimation. The performance of all these techniques depend critically on many system parameters and the input SNR range of interest.

Even though a great deal of research on spread-spectrum communication has been focussed on the performance analysis of various code acquisition techniques [5-10], it is difficult to obtain an exact closed form solution for the mean acquisition time of many acquisition schemes. The general approach to the analysis using signal flow graph techniques developed in [6,9] are seen to provide general expressions for the probability density function of the acquisition time. These analyses, however, require the complete knowledge of the generating function which depends on transition probability distributions of the underlying discrete time

Markov process which describes the acquisition process. In many cases, obtaining the probability distribution of the acquisition time in closed form is quite difficult, and simulation is required to evaluate them before these analytical results can be used. In particular, obtaining the probability density functions of the various random times involved in sequential detection are quite difficult and this was the motivation for the simulation of sequential detector. In this chapter, various Gaussian approximations employed in deriving the mean acquisition time of a single-dwell detector and a digital matched filter have also been considered and an exact performance assessment using Monte-Carlo simulation is carried out.

As discussed in chapter 2, the serial-search is effected by using either a passive correlator or an active correlator. In passive correlation, typically, a SAW tapped delay line or a digital matched filter is employed and the decisions are made at a very high rate (normally at a multiple of the chip rate). The matched filters thus, exhibit a high rejection rate of the wrong code epochs resulting in a rapid acquisition in good SNR conditions. However, since the uncertainty region is normally assumed to be equal to the code length, it suffers from an increased hardware complexity with increasing code length as the correlator length is proportional to the code length. Further, although the acquisition time is normally quite good for moderate to high SNRs, it increases rapidly at low SNRs due to an excessive increase in the miss detections and the false alarm rate since the decision SNR (per-cell basis) becomes smaller. In fact, in the large number of wrong code epochs L-1 (where L is the code length) detected, many of them can result in false alarms due to high noise.

In active correlation, which uses either fixed or variable dwell-time integration, the correlator output is integrated over a period of time which is the dwell-time τ_d, and the decisions are made using a simple threshold detector with threshold η. The samples of the correlator outputs are generally sufficiently decorrelated by sampling at a rate $R_s = 1/T \leq B$, where B is the predetection filter bandwidth, and this provides a longer integration time giving high decision SNR resulting in more reliable decisions. However, as the decision rate is slower compared to the matched filter, it takes much longer to acquire lock (in relatively good SNR conditions). These techniques work well at lower SNRs because of the longer integration time, but, the mean acquisition time is dependent on the various system parameters such as threshold, dwell-time and the search strategy itself, and increases with the worsening of SNR although generally not as rapidly as the matched filter.

Generally, simulations were employed to characterize the sequential detector within a limited range of system parameters and the SNR range of interest [11-12]. A comparison of fixed-dwell detector with the variable-dwell detector and the optimum sequential detector using a numerical approach was presented by Braun [13]. This approach, however, assumes approximations suitable for low SNRs. Further, it assumes truncated sequential tests and the characteristic function is obtained by numerically solving the complex transcendental equations from which the *pdf* of the average sample number is obtained. The results show a comparable improvement in the average dwell-time of this variable-dwell-time detector over a fixed-dwell-time detector at large SNRs, but almost as good as the optimum sequential detector at low SNRs.

In this chapter, comparison is carried out with the serial-search techniques, with a particular emphasis on the sequential detection. The three techniques considered are: i) a non-coherent sequential detector, ii) a digital matched filter and iii) a non-coherent single-dwell detector. The detector operating characteristics of a single-dwell detector and a matched filter were obtained through simulation and the acquisition performance of each detector is evaluated using the analytical results. The dependence of the mean acquisition time on the critical design parameters viz., threshold, dwell-time and input SNR has been assessed and the optimization of these parameters to achieve the minimum mean acquisition time is achieved, and the optimum performance of all three detectors compared.

7.7 DETECTOR THEORY

This section presents the basic theory and analysis of the single-dwell detector and the matched filter considered. Both techniques have received considerable attention recently and a number of models have been produced. Since the statistics of the decision variable depends not only on the input signal but also on the correlator signal and the detector type, in case of many models, a number of assumptions were made as to simplify the analyses to obtain closed form solutions. In this section the analytical results used to compute the acquisition performance of the digital matched filter and the single-dwell detector are presented.

7.7.1 Digital matched filter

The digital matched filter correlates the incoming signal with the *a priori* known code sequence matched to the incoming sequence and makes the decisions on the basis of each incoming chip (or the cell). Normally, the incoming signal is stored in a shift register which is updated on the arrival of every new chip. This is compared against the stored local replica

of the code sequence and the correlation measure is generated which is tested in a threshold detector. As the local code replica matches with the incoming sequence once in a period of code length, the correlation output produces a sequence of impulses at an interval of the code length. For a code sequence of length L, with a chip rate $f_c = 1/T_c$, the envelope of the correlation impulses consists of a train of triangular impulses occurring at an interval L/f_c. Because of the presence of noise on the input signal, these matched filter output samples are corrupted and give rise to miss detections and false alarms.

Let T_v be the time interval in which a false alarm occurring can affect the v^{th} impulse at an instant t_v and P_{dv} be the probability of detecting this correlation impulse. If P_d is the probability of detection of a correlation impulse, n_{fa} is the false alarm rate of the detector with T_{vr} as the false alarm verification time, then the mean acquisition time T_{acq}, is given by [10]:

$$T_{acq} = \frac{L}{2f_c}\left[P_{d1}+\sum_{v=1}^{\infty}(2v+1)P_{dv+1}\prod_{\mu=1}^{v}(1-P_{d\mu})\right] \tag{7.7}$$

where P_{dv} and T_v are given by

$$P_{dv} = P_d \exp(-n_{fa}T_v) \tag{7.8}$$

$$T_v = \min(T_{vr}, [v+0.5]\,L/f_c) \tag{7.9}$$

Using an approximate analysis based on the Gaussian assumption of the decision statistic applicable to the low input SNRs, assuming a practical case of the correlator length M, $1 \ll M \ll L$ for a very long code length L, the probability of detection P_d and the probability of false alarm P_{fa} are given by:

$$P_d = Q(\gamma_d,\beta_d) \equiv \int_{\beta_d}^{\infty} x \exp[-1/2(x^2+\gamma_d^2)]I_o(\gamma_d x)\,dx \tag{7.10}$$

$$P_{fa} = \exp\left\{-1/2\frac{c}{1+\gamma_c G_o(p)}\right\} \tag{7.11}$$

where $Q(\gamma_d,\beta_d)$ is the Marcum Q-function with γ_d and β_d given by

$$\gamma_d = \sqrt{2M\gamma_c\frac{(1-|p|)^2}{1+\gamma_c G_1(p)}} \tag{7.12}$$

$$\beta_d = \sqrt{\frac{c}{1+\gamma_c G_1(p)}} \tag{7.13}$$

and

$$G_i(p) = \begin{cases} p^2 & i=1 \\ 1-2|p|+2p^2 & i=0 \end{cases} \tag{7.14}$$

$$c = 2\frac{R_o^2}{N_o}MT_c \tag{7.15}$$

where c is the normalized threshold, γ_c is the decision *SNR* on a per-cell basis, MT_c is the correlation time (in seconds) and p is the code phase offset.

In the analysis of matched filter using unified theory by Polydoros and Weber [7], exact expressions of a noncoherent I-Q matched filter detector were derived using series solutions. In this, recursive relations were employed to enable the numerical computation of the detector probabilities as the closed form expressions were found to be difficult to obtain.

In the present work, detection probability P_d and false alarm n_{fa} of a digital matched filter was obtained by simulation and the mean acquisition time was computed using (7.7). The series computation in (7.7) has been carried out by employing the convergence of the series which results in the significant reduction in computation time. Appendix 7.1 presents the derivation of the series sum.

7.7.2 Single-dwell detector

The analytical expression for the mean acquisition time, T_{acq}, for the simple case without Doppler, is obtained quite easily either by a heuristic approach or by using a Markov chain model of the acquisition process. The expression derived analytically using Markov chain model is given by the relationship [5]:

$$T_{acq} = \frac{(2-P_d)(1+KP_{fa})}{2P_d} q\tau_d \tag{7.16}$$

where P_d and P_{fa} are the detector decision probabilities and K is the false alarm penalty factor ($T_{vr} = K\tau_d$ sec). The envelope detector output is sampled at a rate $1/T \leq B$ which ensures sufficient sample decorrelation, so that the samples can be treated as independent identically distributed random variables (iid). Then the detector probabilities can be approximated with a Gaussian assumption of the integrator output (for a large number of samples) and given by:

$$P_{fa} = Q[\beta] \tag{7.17}$$

$$P_d = Q[(\beta-\sqrt{B\tau_d}\gamma)/\sqrt{1+2\gamma}] \tag{7.18}$$

where $Q[x]$ is the Gaussian probability integral with β given by

$$\beta = (\eta-B\tau_d)/\sqrt{B\tau_d} \tag{7.19}$$

For a given P_d, P_{fa}, γ, B and η the dwell-time τ_d can be determined easily. However, a basic design problem is to choose the optimum threshold and the dwell-time that provides the minimum mean acquisition time for a given input SNR. Since P_d, P_{fa} are functions of the threshold, the dwell-time and γ and moreover, they are transcendentally related, in this work, these equations are solved numerically as a two dimensional optimization problem and the simulated performance is compared with the numerical results.

7.8 SIMULATION OF THE DETECTORS

Serial-search code acquisition using the three types of detector, was simulated using Monte-Carlo simulation. The direct sequence pseudo-noise signal was simulated by a PN code of length $L = 127$, chip rate $f_c = 1/T_c = 100$ kchips/sec. The channel was assumed to be corrupted by additive white Gaussian noise (*AWGN*) and the corrupted spread-spectrum signal was used with each type of the detectors simulated. For each detector and for each test carried out on the correlator output, the incoming code sequence with a random starting phase was used and the search was carried out by examining the correlator output corresponding to each code cell. Checks were made to record missed detections and false alarms. Whenever either an out-of-sync or a false alarm was observed, the code phase was updated and the test continued. On the successful detection or miss detection, the codes were reset with a new random starting phase and the test was repeated. For each set of system parameters and for each detector, 100 tests were carried out and the number of miss detections and the false alarms were recorded. For the given system parameters, these tests achieve P_d with an accuracy of 1×10^{-2} and the P_{fa} with an accuracy of 1×10^{-4}.

For the case of serial-search using a digital matched filter, the correlator length was assumed equal to the uncertainty region (one code length, $L = 127$) and the search was carried out with one code chip per cell. The input to the matched filter was first passed through a one-bit A/D converter or a hard quantizer and the quantized input signal was fed to the one-bit digital matched filter simulated. The simulation characteristics were obtained for a range of thresholds and input SNRs.

Single-dwell serial-search was simulated for the same input signals without a hard quantizer and the detector operating characteristics (OCF) were determined with respect to the threshold and the dwell-time varied for different input SNRs. The mean acquisition time was then computed and the three dimensional acquisition characteristics were obtained.

7.9 ANALYSES OF ACQUISITION PERFORMANCE

The acquisition performance of all three detectors was obtained for various thresholds, dwell-times and input SNRs From this, the optimization of the various system design parameters was obtained and the optimum performance of the each detector compared.

7.9.1 Sequential detector

For the convenience of comparison with the other two detectors simulated, the main

acquisition characteristics of the sequential detector at Wald's optimum bias, b_1, and the non-optimum bias, b_2, have been reproduced in figures 7.34 and 7.35 which show the variation of ASN and the T_{acq} with γ for the $T_u = 5.0$ and $T_l = -5.0$ for all three variants of the detector. As already observed, the ASN of the sequential detector is seen to increase with the decreasing γ and T_l. However, when biased at $b = b_1$, it is always less than that with the non-optimum bias b_2. The optimum γ at which the minimum T_{acq} occurs (which is considered as the design SNR, γ_{dsn}) is also found to be around 7dB for the QLD and at this operating point T_{acq} = 0.5sec which is minimum. For the BSD, it is around 10dB (at a non-optimum bias, b_2) with a minimum T_{acq} almost same as the QLD. The performance of the QLD is observed to be quite close to that with the LLD whereas the BSD shows better performance at lower SNRs at the optimum bias.

7.9.2 Digital matched filter

The performance of the matched filter is dependent on the threshold and the input SNR as these two parameters can drastically affect the operating characteristics of the detector. The simulation has been used to obtain these characteristics for a threshold range of 0.0 to 0.4 for an input SNR in the range of -10dB to -28dB (predetection SNR γ range of -7dB to 11dB). From the P_d and n_{fa} obtained from the simulation, T_{acq} has been computed using (7.7)-(7.9).

7.9.2.1 Probability of detection and false alarm rate

The variation of the probability of detection P_d and the false alarm rate n_{fa} with the threshold and the input SNR is shown in the figures 7.36 and 7.37. At each input SNR, the P_d decreases with increasing threshold. When the input SNR is reduced, it falls drastically even at much lower thresholds showing a clear upper bound in the maximum attainable detection probability in a noisy condition. The false alarm rate also falls with the threshold, however, there is a saturation seen in the n_{fa} as the SNR is decreased, which is due to the hard limiting employed.

7.9.2.2 Mean acquisition time

The mean acquisition time of the matched filter is shown in figure 7.38 and passes through a minimum with respect to the threshold. The reason for this is that at lower threshold values both P_d and n_{fa} are high and it is the n_{fa} which is dominant in lengthening T_{acq}. At the higher threshold values n_{fa} and P_d are very low and it is the low P_d which affects T_{acq}. Thus, the false alarms at the lower threshold and the miss detections at the higher threshold show

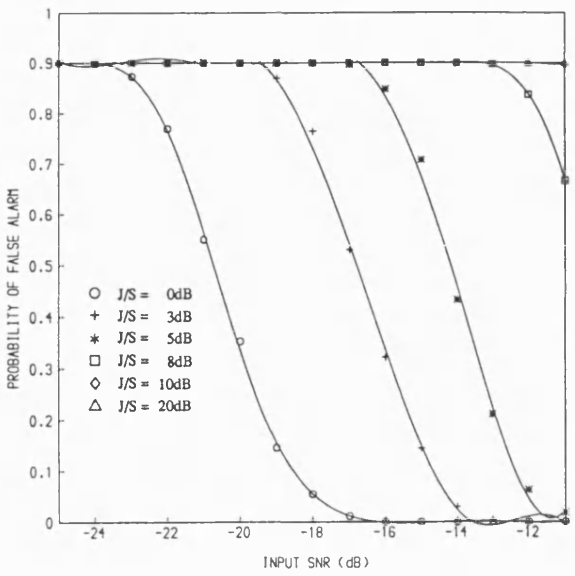

Figure 7.33 P_{fa} vs input SNR for BSD with pulse jammer in Gaussian noise.

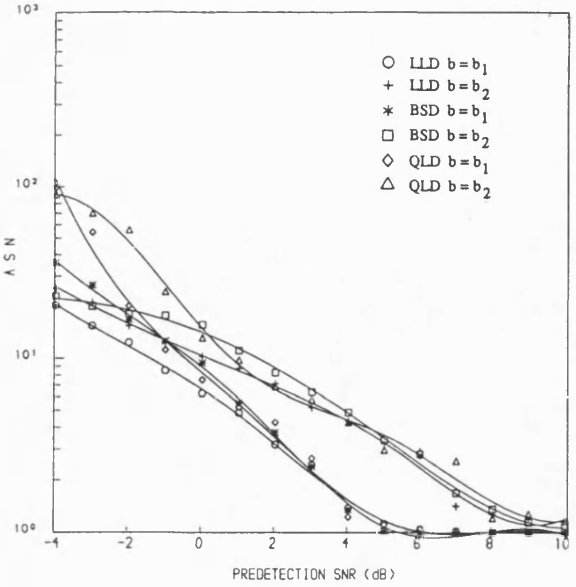

Figure 7.34 A S N vs γ for LLD, BSD and QLD with $b = b_1$, $b = b_2$ at $T_u = 5.0$ and $T_l = -5.0$.

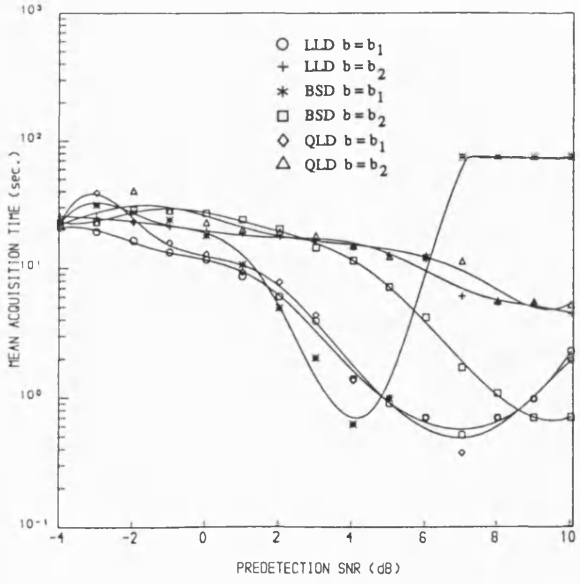

Figure 7.35 T_{acq} vs γ for LLD, BSD and QLD with $b = b_1$, $b = b_2$ at $T_u = 5.0$ and $T_l = -5.0$.

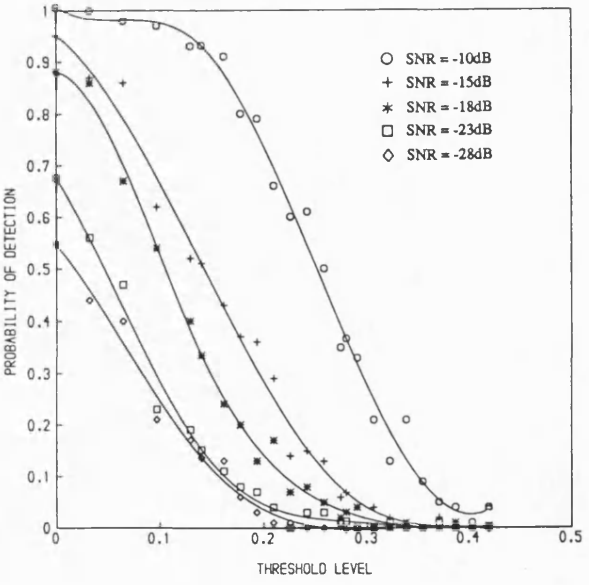

Figure 7.36 P_d vs threshold of a digital matched filter with input SNR = -10, -15, -18, -23 and -28dB.

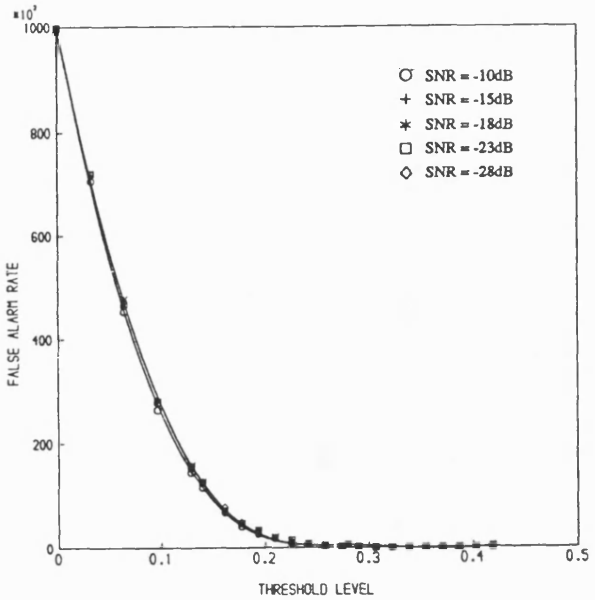

Figure 7.37 False alarm rate (n_{fa}) vs threshold (η) of a digital matched filter with input SNR = -10, -15, -18, -23 and -28dB.

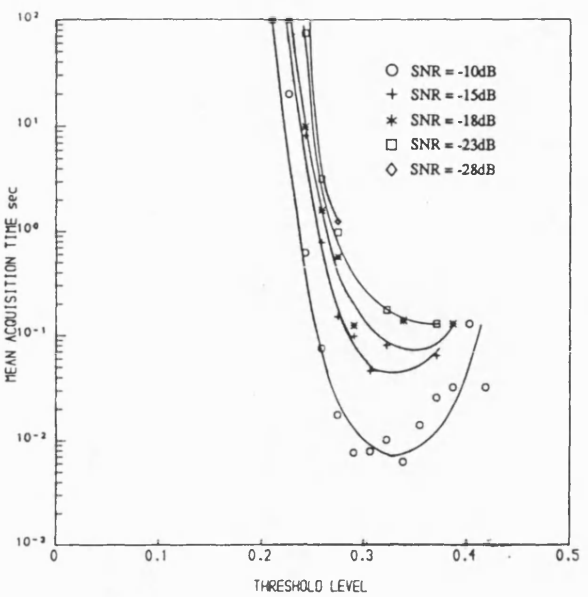

Figure 7.38 T_{acq} vs threshold (η) of a digital matched filter with input SNR = -10, -15, -18, -23 and -28dB.

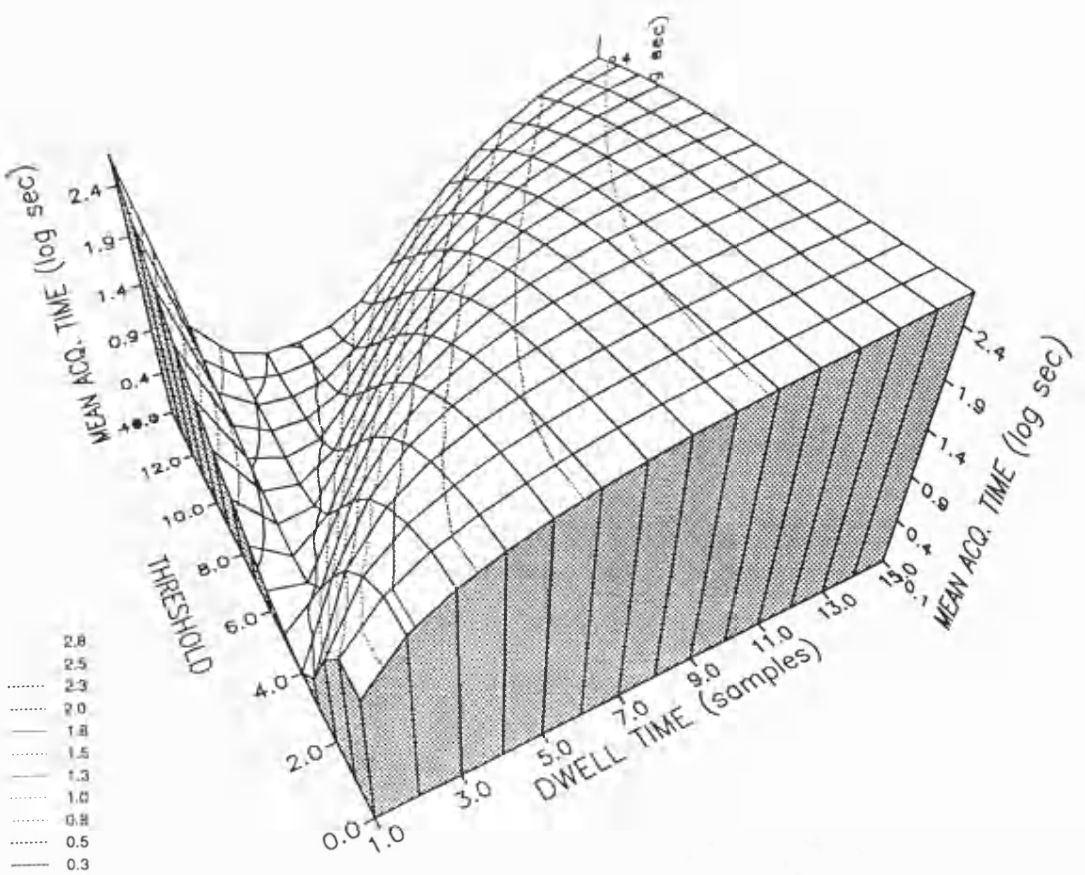

Figure 7.39 T_{acq} vs threshold and the dwell time of a single-dwell detector at input SNR = -15dB with K = 100; numerical results for a narrow range of the dwell time and threshold.

greater influence on the T_{acq}. The optimum threshold is seen to be a function of input SNR and is lower when the matched filter is designed to work at lower SNRs. However, in the region of SNRs considered here, these optimum thresholds are quite close as the P_{fa} (and hence n_{fa}) saturates to a high value and this quickly saturates T_{acq}. The optimum threshold is close to 0.3 for SNR = -15dB whereas it is moved to around 0.28 with SNR = -28dB. The optimum threshold is also quite sharp and this shows the greater sensitivity of T_{acq} with the optimum threshold.

It is also worth noting that the optimum performance of the matched filter is obtained at a much lower probability of detection (always < 0.2) and the false alarm rate n_{fa} is also quite low (< 100). This implies that the optimum detector always performs on the tail end of the probability distributions of both signal and noise. The minimum mean acquisition time with the input SNR (from figure 7.38) shows that the best case minimum acquisition time is close to 1×10^{-2} sec at input SNR = -10dB, but this worsens to 1.2sec when the input SNR falls to -28dB (for the design parameters considered). Considering the fact that the digital matched filter employs one chip per cell for search, the acquisition times are nearly twice when half chip per cell is employed. Further, the acquisition time at lower SNRs has been found to be governed by the accuracy of P_d which is 1×10^{-2} for the 100 runs considered in the present simulation (from the statistical confidence level, the accuracy of the probabilities is still one order less). However, with increased accuracy the T_{acq} is still worse (for example, with 1000 runs the minimum T_{acq} at SNR = -28dB has been found to be close to 4.5sec). This in turn demonstrates the extreme sensitivity of the matched filter al low SNRs.

7.9.3 Single-dwell detector

The acquisition performance of the single-dwell detector depends on the threshold η, dwell-time τ_d, and the predetection SNR γ. The acquisition performance using numerical evaluation as well as the detector characteristics obtained through simulation are presented and compared below.

7.9.3.1 Numerical evaluation

A three dimensional acquisition characteristic was obtained numerically and is shown in figure 7.39 and 7.40 for two different ranges of the dwell-time and threshold for a false alarm penalty factor $K = 100$. These figures show variation of the T_{acq} with η and τ_d for an input SNR at -15dB (γ = 7dB) with the logarithm of T_{acq} represented on the vertical axes. The acquisition characteristics show that T_{acq} passes through a minimum both with respect to τ_d

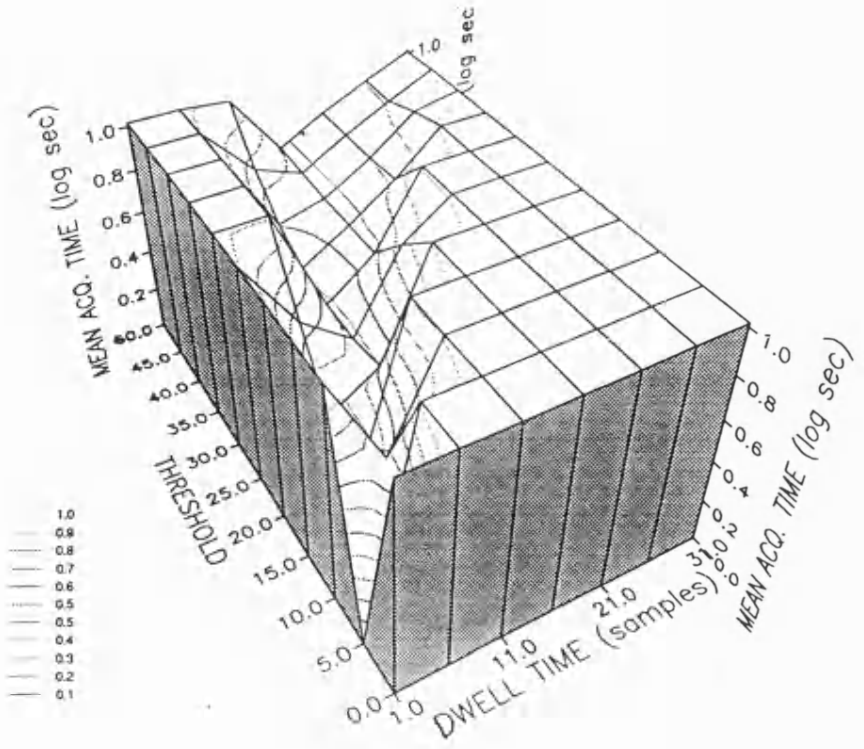

Figure 7.40 T_{acq} vs threshold and the dwell time of a single-dwell detector at input SNR = -15dB with K = 100; numerical results for a wider range of threshold and dwell time (corresponding to simulation).

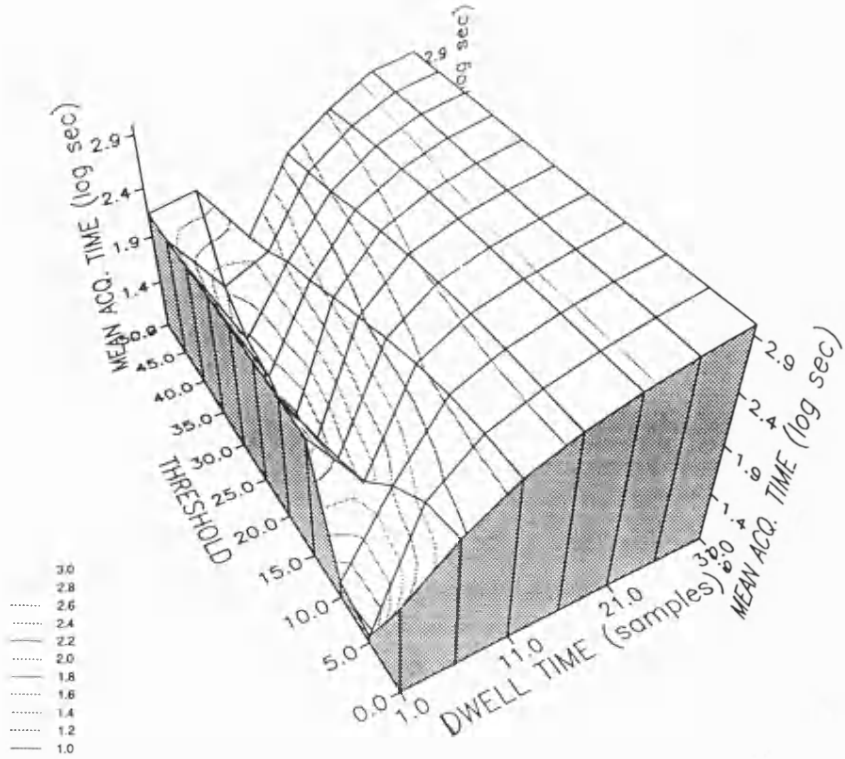

Figure 7.41 T_{acq} vs threshold and the dwell time of a single-dwell detector at input SNR = -15dB with K = 100; simulated characteristics.

and threshold. The minimum T_{acq} with respect to τ_d is due to the fall in P_d at lower integration times (τ_d) and when τ_d is long, P_d reaches saturation and the acquisition time becomes directly proportional to the dwell-time. At the higher values of threshold, T_{acq} is also higher due to increase in the miss detections. Eventhough P_d can be increased by increasing τ_d at these thresholds to achieve a minimum in T_{acq}, this cannot provide the global minimum in T_{acq} as the increasing τ_d can directly increase the T_{acq}. However, when the threshold η is decreased P_d starts increasing even at a lower value of τ_d and the minimum T_{acq} moves in the direction of lower values of threshold. Although it appears, at first instance, that the minimum T_{acq} can be decreased by lowering both η and τ_d, both P_d and P_{fa} start saturating soon, and then the T_{acq} is solely determined by the false alarms. Thus the optimum value for the threshold also exists which determines the global minimum in conjunction with the optimum τ_d. The threshold in combination with the dwell-time determine the optimum detector probabilities (for a given SNR) which results in the global minimum in T_{acq}.

As shown in figure 7.39 (for a narrow range of the parameters), the curves show a clear barrier for the lower values of τ_d and the higher values of η which are due to the rapidly vanishing P_d that causes total miss detections. A similar barrier at the higher values of the τ_d and the lower values of the threshold can also be observed. In figure 7.40 similar characteristics are shown for a much wider range of the parameters with the peak values of the T_{acq} corresponding to both the barriers truncated. This truncation was employed to highlight the lower T_{acq} regions as the T_{acq} at the barriers is extremely high.

In addition to the above characteristics, a three dimensional acquisition characteristic has also been obtained by varying both the input SNR (from -10dB to -30dB) and the dwell-time for a fixed threshold set at 5.0 with $K = 100$ and is shown in figure 7.42. From this characteristics, it can be observed that an optimum dwell-time exists for all the SNRs for a given threshold. However, this optimum dwell-time increases with the decreasing SNR (and also with the increasing threshold) and this causes the minimum T_{acq} to increase with the worsening of SNR. For example, minimum T_{acq} is close to 0.4sec at SNR = -10dB while it is more than 10sec for SNRs less than -25dB at the threshold value considered. The global minimun in T_{acq} corresponding to each input SNR has been used to compare with the acquisition performance of the sequential detectors.

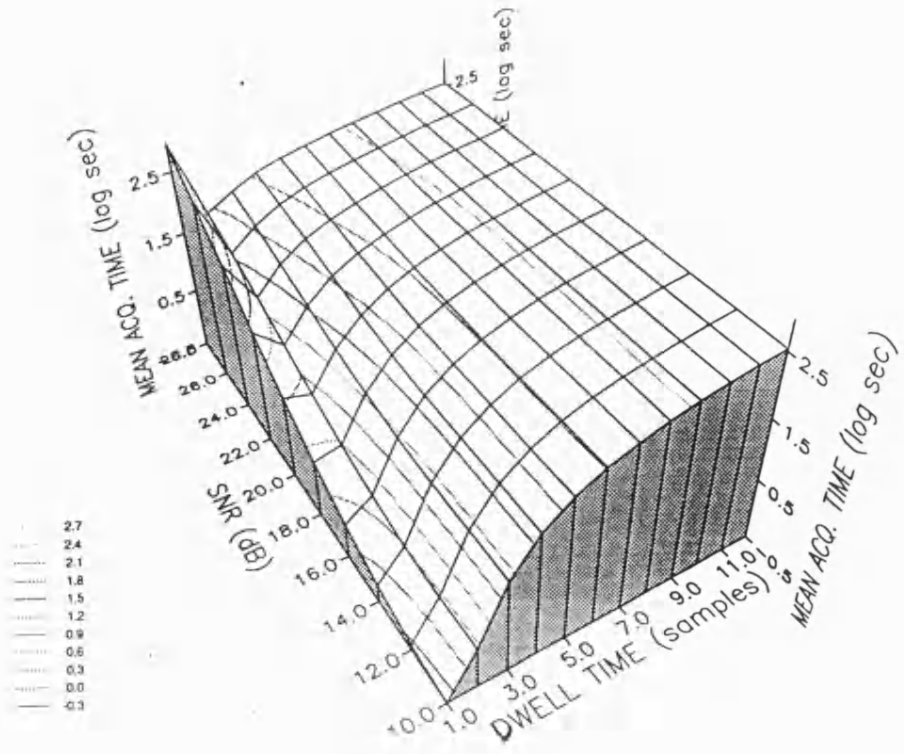

Figure 7.42 T_{acq} vs input SNR and the dwell time of a single-dwell detector at threshold = 5.0 with K = 100; numerical results.

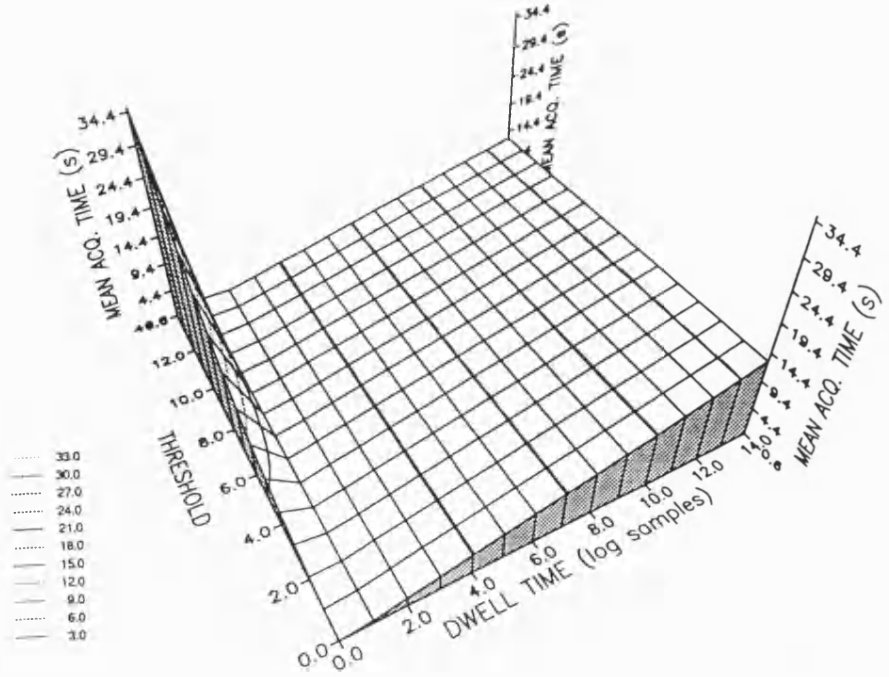

Figure 7.43 T_{acq} vs threshold and the dwell time of a single-dwell detector at input SNR = -15dB with K = 1; numerical results for a wide range of the dwell time and threshold.

7.9.3.2 Simulated characteristics

The single-dwell detector has also been simulated and the simulated detector characteristics have been obtained from which the acquisition performance is computed and shown in figure 7.41 for an input SNR of -15dB. The simulation was carried out using the same ranges of dwell-time and threshold as shown in figure 7.40. The simulation also displays characteristics which are similar to the numerically evaluated analytic results (for the range of parameters considered) and shows both the barriers. However, the T_{acq} at these barriers is controlled by the accuracy of the probabilities obtained through simulation using a limited number of runs (100) and thus are not pronounced. T_{acq} also has an optimum value with respect to the threshold which is, for example, around 5.0 at the optimum $\tau_d \approx 1.3$ *msec* (close to 1 sample) for an input SNR = -15dB. The minimum T_{acq} at this SNR is found to be around 0.88sec which is comparable to that of the matched filter in the worst case situation.

The characteristics of the single dwell-detector have also been obtained for various values of K in the range of 1 to 100. Figures 7.43 and 7.44 show the characteristics obtained numerically for two ranges of the parameters with $K = 1$ and figure 7.45 shows the simulated characteristics computed for the lowest value of $K = 1$. These curves show the optimum with respect to the dwell-time, however, the optimum with respect to the threshold is considerably suppressed due to the higher values at the barriers. The global minimum in T_{acq} corresponding to each SNR has also been obtained with $K = 10$ and used to comapare with the acquisition performance of the sequential detectors and the digital matched filter.

7.10 PERFORMANCE COMPARISON

Figure 7.46 shows the comparison of the optimum mean acquisition times of the three serial-search detectors for the input SNR range from -10dB to -30dB. For this comparison, the SNR optimization characteristics of BSD (biased appropriately at low SNRs) and QLD shown in figures 5.29 and 5.28 in chapter 5 are used. From these characteristics, showing the performance of the three detectors operating at their optimum design parameters, the digital matched filter shows a very good performance at medium to higher SNRs when compared with the single-dwell and the sequential detectors. However, when the input SNR is decreased the performance of all the detectors show a downward trend, *with the performance of the matched filter falling at a much faster rate.* This renders the matched filter difficult to operate in the lower SNRs typically less than -25dB. The quantized log-likelihood detector (QLD) is found to work well at the input SNR close to design SNRs when biased optimally.

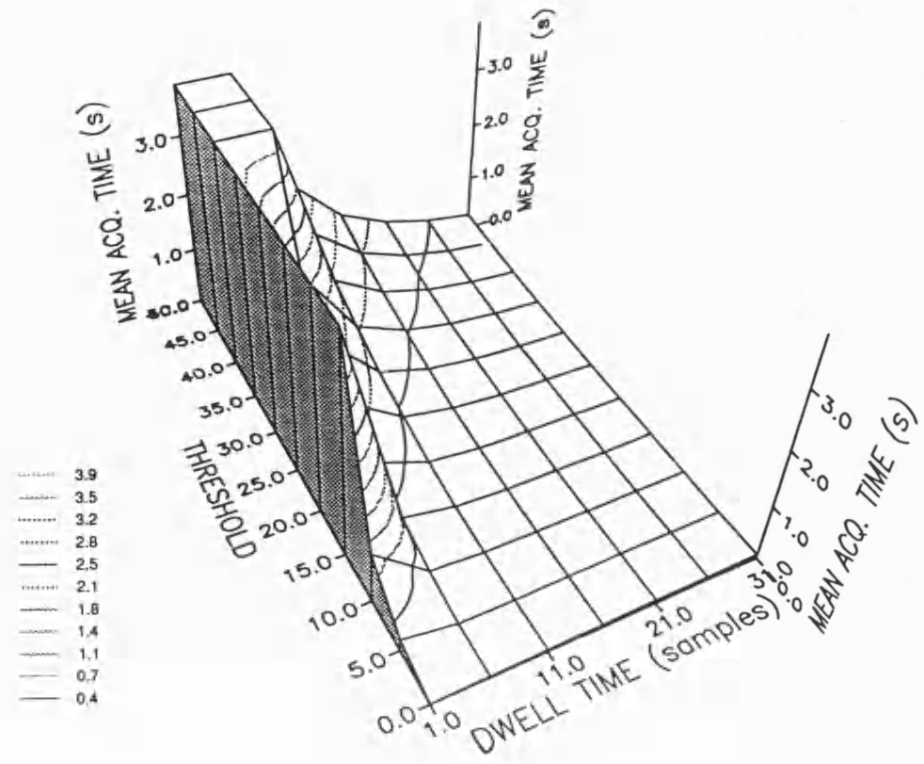

Figure 7.44 T_{acq} vs threshold and the dwell time of a single-dwell detector at input SNR = -15dB $K = 1$; numerical results (corresponding to simulation).

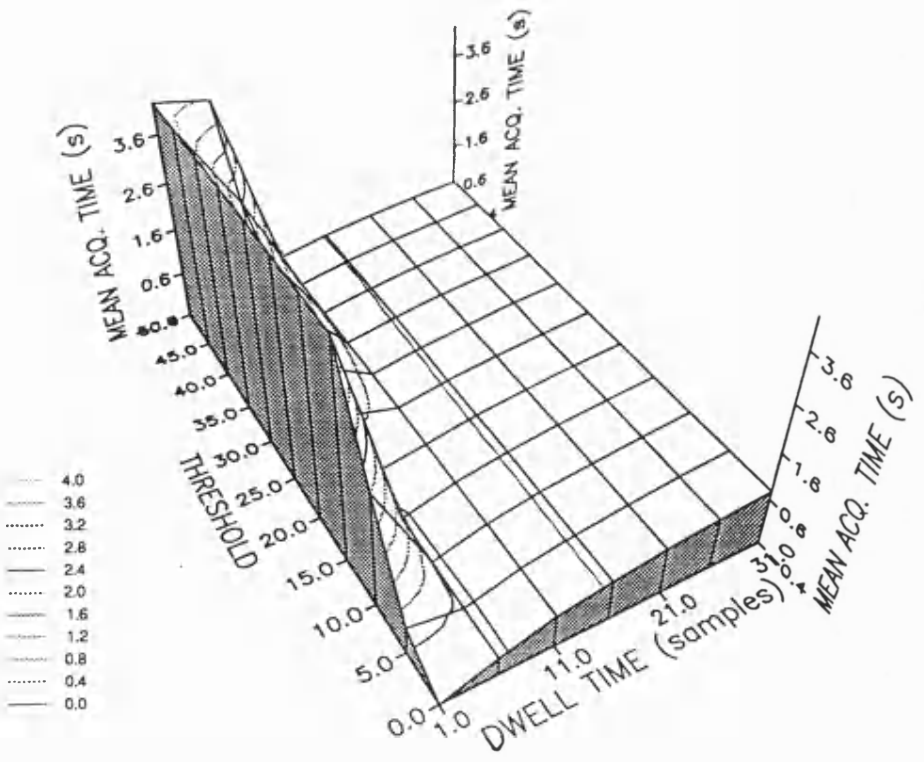

Figure 7.45 T_{acq} vs threshold and the dwell time of a single-dwell detector at input SNR = -15dB with $K = 1$; simulated characteristics.

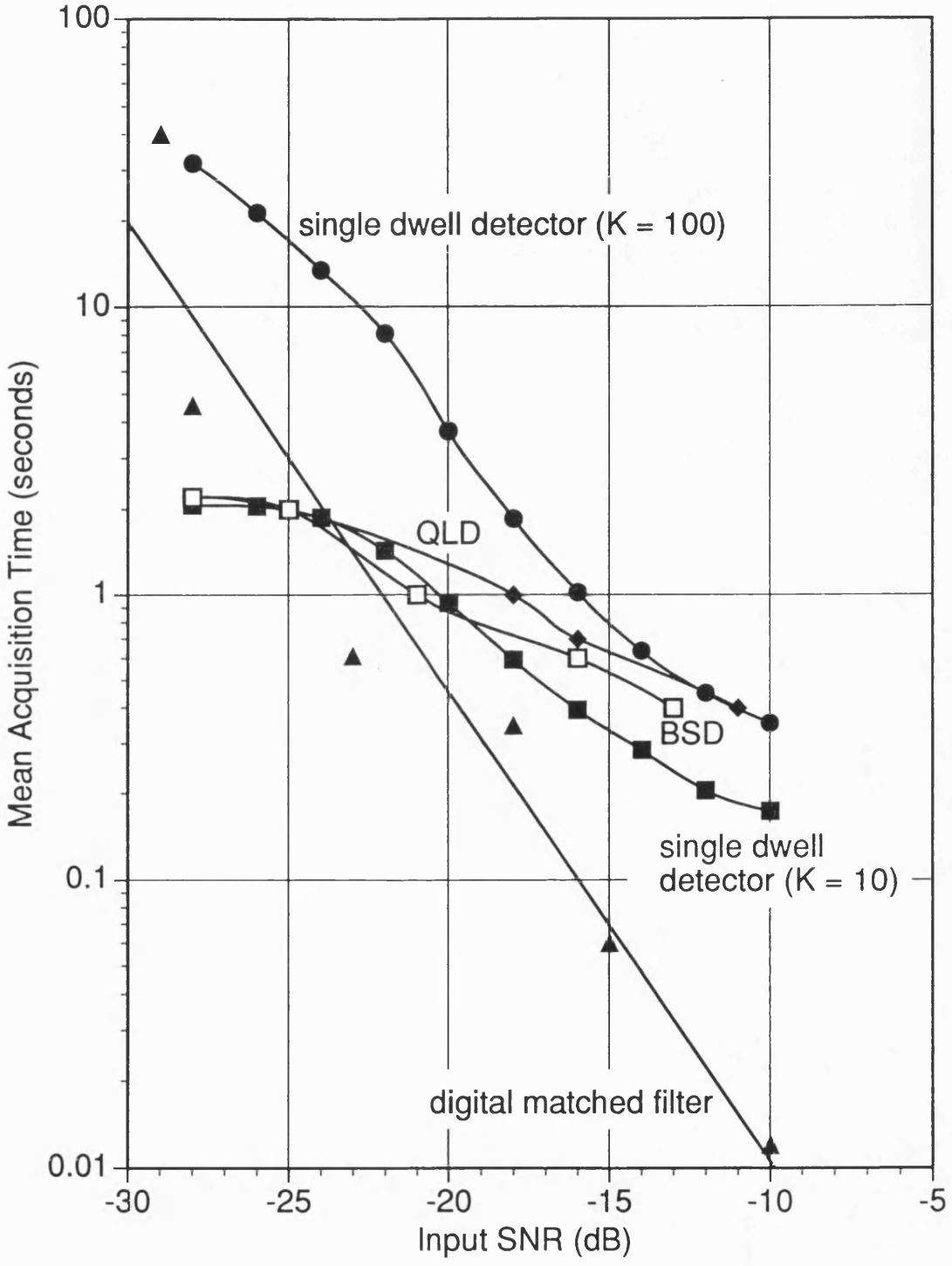

Figure 7.46 Comparison of optimum mean acquisition performance of log-likelihood sequential detector, digital matched filter and single-dwell detector.

However, the biased square law detector (BSD), shows a better low SNR performance at a non-optimum bias. The QLD has achieved minimum T_{acq} close to 0.5sec with optimum design SNR at 7dB. Although the design SNR is different for the BSD (which is 10dB), it also achieves minimum T_{acq} of the same order.

The digital matched filter, however, needs to be optimized at an optimum threshold for each SNR and the optimum threshold is quite sharp. The single-dwell detector needs both the dwell-time and the threshold to be optimized for better performance at each input SNR. The minimum acquisition time is determined by the best combination of P_d and P_{fa} and this influences both the threshold and dwell-time when the input SNR is varied. At lower thresholds the minimum T_{acq} is fully determined by the false alarms (as the effect of lowering threshold completely saturates the detector probabilities). At higher thresholds, increasing dwell-time saturates the detector probabilities and then directly increases T_{acq} .

When compared at a moderate input SNR at -15dB, the single-dwell detector ($K = 100$) has a minimum T_{acq} = 0.88sec whereas for the matched filter T_{acq} is around 0.06sec which shows the superiority of the matched filter. The sequential detector at an equivalent predetection SNR (around 7dB) produces an acquisition time of around 0.5sec. Though the single-dwell detector with $K = 10$) appears to have better performance than with $K = 100$, for the equivalent false alarm penalty time $T_P = 100msec$ used to obtain the performance of the sequential detectors and the matched filter, a comparison of the performance of the single-dwell detector with $K = 100$ is considered to be more appropriate. When the SNR is very poor, for example at an input SNR = -25dB, the matched filter has quite a poor performance (close to 4sec with increased accuracy of P_d). The single-dwell detector (with more than 10sec for $K = 100$) appears to be the worst. However, it shows more than 2sec for $K = 10$ which is better than the matched filter, but is still considered to be poor when compared against the sequential detector, particularly the BSD which produces less than 2sec when appropriately biased. For SNRs less than -25dB the matched filter rises rapidly showing the worst performance when the sequential detector can still perform the best.

7.11 CONCLUSIONS

The acquisition performance of the sequential detector in the presence of CW jammer and the pulse jammer for the case of no data modulation has been analyzed. The results show that when the average pulse power is constrained, the pulse jammer with a suitably selected duty factor causes more degradation than the CW jammer.

The acquisition performance of the sequential detector in Gaussian noise has also been compared with a single-dwell detector and a digital matched filter using Monte-Carlo simulation. The critical dependence of the acquisition time on the system parameters has been examined for both the single-dwell detector and the matched filter, and the optimization of these parameters to result in minimum mean acquisition time has been achieved. The optimized performances of the three detectors have been compared and their merits and demerits assessed. As a result of these comparisons, the sequential detector has been seen to perform better than both the matched filter and the single-dwell detector at a low SNR. The matched filter was particularly poor in the low SNRs, even though it has superior performance at high SNRs.

Although the use of the Monte-Carlo simulation is fully justified for the case of sequential detector, the approximate and precise analytical solutions for the acquisition performance of the single-dwell detector and the matched filter systems can provide easier solutions sometimes. However, the equivalent detector characteristics obtained through the simulation of these detectors provide a more realistic comparison and also provide better insight into the optimum operation of the all three detectors.

7.12 REFERENCES

1) S.W. Houston, "Modulation techniques for communication, Part I : Tone and noise jamming performance of spread-spectrum M-ary FSK and 2, 4-ary DPSK waveforms", NAECON'75, pp 51-58, June 10-12, Dayton, Ohio, USA.

2) M.K. Simon *et al*, *Spread spectrum communications*, Vol I and II, Computer science press, Maryland, USA, 1985.

3) E.W. Siess and C.L. Weber, "Acquisition of direct-sequence signals with modulation and jamming", IEEE Jou. on Sel. Areas in Comm., vol. sac-4, no. 2, pp 254-272, March 1986.

4) L.W. Milstein, "Interference suppression at aid acquisition in direct-sequence spread-spectrum communications", IEEE Trans. on Comm. vol. 36, no. 11, pp 1200-1207, November 1988.

5) J.K.Holmes and C.C.Chen, "Acquisition performance of PN spread-spectrum systems" IEEE Trans. on Comm. vol. com-25, no. 8, pp 778-783, August 1977.

6) A.Polydoros and C.L.Weber, "A unified approach to serial-search code acquisition- Part I: General theory", IEEE Trans. on Comm. vol. com-32, no. 5, pp 542-549, May 1984.

7) A.Polydoros and C.L.Weber, "A unified approach to serial-search code acquisition- Part II: A matched filter receiver" IEEE Trans. on Comm. vol. com-32, no. 5, pp 550-560, May 1984.

8) A.Polydoros and M.K.Simon, "Generalized serial-search code acquisition: The equivalent state diagram approach", IEEE Trans. on Comm. vol. com-32, no. 12, pp 1260-1268, December 1984.

9) V.M.Jovanovic, "Analysis of strategies for serial-search spread-spectrum code acquisition- Direct approach" IEEE Trans. on Comm. vol. 36, no. 11, pp 1208-1220, November 1988.

10) M.Pandit," Mean acquisition time of active and passive correlation acquisition systems for spread spectrum communication systems", IEE Proc. Pt. F, vol. 131, no. 7, pp 742-750, December 1984.

11) R.F.Cobb and A.D,Darby, "Acquisition performance of simplified implementations of the sequential detection algorithm", NTC'78, PP 43.4.1 - 43.4.7, December 4-6, 1978, Birmingham, AL.

12) K.V.Ravi and R.F.Ormondroyd, "Comparison of the acquisition performance of biased square law and quantized log-likelihood sequential detectors for PN acquisition" IEEE International Symposium on Spread Spectrum Techniques and Applications, Symposium Proceedings, pp 53-58, September 24-26,1990, London, UK.

13) W.R.Braun, "Comparison between variable dwell and fixed dwell-time PN acquisition algorithms", ICC'81, pp 59.5.1 - 59.5.5, Denver, CO, 1981.

APPENDIX 7.1

Computation of the acquisition time of a digital matched filter

The acquisition time of the digital matched filter has been computed by using (7.7) to (7.9). A straightforward computation of the series generated by the probabilities of detection of the successive correlation impulses which are denoted as ν^{th} impulse in (7.7), leads to a significantly long computing time particularly at lower probability of detection (P_d) and higher false alarm rate (n_{fa}). However, a series summation using the convergence properties of arithmetic-geometric series can be applied and this provides accurate and faster results. The derivation for the series summation is provided below:

The expression for T_{acq} given by (7.7) can be rewritten as:

$$T_{acq} = \frac{LP_{d1}}{2f_c}\left[1+\sum_{\nu=1}^{\infty}(2\nu+1)\frac{P_{d\nu+1}}{P_{d1}}\prod_{\mu=1}^{\nu}(1-P_{d\mu})\right] \tag{A.1}$$

From the definition of the ν^{th} detection probability given by (7.8) and (7.9), $T_\nu = T_{vr}$ for all correlation impulses with $(\nu+0.5)L/f_c \geq T_{vr}$. If the number of correlation impulses within the verification time T_{vr} are denoted by M, which is given by the integer part of $[T_{vr}/(LT_c)]$, then the series of detection probabilities for a given n_{fa} satisfy the following inequalities:

$$P_{d1} > P_{d2} > P_{d3} > \cdots\cdots > P_{dM} \tag{A.2}$$

$$P_{M+1} = P_{M+2} = P_{M+3} = \cdots \tag{A.3}$$

Hence, $\frac{P_{d\nu+1}}{P_{d1}} < 1$ for all values of ν. Therefore, the product of miss probabilities in (A.1) falls with the increasing ν (number of terms in the series), however, the sum of the series increases due to the presence of the term $(2\nu+1)$. In order to prove that the series converges, the ratio rule can be applied as shown below.

The equation (7.7) can be rewritten using the series sum S_S as:

$$T_{acq} = \frac{L}{2f_c} S_S \tag{A.4}$$

where S_S represents

$$S_S = P_{d1} + 3P_{d2}(1-P_{d1}) + 5P_{d3}(1-P_{d1})(1-P_{d2}) + \cdots \tag{A.5}$$

Using (A.2) and (A.3) the n^{th} term of the series can be obtained as

$$n^{th}\ term = K(2n+1)P_{dn+1}(1-P_{dn})^{n-M} \quad \text{for } n = 0,1,\cdots \tag{A.6}$$

where K is the product of first M miss probabilities (including M^{th} term) which is given by

$$K = (1-P_{d1})(1-P_{d2})\cdots\cdots(1-P_{dM}) \tag{A.7}$$

The $(n+1)^{th}$ term of the series is given by:

$$(n+1)^{th}\ term = K(2n+3)P_{dn+2}(1-P_{dn+1})^{n+1-M} \tag{A.8}$$

Using (A.3) the ratio of $(n+1)^{th}$ term to n^{th} term becomes

$$\frac{(n+1)^{th}\ term}{n^{th}\ term} = \frac{(2n+3)}{(2n+1)}(1-P_{dn}) = \frac{(2n+3)}{(2n+1)}C \tag{A.9}$$

where $C = 1-P_{dn} < 1$.

$$\underset{n\to\infty}{Lt}\ \frac{(n+1)^{th}\ term}{n^{th}\ term} \to C \tag{A.10}$$

Thus, the series tends to be a geometric series with the ratio of successive terms less than one, and hence convergent.

Summation of the series:

The series in (A.5) is summed by splitting it into two parts. First part consists of the varying miss probabilities upto $n = M$ and the second part is the terms with constant miss probabilities with $n > M$, which can be added as a arithmetic-geometric series. Therefore, the sum of the series, S_S, is

$$S_S = S_M + S_T \tag{A.11}$$

where S_M represents the sum of the first M terms and S_T represents the sum of the rest of the terms in the series.

The sum, S_T is given by:

$$S_T = K[(2M+1+3)(1-P_{dn}) + (2M+1+5)(1-P_{dn})^2 + \cdots\cdots] \tag{A.12}$$

The n^{th} term of S_T, with $N = 2M+1$, is given by:

$$n^{th}\ term = K(N+2n+1)(1-P_{dn})^n \tag{A.13}$$

$$S_T = K\sum_{n=1}^{\infty}(N+2n+1)(1-P_{dn})^n \tag{A.14}$$

Substituting C for $(1-P_{dn})$

$$\begin{aligned} S_T &= K\sum_{n=1}^{\infty}(N+2n+1)C^n \\ &= K\left[\sum_{n=1}^{\infty}2nC^n + (N+1)\sum_{n=1}^{\infty}C^n\right] \\ &= K\left[\frac{2C}{(1-C)^2} + (N+1)\left(\frac{1}{(1-C)}-1\right)\right] \end{aligned}$$

The sum S_M can be computed from the P_d and n_{fa} term by term quite easily and thus the sum

of the series S_S can be obtained from which T_{acq} can be computed using (A.4).

It was also observed that the contribution of terms is not uniform throughout the series for various values of P_{dn}. Although, the sum S_S with $P_{dn}(<P_{d1})$ is higher than that with P_{d1}, the sum S_M with P_{dn} is always less than that with P_{d1}. Therefore, the first M terms (S_M) contribute more if P_d is higher whereas the last terms (S_T) contribute more if the P_d is smaller. By using P_{d1} and P_{dn} and computing the sum S_S as a geometric series both the lower and upper bounds of the S_S can also be obtained.

The sum S_S, assuming equal probabilities say P_{dx} for all terms in (A.5), can be obtained as

$$S_S = (2-P_{dx})/P_{dx} \tag{A.15}$$

The upper limit can be obtained as

$$S_{S\,|\,upper} = (2-P_{dn})/P_{dn} \tag{A.16}$$

and the lower limit can be obtained as

$$S_{S\,|\,lower} = (2-P_{d1})/P_{d1} \tag{A.17}$$

These limits provide quick verification of the acquisition time.

CHAPTER 8

CONCLUSIONS

In this thesis, the sequential detector has been applied to the problem of initial code acquisition of direct-sequence spread-spectrum pseudo-noise signals. Three variants of the sequential detector have been considered and their acquisition performances have been compared. The optimization of these detectors and their acquisition performance in various situations have been obtained using a Monte-Carlo simulation approach. As the sequential detector employs a serial search strategy, its performance has also been compared with the more conventional forms of serial search detectors; namely, the single-dwell time detector and the digital matched filter.

Various contributions to the randomness of the acquisition process have been identified as:

i) the initial uncertainty about the code phase

ii) unknown carrier frequency and phase

iii) the presence of data modulation on the spread-spectrum signal

iv) channel noise which is additive white Gaussian (AWGN)

v) additive interference (intentional or unintentional) and

vi) channel distortion (due to fading and multipath)

The acquisition performance of the sequential detector has been analyzed for most of these situations and the performance of each sequential detector variant has been compared. A non-coherent sequential detection system has been employed to counter the carrier frequency and phase uncertainty. The common frequency offset due to Doppler has been analyzed for both the residual carrier frequency and code offset. The performance of the detectors has been obtained both in the presence and the absence of random data modulation, and the degradation in the acquisition performance has been assessed. Two common types of jamming signal, namely, the CW jammer and the pulse jammer have also been employed to examine the degradation in the performance of the sequential detector due to jamming.

The acquisition system is broadly characterized by two main components. One of these is the decision making device, which is the detector and the other is the acquisition strategy, which is the search technique. With regard to the search strategies, various types of strategy were analyzed. A key area of the research was the optimization of the serial search strategy and its parameters. However, in the detector optimization, not all the detector types have received equal attention in spite of the wide concern for the non-coherent single or multiple dwell detectors. In this thesis, major emphasis has been placed on the optimization of the detector and consequently, the sequential detectors which are the variable dwell time detectors have been analyzed. The sequential detector is conceptually known to be optimum in the sense of minimum mean dismissal time for a given probability of detection and false alarm compared to any other detectors which may be either sequential or non-sequential (without considering the detectors that use any form of adaptation). It has been used generally in radar detection for sequential range processing but its use in communications is very much limited. The reason for this has been partially due to the difficulties involved in the theoretical analysis of the sequential detector which is due mainly to the complex relationship with the thresholds, bias and the input SNR governing the various random times involved in the sequential detector. The solutions for the multiple integral equations governing the acquisition process are very difficult, if not impossible and often unwieldy for the wide range of parameters controlling the sequential detector. Hence, the Monte-Carlo computer simulation has been found to be an important tool to investigate the optimum performance of the sequential detectors for spread-spectrum acquisition in various practical situations.

Three variants of the computer models had to be used to simulate two different variations in the sequential detector using practically realizable approximations together with the ideal sequential detector, whose performance forms the baseline for the other two. A number of signal models have been used and various types of received signal structure representing the presence and the absence of data modulation, the code and the residual carrier Doppler frequency offsets have been simulated. Besides, various channel impairments, namely, the jamming and interference signals in an additive Gaussian noise channel have been simulated. The direct-sequence spread-spectrum system models for both the transmitter and receiver have been employed and the sequential detector code acquisition system has been simulated. In order to assess the relative performance of sequential detection PN code acquisition, the more conventional serial search using a single-dwell detector and a digital matched filter have also been simulated.

The design of the acquisition system consists of a set of design parameters relating to the optimum performance of the detector and the search strategy. The threshold settings, correlation time, design SNR etc., specifically govern the optimum detector while the number of tests per chip (number of cells), mean dismissal time and the system complexity are manifested by both the detector and the choice of search strategy and verification logic. However, various parameters relating to the PN code namely, the code rate, code length, code uncertainty region and the parameters such as false alarm penalty explicitly control the mean acquisition time. For the specification of the overall acquisition performance, eventhough the mean acquisition time is generally acceptable, the probability of prompt acquisition (probability of acquiring within a specified search time) is used as an equivalent specification for the situations with intermittent pauses. The probability of detection (or miss detection) is also an important parameter when too many system deadlocks are imposed (viz., a finite search time as well as an absorbing type false alarm state).

For the analysis of the sequential detector, in this thesis, major emphasis has been placed on the mean acquisition time. However, the average sample number, the probability of detection and the probability of false alarm have also been discussed and compared principally to show how each plays a part in determining the mean acquisition time. The effect of the number of quantization levels of the uniform quantizer Q for $Q = 10,16,32,40,50$ and 100 on the acquisition performance of a quantized log-likelihood sequential detector (QLD) has been obtained and compared with the performance of a sequential detector employing an ideal log-likelihood function (LLD). The minimum number of quantization levels for the QLD yielding an acquisition performance close to the ideal sequential detector LLD, has been determined as $Q = 32$ on the basis of minimum mean acquisition time at moderate SNR, although more would be necessary at very low SNRs to minimize quantization effects. The biased square law detector (BSD) which is a more usual approximate model to the ideal log-likelihood function suitable at *low SNR* conditions has also been simulated and the acquisition performance of all the three variants of the sequential detector have been compared at Wald's optimum bias and at a non-optimum bias.

It has been found that the QLD closely agrees with the LLD. In addition, it is less sensitive to the changes in the predetection SNR than the BSD which shows a sharp increase in the mean acquisition time when predetection SNR is above +3dB. At a predetection SNR of 7dB both the LLD and the QLD achieve a minimum mean acquisition time close to 0.5 sec at Wald's

optimum bias while the BSD achieves the same order of minimum mean acquisition time around 10dB with non-optimum bias.

The optimization of the three detectors with respect to various critical system parameters has also been presented and the optimum performances has been compared. In order to obtain the optimum performance of the three detectors, an optimization has been carried out with respect to both upper and lower thresholds of the detectors. The detectors have also been optimized with respect to the input SNR and the design SNR and presented in the form of three dimensional acquisition characteristics.

8.1 Optimization of sequential detectors

Both stages of optimization provide the range of near-optimum values for the thresholds and the SNRs which are dependent on the bias value and the detector type. For the case of thresholds, the optimum lower threshold has been found to vary with the bias whereas the upper threshold has no significant effect. The optimum design SNR and the predetection SNR have also been determined, however, they vary with the bias and the detector type giving a broad range of optimum values.

It is observed that a lower threshold of around -5.0 is optimum for most upper threshold values at Wald's optimum bias for all the detectors. With non-optimum bias the lower threshold must be set to around -1.0 to achieve the optimum. At Wald's optimum bias, the optimum predetection SNR is around 8dB with an optimum design SNR also at 8dB (at the global minimum) for the LLD and QLD whereas for the BSD the optimum design SNR is at 6dB. At the non-optimum bias, all the detectors show minima at a higher design SNR, but the predetection SNR for the LLD and the QLD is reduced to 6dB while it is increased to 10dB for the BSD.

In order to obtain minimum acquisition time at lower SNRs, all three variants of sequential detector need to be biased appropriately with design SNR in the range of 2-4dB and this results in the minimum acquisition times less than 2sec around the input SNR = -25dB

8.2 Data modulation effects

Data modulation has been found to introduce degradation in the minimum mean acquisition time, T_{acq}. This is due principally to a reduction in the probability of detection, P_d rather than an increase in the ASN or the P_{fa}. Even with data modulation, the QLD agrees closely with

the LLD, and has broader optimum SNR characteristics than the BSD which is more sensitive to changes in the predetection SNR. Although the LLD and the QLD do not show significant changes in the optimum design SNR, the optimum design SNR for the BSD is found to be reduced by approximately 3dB. However, for all detectors the minimum mean acquisition time is found to increase by 5-10 times depending on the lower thresholds and the biases.

8.3 Effect of the Doppler shift and data modulation

The degradation due to code and carrier Doppler in the presence of data is quite significant for all the three detectors, however, when only code Doppler is present the degradation seems to be reasonable. Both the QLD and the LLD show a drift of +3dB in the value of optimum predetection SNR, γ_{opt}, at which the T_{acq} is minimum. Nevertheless, the minimum mean acquisition time increases by 10 times without data due to Doppler. With data, the drift in γ_{opt} is 2dB, but minimum T_{acq} increases by more than 10 times. The performance of the BSD is better than that of the QLD and the LLD at lower γ, particularly at Wald's optimum bias. The degradation in γ_{opt} is +3dB and the minimum T_{acq} is increased by 4 times without data; but in the presence of data, γ_{opt} is degraded by +3dB and the minimum T_{acq} is increased by 5 times.

The effect of the code and carrier Doppler with data modulation are seen to degrade the mean acquisition time by 5-10 times and cause a 3-5dB degradation in the γ_{opt}.

8.4 Performance in the presence of jamming

All the detectors show a certain level of immunity to both CW jamming and pulse jamming. In the presence of the CW jammer, no significant degradation in the acquisition performance is seen as long as the jammer to signal power ratio, J/S, is below 30dB. For J/S above 30dB the performance degrades rapidly and becomes intolerable above 40dB. For the case of the pulse jammer, the degradation in the acquisition performance is not significant for the pulse duty factor less than 0.1 with the average power maintained constant (for S/J in the range -10dB to -25dB). However, when the duty factor is reduced below 0.1 then the degradation is found to be significant.

8.5 Comparative analyses with the single-dwell detector and the matched filter

When compared under their various optimum design parameters, the matched filter (as

expected) shows a very good performance at the medium to high SNRs than either the single-dwell detector or the sequential detectors. However, as the input SNR is decreased the performance of all the detectors show a marked deterioration with the performance of the matched filter falling at a much faster rate than the other two rendering it difficult to operate at SNRs lower than -25dB. Below this value the sequential detectors completely outperform both the matched filter and the single-dwell detector.

When working at their respective optimum design parameters, the QLD achieves a minimum T_{acq} close to 0.5sec and requires a predetection SNR of 7dB to achieve this minimum. The BSD also achieves the minimum T_{acq} of the same order but this requires a predetection SNR of 10dB. When compared at a moderate input SNR at -15dB, the single-dwell detector has a minimum T_{acq} = 0.88sec whereas the matched filter shows an acquisition time around 0.06sec. The sequential detector at an equivalent predetection SNR (around 7dB) also produces an acquisition time of around 0.5sec. When the SNR is very poor, for example at an input SNR = -25dB, the matched filter has a very poor performance with minimum achievable T_{acq} around 4.5sec, whereas the single-dwell detector ($K = 10$), even though better than the matched filter, is still considered to be poor with minimum T_{acq} greater than 2sec. The single-dwell detector ($K = 100$) shows the minimum T_{acq} worse than 10 sec and thus is the poorest. However, the sequential detector, particularly the BSD, shows better performance in these SNRs achieving a minimum T_{acq} of less than 2sec. In fact, at input SNRs worse than -25dB the sequential detector still maintains minimum T_{acq} close to 2sec (when appropriately biased) whereas the other two detectors show rapid degradation with the matched filter tending to be the poorest.

Although, the use of Monte-Carlo simulation has been necessary because of the complexity of solving the integral equations for the case of the sequential detector, the application of the technique to the matched filter and the single-dwell detector systems provide a more realistic comparison and also a better insight into the optimum operation of all the three detectors.

8.6 Applications

Sequential detection code acquisition has been shown to provide faster acquisition than its serial search counterparts in low SNR conditions. It is also relatively immune to other channel impairments and can tolerate significant code Doppler offset. Therefore, the technique is very much applicable for the high dynamics GPS receivers and low SNR links like TDRSS down links. Further, the sequential detection requires *a priori* knowledge

regarding the probability distributions of the incoming signal and needs relatively stable design SNR it is particularly applicable in satellite links in which the link characteristics are normally well understood and the SNR fluctuations are relatively low. It is also usable in *push-to-talk* communication systems and in communication scenarios with intermittent pauses where the acquisition needs to be much faster. As the complexity of realizing the optimum quantized log-likelihood sequential detector is quite low, it is relatively inexpensive yet offers better performance at low SNRs permits and this assures it a versatile usage.

8.7 Scope for further study

Although most situations that contribute to the code phase uncertainty have been investigated the effects of fading and multipath could also be of significant importance for the application of spread-spectrum techniques to cellular mobile radio systems or hf radio. As the fading can deteriorate the input SNR significantly for short intervals, the code synchronization system in such situations should be capable of holding lock even during severe fading depths and the acquisition system must be fast enough to acquire code lock in case the loop looses lock due to a severe loss of SNR. The sequential detector with its capability to work at lower SNRs can be optimized to work satisfactorily in fading channels. As the input SNR from a fading dispersive channel can have wide variations, the sequential detector must be designed to operate at various design SNRs which can be adapted depending upon the input SNR. This requires the knowledge of channel SNR which must be estimated to set the design SNR appropriately. The adaptive signal processing techniques offer rich potential for this purpose and the sequential detector operating in conjunction with these techniques can provide a robust code synchronization.

A significant investigation into the performance of sequential detector can be carried out on the effects of partial correlations between the incoming code and the local code which contribute to the excessive false alarm rate. As the present simulation employs relatively a shorter code length $L = 127$, the contribution of partial correlations can be further reduced by increasing the code length which can result in the reduction of the correlation noise while checking the majority of out-of synchronization cells. As the false alarms can be catastropic to the acquisition performance, a detailed analysis of the effect of code length on the sequential detector's performance is of significant importance. From this, a correct dismissal of the majority of false alarms can even speed up the acquisition process further.

A further improvement in the acquisition speed of the sequential detector can be achieved by incorporating a time-out feature in the sequential detection. The use of *truncated sequential tests* by replacing the upper threshold with a time-out feature inherently causes faster detections and offers better potential. However, the effect of partial correlations with such tests become more important as this can outweigh the advantage gained by increasing false alarms. A proper optimization of the truncated sequential test is essential to iminimize the false alarms. Various sub-optimum detector structures can also be employed to improve the robustness of the sequential detectors for varying channel characteristics. A sub-optimum behaviour of such detectors can permit the use of sequential detectors as *non-parametric detectors* in situations that cannot guarantee the required *a priori* knowledge and this would be a major advantage in some applications. Sequential sign-tests and sequential dead-zone limiters provide simplicity and better performance as non-paramertric detectors when the channel statistics are difficult to obtain. However, as these detectors employ two level or three level hard limiting, the hard limiting non-linearity of these devices can be well compensated by increasing the number of quantization levels. A detailed analysis and studies of sequential non-parametric detectors by increasing the number of input quantization levels is necessary to compare the performance of such detectors with the optimum sequential detectors.

A further interest in the code acquisition lies with the parallel-serial search methods which can partly implement the maximum-likelihood approach by dividing the search region into smaller segments and employing faster serial search methods. An investigation of sequential detectors in such situations as a completely parallel or as a serial-parallel scheme provides better understanding of their performance compared to parallel schemes with non-sequential detectors and would achieve significantly faster acquisition times.

Hitherto, much of the analyses of code acquisition have been carried out for the time uncertainty case assuming relatively less Doppler. However, when the accumulated local oscillator frequency drift and/or Doppler shift are significant, the practical situation requires a two-dimensional time/frequency uncertainty region to be searched. Thus a quantization of the compound time/frequency region, resulting in two-dimensional cells needs to be examined. This requires a bank of detectors, each timed for different cell frequency, resulting in a parallel processing to resolve frequency uncertainty and either parallel or serial search for resolving the time uncertainty. Such receivers can well be implemented with sequential

detectors because of their simplicity and better performance and the trade-off between cost and effectiveness of such receiver structures, which would also require to incorporate a conflict resolution logic, would be interesting and worth examining.

Significant improvements can also be carried out in the acquisition performance of digital matched filters. Use of digital matched filters require A/D conversion of the received signal at the input of the correlator. For simplicity and minimum power consumption, especially at chip rates at ten's of MHz, it is generally required to keep the quantization as coarse as possible. At very low SNRs, the penalty for coarse quantization is very high and this adds to the poor performance of the digital matched filters at low SNRs. The use of finer quantization improves the performance at the cost of complexity and the influence of such correlators on the subsequent acquisition process with the problem of optimizing the loop would also be an interesting future work. As the digital matched filter makes decisions at much higher rate which is a multiple of the code rate, the decision SNR is inherently very low and this is the principal reason for its poor performance when SNR is low. An investigation into the digital matched filters with a multiple code length correlator is also important as this accumulates the correlation outputs corresponding to the same uncertainty cell to increase the decision SNR resulting in improved performance at low SNRs. In order to improve the performance of the matched filter with data modulated signals, the use of subsequence matched filtering to match with the different segments of incoming code with a subsequent non-coherent combining of such partial correlation outputs also forms an interesting extention to the present research.

GLOSSARY OF PRINCIPAL SYMBOLS

A	rms signal amplitude of the correlator signal
A_t	upper threshold
$A(\eta)$	decision criterion
$a(t)$	random signal at the correlator output
B_t	lower threshold
B	predetection filter bandwidth
b	bias
b_1	Wald's optimum bias
b_2	a non-optimum bias
b'	normalized bias value
C_{ij}	cost associated with choosing the hypothesis H_i when hypothesis H_j is true
$\overline{C}$	average cost
C_k	k^{th} PN code chip
$c(t)$	PN code sequence
c	normalized threshold of digital matched filter
$D(v)$	detector on input observation v
D_1	detector 1
D_2	detector 2
$D(d/v)$	decision rule or conditional probability of making decision d with a given observation v
d_o	decision that the signal is absent

d_1	decision that the signal is present
d_2	decision to defer a sequential test
$d(t)$	data sequence
$E_{1,2}$	ARE, asymptotic relative efficiency
E_b	energy per bit
$E(Z_n/\theta)$	expectation of the log-likelihood ratio (n samples) conditioned on θ
$E(z/\theta)$	expectation of the log-likelihood ratio for i^{th} sample conditioned on θ
$F(x_i/x_{i-1})$	pdf of the transitions of the Markov process $\{x_i\}$
f_c	PN code rate
f_s	input sampling rate
f_d	frequency difference due to Doppler
$f_m^*(v)$	a derived distribution of observation v
$G(x;c)$	intermediate function defined to derive ASN of the BSD
$G_i(p)$	a function of the correlator output
g	gain
H	a hypothesis
H_o	null hypothesis
H_1	alternate hypothesis
H_i	general hypothesis corresponding to either H_o or H_1 for i=0,1
H^*	a derived hypothesis setting a new distribution for v
$H(x;c)$	intermediate function defined to derive ASN of the BSD
h	a real number
$I_o[\,]$	modified Bessel function of the first kind, zeroth order
$J(t)$	jammer signal
J	rms jammer power
J_P	peak jammer power

J_k	jammer component
K	false alarm penalty factor
K_i	false alarm penalty factor of the i^{th} dwell
L	PN code length
$L(0)$	OCF with signal absent
$L(\theta)$	OCF with signal present
M	correlator length of a matched filter
$M_1(x_o)$	average test duration derived as the first moment of the moment generating function of the duration of test
m	number of adders in a sync-worthiness-indicator
N	number of dwells
N_o	single-sided noise spectral density
N_j	jammer power spectral density
N_{opt}	optimum number of sweeps
N_u	number of code chips in the uncertainty region
N	noise space
N_1, N_2	sample size for the same α, β, hypothesis and the alternative
n_1, n_2	smallest number of samples necessary for the two detectors two achieve a power of $1-\beta$ for same significance level, hypothesis and the alternative
n_{fa}	false alarm rate
n_{agr}	number of agreements
$n(t)$	noise waveform
n	shift register length
P_d	probability of detection
P_{fa}	probability of false alarm
P_{di}	probability of detection of the i^{th} detector of a multiple-dwell detector

P_{fai} probability of false alarm of the i^{th} detector of a multiple-dwell detector

P_D overall system detection probability

P_{FA} overall system false alarm probability

P_{acq} probability of overall acquisition

P_{fd} false dismissal probability

P_c correctness probability of an estimated bit

P_{fak} probabitity of false alarm at the end of the k^{th} examination interval

P_{fdk} probabitity of false dismissal at the end of the k^{th} examination interval

$P_{d\mu}$ probability of detecting μ^{th} correlator impulse

P_{md} miss detection probability

P_e probability of error

$P_J(t)$ jammer pulse

$P(H_o)$ *a priori* probability of hypothesis H_o

$P(H_1)$ *a priori* probability of hypothesis H_1

$P(D_1/H_o)$ conditional probability of decision d_1 with the given hypothesis H_o

$P(D_o/H_1)$ conditional probability of decision d_o with the given hypothesis H_1

$P_i(x_o)$ probability of test truncation

P_L probability of entering lock

$p(n)$ *a priori* pdf of all the points in noise space

$p_m(v/\theta)$ conditional pdf of m data samples

$p(v/s)$ *a priori* pdf of observation v or conditional probability of waveform v with a given signal s

$p(v/o)$ *a priori* pdf of observation v in noise or conditional probability of waveform v with given signal $s=0$

p code phase offset in a matched filter

Q number of quantization levels for the QLD

$Q(\beta)$	Gaussian probability integral
$Q_d(X,Y)$	operating point on the OCF
$Q(\gamma_d,\beta_d)$	Marcum's Q-function
q	number of code cells to be searched
q'	number of cells in the absence of Doppler
$R_c = f_c$	code rate
R_d	data rate
R_s	sampling rate at the envelope detector output
R_o	threshold parameter of digital matched filter
$r(t)$	received signal
S	rms signal power at the input
S_S	sum of the series
S_M	sum of the first M terms of the series
S_T	sum of the tail end of the series
$s(t)$	transmit signal
T_{acq}	mean acquisition time
T_P	false alarm penalty time
T_{un}	total time uncertainty
T	sampling time at the envelope detector output
T_c	PN code chip duration
T_e	examination period
T_i	beginning of an integration interval
T_J	time between the successive pulses of the jammer
T_o	data bit duration
T_r	reset penalty time required to rewind the code
T_s	sampling time at the input of the receiver (PN signal sample time)

T_{dis}	mean dismissal time
T_{vr}	verification time
T_{tr}	truncation time
$T_u = \ln A_t$	upper threshold of a log-likelihood sequential detector
$T_l = \ln B_t$	lower threshold of a log-likelihood sequential detector
T_v	time interval in which a false alarm occuring can affect the v^{th} impulse
t_j	additional time necessary to make the j^{th} decision given that the present cell has not been rejected at the $(j-1)^{th}$ decision in a multiple-dwell detector
t_v	instant of time at which v^{th} correlation impulse occurs
$u(v_k)$	unit step function
$(v_1, v_2, \cdots v_m)$	m-dimensional sample vector
v_i	accumulator output of a sequential detector
W_{ss}	spread bandwidth
$x(t)$	correlator signal
$\{x_i\}$	discrete stationary Markov process
Y_k	k^{th} sample of the envelope detector of a BSD after the bias
$y(t)$	output of the envelope detector
y_k	k^{th} sample of the envelope detector (LLD or QLD) or square-law envelope detector (BSD)
z(t)	accumulator output of the basic form of sequential detector
Z_m	log-likelihood ratio for m samples
α	significance level or size of the test
α_o	a fixed significance level or size of the test
α', β'	significance level and power for test H^* versus H
$\beta(\theta)$	probability of miss detection
$1-\beta$	power of the test

Δ	decision space
ΔT	code phase misalignment
ΔT_c	step size in a serial search
Δf_c	difference in clock frequency of a continuous sliding correlator or code Doppler in a discrete search
δ_{ij}	Kronecker detla function
η	threshold
η_o, η_1	fixed values of detector threshold
η_i'	normalized threshold values for i=1,2
Γ	observation space
Γ_m	m-dimensional sample space
$\Gamma_m^o, \Gamma_m^1, \Gamma_m^2$	decision regions corresponding to the decisions d_o, d_1, d_2
γ	predetection SNR
γ_{in}	input SNR
γ_{dsn}	design SNR
γ_{opt}	optimum SNR
γ_c	decision SNR on a per-cell basis
Λ_i	likelihood ratio function for i samples
$\Lambda_m(v/\theta)$	likelihood ratio function for m samples
$\lambda(v), \lambda(k)$	likelihood ratio
μ	mean search update
ν	number of the correlator impulse
Ω	signal space
ω_c	carrier radian frequency
ω_d	carrier Doppler shift in radians
ω_j	jammer radian frequency

ω_{ca}	radian cut-off frequency of an analog filter
ω_{cd}	radian cut-off frequency of a digital filter
π_j	*a priori* distribution of the code phase uncertainty
$\pi_i(x_o)$	probability of decision i=0,1,2
ρ	duty factor of a pulse jammer
ρ^*	critical duty factor of a pulse jammer
$\sigma(s)$	*a priori* pdf of all the points in signal space
σ^2	variance of the noise process
σ^2_{acq}	variance of the acquisition time
τT_c	local code phase offset
τ'	local code frequency error
τ_d	dwell-time
$\overline{\tau_d}$	mean-dwell time of a search/lock strategy
τ_{di}	dwell-time of the i^{th} dwell of a multiple-dwell detector
τ_J	pulse width
τ_o	test truncation time
θ	signal parameter
θ_c	carrier phase
θ_d	design signal parameter
θ_J	jammer phase
θ_j	j^{th} signal parameter
$\xi T_o+\zeta T_c$	received data bit phase offset
ζT_c	received code phase offset
ζ'	received code frequency offset
$>^{H_1}<_{H_o}$	hypothesis H_1 accepted if likelihood ratio is greater than the R.H.S and hypothesis H_o is accepted if it is less than the R.H.S

ANNEXURE

PUBLISHED PAPERS

This annexure presents the copies of the papers published in the international conferences. The list of the papers presented are:

1) K.V.Ravi and R.F.Ormondroyd, "Computer simulation of a quantized log-likelihood sequential detector for faster acquisition of spread-spectrum pseudo-noise signals." 5th International Conference on Radio Receivers and associated systems, IEE Conference publication No. 325, pp 207-211, July 24-26,1990, Cambridge, UK.

2) K.V.Ravi and R.F.Ormondroyd, "Comparison of the acquisition performance of biased square law and quantized log-likelihood sequential detectors for PN acquisition" IEEE International Symposium on Spread Spectrum Techniques and Applications, Symposium Proceedings, pp 53-58, September 24-26,1990, London, UK.

3) K.V.Ravi and R.F.Ormondroyd, "Performance of sequential detectors for the acquisition of data modulated spread spectrum pseudo noise signals", IEEE International Conference on Communications, ICC'91, June 23-26, 1991, Denver, Colorado, USA.

4) K.V.Ravi and R.F.Ormondroyd, "Simulation performance of a quantized log-likelihood sequential detector for PN code acquisition in the presence of data modulation and Doppler shift", MILCOM'91, November 4-7, 1991, McLean, USA.

5) R.F.Ormondroyd and K.V.Ravi, "Performance of the serial-search PN code acquisition techniques using Monte-Carlo simulation - A comparative evaluation", MILCOM'91, November 4-7, 1991, McLean, USA.

COMPUTER SIMULATION OF A QUANTIZED LOG-LIKELIHOOD SEQUENTIAL DETECTOR FOR FASTER ACQUISITION OF SPREAD SPECTRUM PSEUDO-NOISE SIGNALS.

K.V. Ravi, R.F. Ormondroyd

University of Bath, UK

ABSTRACT

This paper presents the performance of a quantized log-likelihood sequential detector for the acquisition of psuedo-noise signals in direct-sequence spread spectrum systems. This new sequential detector improves the ease of implementation through the use of a digitally implementable look-up table approach, and it also simultaneously provides the minimum mean acquisition time for a lower input signal-to-noise (SNR) ratio when compared with a fixed dwell serial-search or matched filter acquisition system. The effect of the number of quantization levels on the acquisition performance of the quantized log-likelihood sequential detector has been obtained by computer simulation and compared with the performance of a sequential detector employing an ideal log-likelihood function. It has been found that the quantized log-likelihood sequential detector with 32 quantization levels yields an acquisition performance close to the ideal sequential detector. Optimization of various sequential detector system parameters to result in the minimum mean acquisition time has also been discussed.

INTRODUCTION

There is a pressing need for faster code acquisition in direct-sequence spread-spectrum receivers and consequently the acquisition problem has received considerable attention recently. Spread-spectrum code acquisition schemes can be broadly classified in terms of the underlying search algorithm and the detector type. Three major types of commonly used search algorithm are: maximum likelihood, serial search and sequential estimation. These methods trade system complexity for acquisition performance, and the sequential estimator, for example, has a poor SNR performance. The detectors used with these schemes generally employ either fixed-dwell detection or matched filtering. For serial search algorithms, however, sequential detection, employing a *variable dwell* time, has been shown (1) to be the optimum for achieving the minimum acquisition time in low SNR conditions and forms the basis of this paper.

Sequential Detection of Spread-spectrum Signals

The classical sequential detection technique was initially proposed by Wald (2) for radar detection but it has also been applied to the problem of spread-spectrum acquisition by Cobb and Darby (3). Figure 1 shows a schematic diagram of a serial search p-n code synchronizer using a sequential detector in place of the more usual fixed dwell system. As for fixed dwell systems, the timing error between the received pseudo noise (PN) code and the locally generated replica code is obtained from the measure of correlation existing between them. Because of the effect of noise, the correlation function is corrupted. This means that the detection of the wanted (ie. in-lock) correlation can be missed or that "false alarm" conditions can occur. The code is split into cells of typically two cells per chip and samples of the corrupted correlation output are obtained.

In the sequential detector, these samples are checked to establish the measure of the likelihood that they contain the wanted correlation signal (plus noise) or are simply noise alone. This likelihood measure is accumulated and tested against normally two thresholds to detect the correct synchronization. The accumulator output rises linearly at different slopes depending upon whether the cell being searched corresponds to noise only or signal plus noise.

By adding a proper bias to the log-likelihood function, which is between the means of the detector outputs under the two hypotheses, say, the accumulator output will tend to decrease linearly when noise alone is present and increase linearly when signal plus noise is present. When the accumulator output falls below the lower threshold, the cell is dismissed and the local code is advanced by one cell and synchronization is re-checked. If the accumulator output exceeds the upper threshold, then synchronization is declared (however it may be a false alarm). By appropriate choice of the lower threshold level and bias level, the dismissal time can be minimized. Since the detector spends most of the time dismissing out of synchronization cells, which occur in all but one cell per pass through the uncertainty region, the sequential detector can be designed to reduce the mean time to dismiss the out of synchronization cells; resulting in minimum mean acquisition time.

This mechanism of quick dismissal of the out of synchronization cells forms the heart of the sequential detection system that provides the acquisition time advantage not possible with other schemes.

Wald has provided an analysis of the sequential detector based on approximations which are valid only in situations of low signal-to-noise ratios as the 'excess-over-boundary' problem was not treated (4). Kendall analyzed the performance of a simplified version of the sequential detector called the 'biased square law sequential detector' for the case of dismissing the out of synchroniszation cells (1). However, the exact analysis in the range of moderate signal-to-noise ratios (ie. a predetection signal-to-noise ratio in the range of -3dB to +3dB in the IF bandwidth) has been found to be difficult (1,5) as the integral equations governing the decision probabilities and the expected sample size of a sequential probability ratio test are very difficult to solve by methods that will give useful numerical results. Some simulation results of the detection probability, P_d, and false alarm probability, P_{fa}, with simplified detector implementations have been presented by Cobb and Darby (3), where the authors simulated the ideal log-likelihood sequential detector transformation, 'ln $I_0[\ ]$', (ie. the natural logarithm of the modified Bessel function of first kind and zero order) and employed square law detector, envelope detector and absolute value detector implementations.

In this paper, the ideal sequential detector's 'ln $I_0[\ ]$' transformation has been quantized and the spread spectrum acquisition has been simulated by a Monte Carlo method

Paper presented in the 5th International Conference on Radio Receivers and associated systems, July 24-26, 1990, Cambridge, UK, IEE Conference publication No. 325, pp 207-211.

and new results for the quantized log-likelihood sequential detector are presented. The minimum number of quantization levels to achieve satisfactory performance has been derived with this simulation and the performance characteristics of the quantized log-likelihood sequential detector are compared with the simulated performance of the ideal log-likelihood sequential detector.

SIMULATION OF SEQUENTIAL DETECTION

The incoming signal is modelled as a baseband direct-sequence spread-spectrum signal with pseudo random code modulation. The transmit signal has been simulated as a PN code of length 127 chips running at a rate of 100Kb/s. Two cells per chip have been assumed. Additive white Gaussian noise (AWGN) has been assumed and the channel characteristics have been simulated by generating Gaussian random noise with unit variance and the corrupted spread spectrum signal is used as the input to the PN receiver. In the simulation of the receiver, the incoming signal is correlated with the local code generated with an arbitrary starting state and the correlated signal is low pass filtered and sampled at the rate equal to 1/B, where B is the predetection filter bandwidth.

Definition of the Log-likelihood Function

In the baseband simulation of the sequential detection system it has been assumed that the output of the low pass filter is equivalent to the filter output of a band pass model which has a Gaussian noise corrupted sinusoidal (IF) signal as its input. The output of the envelope detector is assumed to have a Rician probability density function (pdf) with signal plus noise and a Rayleigh pdf with noise only. When this envelope is sampled at the rate 1/B, the log-likelihood function, which is defined as the logarithm of the ratio of probability of signal plus noise, $p_1(y_k)$, to the probability of noise only, $p_0(y_k)$, with y_k as the k^{th} sample, is given by:

$$\lambda(k) = \ln\frac{p_1(y_k)}{p_0(y_k)} \qquad (1)$$

$$= -\gamma + \ln[\, I_0(2y_k\sqrt{\frac{\gamma}{2\sigma^2}})] \qquad (2)$$

The accumulator output, which is the running sum of the log-likelihood function, is given by:

$$v_i = \sum_{k=1}^{i} \lambda(k) \qquad (3)$$

$$= \sum_{k=1}^{i} (-\gamma + \ln[\, I_0(2y_k\sqrt{\frac{\gamma}{2\sigma^2}})]) \qquad (4)$$

where σ is the standard deviation of the noise, and γ is the predetctor SNR. In the double threshold sequential detector, this sum is compared against two thresholds viz., the upper threshold T_u and the lower threshold T_l.

Performance Parameters Examined

The sequential detection system employing the ideal log-likelihood function was simulated and various performance characteristics of the sequential detector viz., average sample number(ASN), probability of detection (P_d) and probability of false alarm (P_{fa}) were recorded for multiple runs with random starting states of the local code generator. The phase of the local code was changed in steps of 1/2 chip interval (the cell length) and all the four possible successive cells of the autocorrelation curve were searched for detection.

The log-likelihood function was then quantized using a uniform step size and the acquisition characteristics were compared for a different number of quantization levels. Using this technique, the quantized log-likelihood sequential detector with the minimum acceptable number of quantization levels has been obtained for two different bias levels (Wald's optimum value and a non-optimum value) and from this the acquisition performance has been determined.

The critical system parameters determining the performance of the system are the upper threshold, lower threshold, bias and gain. In order to obtain a valid performance of the detector, the loop gain had to be carefully optimized to achieve acceptable probabilities of detection and false alarm over the input SNR range of interest. The bias was set as a function of the predetection SNR and the input SNR was then varied to obtain the required performance characteristics. The mean acquisition time was computed from these observations and the acquisition performance for the input signal-to-noise ratio ranging from -25dB to -10dB was then obtained.

SIMULATION RESULTS

For the ideal log-likelihood sequential detector (LLD) and the quantized log-likelihood sequential detector (QLD), ASN, P_d and P_{fa} have been recorded for the predetection SNR, γ, ranging from -4dB to +10dB (for a 21dB process gain). Generally, it has been observed that P_d is decided mainly by both the lower threshold and the bias while P_{fa} is mainly controlled by the upper threshold and the bias point. The effect of the other threshold seems to be minor in both cases. Normally, in all the characteristics, the upper threshold has been fixed at 5.0 and the lower threshold is set to -5.0, -2.0 and -0.5. For each set of thresholds, two different bias levels, b, are employed, one at Wald's optimum value ie., $b = \gamma(1+\gamma/2)$ and the other at the non-optimum bias equal to $b = \gamma$. The characteristics with the upper threshold at 5.0 and the lower threshold at -5.0 for both these bias values are shown in figures 2-5.

The characteristics of the ASN versus predetection SNR and the mean acquisition time versus predetection SNR for the ideal LLD are shown in figures 2 and 3.

The effect of the number of quantization levels, Q, on the performance of the QLD has been obtained for Q=10,16,32,40,50 and 100 with the upper and lower thresholds at 5.0 and -5.0 respectively, and these results are shown in figures 4 and 5.

Discussion of the ASN Results

The ASN for the sequential detection system depends both on the lower threshold and the bias. Although the ASN appears to be reducing with an increasing lower threshold, the false alarm probability starts increasing, and this starts to control the mean acquisition time. This factor limits the choice of the lower threshold to moderate values. With the optimum bias, the ASN is seen to be always less than that with the non-optimum bias.

From the characteristics shown in figure 2, it can be observed that the ASN increases with decreasing predetection SNR. For example, for the ideal LLD at SNR=0dB with the optimum bias, the ASN is 6.25 for the lower threshold at -5.0 while at SNR=-3dB the ASN is 15.54 for the same threshold. With the non-optimum bias the ASN is slightly higher than that with the optimum bias ie., 10.2 for SNR=0dB; 21.1 for SNR=-3dB. The ASN for the quantized log-likelihood detector with Q=32 (QLD)

closely agrees with the LLD at SNR=0db. However, at SNR=-3dB the QLD appears to be overshooting the LLD showing a sharp increase in the ASN with the decreasing SNR which can be attributed to the effect of quantization at low SNR's. This effect of coarse quantization on the ASN at lower predetection SNR's can be seen in figure 4.

Discussion of the Acquisition Time Results

The mean acquisition time depends on the combination of ASN, P_d and P_{fa} and is seen to pass through a minimum as the SNR varies. The minimum mean acquisition time and the optimum SNR at which it occurs vary with the thresholds, the biases and the type of the detector. Figure 3 shows the minimum mean acquisition time for two biases with the upper threshold at 5.0 and the lower threshold at -5.0. The mean acquisition time has been calculated under the assumption of multiple passes based on the probability of detection and a false alarm penalty time based on the probability of false alarm. Typical values for the truncation time (T_{tr}) and the verification time (T_{vr}) of the sequential test have been assumed as T_{tr}=50 ms and T_{vr}=50 ms respectively and the total mean acquisition time has been computed by using the relationship

$$T_p = T_{dis}\left[1 + \frac{P_{fa}(T_{tr} + T_{vr})}{T_{dis}}\right] q\left[\frac{\ln(1-P)}{\ln(1-P_d)}\right] \qquad (5)$$

where T_{dis} is the mean dismissal time given by

$$T_{dis} = ASN/B \qquad (6)$$

where B is the predetection filter bandwidth, which is equal to the data bandwidth, q is the number of the code cells being searched and T_p is the acquisition time with probability P. In these results, P is assumed to be 0.9.

The mean acquisition time as a function of the pre-detection SNR has been plotted for both the LLD and the QLD (for Q=10,16,32,40,50 and 100), and the results are shown in figure 5. Typically, the mean acquisition time shows a downward trend with an increase in the SNR from -4dB and passes through a minimum. At the lower predetection SNR=-4dB the ASN and the P_{fa} are at their maximum, and even though the P_d is also at its maximum, this causes a higher acquisition time. With increasing SNR, the initial fall in the mean acquisition time is due to decreases in both the ASN and the P_{fa}. Further increase in the SNR, even though this causes the ASN and the P_{fa} to be reduced, increases the mean acquisition time. This is because P_d significantly reduces, causing the number of passes to rise sharply.

The optimum SNR with the non-optimum bias is seen to be broader than that with the optimum bias while the minimum mean acquisition time with the optimum bias is always less than that with the non-optimum bias as seen from figure 3.

For the QLD with the number of quantization levels set at Q=10 and 16, although the acquisition time maintains a minimum, it is greater than the minimum achievable and rises very fast with a varying SNR. However, for Q=32 and above, this minimum almost merges with that of the LLD and the characteristic closely agrees with the LLD's characteristic throughout the SNR range of interest. The optimum SNR occurs around 7 dB for both the LLD and the QLD with a minimum achievable acquisition time of approximately 0.5 sec for the given system parameters.

The minimum mean acquisition time obtainable from the QLD appears to be considerably less than for fixed dwell serial search systems with the same system parameters. However, the SNR to achieve this optimum seems to be higher. This is due to the fact that the simulation employs a bias which depends on the predetection SNR. A sequential detector designed with this input SNR as the optimum, with the bias derived from the predetection SNR, can provide the optimum performance for an input SNR around -15dB for a 127 chip sequence. However, as seen from figure 3, the bias of the sequential detector plays an important part in determining the optimum input SNR, and hence, on the choice of the design SNR. As Wald's optimum bias is valid only for the lower input SNR's and the exact expressions for the decision probabilities and the average test duration do not require the bias to correspond to Wald's optimum bias (5), changing the bias independently from the predetection SNR would allow the choice of a design SNR suitable for a wider range of input SNR's. The effects of the bias variation, with a fixed design SNR, on the acquisition performance need to be assessed.

CONCLUSIONS

The quantized log-likelihood sequential detector with 32 quantization levels is seen to have a performance close to that of the ideal log-likelihood sequential detector. With this number of quantization levels, a simple realization of the QLD using a look-up table approach can be implemented digitally with an easily manageable size of ROM, thus reducing the hardware complexity. The performance of such a sequential detector can be quite robust providing the minimum acquisition time for a wide range of input signal-to-noise ratios. Since the total average acquisition time of the spread spectrum receiver employing the sequential detector can be quite low, the use of direct-sequence spread-spectrum techniques in such diverse applications as push-to-talk digital mobile communication systems, satellite navigation systems and LAN systems etc. becomes more practicable.

The sequential detector has been found to have a good acquisition performance at low signal-to-noise ratios when compared with serial search or matched filter systems and is an attractive alternative for many present day spread spectrum communication systems.

ACKNOWLEDGEMENTS

The authors wish to thank the Commonwealth Scholarship Commission and the British Council for their provision of a Commonwealth Scholarship to one of the authors (KVR) to carry out postgraduate research. The authors also wish to acknowledge the support provided by the Indian Space Research Organization to one of the authors in allowing study leave to pursue research in the University of Bath.

REFERENCES

1) Kendall.W.B., 1965 "Performance of the Biased Square Law Sequential Detector in the absence of signal" IEEE Trans. Inform. Theory, IT-11, 83-90.

2) Wald.A., 1947, " Sequential Analysis", John Wiley,New York.

3) Cobb.R.F., and Darby.A.D., 1978 "Acquisition performance of simplified implementations of the sequential detection algorithm" National Telecommunications conference Record, Birmingham,AL.

4) Wald.A., and Wolfowitz.J., 1948 "Optimum character of the Sequential Probability Ratio Test", Ann. Math. Stat., 19, 326-339.

5) Simon.M.K., Omura.J.K., Scholtz.R.A., and Levitt.B.K., 1985 "Spread Spectrum Communications" Computer Science Press,Inc.,U.S.A.,Volume No.3.

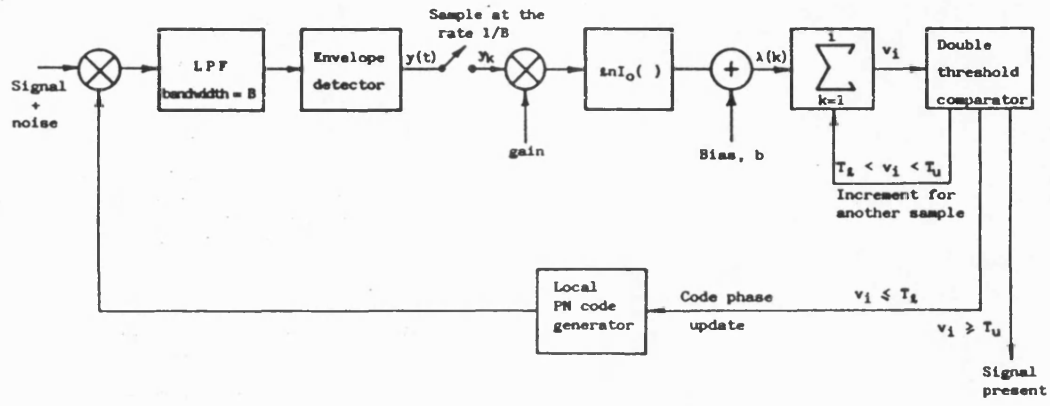

Figure 1 Block diagram of a sequential detection PN acquisition system.

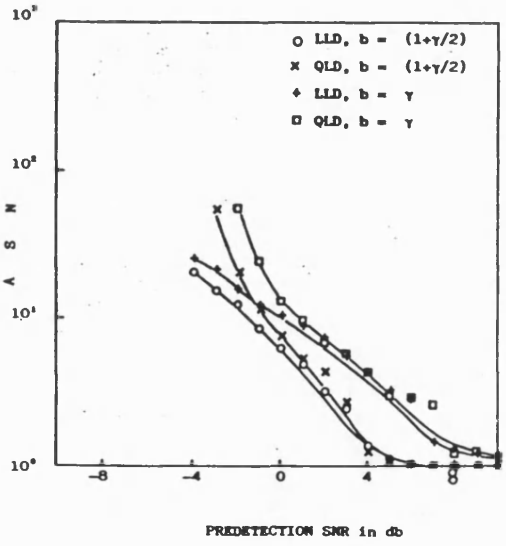

Figure 2 Average sample number (ASN) vs. predetection SNR for LLD and QLD with Q=32 for Wald's optimum and non-optimum bias.

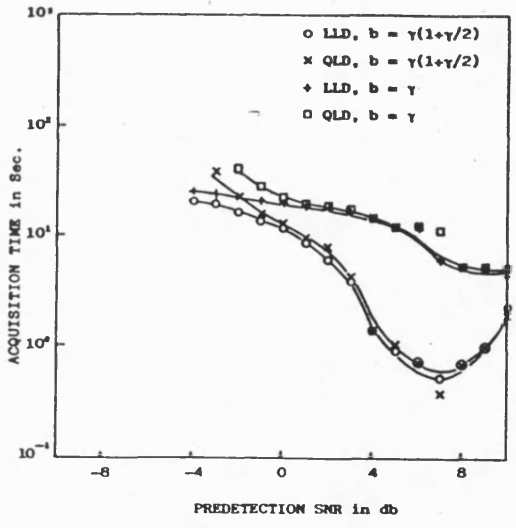

Figure 3 Mean acquisition time vs. predetection SNR for LLD and QLD with Q=32 for Wald's optimum and non-optimum bias.

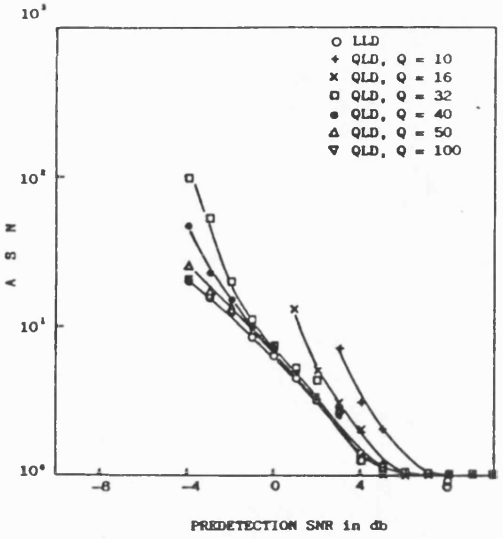

Figure 4 ASN vs. predetection SNR for LLD and QLD with Q=10, 16, 32, 40, 50, 100

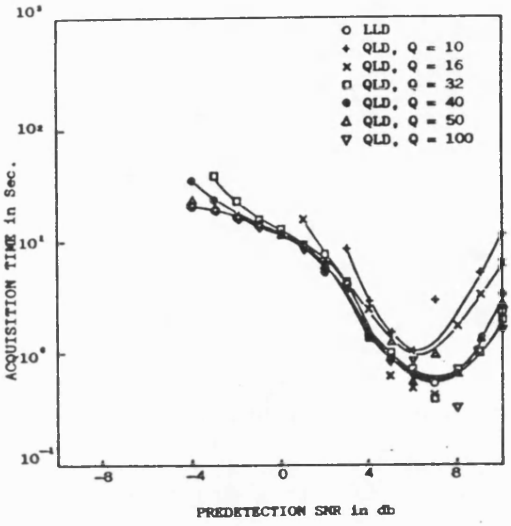

Figure 5 Mean acquisition time vs. predetection SNR for LLD and QLD with Q=10, 16, 32, 40, 50, 100

COMPARISON OF THE AQUISITION PERFORMANCE OF BIASED SQUARE LAW AND QUANTIZED LOG-LIKELIHOOD SEQUENTIAL DETECTORS FOR PN ACQUISITION.

K.V.Ravi and R.F.Ormondroyd

University of Bath, UK

1.0 ABSTRACT

This paper compares the acquisition performance of a new type of sequential detector, the quantized log-likelihood sequential detector (QLD), with the biased square law sequential detector (BSD) for the acquisition of direct-sequence spread-spectrum pseudo noise signals. The ideal log-likelihood function of the sequential detector has been quantized and the quantized log-likelihood sequential detector is simulated. It has been found that the QLD with 32 quantization levels has an acquisition performance close to that of the ideal log-likelihood sequential detector. The BSD has also been simulated and its acquisition performance is obtained for the same system parameters as the QLD.

In this paper, the acquisition performance of the QLD and the BSD have been compared both at Wald's optimum bias and at a non-optimum bias for a predetection signal-to-noise ratio (SNR) ranging from -4dB to +10dB. It has been found that the QLD is less sensitive to the changes in the predetection SNR than the BSD which shows a sharp increase in the minimum mean acquisition time when the predetection SNR is increased beyond +3dB. Because the QLD can be easily realized by a look-up table approach using digital techniques, and yet can provide a better aquisition performance, it is attractive for use in many spread spectrum systems requiring faster acquisition when working at low input signal-to-noise ratios.

2.0 INTRODUCTION

Direct-sequence spread-spectrum (DS-SS) receivers usually accomplish code despreading using active correlation by generating a local replica of the pseudo noise (PN) code which is synchronized to the code superimposed on the incoming waveform. Synchronization is ordinarily achieved in two stages. In the first stage, a coarse alignment of the two PN codes is obtained to within a small relative timing offset, typically less than a chip duration. This is referred to as 'PN acquisition'. In the second stage, fine synchronization is performed by continuously tracking the relative code error and maintaining the best possible code alignment by means of a closed loop system. In this paper, only the acquisition problem is considered.

A common method of achieving initial synchronization is to use a serial search of all the code epochs using the correlation between the two codes as the input to an appropriate detector to indicate coarse lock. The simplest systems use fixed dwell integration and a threshold detector. The sequential detector (1), which employs a *variable* dwell time serial search algorithm, has been found to be optimum for achieving a minimum acquisition time (2), and forms the basis of this paper. The basic structure of the sequential detection system is shown in figure 1. In this system, the samples of the correlation between the two codes, after the envelope detector, are transformed by a $\log_e I_o[\ ]$ function, where $I_o[\ ]$ is the modified Bessel function of the first kind and zero order. The output of this transformation gives a measure of the likelihood that the signal contains the wanted correlation information (ie. the in-lock signal) or is mostly noise containing only the out of sync. correlation value. The sequential detector accumulates these samples and tests the accumulated output continuously against two thresholds to determine the presence of the signal (plus noise) or the noise only. If the accumulator output crosses the upper threshold, the in-lock signal is declared (although it may be a false alarm). When the accumulated output is between the thresholds a new sample is taken and the test is repeated. When the lower threshold is crossed, it is assumed that the two codes are not in synchronization and the local code is advanced by one code cell relative to the incoming code (usually 1/2 chip interval) and the test is repeated; thus the search is continued until the presence of the signal is detected.

The realization of the sequential detection algorithm involves an exact realization of the transformation, '$\log_e I_o[\ ]$'. In the past this was found to be difficult and a number of different approximations have been employed. Cobb and Darby have reported the simulation results of simplified sequential detector implementations, employing a square law detector, envelope detector and absolute value detector (3). The exact analysis of the sequential detector was found to be difficult as the solutions for the characteristic

Paper presented in the IEEE International Symposium on Spread Spectrum Techniques and Applications, September 24-26, 1990, London, UK, Symposium Proceedings, pp 53-58.

integral equations become quite difficult even using numerical methods (4). Wald's analysis of a sequential detector is based on approximations and valid only to situations of low signal-to-noise ratios (1). Kendall analyzed the performance of a simplified version of the sequential detector called the 'Biased square law sequential detector' giving the analysis only in the absence of the signal (4).

In this paper, the ideal log-likelihood sequential detector's '$\log_e I_o[\ ]$' transformation has been quantized and the spread-spectrum acquisition system is simulated by using a Monte Carlo method. The performance results for a quantized log-likelihood sequential detector (QLD) are also presented. The minimum number of quantization levels to achieve a satisfactory performance has been determined. The biased square law sequential detector (BSD) has also been simulated and it's acquisition performance is assessed and compared with that of the QLD.

3.0 TYPES OF SEQUENTIAL DETECTOR

The sequential detectors simulated here employ three different realizations of the likelihood function which is a ratio of the *a priori* probabilities of the two hypotheses corresponding to: i) the presence of signal plus noise or ii) noise only. The different likelihood functions are described in the following sections.

3.1 Ideal Log-likelihood Sequential Detector (LLD)

For a baseband model of the spread-spectrum sequential detection system, the probability density function (pdf) of the envelope detector's output is given by a Rician distribution for signal plus noise, $p_1(y_k)$, and by a Rayleigh distribution for noise only, $p_0(y_k)$ for the k^{th} sample, y_k (assuming the out of sync. correlation signal is negligible in amplitude). The log-likelihood function is:

$$\lambda(k) = \log_e\left[\frac{p_1(y_k)}{p_0(y_k)}\right] \tag{1}$$

$$= -\gamma + \log_e[I_o(2y_k\sqrt{\gamma/2\sigma^2})] \tag{2}$$

The accumulator output is:

$$v_i = \sum_{k=1}^{i}\lambda(k) \tag{3}$$

$$= \sum_{k=1}^{i}(-\gamma + \log_e[I_o(2y_k\sqrt{\gamma/2\sigma^2})]) \tag{4}$$

where γ is the predetection signal-to-noise ratio, and σ is the standard deviation of the noise.

An LLD realizes this function ideally, and the sum of the accumulator output is compared to an upper threshold T_u and a lower threshold T_l in a double threshold sequential detector.

3.2 Quantized Log-likelihood Sequential Detector (QLD)

In this case, the ideal log-likelihood function is quantized using a 'uniform quantizer' which facilitates a look-up table implementation using digital techniques. A choice of the acceptable number of quantization levels, Q, has been made based on the comparison of the simulated performance with the LLD. The QLD with a minimum acceptable number of quantization levels has been simulated and its acquisition performance is obtained.

3.3 Biased Square Law Sequential Detector (BSD)

For low SNRs, the '$\log_e I_o[\,x\,]$' function can be approximated by the first two terms of a power series expansion:

$$\log_e I_o[x] \approx \frac{x^2}{4} - \frac{x^4}{64} \tag{5}$$

and this leads to a biased square law sequential detector (BSD) whose accumulated log-likelihood function becomes:

$$v_i = \sum_{k=1}^{i}\left(-\gamma + \gamma\frac{y_k}{2\sigma^2} - \frac{1}{4}\gamma^2\left(\frac{y_k}{2\sigma^2}\right)^2\right) \tag{6}$$

$$= \sum_{k=1}^{i}\left(-\gamma + \gamma\frac{y_k}{2\sigma^2} - \frac{\gamma^2}{2}\right) \tag{7}$$

$$= \sum_{k=1}^{i}(y_k - b) \tag{8}$$

where b is the bias of the log-likelihood function, $b = N_o B(1+\gamma)$, and N_o is the single-sided noise spectral density. For the BSD, two bias values, one at Wald's optimum bias and one at a non-optimum bias, have been considered.

4.0 SIMULATION OF SEQUENTIAL DETECTORS

A baseband model of a direct-sequence spread-spectrum system was developed. The transmitted signal was represented by a pseudo random noise (PN) code running at a rate of 100Kb/s with a code length of 127 chips. The transmission characteristics of the channel were simulated under the assumption of additive white Gaussian noise (AWGN) by generating a Gaussian random noise signal with unit variance and the corrupted spread-spectrum signal was fed to the DS-SS receiver. The receiver correlates the incoming signal with the locally generated PN code. The correlator output was then low pass filtered and the envelope was sampled at a rate equal to $1/B$, where B is the predetection filter bandwidth, which ensured sufficiant sample decorrelation for the tests of the two hypotheses to be valid. An absolute-value detector was employed and all four possible cells under the auto correlation curve were searched for detection of the wanted correlation signal.

The tests were carried out for multiple runs with an arbitrary code starting phase and the average sample number, ASN, the probability of detection, P_d, and the probability of false alarm, P_{fa}, were recorded at each input SNR. For each set of ASN, P_d and P_{fa}, the mean acquisition time was then calculated. The input SNR was varied from -25dB to -10dB ie. a predetection SNR in the range: -4dB to +11dB (assuming a process gain of 21dB) in steps of 1 dB and the acquisition characteristics determined for each SNR.

4.1 Total mean acquisition time (T_p)

The mean acquisition time of a sequential detector depends on a combination of ASN, P_d and P_{fa}. P_{fa} causes a false alarm penalty time which adds to the mean acquisition time, whereas a non-unity P_d increases the number of passes of search through the uncertainty region, depending on the required probability of overall acquisition P_{ac}. Even though the total mean acquisition time is the sum of the search times required to search that part of the uncertainty region where the signal is *not* present and the search time for the cell where the signal *is* present, the time for the latter is normally neglected due to the large number of cells where the signal is not present. The time for verification of a false alarm (T_w) and the time to reach truncation to declare the signal present (T_v) are typically assumed to be 50ms each. Thus the mean acquisition time T_p with probability of acquisition P_{ac} is given by:

$$T_p = T_{dis}\left[1 + \frac{P_{fa}(T_v + T_w)}{T_{dis}}\right]q\left[\frac{\log_e(1-P_{ac})}{\log_e(1-P_d)}\right] \tag{9}$$

where T_{dis} is the mean dismissal time given by:

$$T_{dis} = ASN/B \tag{10}$$

and q is the total number of code cells to be searched.

5.0 COMPARISON OF SIMULATED ACQUISITION PERFORMANCES

The total mean acquisition time is not only directly related to the mean dismissal time but also to P_d and P_{fa}. Consequently, the simulation results are presented to facilitate the comparisons of ASN as well as the mean acquisition time. It has been observed that P_d is mainly decided by the lower threshold, T_l, and the bias value, b, whereas P_{fa} is mainly decided by the upper threshold, T_u, and the bias value; with the other thresholds showing a minor influence on both P_{fa} and P_d. In this paper, the upper threshold has been fixed at 5.0 and the lower threshold is set to -5.0,-2.0 and -0.5 for two different bias values, b, viz: Wald's optimum, $b_1 = \gamma(1+\gamma/2)$ and a non-optimum bias equal to $b_2 = \gamma$ and the simulation repeated for each set of values.

For the QLD with a uniform quantizer, the acquisition performance has been obtained for Q=10,16,32,40,50 and 100 with upper and lower thresholds set at 5.0 and -5.0 respectively and the comparative performance is shown in figure 2 together with the acquisition performance of the LLD. When $Q \geq 32$ the acquisition performance closely agrees with that of the LLD but when $Q < 32$, it is worse than the LLD and T_p varies rapidly with SNR. The complete acquisition performance of the QLD for both bias values with different threshold settings has been obtained, and the variation of the ASN and the mean acquisition time with the predetection SNR are shown in figures 3a-3b and 4a-4b for both types of detector. The ASN of the sequential detector depends both on the lower threshold and the bias value and is always seen to be less when optimally biased than when non-optimally biased. From the characteristics shown in figure 3a, it can be seen that the ASN increases with decreasing predetection SNR. For the QLD, the ASN is lower than the BSD at SNR=0dB and almost as good as the LLD. The difference is mainly due to the effect of the coarse approximation employed in the BSD by truncating the power series expansion of the $\log_e I_o[\ ]$ function to the fourth power. However, at SNR=-3dB the QLD overshoots the BSD and shows a sharp increase in the ASN when the SNR is further decreased. This rise is seen to be due to the effect of quantization at low SNR's.

The mean acquisition time has been computed for all three detector types for a probability of acquisition, $P_{ac} = 0.9$ and plotted as a function of the predetection SNR in the range of -4dB to 10dB for both the optimum and the non-optimum bias points. The mean acquisition time shows a downward trend with increase in SNR from -4dB and passes through a minimum. The initial fall in T_p is attributed to a decrease in the ASN and P_{fa} with an increasing SNR. Further increase in the SNR causes a significant reduction in P_d and this increases the number of passes required, and consequently T_p increases. It is observed that the minimum acquisition time and the optimum SNR at which it occurs, depend on the thresholds and the biases. For the case of the QLD, this minimum is always less with the optimum bias than with the non-optimum bias. However, for the BSD the minimum occurs with the *non-optimum* bias. This leads to the observation that the truncation error in the $\log_e I_o[\ ]$ function when approximated with the BSD requires that the bias needs to be carefully tuned for optimum performance. The optimum SNR is higher in the case of the non-optimum bias than with the optimum bias. For the QLD, the optimum SNR occurs around 7dB. For the BSD, the optimum SNR occurs around 10dB (with non-optimum bias) and is higher than either the LLD or the QLD, thus limiting its use to operation in high SNR's. In all cases, minimum mean acquisition times of around 0.5s are achieved.

6.0 CONCLUSIONS

The simulated acquisition performance of a quantized log-likelihood sequential detector with 32 quantization levels and a biased square law sequential detector have been compared. The performances are found to be quite different. The QLD performs better with the optimum bias at low SNR's than the BSD. The mean acquisition time of the BSD at the optimum bias rises rapidly with increasing SNR and is also highly sensitive to the predetection SNR whereas the QLD has a relatively robust performance at the optimum SNR. The BSD achieves minimum mean acquisition time for the non-optimum bias at a higher predetection SNR. The QLD is also seen to perform well in comparison with the ideal log-likelihood sequential detector. Performance of the biased square law detector is found to be worse than the QLD and the exact realization of a square law detector is also quite difficult. With 32 quantization levels (for example) realization of the QLD using a look-up table approach can be implemented digitally with a relatively small ROM size. This not only results in reduced hardware complexity but also a faster acquisition performance in low SNR's than the BSD. With an appropriate choice of predetection SNR, the performance of such a sequential detector can be quite robust providing an acquisition time which is virtually optimum for a wide range of input SNRs.

7.0 ACKNOWLEDGEMENTS

The authors wish to thank the Commonwealth Scholarship Commission and the British Council for their provision of a Commonwealth Scholarship to one of the aurthors (KVR) to carry out postgraduate research. The authors also wish to acknowledge the support provided by the Indian Space Research Organization to one of the authors in allowing study leave to pursue research at the University of Bath.

8.0 REFERENCES

1) A.Wald, Sequential Analysis, John Wiley,New York, 1947.

2) A.Wald and J.Wolfowitz, "Optimum character of the Sequential Probability Ratio Test", Annals of Math. Stat., vol.19, pp 326-339, 1948.

3) R.F.Cobb and A.D.Darby, "Acquisition performance of simplified implementations of the sequential detection algorithm", NTC Conference Record,pp 43.4.1-43.4.7, December 4-6, 1978, Birmingham, AL.

4) W.B.Kendall, "Performance of the Biased Square Law Sequential Detector in the absence of signal", IEEE Trans. Inform. Theory, IT-11, pp 83-90, January 1965.

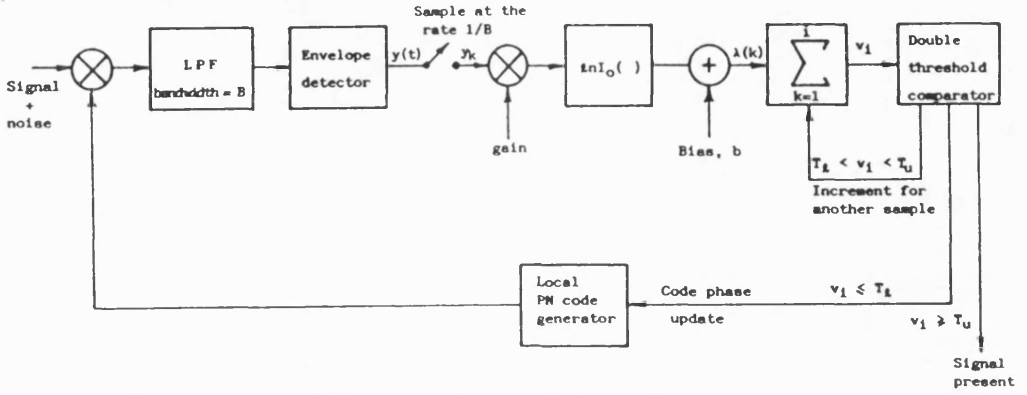

Figure 1 Block diagram of a sequential detection PN acquisition system.

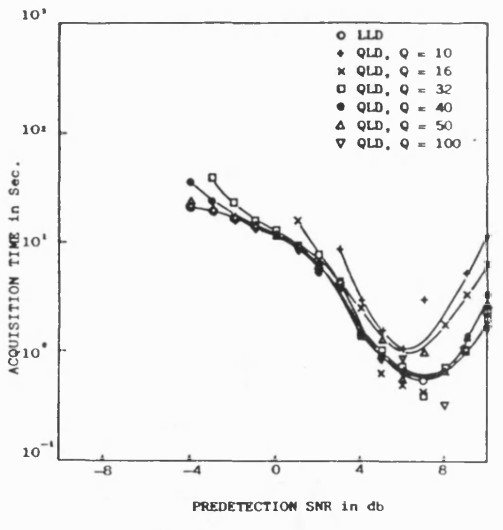

Figure 2 Comparison of acquisition performance of QLD with Q=10,16,32,40,50,100.

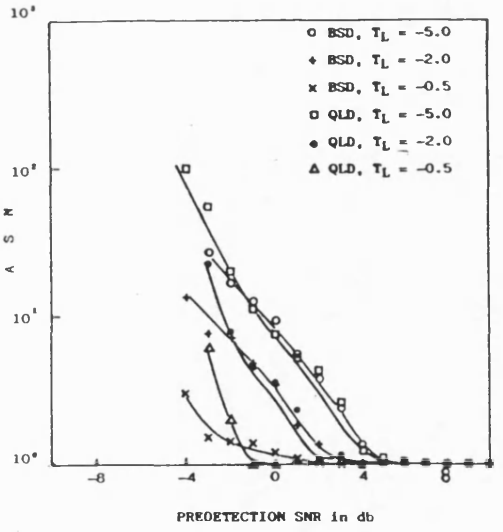

Figure 3a ASN vs predetection SNR for BSD and QLD with Wald's optimum bias.

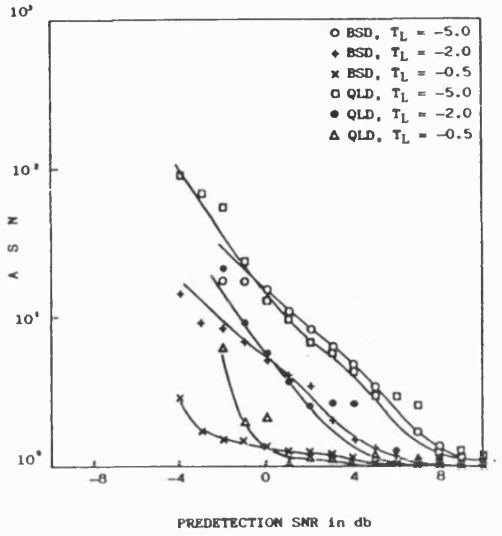

Figure 3b ASN vs predetection SNR for BSD and QLD with non-optimum bias.

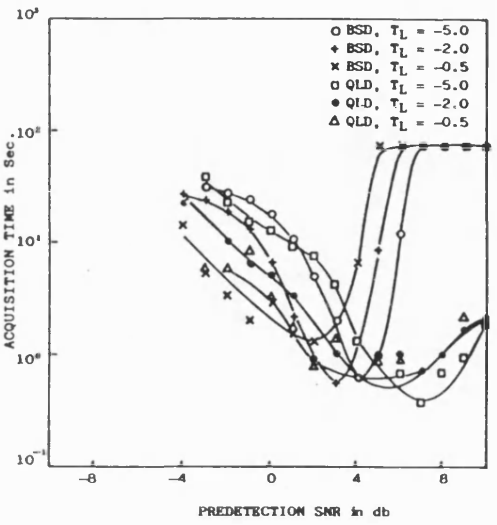

Figure 4a Mean acquisition time vs predetection SNR for BSD and QLD with Wald's optimum bias.

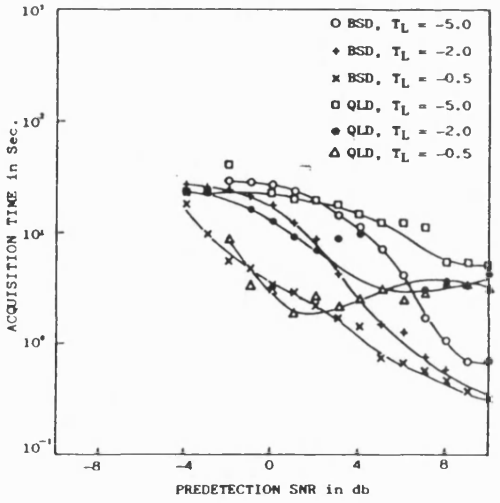

Figure 4b Mean acquisition time vs predetection SNR for BSD and QLD with non-optimum bias.

PERFORMANCE OF SEQUENTIAL DETECTORS FOR THE ACQUISITION OF DATA MODULATED SPREAD SPECTRUM PSEUDO NOISE SIGNALS

K.V.Ravi and R.F.Ormondroyd

School of Electronic and Electrical Engineering
University of Bath, Claverton Down
Bath, BA2 7AY, UK

ABSTRACT

The paper addresses the problem of fast initial acquisition of spread-spectrum PN sequence synchronization in low SNR conditions. The sequential detector offers optimum performance by minimizing the time taken to eliminate the wrong code epochs for a given probability of detection and false alarm in a serial search strategy, but its analysis using analytical techniques is extremely complex. In this paper the effect of data modulation on the acquisition performance of several sequential detectors is obtained using a Monte Carlo computer simulation technique.

The effects of data modulation on the quantized log-likelihood sequential detector and biased square law device are compared with the ideal log-likelihood sequential detector for moderate predetection SNRs (in the range -4dB to 10dB). The performance of the quantized log-likelihood function at moderate SNRs is found to be better than the biased square law device (which is an approximate model, optimized at low SNRs) and is shown to be close to the performance of the ideal log-likelihood sequential detector. However, all three detectors are found to be slower by a factor of 5-10 due to the effect of data modulation.

INTRODUCTION

Acquisition of pseudo-noise codes plays a vital role in the detection of direct-sequence spread-spectrum signals. Recently, emphasis has been placed on the need for faster code acquisition in low input signal to noise ratio (SNR) conditions, particularly in certain satellite communication and navigation applications. Commonly, a serial search is employed to acquire the initial synchronization using the correlation between the incoming signal and the locally generated code replica by searching through all possible code epochs to indicate coarse lock. This works well in low SNRs but the acquisition time can be unacceptably long. Various detectors have been used with the serial search synchronizer to detect the correlation signal, including single or multiple dwell time detectors and matched filters. All these detectors have disadvantages. The single and multiple dwell detectors take as long to dismiss each *incorrect* code epoch as to detect the *correct* code epoch while the matched filter, even though faster in detection/dismissal of the correct/incorrect code epoch, suffers from an increase in the hardware complexity proportional to the lengh of the PN code. Sequential detectors, however, employ a serial search strategy but use a variable dwell time integration. These detectors are relatively easy to implement and are capable of dismissing the larger number of incorrect code epochs quickly, allowing for longer integration of the correct code epoch resulting in reliable and faster code acquisition. For this reason, sequential detectors are the optimum in the sense of minimum dismissal time of the wrong code epoch for a given probability of detection and false alarm [1].

The integral equations governing the decision probabilities and the average sample number (ASN) required for the dismissal of each incorrect code epoch are difficult to solve analytically and by methods that will give useful numerical solutions. In the previous work a number of simplifying assumptions have been made. Wald's analysis of sequential detection does not include the 'excess over boundaries' problem and is valid only for low SNRs [2]. An approximate simplified version of the sequential detector viz., the biased square law sequential detector, has been analyzed by Kendall [3] who considered only the case of dismissing the out of sychronization cells whilst Cobb and Darby have characterized the acquisition performance of a sequential detector using a computer simulation [4]. However, their simulation did not include the presence of the data modulation and also employed various simplifications. Recently, results on the computer simulation of more complete implementations of the biased square law and a quantized log-likelihood sequential detector in the absence of data modulation were presented by Ravi and Ormondroyd [5]-[6]. In the present paper, new results on the acquisition performance of sequential detectors in the presence of random BPSK data modulation are presented and these are compared with the performance without data modulation. Further, the performance of a new type of sequential detector, the quantized log-likelihood detector (QLD), is compared with the ideal log-likelihood sequential detector (LLD) and the biased square law sequential detector (BSD) in the presence of data modulation.

SEQUENTIAL DETECTORS FOR PN ACQUISITION

Sequential detectors are used to check the output of the discrete-step serial-search correlator for the presence of a correlation signal representing the coarse in-lock condition. Because of the large noise levels encountered in spread-spectrum systems, this correlation signal is often heavily corrupted by noise. Sequential detection employs the ratio of the *a priori* probabilities of the incoming samples (at the output of the envelope detector) as a measure of the likelihood of the samples belonging to the wanted correlation sig-

ICC '91 CH2984-3/91/0000-0575 $1.00 © 1991 IEEE

Paper presented in the IEEE International Conference on Communications, ICC'91, June 23-26, 1991, Denver, Colorado, USA, Proceedings of the ICC'91, vol.2, pp 575-579.

nal plus noise (corresponding to the in-lock condition) or noise only (corresponding to the out-of-lock condition). The n ratios of n samples are multiplied to give the likelihood that the envelope detector output is signal or noise averaged over n samples. This likelihood ratio is tested against two thresholds. If the ratio lies between the thresholds, a new sample of the correlator output is taken and the likelihood of it being signal or noise is found. Exceeding either threshold indicates the presence or absence of the correlation signal, respectively.

The input signal without data modulation, $s(t)$ is represented as:

$$s(t) = A\cos(\omega_o t + \psi) + n(t) \tag{1}$$

where A is the rms signal amplitude, ω_o is the carrier frequency, ψ is the random phase of the carrier and $n(t)$ is the noise which is an independent white Gaussian process with a variance, $\sigma^2 = N_o B/2$ where B is the predetection filter bandwidth which is equivalent to the data bandwidth and N_o is the single-sided noise spectral density.

When the signal $s(t)$ is passed through an envelope detector, the output of the envelope detector samples follow a Rayleigh distribution, $P_0(y_k)$, for the case of noise only; and a Rician distribution, $P_1(y_k)$ for the case of signal plus noise. The samples of the envelope detector output are assumed to be sufficiently decorrelated by sampling at an interval $\geq 1/B$. The likelihood function is defined as the ratio of the *a priori* probability distributions and is given by:

$$\lambda(k) = \frac{P_1(y_k)}{P_0(y_k)} \tag{2}$$

The likelihood ratio after n samples is:

$$\Lambda_n = \frac{\prod_{k=1}^{n} P_1(y_k)}{\prod_{k=1}^{n} P_0(y_k)} \tag{3}$$

The sequential probability ratio test (SPRT) is carried out by comparing Λ_n with two thresholds, an upper threshold, T_u and a lower threshold T_l.

If $\Lambda_n \geq T_u$ hypothesis H_1(*signal present*) is decided and the search is stopped.
If $\Lambda_n \leq T_l$ hypothesis H_0(*signal absent*) is decided and the code epoch is updated.
If $T_l \leq \Lambda_n \leq T_u$ sample Λ_{n+1} is taken and the test is repeated for the same relative phase between the codes.

Substituting the density functions in (3) and taking the logarithm, the accumulated log-likelihood function over i samples becomes:

$$v_i = \sum_{k=1}^{i} (-\gamma + \ln[I_o(2y_k\sqrt{\gamma/2\sigma^2})]) \tag{4}$$

where

$$\gamma = A^2/2\sigma^2 \tag{5}$$

and γ is the predetection SNR.

On approximating the '$\ln I_o[\ ]$' by the first two terms of its power series expansion, v_i can be reduced to a simple form:

$$v_i = \sum_{k=1}^{i} (y_k - b) \tag{6}$$

where b is the bias of the log-likelihood function, $b = N_o B(1+\gamma)$ with the symbols same as defined earlier.

EFFECT OF DATA MODULATION ON THE CORRELATION FUNCTION

The log-likelihood function defined above does not model the loss of correlation due to the data modulation present on the carrier. When the data is added, the received signal with data modulation, $r(t)$ can be written as:

$$r(t) = A\,d(t+\xi T_o+\zeta T_c)\,c(t+\zeta T_c)\cos(\omega_c t + \theta) + n(t) \tag{7}$$

where $d(t)$ and $c(t)$ are the data and code sequences, T_c is the chip time of the PN code, T_o is the data bit time which is assumed to be a multiple of T_c, ζT_c is the received code phase offset, $\xi T_o + \zeta T_c$ is the received data bit phase offset assuming that the data stream timing is synchronized to the code chip time , ω_c and θ are the carrier frequency and random phase respectively and $n(t)$ is the additive white Gaussian noise with one-sided power spectral density N_o.

The code despreading is done at baseband and the correlator signal representing a sample value on the correlator curve is:

$$x(t) = u\cos(\theta) + n(t) \tag{8}$$

$$u = A\,d(t+\xi T_o+\zeta T_c)\,c(t+\zeta T_c)\,c(t+\tau T_c) \tag{9}$$

where τT_c represents the local code phase offset.

When $x(t)$ is passed through the envelope detector, the presence of data in the carrier causes degradation in the output of the correlator since the correlation across the data bit boundaries can result in the loss of the wanted signal when the data bit polarity changes. Normally, this data modulation distortion effect can be reduced by using a combined output from a bank of parallel I-Q detectors, each matched to a different pattern, which the data sequence can assume within the correlation interval. However, the number of such detectors could be quite high as it depends on the number of data bits integrated and the resolution of data epoch uncertainty. Another method is to employ square law noncoherent combining detection in which the correlation time is partitioned into a number of subintervals. The integration results in these subintervals can then be combined noncoherently for detection. Recently, such a scheme has been analyzed by Cheng [7]. Using this method the effect of data modulation is reduced at the cost of combining loss. Although this is not as efficient as the parallel bank of I-Q detectors, it does not suffer from the penalty of complexity.

In the sequential detectors simulated here, the envelope detector samples are directly emphasized by the nonlinearity function '$\ln I_o[\ ]$' and the result is accumulated for the threshold comparisons. Therefore, the correlation interval cannot be partitioned into subintervals for combining directly. However, a parallel implementation is possible, whereby a bank of detectors each with

its own sequential detection algorithm can be matched to a different data pattern. In this paper, a single sequential detector's acquisition performance with data modulated PN signals has been evaluated.

COMPUTER SIMULATION OF THE SEQUENTIAL DETECTORS

The acquisition performance of three types of sequential detector viz., an ideal log-likelihood sequential detector, a quantized log-likelihood sequential detector and a biased square law sequential detector in noise were simulated by means of a Monte Carlo computer simulation. A pseudo-noise code sequence of length $L = 127$ and chip rate $R_c = 1/T_c = 100Kb/s$ was modulated by a random binary data sequence at a rate, $1/T_s = R_c/L = 1/LT_c$ with random data transitions. The channel was assumed to be the additive white Gaussian noise (AWGN).

For the quantized log-likelihood sequential detector, shown in figure 1, the number of quantization levels required for acceptable performance was found to be $Q = 32$, [5] and consequently in this paper the performance of the QLD with 32 quantization levels for data modulated PN signals has been examined. For the case of the biased square law detector, the log-likelihood function was approximated to the first two terms of the power series expansion and the simplified detector's performance was assessed. The ASN performance and the acquisition performance of all three detectors were determined for two bias values viz., Wald's optimum bias given by: $b_1 = \gamma(1 + \gamma/2)$ and a non-optimum bias given by: $b_2 = \gamma$.

DISCUSSION OF THE RESULTS

The acquisition performance of the sequential detectors depend critically on the threshold settings and the bias of the log-likelihood function, which is generally a function of the predetection SNR. As a result of our simulation, the average sample number (ASN), and the probability of detection (P_d) are observed to depend more on the lower threshold than the upper threshold whereas the probability of false alarm (P_{fa}) depends more on the upper threshold. Bias has the influence of changing all these variables. The signal gain after the envelope detection has been optimized to result in maximum probability of detection for a given probability of false alarm and predetection SNR. Three lower threshold values $T_l = -5.0, -2.0, -0.5$ and an upper threshold $T_u = 5.0$ are employed and the acquisition performance has been recorded for both the bias values b_1 and b_2.

The variation of the ASN with the predetection SNR has been observed to fall due to the increase in the bias. With the reduction in the level of the lower threshold, a rapid fall in the ASN with the predetection SNR has been observed [6]. The ASN for various sequential detectors with and without data is shown in figures 2 and 3 with the threshold values, $T_u = 5.0$ and $T_l = -5.0$. The presence of data does not significantly degrade the ASN performance, however, the acquisition performance is found to be affected as shown in figures 4 - 9 for each of the detectors and this is attributed to the reduced probability of detection as a result of correlation loss due to the data modulation.

The probability of detection and the probability of false alarm have been observed to fall with the increase in the predetection SNR for both the cases of with and without data modulation. This causes the minimum mean acquisition time, which is a function of the ASN, P_d and P_{fa}, to pass through a minimum as the predetection SNR increases. The increase in the ASN is responsible for the initial increase in the mean acquisition time at lower predetection SNRs whereas the reduction in P_d causes the mean acquisition time to increase after passing the optimum SNR. The optimum SNR and the minimum mean acquisition time have been observed to change with the bias and the figures show the performances for both bias values.

The acquisition performance of each detector with and without data modulation is plotted separately with $T_l = -5.0, -2.0, -0.5$ and $T_u = 5.0$. In all cases the curves are found to shift upwards, showing the degradation in the minimum mean acquisition time due to the loss in correlation due to filtering and envelope detection at the polarity changes caused by the data modulation.

The acquisition performance of the QLD closely agrees with that of the LLD with and without data modulation. For example, with the optimum bias the optimum SNR for the LLD and the QLD without data modulation is around 5-7dB with the minimum mean acquisition time ranging from 0.5-1.0sec (depending upon the value of the lower threshold) and 4-8sec for the same range of optimum SNR with data modulation. When the bias is changed, both the LLD and the QLD show similar changes in the performance for both with and without data modulation. The minimum mean acquisition time without data has now increased to 2-5sec whereas with data it does not show significant change. For the BSD at the optimum bias without data, the optimum SNR occurs around 3-4dB with the minimum mean acquisition time around 0.5-1.0sec. However with data, the optimum SNR reduces to between -1dB and 2dB with an increase in the minimum mean acquisition time of approximately 10sec. The actual minimum for the BSD occurs with a *non-optimum* bias around 10dB without data and around 8dB with data.

CONCLUSIONS

Three types of sequential detector have been simulated and their acquisition performance with and without data modulation has been compared. The degradation in the minimum mean acquisition time due to data modulation has been found to occur for all three types of detector and this is due principally to a reduction in the probability of detection, P_d rather than an increase in the ASN. Although the LLD and the QLD do not show significant changes in the optimum design SNR, the optimum design SNR for the BSD is found to be reduced by approximately 3dB. However, for all detectors the minimum mean acquisition time is found to increase by 5-10 times depending on the lower thresholds and the biases.

The quantized log-likelihood sequential detector agrees closely with the ideal log-likelihood sequential detector with and without data modulation and has broader optimum SNR characteristics than the BSD which shows a sharp increase in the mean acquisition time with increase in the predetection SNR. The use of the QLD for the

acquisition of PN spread-spectrum signals represents an easy to implement digital approach with a minimum mean acquisition time and is thus attractive for applications such as satellite communication and navigation and spread-spectrum mobile radio and data communication networks.

ACKNOWLEDGEMENTS

The authors wish to thank the Commonwealth Scholarship Commission and the British Council for their provision of a Commonwealth Scholarship to one of the aurthors (KVR) to carry out postgraduate research. The authors also wish to acknowledge the support provided by the Indian Space Research Organization to one of the authors in allowing study leave to pursue research at the University of Bath.

REFERENCES

1) A.Wald, Sequential Analysis, John Wiley,New York, 1947.

2) A.Wald and J.Wolfowitz, "Optimum character of the sequential probability ratio test", Annals of Math. Stat., vol.19, pp 326-339, 1948.

3) W.B.Kendall, "Performance of the biased square law sequential detector in the absence of signal", IEEE Trans. Inform. Theory, IT-11, pp 83-90, January 1965.

4) R.F.Cobb and A.D.Darby, "Acquisition performance of simplified implementations of the sequential detection algorithm", NTC Conference Record, pp 43.4.1-43.4.7, December 4-6, 1978, Birmingham, AL.

5) K.V.Ravi and R.F.Ormondroyd, "Computer simulation of a quantized log-likelihood sequential detector for faster acquisition of spread-spectrum pseudo-noise signals." 5th International Conference on Radio Receivers and associated systems, IEE Conference publication No. 325, pp 207-211, July 24-26,1990, Cambridge, UK.

6) K.V.Ravi and R.F.Ormondroyd, "Comparison of the acquisition performance of biased square law and quantized log-likelihood sequential detectors for PN acquisition" IEEE International Symposium on Spread Spectrum Techniques and Applications, Symposium Proceedings, pp 53-58, September 24-26,1990, London, UK.

7) U.Cheng, "Performance of a class of parallel spread-spectrum code acquisition schemes in the presence of data modulation" IEEE Trans. Comm, vol.36, No.5, pp 596-604, May 1988.

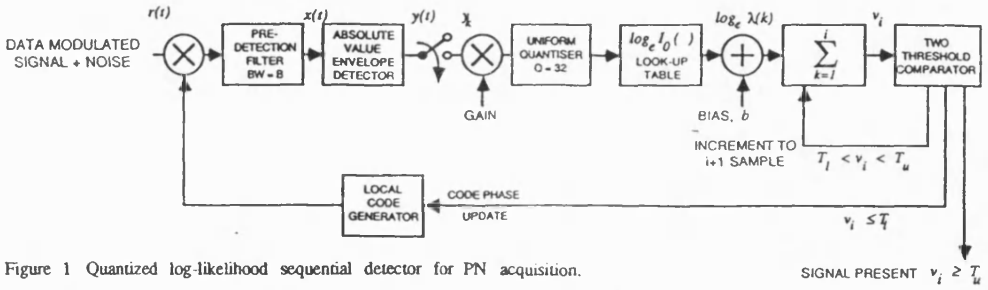

Figure 1 Quantized log-likelihood sequential detector for PN acquisition.

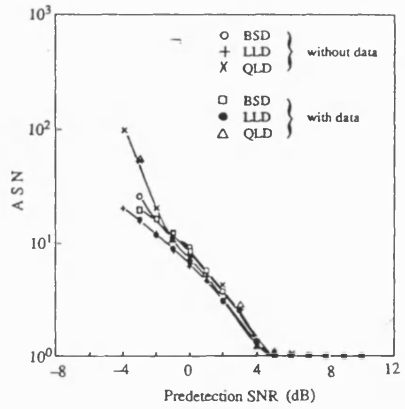

Figure 2 A S N vs Predetection SNR with $b = b_1$ for BSD,LLD and QLD.

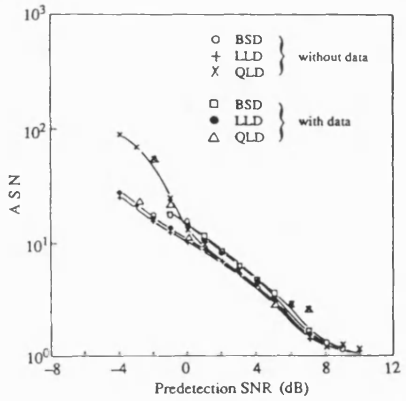

Figure 3 A S N vs Predetection SNR with $b = b_2$ for BSD,LLD and QLD.

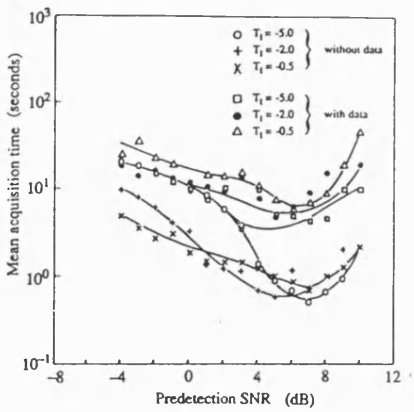

Figure 4 Mean acquisition time vs Predetection SNR with $b = b_1$ for LLD.

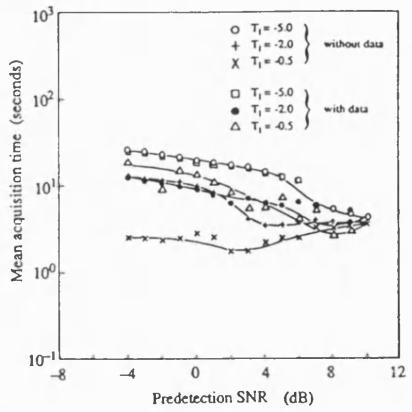

Figure 5 Mean acquisition time vs Predetection SNR with $b = b_2$ for LLD.

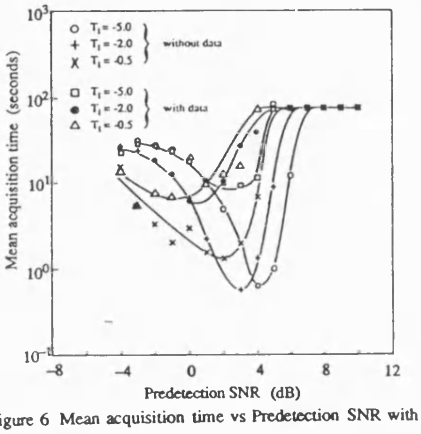

Figure 6 Mean acquisition time vs Predetection SNR with $b = b_1$ for BSD.

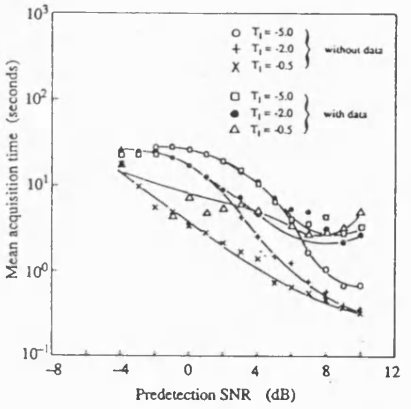

Figure 7 Mean acquisition time vs Predetection SNR with $b = b_2$ for BSD.

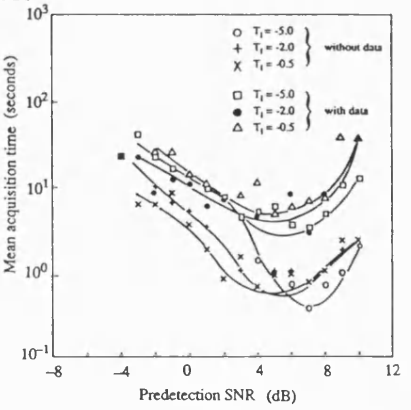

Figure 8 Mean acquisition time vs Predetection SNR with $b = b_1$ for QLD.

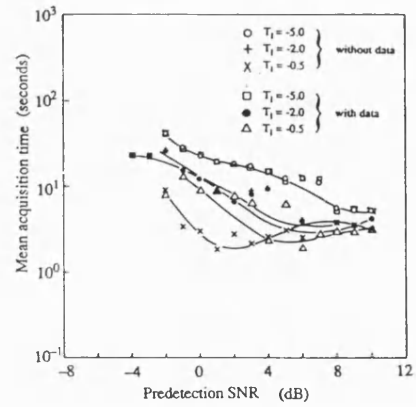

Figure 9 Mean acquisition time vs Predetection SNR with $b = b_2$ for QLD.

SIMULATION PERFORMANCE OF A QUANTIZED LOG-LIKELIHOOD SEQUENTIAL DETECTOR FOR PN CODE ACQUISITION IN THE PRESENCE OF DATA MODULATION AND DOPPLER SHIFT

K.V.Ravi and R.F.Ormondroyd

School of Electronic and Electrical Engineering
University of Bath, Bath, BA2 7AY, UK

ABSTRACT

The problem of initial acquisition of data modulated spread-spectrum PN codes in low SNR conditions using a variable-dwell time serial search synchronizer controlled by a sequential detector is addressed. The effect of carrier and code rate Doppler frequency offsets on the acquisition characteristics of three variants of sequential detector is assessed by means of a Monte-Carlo computer simulation and their performances are compared. The sequential detectors examined use : a) an ideal log-likelihood function, b) a quantized log-likelihood function and c) a 'biased square law' approximation to the log-likelihood function. In each case, the optimum operating conditions giving the minimum mean acquisition time have been found over the predetection SNR range from -4dB to 10dB. It is found that high code rate Doppler shifts are tolerated in the absence of data modulation and residual carrier Doppler frequency offsets. However, in the presence of data modulation with carrier Doppler frequency offset of 1 kHz and code rate Doppler frequency offset of 100 chips/s in a code rate of 100 kchips/s, the minimum mean acquisition time is degraded by 5-10 times, depending on the detector type and this requires the predetection SNR to be improved by 3-5 dB.

1.0 INTRODUCTION

Acquisition of pseudo-noise code synchronization in direct-sequence spread-spectrum systems is usually the first of a series of synchronization procedures which are required before the communication link can be established. Consequently, it is vital that it is achieved very quickly even though the channel condition may be such that the input SNR is worse than -30dB. This is particularly important for military communications and also for some satellite communication links where the time for synchronization needs to be a relatively small proportion of the available link time as in the case of low-earth orbit satellites and satellite navigation.

It is common to acquire coarse synchronization to within half a chip by performing a fixed-dwell serial search using either active or passive correlation. Such a technique does not take advantage of any *a priori* knowledge of the noise statistics in the channel and consequently these methods take as long to dismiss each wrong code epoch as to detect the correct code epoch. For most of the satellite communication links, the conditions of the channel are usually well defined and it is possible to take advantage of this to reduce the mean acquisition time of a spread-spectrum satellite link using a sequential detector. This type of synchronizer uses a variable-dwell serial search strategy in which the overall acquisition time is determined by the likelihood that the samples of the correlation between the local and wanted codes correspond to either the in-lock condition or the out-of-lock condition. The average number of samples of the correlation signal which is required to dismiss a code epoch (to a given probability) and step the relative code phase by one cell (usually half a chip), is known as the average sample number (ASN). The time to dismiss each wrong epoch is usually much less than the optimum dwell-time of a fixed-dwell serial search synchronizer, and this largely determines the mean acquisition time of the sequential detector. In this sense, the sequential detector is optimum because it minimizes the time taken to dismiss the wrong code epochs for a given false alarm rate and a given probability of correctly detecting the wanted code epoch.

The performance of sequential detectors with an ideal log-likelihood function (LLD) and a quantized log-likelihood function (QLD) have been analyzed by Ravi and Ormondroyd for the cases of no data modulation [1] and with data modulation [2]. However, for many satellite communication systems, a particular problem is that of Doppler frequency offset, with respect to both the carrier frequency and the clock frequency of the incoming PN codes. The carrier Doppler frequency offset has a detrimental effect because the IF bandwidth (and hence noise bandwidth) must be wider to accomodate the frequency offset. The code rate Doppler offset causes the two codes to be decorrelated, which reduces the probability of correctly detecting the wanted code epoch and also causes the generation of *self-noise* [3].

Though the code acquisition problem has attracted considerable attention recently, very few published analyses have considered both data modulation and Doppler effects. Of these, Holmes [4] has presented an approximate analysis of the performance degradation of a single-dwell serial search scheme due to Doppler offset on the code rate, but this analysis did not include the effect of the change in detection probability. Davisson and Flikkema [5] presented the performance results of a parallel acquisition scheme using maximum likelihood detectors for signals carrying data and affected by Doppler whilst Cheng *et al* [6] have considered the effect of code and carrier Doppler on spread spectrum acquisition using square law non-coherent combining detection with parallel/hybrid architectures.

The purpose of this paper is to examine, for the first time, the effect of both carrier and code Doppler on the mean acquisition time of a sequential detector. The degradation in the mean acquisition time due to both Doppler effects in the presence and absence of random binary data modulation will be analyzed for three types of sequential detector. The detectors examined are: a) the ideal

Paper to be presented in the 1991 IEEE Military Communications Conference, MILCOM'91, November 4-7, 1991, McLean, USA.

5) DS spread-spectrum signal with code Doppler frequency offset and data modulation.

6) DS spread-spectrum signal with code and carrier Doppler frequency offsets with data modulation.

These signals are represented as follow:
Signal type 1:

$$r_1(t) = A\,c(t-\zeta T_c)\cos(\omega_c t + \theta_c) + n(t) \quad (7)$$

Signal type 2:

$$r_2(t) = A_2(t)\cos(\omega_c t + \theta_c) + n(t) \quad (8)$$

$$A_2(t) = A\,c\left(\frac{t}{1-\zeta'} - \zeta T_c\right) \quad (9)$$

Signal type 3:

$$r_3(t) = A_3(t)\cos(\omega_c t) + n(t) \quad (10)$$

$$A_3(t) = A\,c\left(\frac{t}{1-\zeta'} - \zeta T_c\right)\cos(\omega_d t + \theta_c) \quad (11)$$

Signal type 4:

$$r_4(t) = A\,d(t-\xi T_o - \zeta T_c)\,c(t-\zeta T_c)\cos(\omega_c t + \theta_c) + n(t) \quad (12)$$

Signal type 5:

$$r_5(t) = A_5(t)\cos(\omega_c t + \theta_c) + n(t) \quad (13)$$

$$A_5(t) = A\,c\left(\frac{t}{1-\zeta'} - \zeta T_c\right) d\left(\frac{t-T}{1-\zeta'} - \xi T_o\right) \quad (14)$$

Signal type 6:

$$r_6(t) = A_6(t)\cos(\omega_c t) + n(t) \quad (15)$$

$$A_6(t) = A\,c\left(\frac{t}{1-\zeta'} - \zeta T_c\right) d\left(\frac{t-T}{1-\zeta'} - \xi T_o\right)\cos(\omega_d t + \theta_c) \quad (16)$$

The symbols used in the above equations are defined as: $d(t)$ and $c(t)$ are the data and code sequences with T_c the chip time of the PN code, T_o is the data bit time which is assumed to be an integral multiple of T_c, ζT_c is the received code phase offset, $\xi T_o + \zeta T_c$ is the received data bit phase offset assuming that the data stream timing is synchronized to the code chip time, ζ'/T_c is the received code frequency offset, ω_d is the received carrier radian frequency offset, T represents the beginning of the integration interval, ω_c and θ_c are the carrier radian frequency and random phase, and $n(t)$ is the additive white Gaussian noise with one-sided power spectral density N_o.

The output of the correlator at baseband representing a sample value on the correlator curve is

$$x(t) = u(t)\cos(\theta_c) + n(t) \quad (17)$$

$$u(t) = A\,c\left(\frac{t}{1-\zeta'} - \zeta T_c\right) d\left(\frac{t-T}{1-\zeta'} - \xi T_o\right) c\left(\frac{t}{1-\tau'} - \tau T_c\right) \quad (18)$$

where τT_c represents the local code phase offset and τ' represents the local code frequency error ($\zeta' - \tau' \ll 1$).

It is this correlator signal which is envelope detected and whose samples are directly emphasized by the nonlinearity function 'ln $I_o[\ ]$' of the sequential detector. The analytical solution of the log-likelihood sequential detector is extremely complex and this is the prime motivation for our computer simulation.

5.0 SYSTEM DESCRIPTION

The three types of sequential detector, were simulated by means of a baseband Monte-Carlo computer simulation. Direct-sequence spread-spectrum signals were simulated with a PN code length L = 127 and chip rate $R_c = 1/T_c = 100$ kchips/sec. These codes were modulated by a random binary data sequence at a rate, $1/T_o = R_c/L = 1/LT_c$ with random data transitions. A Doppler code frequency offset of 100 chips/sec was impressed on the transmit PN code clock and a residual carrier frequency offset of 1kHz was also generated. An additive white Gaussian noise (AWGN) channel was simulated and the composite spread-spectrum signal was used to examine the acquisition performance of the sequential detectors.

All six signal structures described were generated and the performance of each detector has been obtained. For the quantized log-likelihood sequential detector shown in figure 1, the number of quantization levels required for acceptable performance has been found to be Q=32 [1], and consequently in this paper the performance of the QLD with 32 quantization levels, for all six signals, has been examined. For the case of the biased square law detector, the log-likelihood function was approximated to the first two terms of the power series expansion and the simplified detector's performance was assessed. The ASN performance and the acquisition performance of all three detectors were determined for two bias values viz., the normalized Wald's optimum bias given by: $b_1 = \gamma_{dm}(1 + \gamma_{dm}/2)$ and a non-optimum bias given by: $b_2 = \gamma_{dm}$ with γ_{dm} representing the design predetection SNR [7].

6.0 SIMULATION RESULTS AND DISCUSSION

The basic system parameters of the sequential detection system are i) T_u, ii) T_l, iii) bias, b and iv) design predetection SNR, γ_{dm}. The performance parameters are i) ASN, ii) probability of detection, P_d iii) probability of false alarm, P_{fa} and iv) total mean acquisition time, T_{acq}. The sequential detector's acquisition performance was found to depend on the threshold settings, the bias and the detector type itself. From earlier simulation results [1,2] it had been found that the variation of ASN and P_d depend more on T_l than on T_u whereas P_{fa} depends more on T_u and that the bias value, b, influences all these variables. The total mean acquisition time is dependent on a combination of ASN, P_d and P_{fa} as shown in [1].

For the purpose of the present simulation, three lower threshold values, T_l = -5.0,-2.0,-0.5 and an upper threshold value T_u = 5.0 are employed and the acquisition performance has been obtained for both the bias values b_1 and b_2. An overall acquisition probability of 0.9 is assumed. The sequential detector's acquisition performance for the predetection SNR range of -4dB to 10dB has been assessed and the optimum design SNR, γ_{dm} for the given system parameters, namely, b, T_u and T_l is determined. The acquisition characteristics have been obtained using this design SNR, γ_{dm} with γ varied about γ_{dm}.

Although the ASN characteristics provide an important insight into the detector's dismissal behaviour of wrong code epochs, in this paper emphasis is placed mainly on the mean acquisition time. In the figures which follow, the mean acquisition time is plotted as a function of the predetection SNR, γ. The six curves on each graph

correspond to the six signal types 1-6 as defined earlier. Signal type 1 is used as the reference signal for the purpose of comparison. In all the figures T_{acq} is maximum at very low γ and decreases with increasing γ. However, as γ is increased further, T_{acq} passes through a minimum. The reasons for this are attributed to the dominance of P_d and P_{fa} which are dependant on γ. At a very low γ both P_d and P_{fa} are very low and it is the reduced P_d that causes a high T_{acq} whereas at a very high γ both P_d and P_{fa} are very high and it is the false alarm penalty which causes the T_{acq} to increase once again. The best combination of P_d and P_{fa} produces the minimum T_{acq} and the γ at which it occurs is the optimum γ, referred to as γ_{opt}. However, with changing system parameters, the ASN and the rate at which P_d and P_{fa} vary also change. This causes a change in both the minimum T_{acq} and the γ_{opt}.

Figures 2 and 3 show the characteristics of the LLD with bias values b_1 and b_2. With Wald's optimum bias, b_1, signal type 1 produces the minimum T_{acq}. This is approximately 0.5sec and γ_{opt} occurs at 7dB. The addition of Doppler shift and/or data modulation is found to degrade both the minimum T_{acq} and the γ_{opt}. The addition of code Doppler only (signal type 2), degrades T_{acq} slightly whereas with the addition of both the Doppler frequency offsets (signal type 3), the degradation is severe. For signal type 2, the minimum T_{acq} is 1.5sec with a γ_{opt} at 8dB, representing a 1dB degradation in the γ_{opt} and a threefold increase in minimum T_{acq}. Signal type 3 causes 3dB degradation in γ_{opt} and an almost eightfold increase in the minimum T_{acq}. When data is added the degradation is seen to be worse still. With the addition of data (signal type 4), the minimum T_{acq} is increased to 2sec whereas with Doppler shift ie., signal types 5 and 6, it is 4sec and 5sec respectively. The degradation in γ_{opt} for these signal types is more than 3dB. When the bias is changed to a non-optimum value, b_2, as shown in figure 3 the degradation in the minimum T_{acq} at higher values of γ is similar for all signal types, and the minimum T_{acq} is around 5sec. However, the degradation in T_{acq} is quite different at lower predection SNRs.

In figures 4 and 5, the performance of the QLD is considered. With the bias values, b_1 and b_2 the QLD has a performance which closely matches with that of the LLD. The worst case minimum T_{acq} for this detector is also found to occur with signal type 6 and it is approximately 6sec for a value of γ_{opt} at 10dB. The performance of the BSD, which is shown in figures 6 and 7, is slightly different from the performance of the LLD and the QLD. It has better characteristics at lower γ with Wald's optimum bias, b_1. The minimum T_{acq} varies from 3sec to 5sec for signal types 2-6 resulting in an increase of 3-5 times compared to that of signal type 1. The γ_{opt} is close to 8dB for signal types 3-6 which amounts to a degradation of 2dB only compared to the performance of signal type 1. However, for signal type 2, it is at 4dB, representing an improvement of 2dB in the γ_{opt}. With the non-optimum bias b_2, signal types 1 and 4 show a minimum T_{acq} at a higher γ; however, the drift towards lower γ is prominant with the rest of the signal types. The minimum T_{acq} remains to be close to 5sec for signal types 3-6 and 1sec for signal type 2. This drift in γ towards lower values is expected because the BSD has been found to be a good approximation to the log-likelihood function at low SNRs [8].

7.0 CONCLUSIONS

The degradation due to both carrier and code Doppler frequency offsets in the presence of data modulation is found to be quite significant for all the three types of sequential detector. However, the degradation in the performance of the QLD is similar to that of the LLD. Both detectors show a drift of +3dB in γ_{opt} and the minimum mean acquisition time is found to increase by 10 times without data modulation. With the data modulation, there is a drift of +2dB in γ_{opt} and minimum T_{acq} increases by more than 10 times. The performance of the BSD is better at lower γ than either the QLD or the LLD, particularly at Wald's optimum bias. However, the degradation in γ_{opt} with code and carrier Doppler frequency offsets is 3dB and the minimum T_{acq} is increased by 4 times without data modulation; but with data modulation, γ is degraded by 3dB and the minimum T_{acq} is increased by 5 times.

Even though degradation due to code and carrier Doppler in the presence of data is quite significant for all the three detectors, when only code Doppler is present the degradation seems to be tolerable.

8.0 ACKNOWLEDGEMENTS

The authors wish to thank the Commonwealth Scholarship Commission and the British Council for their provision of a Commonwealth Scholarship to one of the authors (KVR) to carry out postgraduate research. The authors also wish to acknowledge the support provided by the Indian Space Research Organization to K.V.Ravi in allowing him study leave to pursue research at the University of Bath.

9.0 REFERENCES

1) K.V.Ravi and R.F.Ormondroyd, "Comparison of the acquisition performance of biased square law and quantized log-likelihood sequential detectors for PN acquisition" IEEE International Symposium on Spread Spectrum Techniques and Applications, Symposium Proceedings, pp 53-58, 1990, London, UK.

2) K.V.Ravi and R.F.Ormondroyd, "Performance of sequential detectors for the acquisition of data modulated spread spectrum pseudo noise signals", IEEE International Conference on Communications, ICC'91, Conference Record, vol. 2, pp 19.7.1-19.7.5, June 23-26, 1991, Denver, Colorado, USA.

3) R.F.Ormondroyd and V.E.Comley, "Limits on the search rate of a sliding correlator synchroniser due to the effects of self-noise and decorrelation" IEE Proceedings, Part F, vol. 131, no. 7, pp 742-750, December 1984.

4) J.K.Holmes, *Coherent Spread Spectrum Systems*, John Wiley & Sons, New York, 1982.

5) L.D.Davisson and P.G.Flikkema, "Fast single-element PN acquisition for the TDRSS MA system" IEEE Trans. on Communications, vol.36, no. 11, pp 1226-1235, November 1988.

6) U.Cheng, W.J.Hurd and J.I.Statman, "Spread-spectrum code acquisition in the presence of Doppler shift and data modulation" IEEE Trans. on Communications, vol. 38, no. 2, pp 241-250, February 1990.

7) A.Wald, *Sequential Analysis*, John Wiley, New York, 1947.

8) W.B.Kendall, "Performance of the biased square-law sequential detector in the absence of signal" IEEE Trans. on Inform. Theory, IT-11, pp 83-90, January 1965.

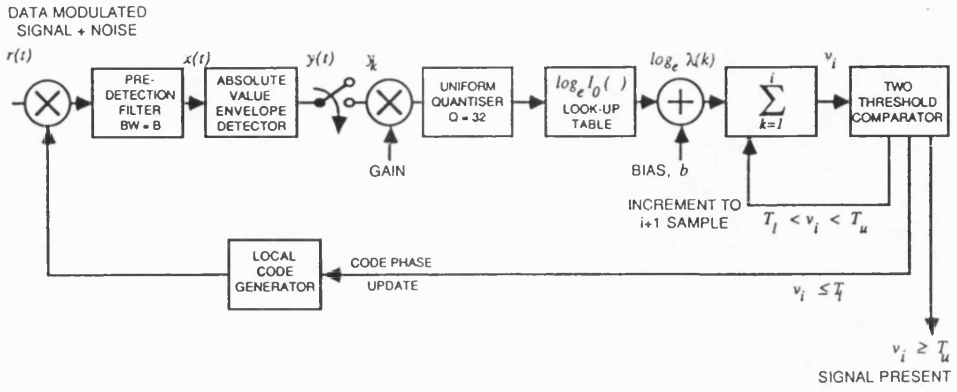

Figure 1. Schematic diagram of the quantized log-likelihood sequential detection PN acquisition system.

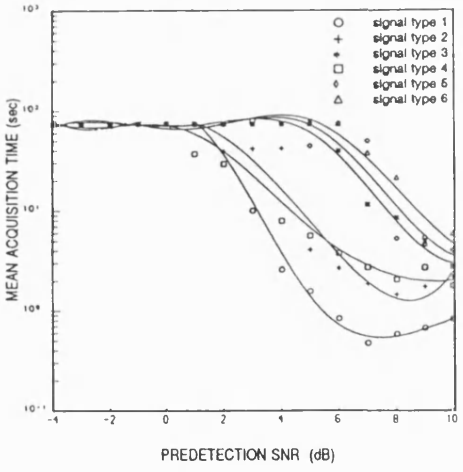

Figure 2. Mean acquisition time vs. predetection SNR for the LLD at bias $b = b_1$.

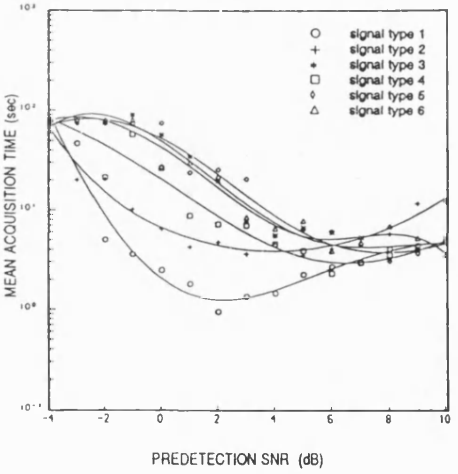

Figure 3. Mean acquisition time vs. predetection SNR for the LLD at bias $b = b_2$.

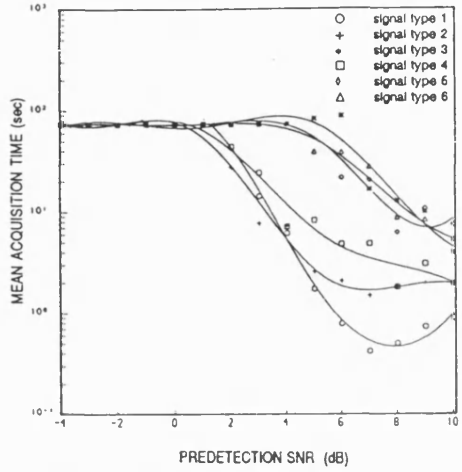

Figure 4. Mean acquisition time vs. predetection SNR for the QLD at bias $b = b_1$.

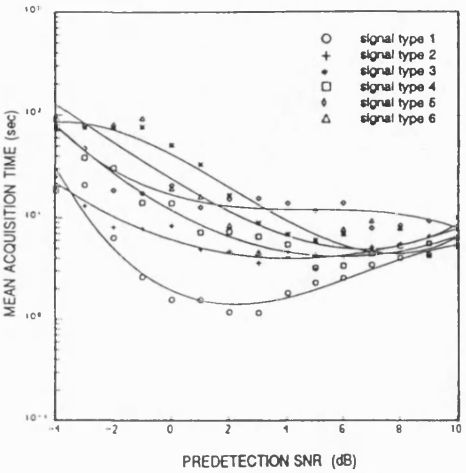

Figure 5. Mean acquisition time vs. predetection SNR for the QLD at bias $b = b_2$.

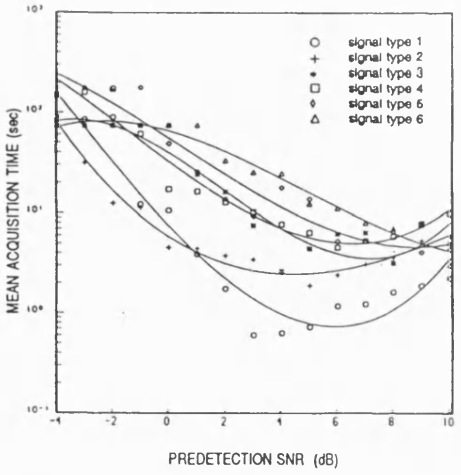

Figure 6. Mean acquisition time vs. predetection SNR for the BSD at bias $b = b_1$.

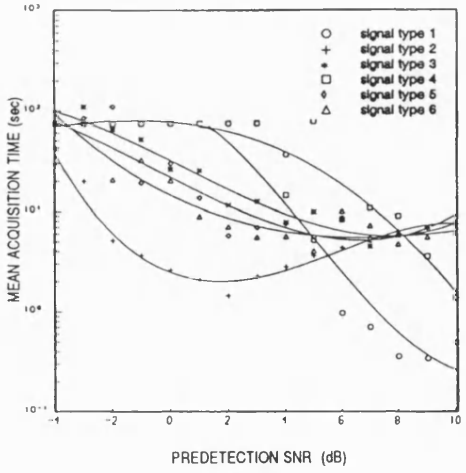

Figure 7. Mean acquisition time vs. predetection SNR for the BSD at bias $b = b_2$.

PERFORMANCE OF THE SERIAL-SEARCH PN CODE ACQUISITION TECHNIQUES USING MONTE CARLO SIMULATION - A COMPARATIVE EVALUATION

R.F.Ormondroyd and K.V.Ravi

School of Electronic and Electrical Engineering
University of Bath, Bath, BA2 7AY, UK

ABSTRACT

A comparative performance analysis of: a) the non-coherent fixed-dwell detector serial-search PN code acquisition, b) the digital matched filter and c) the non-coherent sequential detector methods is presented using Monte-Carlo simulations to obtain the detector characteristics. Their performance was assessed over a predetection SNR range of -4dB to 10dB for the case of no data modulation. The critical dependance of the mean acquisition time on the system parameters has been analyzed and the optimization of these parameters to obtain minimum mean acquisition time has been achieved for each detector.

The results show that the sequential detector, working at an optimized design predetector SNR, performs better than both the single-dwell detector and the matched filter at low input SNRs. However, as the predetection SNR is increased, the matched filter has a significantly improved performance and performs the best at high SNRs.

1.0 INTRODUCTION

Code acquisition is a critical aspect of spread-spectrum receivers and several code acquisition strategies, namely, serial search techniques, maximum likelihood detection and sequential estimation, have been used for this purpose. In this paper, our examination is restricted to serial search techniques. PN code synchronization is generally carried out prior to carrier synchronization and data bit synchronization and it is usual to use a non-coherent synchronizer to remove the effects of data modulation and residual carrier Doppler frequency offsets. Figure 1 shows a schematic of a typical non-coherent serial search synchronizer using an active correlator. The code is first correlated with the local code, and the baseband output gives a measure of phase synchronization between the two codes. This output is corrupted by noise however, and it must be further processed in the detector to improve the probability of correctly identifying whether the signal corresponds to a coarse in-lock correlation or an out-of-lock correlation. If the latter decision is made, the local code phase is advanced by one cell (usually half a chip) and the search is continued. If the former decision is made, the search is stopped and code synchronization is then verified by longer term correlation and a tracking loop initiated.

The acquisition performance of the system is determined by the correlator type, the detector type and the SNR at the input to the detector (defined here as the predetector SNR, which is related to the receiver input SNR *via* the spread-spectrum process gain). Three acquisition systems are considered, namely: a) a non-coherent single-dwell detector, b) a matched filter and c) a non-coherent sequential detector. In the fixed-dwell detector, the baseband samples from the active correlator are simply accumulated for a fixed time period. At the end of this period a simple threshold detector is used to decide whether the correlator output signal corresponds to the coarse in-lock case or the out-of-lock case. Because of the noise, short integration periods result in a low probability, P_d, of detecting the wanted (ie in-lock) signals and a high probability of false alarm detections, P_{fa}. Long integration periods, on the other hand, improve the probability of a correct decision, but the time taken to dismiss each code cell is longer. Consequently, at every value of predetector SNR there is an optimum dwell-time which results in minimum acquisition time.

In the digital matched filter, the known code sequence is stored as the tap weights of the filter. The matched filter combines the action of the correlator and fixed-dwell integrator, and the output samples from the matched filter are fed directly to the threshold detector. In this case, if the signal does not exceed the threshold the out-of-lock condition is assumed and the next sample of the incoming sequence is clocked into the matched filter and a new filtered output sample is obtained which is checked against the threshold. If the threshold is exceeded, coarse synchronization is declared. Due to the effects of noise, it is possible to either miss wanted signal samples or for false alarm synchronization decisions to be made. Both of these events lengthen the acquisition time, as for the the fixed-dwell system.

The fixed-dwell detector supplies samples to the threshold detector at a relatively slow rate (typically the sequence repetition frequency), whereas the digital matched filter provides samples at the chip rate. It would appear, therefore, that the matched filter should always offer faster acquisition than the fixed-dwell detector. However, as will be shown, at low SNRs, P_d can be lower and P_{fa} can be much higher for the matched filter than the fixed-dwell detector and this overturns any benefits resulting from the higher sample rate.

Fixed-dwell systems are inefficient because they take just as long to dismiss each of the many wrong code epochs as to obtain the correct epoch. Serial-search techniques employing a variable-dwell time controlled by a sequential detector can overcome this problem by minimizing the time taken to dismiss out-of-lock signals. The incoming and locally generated codes are actively correlated, as before, and the likelihood that each correlator sample is either the in-lock signal or an out-of-lock signal is obtained in the

Paper to be presented in the 1991 IEEE Military Communications Conference, MILCOM'91, November 4-7, 1991, McLean, USA.

sequential detector using *a priori* information regarding the noise statistics of the channel. These likelihood ratios are accumulated and the accumulator value is tested against two thresholds. The lower threshold T_l, indicates that the two codes are not in-lock, and causes the local code epoch to be incremented by one cell and the search continued. The upper threshold T_u, indicates detection of the correct code epoch. If the accumulated likelihood ratio falls between the two threshold levels, a further correlator sample is taken without advancing the local code epoch, and the sequential probability ratio test repeated.

The performance of all these techniques depends critically on many system parameters and the input SNR range of interest [1-3]. The analytical approch, using signal flow graph techniques developed in [1,2], present general expressions for mean acquisition time and its variance. These analyses require the knowledge of the *generating function* of the acquisition time which depends on the transition probability distributions of the underlying discrete-time Markov process that describes the acquisition process. In many cases however, obtaining the probability distribution of the acquisition time in closed form is extremely difficult and a system simulation is required to evaluate these probability distibutions before the analytical expressions can be used. In this paper, a performance analysis of the three types of detector employing a serial-search strategy is presented by means of the Monte-Carlo simulation method. This is used to obtain the operating characteristics of each detector and from this the acquisition performance of each search strategy has been evaluated analytically. Because the detector characteristics are being found by simulation, fewer approximations have been made than would be the case for a fully analytic solution of the integral equations describing the detector characteristics.

2.0 DETECTOR THEORY

A. Sequential detector

In the sequential detector, the likelihood ratio, which is the ratio of the *a priori* probabilities of the incoming signal sample corresponding to the in-lock and the out-of-lock conditions, is accumulated and compared against thresholds T_l and T_u to decide whether the in-lock signal is present or absent. The test is expressed as:

$$\begin{aligned} d_0 &: v_i \geq T_u \Rightarrow \textit{hypothesis } H_1(\textit{signal present}) \\ d_1 &: v_i \leq T_l \Rightarrow \textit{hypothesis } H_0(\textit{signal absent}) \\ d_2 &: T_l < v_i < T_u \Rightarrow \textit{take sample } v_{i+1} \textit{ and continue} \end{aligned} \tag{1}$$

where $T_l < 0 < T_u$ and v_i is the log-likelihood ratio for i samples given by:

$$v_i = \ln \frac{\prod_{k=1}^{i} P_1(y_k)}{\prod_{k=1}^{i} P_0(y_k)} \tag{2}$$

$P_1(y_k)$ and $P_0(y_k)$ are the *a priori* probabilities corresponding to the in-lock signal plus noise and the out-of-lock signal plus noise, respectively. If the noise in the spread-spectrum channel is assumed to be broadband Gaussian noise, $P_1(y_k)$ has a Rician distribution and $P_0(y_k)$ has a Rayleigh distribution if the out-of-lock signal level is assumed to be zero. On substituting these distributions into (2), the log-likelihood function becomes :

$$v_i = \sum_{k=1}^{i} (-\gamma + \ln[I_o(2y_k\sqrt{\gamma/2\sigma^2})]) \tag{3}$$

$$\gamma = A^2/2\sigma^2 \tag{4}$$

where $I_o(\,)$ is the modified Bessel function of the first kind and zero order, γ is the predetection SNR, A is the rms signal amplitude, $\sigma^2 = N_o B/2$ is the variance of the Gaussian noise process with N_o as the one sided noise spectral density and B is the predetector filter bandwidth.

The mean acquisition time of the sequential detector can be approximately related to the average sample number, *ASN*, and the detector probabilities by:

$$T_{acq} = T_{dis}\left[1 + \frac{(T_{tr}+T_{tr})P_{fa}}{T_{dis}}\right] q \left[\frac{\ln(1-P_{acq})}{\ln(1-P_d)}\right] \tag{5}$$

where T_{dis} is the mean dismissal time given by:

$$T_{dis} = ASN/B \tag{6}$$

P_{acq} is the probability of overall acquisition (assumed to be equal to 0.9 in the present simulation), T_{tr} and T_{tr} are the false alarm verification and truncation times (each assumed to be 50ms) and q is the total number of code cells in the uncertainty region to be searched.

The decision probabilities P_d and P_{fa} and the *ASN* of the sequential detector are governed by integral equations of the form shown below. The probability that the test ends with either decision d_0 or d_1 satisfies the integral equation [4]:

$$p_i(x_o) = \pi_o(x_o) + \pi_o(x_o)\int_{-\infty}^{\infty} p_i(y)\, dF(y/x_o) \tag{7}$$

where $\{x_i\}$ represents the sample sequence, $p_i(x_o)$ represents the probability that the sequential test starting at sample x_o ends with the decision d_i, $i=0,1,2$, $F(x_i/x_{i-1})$ is the probability distribution function governed by the transitions of the stationary Markov process describing the samples and $\pi_i(x_o)$ is the probability of making one of the decisions d_i.

The average sample number (*ASN*) also satisfies a similar integral equation [4]:

$$m_1(x_o) = \pi_o(x_o) + \pi_o(x_o)\int_{-\infty}^{\infty} m_1(y)\, dF(y/x_o) \tag{8}$$

where $m_1(x_o)$ is the first moment of the distribution of the test duration which is the *ASN*. The rest of the symbols are as defined earlier. These equations are extremely difficult solve analytically for realistic system configurations, and for this reason the detector characteristics have been found by simulation.

B. Digital matched filter

For a code sequence of length L, with a chip rate $f_c = 1/T_c$, the correlator signal consists of a train of impulses occuring at a frequency L/f_c corresponding to the in-lock condition. Because of noise on the input signal, the matched filter output samples have a random component giving rise to false alarms and missed detections of this in-lock signal. Let T_v be the time interval in which a false alarm occuring can affect the v^{th} impulse at an instant t_v, and

let P_{dv} be the probability of detecting this correlation impulse. If P_d is the probability of detection of a correlation impulse, n_{fa} is the false alarm rate of the detector with T_w as the false alarm verification time, then the mean acquisition time T_{acq}, is given by [5]:

$$T_{acq} = \frac{L}{2f_c}\left[P_{d1}+\sum_{v=1}^{\infty}(2v+1)P_{dv+1}\prod_{p=1}^{v}(1-P_{dp})\right] \quad (9)$$

where P_{dv} and T_v are given by:

$$P_{dv} = P_d \exp(-n_{fa}T_v) \quad (10)$$

$$T_v = \min(T_w, [v+0.5]\,L/f_c) \quad (11)$$

Using an approximate analysis based on the Gaussian assumption of the decision statistic applicable to the low input SNRs, and assuming a practical case where the correlator length M, satisfies $1 << M << L$ for a very long code length L, the probability of detection P_d and the probability of false alarm P_{fa} are given by:

$$P_d = Q(\gamma_d,\beta_d) = \int_{\beta_d}^{\infty} x \exp[-1/2(x^2+\gamma_d^2)]I_o(\gamma_d x)\,dx \quad (12)$$

$$P_{fa} = \exp\left\{-1/2\frac{c}{1+\gamma_c G_o(p)}\right\} \quad (13)$$

where $Q(\gamma_d,\beta_d)$ is the Marcum Q-function with γ_d and β_d given by

$$\gamma_d = \sqrt{2M\gamma_c\frac{(1-|p|)^2}{1+\gamma_c G_1(p)}} \quad (14)$$

$$\beta_d = \sqrt{\frac{c}{1+\gamma_c G_1(p)}} \quad (15)$$

and

$$G_i(p) = p^2 \qquad i=1$$
$$= 1-2|p|+2p^2 \qquad i=0 \quad (16)$$

$$c = 2\frac{R_o^2}{N_o}MT_c \quad (17)$$

where c is the normalized threshold with R_o as the correlator output, γ_c is the decision SNR on a per cell basis, MT_c is the correlation time in seconds and p is the code phase offset. Alternatively, an exact analysis of the noncoherent I-Q matched filter detector has been derived by Polydoros and Weber [2].

C. Single-dwell detector

The mean acquisition time of the single-dwell detector can be derived analytically using the Markov chain model of the acquisition process, and is given by the relationship:

$$T_{acq} = \frac{(2-P_d)(1+KP_{fa})}{2P_d}q\tau_d \quad (18)$$

where P_d and P_{fa} are the detector decision probabilities and K is the false alarm penality factor ($T_w = K\tau_d$ sec). The envelope detector output is sampled at a rate $1/T_s \le B$ which ensures sufficiant sample decorrelation so that the samples can be treated as independant identically distributed random variables. In this case the integrator output (for a large number of samples to enable the application of the central-limit theorem) may be assumed to have Gaussian statistics and the detector probabilities are given by:

$$P_{fa} = Q[\beta] \quad (19)$$

$$P_d = Q[(\beta-\sqrt{B\tau_d}\,\gamma)/\sqrt{1+2\gamma}] \quad (20)$$

where $Q[x]$ is the Gaussian probability integral with β given by

$$\beta = (\eta-B\tau_d)/\sqrt{B\tau_d} \quad (21)$$

For a given P_d, P_{fa}, γ, B and normalized threshold level, η; the dwell time τ_d can be determined easily. However, a basic design problem is to choose the optimum threshold and dwell time that can provide a minimum mean acquisition time for a given input SNR. Since P_d and P_{fa} are functions of the threshold, the dwell time and γ and, moreover, they are related transcendentally, in this paper, these equations are solved numerically as a two dimensional problem and the simulated performance is compared with these results.

3.0 SYSTEM DESCRIPTION

The generalized block diagram of the serial search process is shown in figure 1. For comparison purposes, the direct-sequence PN code was simulated as a maximal length sequence of length $L = 127$, chip rate $f_c = 1/T_c = 100$ kchips/sec. For each detector, the correlator output samples was assumed to be corrupted with additive white Gaussian noise.

For each set of system parameters and for each detector, at least 100 tests were carried out. In each test, the incoming code sequence was started with a random phase and the search was carried out by examining the correlator output corresponding to each code cell and the number of correct detections, missed detections and false alarms were recorded to obtain the detector characteristics. For the given system parameters, these tests achieve P_d to an accuracy of 1×10^{-2} and P_{fa} to an accuracy of 1×10^{-4}.

For the case of the sequential detector, both the ideal log-likelihood function and the biased square law approximation to the log-likelihood function were simulated. The ASN and the acquisition characteristics of the two versions were obtained for two bias values, namely, Wald's normalized optimum bias $b_1 = \gamma(1+\gamma/2)$ and a non-optimum bias $b_2 = \gamma$ for three different threshold settings. From the acquisition characteristics obtained over the predetector SNR range -4dB to +10dB, corresponding to a receiver input SNR range of -25dB to - 11dB, the optimum design SNR to achieve minimum mean acquisition time was determined.

For the case of the serial-search system using a digital matched filter, the input to the matched filter was first passed through a one-bit A/D converter and the quantized input signal was fed to the one-bit digital matched filter, of length equal to the code length. The detector characteristics were obtained for a range of thresholds and the input SNRs and the acquisition performance was computed. The single dwell serial-search system was simulated for the same input signals without a hard quantizer and the detector operating characteristics were determined with the threshold and the dwell time varied for different input SNRs. The mean acquisition time was computed using the simulated values of P_d and P_{fa} and the three dimensional acquisition characteristcs were obtained and compared with the acquisition characteristics evaluated numerically.

4.0 SIMULATION RESULTS

A. Sequential detector

The acquisition performance of the sequential detector depends on the thresholds, T_u and T_l, the bias, b and the predetection SNR, γ. The total mean acquisition time is a function of *ASN*, P_d, P_{fa} *via* (5), but all these parameters are interrelated. From the simulation results [6,7] it was found that P_d is mainly decided by T_l and b while P_{fa} is decided by T_u and b. However, in each case the other threshold has a minor influence. In this simulation, three sets of thresholds have been employed with T_u = 5.0 and T_l = -5.0, -2.0 and -0.5 and for each set two bias values b_1 and b_2 are used.

Figures 2 and 3 show the variation of ASN and the T_{acq} with γ for various threshold levels of the ideal log-likelihood sequential detector (LLD) and the biased square law sequential detector (BSD). These results are obtained entirely from the simulation. The ASN of the sequential detector increases with decreasing γ and T_l. However, when biased at Wald's optimum b_1, the ASN is always better than for the non-optimum bias b_2. There is an optimum value of input SNR at which the acquisition time T_{acq} is a minimum for both types of sequential detector. The reason is that at low SNRs P_{fa} and hence ASN are high (equivalent to a long dwell-time), whereas at higher SNRs, although the ASN is low, P_d is reduced due to a very high bias b (which is related to γ) and this becomes the dominant term in (5).

For the LLD, the minimum T_{acq} is always better with b_1 than with b_2 whereas for the BSD it is better at the non-optimum bias b_2. This is due to the nature of the approximations of the BSD to the ideal log-likelihood function, which are more applicable at low SNRs and the non-optimum bias, b_2 is always lower than the optimum bias, b_1. The optimum γ at which the minimum T_{acq} occurs is considered as the design γ denoted by γ_{dm} for that set of parameters. It is found to be around 7dB for the LLD with a minimum T_{acq} of typically 0.5sec. For the BSD, it is around 10dB (at a non-optimum bias, b_2) with a similar value for the minimum T_{acq}. At lower input SNRs the BSD at the non-optimum bias has a better performance than the LLD at the optimum bias.

B. Digital matched filter

The performance of the matched filter system is dependant on the detector threshold and the receiver input SNR. The simulation has been used to obtain the detector characteristics, P_d and P_{fa} over a range of detector thresholds from 0.0 to 0.4 with the input SNR in the range of -28dB to -10dB (corresponding to an equivalent predetection SNR γ range of -7dB to +11dB). Using these simulated detector characteristics, T_{acq} has been computed using (9), (10) and (11). The variations of the probability of detection P_d and the false alarm rate n_{fa} with the threshold and input SNR are shown in figures 4 and 5.

For the 1 bit digital matched filter, the probability of detecting the wanted signal falls with input SNR, whilst the false alarm rate is largely independent of the input SNR, (when the SNR is sufficiently low). This is due to the effects of quantization which acts like an AGC system operating on the total input level to the receiver. At SNRs worse than -10dB this is effectively the noise level, so the false alarm rate, which is determined almost entirely by the noise level, remains constant. As the input SNR is reduced however, the effective wanted signal power is reduced by AGC action to maintain the total input power constant, and this causes P_d to be reduced. As the input SNR is reduced, it is necessary to reduce the threshold level in order to attempt to maintain P_d. However, there is a very heavy penalty in reducing the threshold below about 0.2 because this causes the probability of false alarm P_{fa}, and equivalently the false alarm rate, n_{fa}, to increase significantly, as shown in figure 5. As for the cases of the sequential detector and the single-dwell system, there is a tradeoff between setting the threshold level low so that P_d is high, with a correspondingly high P_{fa} and setting the threshold high so that P_d is low but with a low P_{fa}. This is clearly illustrated in figure 6 which shows that the mean acquisition time of the matched filter passes through a minimum as the threshold level is varied for a wide range of receiver input SNRs

It will be noted that the acquisition time is *extremely* sensitive to the threshold value and for practical implementations this effect could pose many practical problems. It is also of interest to note that the optimum performance of the matched filter is obtained at a much lower probability of detection P_d (always < 0.2) and at a false alarm rate n_{fa} which is also quite low (< 100). This implies that the optimum detector always performs on the tails of the probability distributions of both signal and noise. From figure 6, it is seen that the best case minimum mean acquisition time is close to 1×10^{-2} sec at -10dB input SNR but this increases to about 1sec when the input SNR is -28dB (for the design parameters considered).

C. Single-dwell detector

The acquisition performance of the single dwell detector depends on the threshold η, τ_d, and the predetection SNR γ. A three dimensional acquisition characteristic was obtained by numerical solution to (18) - (21) and is shown in figure 7. This shows T_{acq} as a function of η and τ_d for an input SNR at -15dB (corresponding to an equivalent predetector SNR, γ = 6dB). The acquisition characteristics show a minimum with τ_d. On the low τ_d side of the minimum, this is due to the fall in P_d with lower τ_d. Although P_{fa} increases over the same range of τ_d, unless the penalty factor K is very large, from (18) T_{acq} is reduced. At higher values of τ_d, T_{acq} increases due to the direct effect of τ_d in (18). However, as the threshold η is decreased, P_d starts increasing even at a lower values of τ_d and the minimum T_{acq} can be reduced further. Although the minimum value of T_{acq} can be decreased by lowering both the η and the τ_d, P_d and P_{fa} start saturating, and then T_{acq} is solely determined by the optimum value of τ_d. The curves also show a barrier for lower values of τ_d and higher values of η which is due to the wanted signal always being below the threshold level which gives 100% missed detections. The single dwell detector has also been simulated at a fixed value of SNR to obtain its detector characteristics, rather than solving (19) - (21). The simulated detector characteristics are shown in figure 8 for an input SNR of -15dB. The simulation also shows similar characteristics (for the limited range of parameters considered) with the barrier at low τ_d and high η. The T_{acq} characteristic also shows the minimum with dwell-time which is typically τ_d = 25 msec for an input SNR = -15dB. The minimum T_{acq} for this SNR is found to be around 0.88sec which is comparable to that of the matched filter in the worst case situation.

5.0 COMPARISON OF ACQUISITION PERFORMANCE AND CONCLUSIONS

From the simulated performance of the three detectors operating at their optimum design parameters, the matched filter shows a very good performance at the higher SNR when compared with the single-dwell detector and the sequential detectors. However, when the input SNR is decreased the performance of all the detectors show a deterioration. The performance of the matched filter however, falls at a much faster rate, rendering it difficult to operate in SNRs less than typically -25dB. The ideal log-likelihood detector is found to work well at predetection SNRs close to the design SNR when biased optimally. However, the biased square law detector (BSD), shows a better low SNR performance at a non-optimum bias. The LLD achieves a minimum T_{acq} close to 0.5 sec at an optimum design SNR of 7dB, corresponding to a receiver input SNR of -14dB. Though the design SNR is different for the BSD, it also achieves minimum T_{acq} of the same order as the LLD. The digital matched filter, however, needs to be optimized at an optimum threshold $\eta = 0.3$ and the optimum threshold is quite sharp with respect to the input SNR. The single-dwell detector needs the dwell-time to be optimized for better performance at higher thresholds. Nevertheless, at lower thresholds the minimum T_{acq} is fully determined by the dwell-time itself if the verification penalty factor, K, is small.

At a moderate input SNR of -15dB, the single dwell detector has a minimum T_{acq} = 0.88sec whereas the matched filter shows an acquisition time around 0.6sec. The sequential detector at an equivalent predetection SNR (around 7dB) produces an acquisition time of around 0.5sec. When the SNR is very poor, for example at an input SNR = -25dB, the sequential detector, particularly the BSD, shows the best performance.

6.0 REFERENCES

1) J.K. Holmes and C.C. Chen, "Acquisition performance of PN spread-spectrum systems" IEEE Trans. on Comm. vol. com-25, no. 8, pp 778-783, August 1977.

2) A. Polydoros and C.L. Weber, "A unified approach to serial-search code acquisition- Part II: A matched filter receiver" IEEE Trans. on Comm. vol. com-32, no. 5, pp 550-560, May 1984.

3) V.M. Jovanovic, "Analysis of strategies for serial-search spread-spectrum code acquisition- Direct approach" IEEE Trans. on Comm. vol. 36, no. 11, pp 1208-1220, November 1988.

4) W.B. Kendall, "Performance of the biased square-law sequential detector in the absence of signal" IEEE Trans. on Inform. Theory, IT-11, pp 83-90, January 1965.

5) M. Pandit, "Mean acquisition time of active and passive correlation systems for spread-spectrum communications", IEE Proceedings, vol. 128 Part F, pp 100-109, 1981.

6) K.V. Ravi and R.F. Ormondroyd, "Comparison of the acquisition performance of biased-square-law and quantized log-likelihood sequential detectors for PN acquisition", Proceedings of the IEEE International Symposium on Spread-spectrum Techniques and Applications, pp 53-58, 1990, London, U.K.

7) K.V. Ravi and R.F. Ormondroyd, "Performance of sequential detectors for the acquisition of data modulated spread-spectrum pseudo noise signals", IEEE International Conference on Communications, ICC'91, Conference Record, vol. 2, pp 19.7.1-19.7.5, June 23-26, 1991, Denver, Colorado, USA.

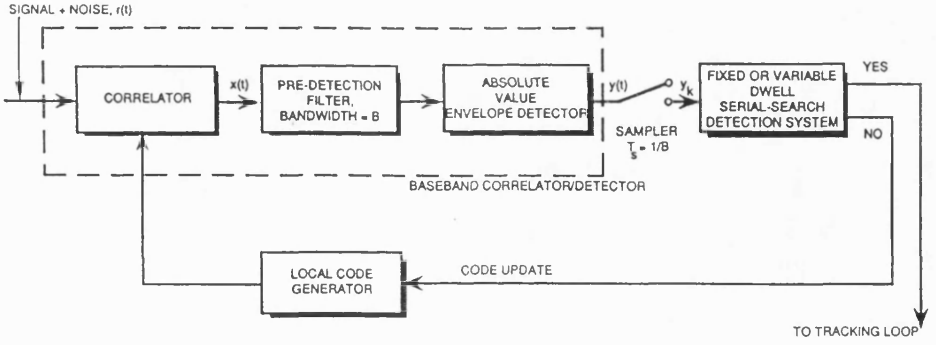

Figure 1 Schematic block diagram of the serial-search PN code acquisition system

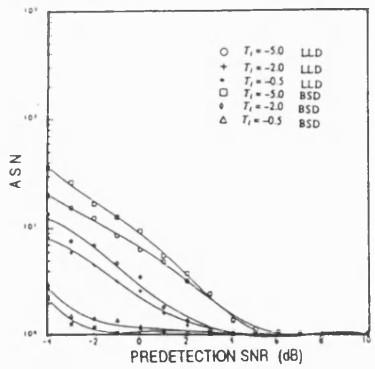

Figure 2a A S N vs predetection SNR for the LLD and the BSD with $b = b_1$ at $T_u = 5.0$.

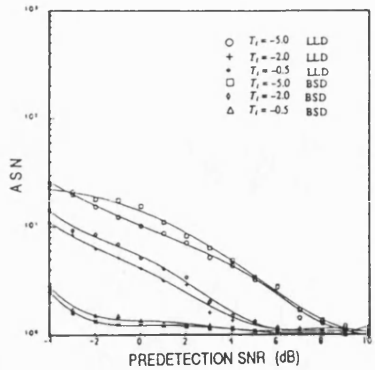

Figure 2b A S N vs predetection SNR for the LLD and the BSD with $b = b_2$ at $T_u = 5.0$.

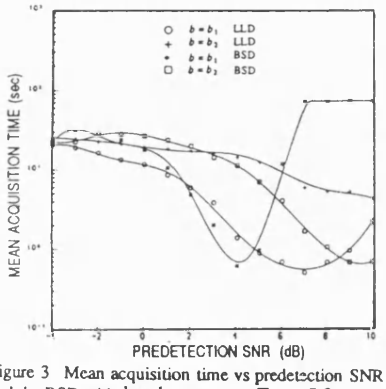

Figure 3 Mean acquisition time vs predetection SNR for the LLD and the BSD with $b = b_1$ and b_2 at $T_l = -5.0$.

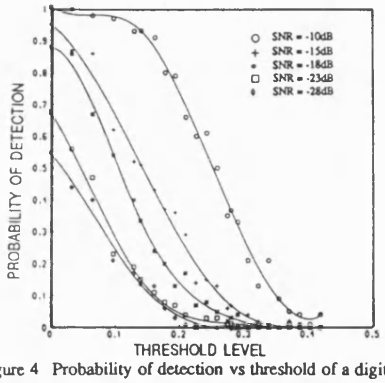

Figure 4 Probability of detection vs threshold of a digital matched filter with input SNR = -10, -15, -18, -23 and -25dB.

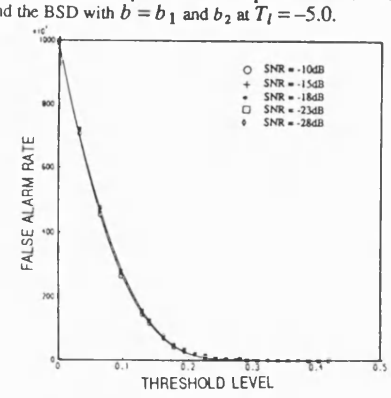

Figure 5 False alarm rate vs threshold of a digital matched filter with input SNR = -10, -15, -18, -23 and -25dB.

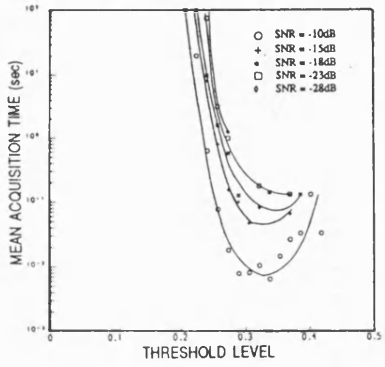

Figure 6 Mean acquisition time vs threshold of a digital matched filter with input SNR = -10, -15, -18, -23 and -25dB.

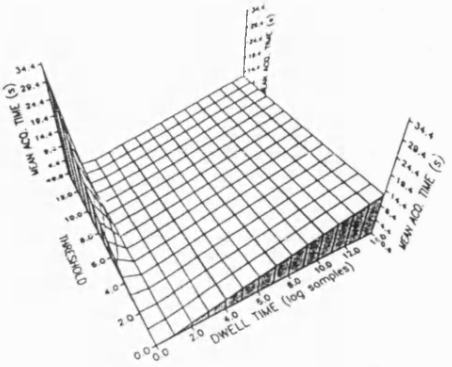

Figure 7a Mean acquisition time vs threshold and the dwell time of a single dwell detector with input SNR = -15dB ; numerical results for a wide range of dwell time.

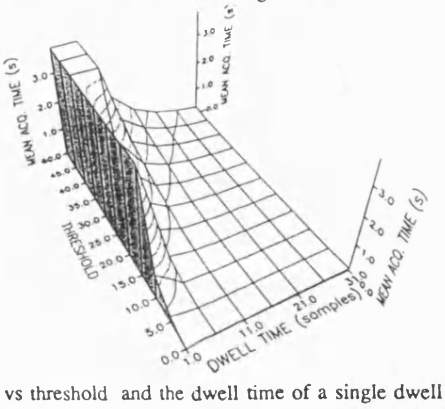

Figure 7b Mean acquisition time vs threshold and the dwell time of a single dwell detector with input SNR = -15dB ; numerical results for normal range of threshold and dwell time (corresponding to simulation).

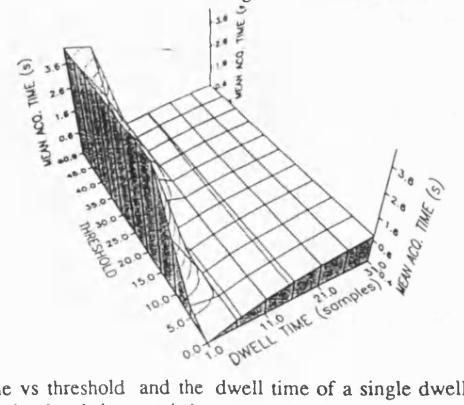

Figure 8 Mean acquisition time vs threshold and the dwell time of a single dwell detector with input SNR = -15dB ; simulated characteristics.